Modélisation Mathématique et Simulation Numérique de Systèmes Fluides Quantiques

Samy Gallego

THÈSE

présentée en vue de l'obtention du
Doctorat de l'Université de Toulouse
délivré par l'Université Toulouse III Paul Sabatier
Spécialité: Mathématiques Appliquées

Samy GALLEGO

MODÉLISATION MATHÉMATIQUE ET SIMULATION NUMÉRIQUE DE SYSTÈMES FLUIDES QUANTIQUES

(MATHEMATICAL MODELING AND NUMERICAL SIMULATION OF QUANTUM FLUID SYSTEMS)

Soutenue le 12 Décembre 2007, devant le jury composé de:

F. Castella	Université de Rennes	*(Examinateur)*
T. Colin	Université de Bordeaux	*(Rapporteur)*
P. Degond	Université de Toulouse	*(Directeur de thèse)*
C. Gardner	Arizona State University	*(Rapporteur)*
G. James	INSA de Toulouse	*(Examinateur)*
F. Méhats	Université de Rennes	*(Directeur de thèse)*
P. Raphaël	Université de Toulouse	*(Examinateur)*

Laboratoire de Mathématiques appliquées à l'Industrie et la Physique
Institut de Mathématiques de Toulouse
Université Paul Sabatier UFR MIG
118 Route de Narbonne 31062 Toulouse cedex 9 France

“ Le doute est le sel de l’esprit; sans la pointe du doute, toutes les connaissances sont bientôt pourries. J’entends aussi bien les connaissances les mieux fondées et les plus raisonnables. Douter quand on s’aperçoit qu’on s’est trompé ou que l’on a été trompé, ce n’est pas difficile; je voudrais même dire que cela n’avance guère; ce doute forcé est comme une violence qui nous est faite; aussi c’est un doute triste; c’est un doute de faiblesse; c’est un regret d’avoir cru, et une confiance trompée. Le vrai c’est qu’il ne faut jamais croire, et qu’il faut examiner toujours. L’incrédulité n’a pas encore donné sa mesure. Croire est agréable. C’est une ivresse dont il faut se priver. Ou alors dites adieu à liberté, à justice, à paix. Il est naturel et délicieux de croire que la République nous donnera tous ces biens; ou, si la République ne peut, on veut croire que Coopération, Socialisme, Communisme ou quelque autre constitution nous permettra de nous fier au jugement d’autrui, enfin de dormir les yeux ouverts comme font les bêtes. Mais non. La fonction de penser ne se délègue point. Dès que la tête humaine reprend son antique mouvement de haut en bas, pour dire oui, aussitôt les rois reviennent. ”

Alain, Propos I (1931)

Remerciements (Acknowledgements)

Chacun sait qu'une thèse, c'est long, et que ce n'est pas l'histoire d'une seule personne. Je tiens donc à remercier ici tous ceux qui ont contribué plus ou moins directement à ce que je parvienne au bout de ce manuscrit.

Mes premiers remerciements vont tout naturellement à mes deux directeurs de thèse Pierre Degond et Florian Méhats qui m'ont accordé leur confiance en me proposant un sujet original et prometteur. Ils ont été très disponibles tout au long des trois dernières années et malgré leur emploi du temps surchargé, ils ont toujours pris le temps de répondre très clairement à mes questions (même quand elles étaient confuses). Leurs qualités scientifiques ne sont plus à démontrer et je peux témoigner comme beaucoup de gens de leurs grandes qualités humaines. Ils ont su me laisser ce qu'il me fallait d'autonomie en me remotivant quand j'en avais besoin. Leur enthousiasme et leur énergie restera un exemple pour moi. Enfin, j'ai beaucoup apprécié qu'ils m'encouragent à voyager et à participer à des conférences internationales.

Je tiens ensuite à exprimer ma gratitude à mes deux rapporteurs Thierry Colin et Carl Gardner qui ont gentiment accepté de se plonger dans mon manuscrit, ainsi que les autres membres de mon jury, François Castella, Guillaume James et Pierre Raphaël qui ont témoigné de l'intérêt pour mon sujet de thèse en acceptant le rôle d'examinateur.

Je remercie aussi Naoufel Ben Abdallah qui n'a malheureusement pas pu être présent dans mon jury le jour de ma soutenance mais qui m'a accordé du temps quand j'ai eu des questions à lui poser, et qui reste pour moi un excellent exemple à suivre tant dans le domaine de la recherche que de l'enseignement. J'associe à ces remerciements tout les autres chercheurs du laboratoire MIP, mais aussi le personnel non chercheur qui contribue à créer au sein du laboratoire une ambiance propice au travail. Je pense en particulier à Christine Marty qui nous a quitté pour Bordeaux, son efficacité et sa gentillesse en font une personne très rare qui je suis sûr va beaucoup manquer au MIP.

Je dis un grand merci à tous les gens du Wolfgang Pauli Institute qui m'ont accueilli pendant deux mois à Vienne, en particulier Norbert Mauser qui s'est particulièrement bien occupé de moi. Ce séjour m'a donné l'occasion de rencontrer et de pouvoir travailler avec Christian Ringhofer qui est en quelque sorte la troisième personne à la base de mon sujet de thèse et qui me fait l'honneur de suivre de près mes travaux.

Je suis bien obligé de remercier mes collègues qui sont dans la même galère que moi depuis le DEA, je pense à Marc, Michaël, Raymond, Elie, Davuth et puis mes collègues de bureau Jean-Luc et Yogesh. Je pense aussi aux petits nouveaux, Sébastien, Dominique et à tous les anciens, Claudia bien sûr pour sa légendaire bonne humeur

et son entrain, Nicolas et Raphaël, Pierre et les autres. Merci à Stéphane et Rémi pour les parties d'échecs et merci aussi à Afeintou pour son sourire et pour m'avoir parlé de son pays le Togo que je vais bientôt visiter. Je remercie aussi tous ceux que j'oublie de citer pour contribuer à ne pas encombrer ma mémoire.

Je remercie celles et ceux extérieurs au laboratoire qui m'ont soutenu plus ou moins consciemment pendant la thèse. Diego, Laurent, Patrick et Bourras par exemple, qui font régulièrement semblant de s'intéresser à mes travaux. Mon parapente aussi, qui ne m'a jamais laissé tomber (sauf une fois...) et qui m'a très souvent fait rêver en me permettant de voir quelques jolis coins de notre planète vue d'en haut. Plus sérieusement, je remercie ma famille qui m'a toujours encouragé à continuer les études en me témoignant sa confiance. Merci Maman, Christophe, Caroline et j'ai aussi une pensée émue pour mon père et ma grand-mère qui seraient probablement fiers de moi.

Et puis forcément j'ai gardé le meilleur pour la fin, merci pour tout à toi Sandra avec qui je me sens si bien.

Table des matières (Table of contents)

Liste des figures (List of figures)

Introduction générale (version française)

Cette thèse s'intéresse à des modèles de transport de particules bien précis: les modèles fluides quantiques issus du principe de minimisation d'entropie. Dans cette introduction nous allons dans un premier temps donner quelques motivations pour l'étude de tels modèles, puis nous allons rappeler comment ces modèles ont été dérivés, et pour cela nous ferons un résumé des articles [14, 11, 12] qui sont à la base du sujet de thèse. Ensuite, nous introduirons quelques notions sur les semiconducteurs qui constituent un champ d'application possible de ces modèles. Enfin, nous présenterons les résultats originaux qui ont été obtenus durant cette thèse.

1 Motivations

La physique n'ayant pas encore été unifiée, il n'existe pas de théorie qui permettrait de décrire de manière universelle un système de particules quelconque. En revanche, il existe plusieurs théories différentes qui s'appliquent dans des domaines particuliers. Par exemple, la mécanique classique développée au $17^{\text{ème}}$ siècle par Newton n'est valable que pour des particules ayant des vitesses v faibles devant la vitesse de la lumière c et elle n'est valable qu'à des échelles d'espace relativement grandes. Pour décrire correctement des particules avec des vitesses élevées, il faudra plutôt utiliser la mécanique relativiste développée par Einstein au tout début du $20^{\text{ème}}$ siècle, et à de très petites échelles, il faudra utiliser la mécanique quantique développée par Bohr, Dirac, de Broglie, Heisenberg, Jordan, Pauli, Planck et Schrödinger dans le premier quart du $20^{\text{ème}}$ siècle. La figure 1 décrit plusieurs théories physiques et leurs liens à travers trois constantes universelles qui apparaissent ou non dans leurs théories: la vitesse de la lumière c, la constante gravitationnelle G et la constante de Planck $\hbar$. Dans cette thèse, nous nous intéresserons à la théorie quantique et aussi aux liens qui existent avec la théorie classique à travers ce que l'on appelle la limite semi-classique.

Par ailleurs, à l'intérieur de chaque théorie il existe différentes échelles de description. L'échelle la plus élémentaire et la plus précise est l'échelle microscopique[1]

[1] Attention, les mots microscopiques, mésoscopiques et macroscopiques n'indiquent pas nécessairement l'échelle spatiale à laquelle on se place, mais plutôt le niveau de description que l'on choisit. Ainsi, il est possible d'utiliser un modèle microscopique pour décrire les mouvement des planètes dans le système solaire, et par ailleurs on peut utiliser un modèle macroscopique pour décrire le déplacement d'électrons dans une puce électronique!

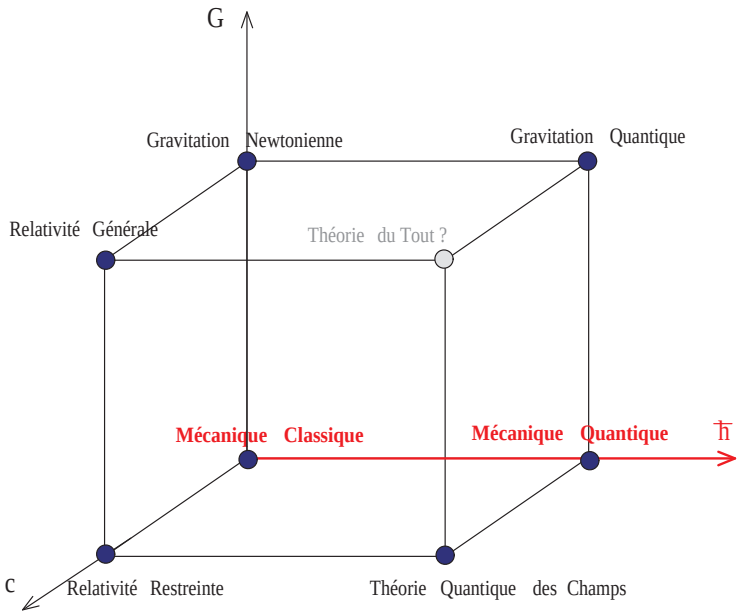

Figure 1: Les différentes théories physiques et leurs constantes universelles, c étant la vitesse de la lumière, G la constante gravitationnelle et $\hbar$ la constante de Planck.

(ou particulaire), l'échelle intermédiaire est l'échelle mésoscopique (ou cinétique), et l'échelle à laquelle nous nous intéresserons est l'échelle macroscopique (ou fluide). Bien évidemment, chaque passage d'une échelle à l'autre entraîne une perte de précision, mais la modélisation devient de moins en moins coûteuse d'un point de vue numérique.

Les modèles fluides en mécanique classique sont employés depuis bien longtemps pour modéliser de grands ensembles de particules, le plus connu étant peut-être celui de Navier-Stokes qui permet de modéliser les mouvements de l'air dans l'atmosphère, les courants océaniques, l'écoulement de l'eau dans un tuyau, etc... Dans l'industrie des semiconducteurs, les équations de Dérive-Diffusion [10, 19, 31, 33] sont très utilisées pour modéliser le transport électronique. Cependant, la taille des composants électroniques ne cessant de diminuer (on arrive à des échelles de l'ordre de 100 nanomètres), ce modèle commence à montrer ces limites et des effets quantiques apparaissent. Certains dispositifs, comme la diode à effet tunnel résonnant, sont même basés sur des effets que seule la mécanique quantique permet d'expliquer. Pour modéliser de tels dispositifs, très peu de modèles fluides existent et il faut la plupart du temps utiliser des modèles microscopiques très coûteux d'un point de vue numérique, et qui tiennent difficilement compte des effets de collision. Les seuls modèles fluides existants ne sont souvent que des modèles fluides classiques auxquels on rajoute des termes de correction quantiques.

Les modèles étudiés dans cette thèse ont été dérivés dans un article de 2003 [14] par Degond et Ringhofer et un article de 2005 [11] par Degond, Méhats et Ringhofer et tentent de combler ce vide en étant "réellement" quantiques. Le tableau 1 donne différents modèles classiques et quantiques qui permettent de modéliser un ensemble de particules aux trois échelles décrites précédemment et permet de situer les quatres modèles étudiés dans la case des modèles macroscopiques et quantiques:

1. le modèle de Dérive-Diffusion Quantique (QDD),

2. le modèle d'Euler Quantique Isotherme,

3. le modèle de Transport d'Énergie Quantique (QET),

4. le modèle d'Hydrodynamique Quantique (QHD).

	Classique	*Quantique*
Microscopique	Newton	Schrödinger
Mésoscopique	Vlasov/Boltzmann	Liouville/Wigner
Macroscopique	Dérive-Diffusion	**Dérive-Diffusion Quantique**
	Euler Isotherme	**Euler Quantique Isotherme**
	Transport d'Énergie	**Transport d'Énergie Quantique**
	Hydrodynamique	**Hydrodynamique Quantique**

Table 1: Quelques modèles classiques et quantiques décrivant un système de particules à différentes échelles.

Le but de cette thèse est d'étudier plus en détail ces modèles et de mettre au point des stratégies numériques pour effectuer des simulations. Mais avant de présenter les résultats obtenus dans cette thèse, il est nécessaire de rappeler comment ces modèles ont été dérivés. Pour cela, nous allons tout d'abord dériver les équations macroscopiques à partir des équations microscopiques dans le cadre de la mécanique classique, cela permettra de mettre en place les limites hydrodynamiques et diffusives et de mieux aborder la dérivation en mécanique quantique qui est basée sur la même méthode.

2 Dérivation des modèles fluides quantiques

2.1 Rappel de la méthode pour le cas classique

2.1.1 Des équations de Newton à l'équation de Boltzmann

Commençons par considérer un système simple à N particules de masse m qui évoluent sans collision. Au niveau le plus fondamental, on peut décrire l'évolution de ce système en appliquant les lois fondamentales de la dynamique sur chaque particule (ces lois ont été exposées pour la première fois en 1687 par l'Anglais Isaac Newton dans le livre "Philosophiae Naturalis Principia Mathematica"). Chaque particule numérotée i est décrite par sa position $x_i \in \mathbb{R}^3$ et son impulsion (le produit de la masse et de la vitesse) $p_i \in \mathbb{R}^3$ avec $i = 1, ..., N$. On obtient ainsi un système d'équations de la forme:

$$\partial_t x_i = \frac{p_i}{m}, \tag{2.1}$$

$$\partial_t p_i = F_i(x_1, ..., x_N), \tag{2.2}$$

où $F_i \in \mathbb{R}^3$ est la force exercée sur la $i^{\text{ème}}$ particule par les autres particules et par les forces extérieures.

En pratique, il est rare de connaître le nombre exact de particules contenues dans un système ainsi que leurs positions et leurs impulsions initiales. Et même si l'on connaissait toutes ces informations, la résolution du système serait trop coûteuse et inutile. C'est pourquoi on utilise un niveau de description plus grossier que l'on appelle mésoscopique ou cinétique. A cette échelle, le système est décrit par une fonction de distribution $f(x,p,t)$. Cette fonction représente une densité dans l'espace des phases décrit par la position et l'impulsion. C'est à dire que $f(x,p,t)dxdp$ est le nombre de particules contenues dans un élément de volume $dxdp$ au point (x,p) et à l'instant t.

Pour obtenir l'équation de Vlasov, on écrit que toutes les particules issues du même point (x,p) de l'espace des phases suivent la même trajectoire:

$$\partial_t X = \frac{P}{m} \quad ; \quad \partial_t P = F(X,t).$$

Pour obtenir l'équation satisfaite par f, on écrit que la densité est conservée le long des trajectoires:

$$\frac{d}{dt} f(X(t),P(t),t) = 0.$$

En développant, on obtient l'équation de Vlasov suivante:

$$\partial_t f + \frac{p}{m} \cdot \nabla_x f + F(x,t) \cdot \nabla_p f = 0. \tag{2.3}$$

A présent, si l'on veut prendre en compte les collisions entre particules, il faut faire intervenir un opérateur de collision que l'on note $Q(f)$ et qui contient toute la physique du système que l'on veut modéliser. L'équation de Vlasov est alors remplacée par l'équation de Boltzmann (introduite initialement par l'Autrichien Ludwig Boltzmann à la fin du XIX$^{\text{ème}}$ siècle pour décrire les gaz):

$$\partial_t f + \frac{p}{m} \cdot \nabla_x f + F(x,t) \cdot \nabla_p f = \frac{Q(f)}{\tau},$$

avec τ le temps moyen entre deux collisions. Si la force extérieure $F(x,t)$ est conservative, elle dérive d'un potentiel $V(x,t)$ tel que $F(x,t) = -\nabla_x V(x,t)$ et on a:

$$\partial_t f + \frac{p}{m} \cdot \nabla_x f - \nabla_x V \cdot \nabla_p f = \frac{Q(f)}{\tau}. \tag{2.4}$$

On peut aussi noter cette équation de Boltzmann sous forme hamiltonienne grâce au crochet de Poisson:

$$\partial_t f = \left\{ \hat{H}, f \right\} + \frac{Q(f)}{\tau}, \tag{2.5}$$

où $\hat{H}(x,p) = \frac{p^2}{2m} + V(x)$ est l'Hamiltonien du système et $\{a,b\}$ dénote le crochet de Poisson:

$$\{a,b\} = \nabla_x a \cdot \nabla_p b - \nabla_x b \cdot \nabla_p a. \tag{2.6}$$

Il est important de rappeler que l'introduction de l'opérateur de collision fait perdre l'aspect réversible de l'équation de Vlasov. Il permet de réconcilier les mécanismes de Newton, qui sont réversibles, avec la thermodynamique qui est, elle, irréversible. Nous ne donnerons pas la forme générale des opérateurs de collision mais nous introduirons des opérateurs qui auront les bonnes propriétés pour dériver les modèles macroscopiques qui nous intéressent. Il y a tant d'articles dédiés à cette équation de Boltzmann que nous ne donnons que quelques références sur son utilisation en physique des semiconducteurs [23, 38].

2.1.2 Scaling de l'équation de Boltzmann

Les deux valeurs de références que l'on choisit sont la longueur de référence $\overline{x} = L$ et la température de référence $\overline{T} = T_0$. On en déduit toutes les autres valeurs de références:

- Temps de référence: $\overline{t} = L\sqrt{\frac{m}{k_B T_0}}$,
- Impulsion de référence: $\overline{p} = \sqrt{k_B T_0 m}$,
- Potentiel de référence: $\overline{V} = k_B T_0$,

avec k_B la constante de Boltzmann, puis on fait les changements de variables: $t' = \frac{t}{\overline{t}}, x' = \frac{x}{\overline{x}}, p' = \frac{p}{\overline{p}}, V' = \frac{V}{\overline{V}}$ et on omet les primes pour obtenir l'équation de Boltzmann adimensionnée:

$$\partial_t f + p \cdot \nabla_x f - \nabla_x V \cdot \nabla_p f = \frac{Q(f)}{\varepsilon}. \tag{2.7}$$

avec ε le temps de relaxation adimensionné[2] suivant:

$$\varepsilon = \frac{\tau}{\overline{t}} = \frac{\lambda_{\text{mfp}}}{L}, \tag{2.8}$$

où $\lambda_{\text{mfp}} = \tau\sqrt{\frac{k_B T_0}{m}}$ dénote le libre parcours moyen ("mean free path" en anglais).

2.1.3 Opérateurs de collision et Maxwelliennes

Plus le temps de relaxation est faible (cela correspond à la limite $\varepsilon \to 0$), plus il y a de collisions et la fonction de distribution tend vers un "équilibre local" qui est défini comme le noyau de l'opérateur $Q(f)$. L'approche de Levermore [25] consiste à définir cet équilibre local comme le minimiseur de l'entropie sous la contrainte que certains moments sont donnés. C'est donc l'entropie qui va décrire la statistique des particules que l'on considère. Dans cette section, nous allons choisir comme entropie l'entropie de Boltzmann (l'équilibre local s'appelle alors Maxwellienne) et dans le cas quantique, nous généraliserons au cas d'une entropie quelconque.

Maxwelliennes: Nous allons définir quatre Maxwelliennes qui vont nous être utiles pour définir les quatres opérateurs de collision nécessaires à la dérivation des modèles macroscopiques. Tout d'abord la Maxwellienne la plus générale est définie comme le minimiseur de l'entropie sous contrainte que la masse, le courant et l'énergie sont donnés. La notion d'entropie, sa définition et le terme lui-même furent introduits dans la thermodynamique en 1854 par l'Allemand Rudolf Clausius. Ludwig Boltzmann fut le premier à proposer une interprétation microscopique de la notion d'entropie. Dès 1877, il reliait celle-ci à une mesure du désordre moléculaire. Il a obtenu l'expression de l'entropie suivante:

$$S(f) = \int f(\log f - 1)\, dp\, dx. \tag{2.9}$$

Les quantités macroscopiques susceptibles de nous intéresser s'expriment en fonction des moments de f: la densité $n = \int f\, dp$, le courant $nu = \int p\, f\, dp$ et l'énergie

[2] pour les équations de Navier-Stokes, ε s'appelle le nombre de Knudsen et se note Kn.

$\mathcal{W} = \int \frac{p^2}{2} f\, dp$. Maintenant on définit le problème suivant: Pour $(n, nu, \mathcal{W})$ donné, trouver

$$\min_f \left(S(f) / \int f \begin{pmatrix} 1 \\ p \\ \frac{|p|^2}{2} \end{pmatrix} dp = \begin{pmatrix} n \\ nu \\ \mathcal{W} \end{pmatrix} \right). \tag{2.10}$$

L'unique solution est donnée par la Maxwellienne suivante:

$$M_{n,nu,\mathcal{W}} = \frac{n}{(2\pi T)^{3/2}} \exp\left(-\frac{1}{2T}(p-u)^2 \right), \tag{2.11}$$

avec $T = \frac{2}{3}\frac{\mathcal{W}}{n} - \frac{1}{3}u^2$.

Maintenant définissons une autre Maxwellienne avec un courant nul qui est solution de:

$$\min_f \left(S(f) / \int f \begin{pmatrix} 1 \\ \frac{|p|^2}{2} \end{pmatrix} dp = \begin{pmatrix} n \\ \mathcal{W} \end{pmatrix} \right). \tag{2.12}$$

L'unique solution est donnée par la Maxwellienne suivante:

$$M_{n,\mathcal{W}} = \frac{n}{(2\pi T)^{3/2}} \exp\left(-\frac{p^2}{2T} \right), \tag{2.13}$$

avec $T = \frac{2}{3}\frac{\mathcal{W}}{n}$.

Enfin, nous nous intéresserons dans cette thèse à des modèles isothermes, cela revient à dire que les particules que l'on considère sont dans un "bain thermostaté" et donc que la temperature est constante et égale à la température de référence T_0 (et donc une fois adimensionnée, $T = 1$). Cette interaction ne conserve pas l'énergie des particules et la bonne notion d'entropie pour décrire une telle situation est l'entropie relative (ou énergie libre) du système, définie comme la somme de l'énergie totale et de l'entropie:

$$G(f) = E(f) + S(f) = \int \hat{H} f + f(\log f - 1)\, dp\, dx, \tag{2.14}$$

avec l'Hamiltonien $\hat{H}(x,p) = \frac{p^2}{2} + V(x)$. On définit ainsi une nouvelle Maxwellienne solution de

$$\min_f \left(G(f) / \int f \begin{pmatrix} 1 \\ p \end{pmatrix} dp = \begin{pmatrix} n \\ nu \end{pmatrix} \right). \tag{2.15}$$

L'unique solution est donnée par la Maxwellienne suivante:

$$M_{n,nu} = \frac{n}{(2\pi)^{3/2}} \exp\left(-\frac{(p-u)^2}{2} \right). \tag{2.16}$$

Et enfin la dernière Maxwellienne est solution de

$$\min_f \left(G(f) / \int f\ dp = n \right). \tag{2.17}$$

L'unique solution est donnée par la Maxwellienne suivante:

$$M_n = \frac{n}{(2\pi)^{3/2}} \exp\left(-\frac{p^2}{2} \right).$$

Opérateurs de collision: On peut à présent définir les opérateurs de collision dont on a besoin pour la dérivation des modèles macroscopiques. On va s'intéresser à 4 opérateurs: Q_h qui nous donnera le modèle hydrodynamique, Q_{hi} qui nous donnera le modèle hydrodynamique isotherme, Q_d qui nous donnera le modèle diffusif, et Q_{di} qui nous donnera le modèle diffusif isotherme. Pour avoir de bonnes propriétés physiques, chaque opérateur doit satisfaire 3 propriétés, la première étant qu'il conserve un certain nombre de moments, la deuxième étant que l'équilibre local est une Maxwellienne, et enfin la troisième étant qu'il fasse décroître l'entropie (ou l'énergie libre).
Plus précisément, Q_h doit satisfaire les propriétés suivantes:

1. $\forall f : \int Q_h(f) \begin{pmatrix} 1 \\ p \\ \frac{|p|^2}{2} \end{pmatrix} dp = 0,$
2. $Q_h(f) = 0 \Longleftrightarrow \exists (n, nu, \mathcal{W}) \ \mid \ f(x,p) = M_{n,nu,\mathcal{W}},$
3. $\int Q_h(f) \ln f dp \leq 0.$

D'autre part, Q_{hi} doit satisfaire les propriétés suivantes:

1. $\forall f : \int Q_{hi}(f) \begin{pmatrix} 1 \\ p \end{pmatrix} dp = 0,$
2. $Q_{hi}(f) = 0 \Longleftrightarrow \exists (n, nu) \ \mid \ f(x,p) = M_{n,nu},$
3. $\int Q_{hi}(f)(\ln f + \hat{H}(x,p)) dp \leq 0.$

L'opérateur Q_d doit satisfaire quant à lui les propriétés suivantes:

1. $\forall f : \int Q_d(f) \begin{pmatrix} 1 \\ \frac{p^2}{2} \end{pmatrix} dp = 0,$
2. $Q_d(f) = 0 \Longleftrightarrow \exists (n, \mathcal{W}) \ \mid \ f(x,p) = M_{n,\mathcal{W}},$
3. $\int Q_d(f) \ln f dp \leq 0.$

Et enfin Q_{di} doit satisfaire les propriétés suivantes:

1. $\forall f : \int Q_{di}(f) dp = 0,$
2. $Q_{di}(f) = 0 \Longleftrightarrow \exists n \ \mid \ f(x,p) = M_n,$
3. $\int Q_{di}(f)(\ln f + \hat{H}(x,p)) dp \leq 0.$

Pour dériver les modèles hydrodynamiques, on n'a pas besoin de connaître la forme exacte des opérateurs de collision. En revanche, pour dériver les modèles diffusifs, il faut connaître la forme exacte des opérateurs de collision car les coefficients des matrices de diffusion en dépendent. Nous ne considérerons dans cette thèse que des opérateurs de type BGK (introduits par Bathnagar, Gross et Krook [4]) qui sont de la forme:

$$Q_d(f) = M_{n,nu}(f) - f \ \ ; \ \ Q_{di} = M_n(f) - f, \tag{2.18}$$

où l'on note $M_{n,nu}(f)$ la Maxwellienne associée à f qui a la même densité et le même courant que f, et $M_n(f)$ la Maxwellienne associée à f qui a la même densité que f. Il est facile de vérifier que ces opérateurs vérifient bien les 3 propriétés définies juste au dessus.

2.1.4 Modèles macroscopiques

On va maintenant pouvoir montrer le lien qui existe entre l'équation de Boltzmann et les modèles hydrodynamiques et diffusifs grâce à la méthode des moments définie par Levermore [25].

Limite hydrodynamique: Nous allons considérer l'équation de Boltzmann associée à l'opérateur Q_h. Pour bien montrer que la solution dépend du paramètre ε, nous allons noter la fonction de distribution f^ε:

$$\partial_t f^\varepsilon + p \cdot \nabla_x f^\varepsilon - \nabla_x V \cdot \nabla_p f^\varepsilon = \frac{Q_h(f^\varepsilon)}{\varepsilon}. \tag{2.19}$$

La méthode des moments consiste à prendre les moments de l'équation de Boltzmann (2.19), c'est à dire de la multiplier par $\begin{pmatrix} 1 \\ p \\ \frac{|p|^2}{2} \end{pmatrix}$ et de l'intégrer par rapport à p. Grâce à la conservation de masse, de courant et d'énergie de l'opérateur de collision (propriété 1 de l'opérateur Q_h), on obtient le système suivant:

$$\begin{aligned} \partial_t n^\varepsilon + \nabla \cdot n u^\varepsilon &= 0, \\ \partial_t (n u^\varepsilon) + \nabla \cdot \Pi^\varepsilon &= -n^\varepsilon \nabla V, \\ \partial_t \mathcal{W}^\varepsilon + \nabla \cdot \Phi^\varepsilon &= -n u^\varepsilon \cdot \nabla V, \end{aligned}$$

avec le tenseur de pression Π^ε et le flux d'énergie Φ^ε donnés par:

$$\begin{aligned} \Pi^\varepsilon &= \int f^\varepsilon (p \otimes p)\, dp, \\ \Phi^\varepsilon &= \int f^\varepsilon \frac{|p|^2}{2} p\, dp. \end{aligned}$$

On voit bien que ce système n'est pas fermé puisque Π^ε et Φ^ε ne peuvent pas s'écrire en fonction de n^ε, nu^ε et $\mathcal{W}^\varepsilon$. Maintenant, si l'on regarde un système fortement collisionnel, on va avoir ε qui tend vers 0 et l'équation (2.19) ainsi que la propriété 2 de Q_h nous donne $f^\varepsilon \overset{\varepsilon \to 0}{\longrightarrow} f^0 = M_{n^0, nu^0, \mathcal{W}^0}(f^0) = \frac{n^0}{(2\pi T^0)^{3/2}} \exp(-\frac{1}{2T^0}(p - u^0)^2)$.

A la limite $\varepsilon \to 0$, on obtient donc le modèle **hydrodynamique** suivant (après un simple calcul des intégrales et en omettant les indices correspondant à $\varepsilon = 0$):

$$\partial_t n + \nabla \cdot nu = 0, \tag{2.20}$$

$$\partial_t (nu) + \nabla \cdot (nu \otimes u) + \nabla (nT) = -n \nabla V, \tag{2.21}$$

$$\partial_t \mathcal{W} + \nabla \cdot (\mathcal{W} u) + \nabla \cdot (nuT) = -nu \cdot \nabla V. \tag{2.22}$$

Le modèle isotherme s'obtient par la même méthode en prenant l'opérateur de collision Q_{hi} et en ne considérant que les 2 premiers moments. On obtient le modèle d'**Euler isotherme**:

$$\partial_t n + \nabla \cdot nu = 0, \tag{2.23}$$

$$\partial_t (nu) + \nabla \cdot (nu \otimes u) + \nabla n = -n \nabla V. \tag{2.24}$$

Limite de diffusion: Si on prend le même scaling que pour la limite de diffusion mais que l'on remplace l'opérateur de collision Q_h par l'opérateur Q_d, on obtient l'équation de Boltzmann:

$$\partial_t f^\varepsilon + p \cdot \nabla_x f^\varepsilon - \nabla_x V \cdot \nabla_p f^\varepsilon = \frac{Q_d(f^\varepsilon)}{\varepsilon}. \tag{2.25}$$

Maintenant, si l'on intègre cette équation contre le vecteur $\begin{pmatrix} 1 \\ p \\ \frac{|p|^2}{2} \end{pmatrix}$ on obtient:

$$\begin{aligned} \partial_t n^\varepsilon + \nabla \cdot n u^\varepsilon &= 0, \\ \partial_t (n u^\varepsilon) + \nabla \cdot \Pi^\varepsilon &= -n^\varepsilon \nabla V - \frac{n u^\varepsilon}{\varepsilon}, \\ \partial_t \mathcal{W}^\varepsilon + \nabla \cdot \Phi^\varepsilon &= -n u^\varepsilon \cdot \nabla V. \end{aligned}$$

Maintenant si on fait tendre ε vers 0, on va avoir $f^\varepsilon \overset{\varepsilon \to 0}{\longrightarrow} f^0 = M_{n^0, \mathcal{W}^0}(f^0) = \frac{n^0}{(2\pi T^0)^{3/2}} \exp(-\frac{p^2}{2T^0})$ et donc $n u^\varepsilon \overset{\varepsilon \to 0}{\longrightarrow} n u^0 = 0$. Comme f^0 est paire par rapport à p, on a aussi $\Phi^0 = 0$ et on obtient le système:

$$\begin{aligned} \partial_t n &= 0, \\ n u &= 0, \\ \partial_t \mathcal{W} &= 0, \end{aligned}$$

c'est à dire que rien ne bouge! Il faut donc regarder à une échelle de temps plus grande et il convient donc d'utiliser un autre scaling pour le temps. On va prendre non pas $\bar{t} = L\sqrt{\frac{m}{k_B T_0}}$ mais plutôt $\bar{t} = \varepsilon^{-1} \times L\sqrt{\frac{m}{k_B T_0}} = L^2 \frac{m}{\tau k_B T_0}$. On a donc:

$$\varepsilon \partial_t f^\varepsilon + p \cdot \nabla_x f^\varepsilon - \nabla_x V \cdot \nabla_p f^\varepsilon = \frac{Q_d(f^\varepsilon)}{\varepsilon}. \tag{2.26}$$

A nouveau si on fait tendre ε vers 0, on va avoir $f^\varepsilon \overset{\varepsilon \to 0}{\longrightarrow} f^0 = M_{n^0, \mathcal{W}^0}(f^0) = \frac{n^0}{(2\pi T^0)^{3/2}} \exp(-\frac{p^2}{2T^0})$. Ensuite, on introduit le développement de Chapman-Enskog suivant:

$$f^\varepsilon = M_{n, \mathcal{W}}(f^\varepsilon) + \varepsilon f_1^\varepsilon, \tag{2.27}$$

ce qui définit f_1^ε de la façon suivante (on note $\mathcal{T}$ l'opérateur de transport $\mathcal{T} f^\varepsilon = p \cdot \nabla_x f^\varepsilon - \nabla_x V \cdot \nabla_p f^\varepsilon$):

$$f_1^\varepsilon = -\frac{1}{\varepsilon} Q(f^\varepsilon) = -\mathcal{T} f^\varepsilon - \varepsilon \partial_t f^\varepsilon. \tag{2.28}$$

A la limite, on a donc $f_1 = -\mathcal{T} f^0$. Ensuite, on multiplie (2.26) par $\begin{pmatrix} 1 \\ \frac{|p|^2}{2} \end{pmatrix}$ et on intègre par rapport à p pour obtenir:

$$\partial_t \int f^\varepsilon \begin{pmatrix} 1 \\ \frac{|p|^2}{2} \end{pmatrix} dp + \frac{1}{\varepsilon} \int \mathcal{T} f^\varepsilon \begin{pmatrix} 1 \\ \frac{|p|^2}{2} \end{pmatrix} dp = 0, \tag{2.29}$$

puis on utilise le développement (2.27) pour avoir:

$$\mathcal{T} f^\varepsilon = \mathcal{T} M_{n,\mathcal{W}}(f^\varepsilon) + \varepsilon \mathcal{T} f_1^\varepsilon.$$

La Maxwellienne $M_{n,\mathcal{W}}(f^\varepsilon)$ étant paire par rapport à p, il est facile de vérifier que $\mathcal{T} M_{n,\mathcal{W}}(f^\varepsilon)$ est impaire par rapport à p. On a donc

$$\int \mathcal{T} M_{n,\mathcal{W}}(f^\varepsilon) \begin{pmatrix} 1 \\ \frac{|p|^2}{2} \end{pmatrix} dp = 0,$$

et donc à la limite $\varepsilon \to 0$:

$$\partial_t \int f^0 \begin{pmatrix} 1 \\ \frac{|p|^2}{2} \end{pmatrix} dp + \int \mathcal{T}\mathcal{T} f^0 \begin{pmatrix} 1 \\ \frac{|p|^2}{2} \end{pmatrix} dp = 0. \tag{2.30}$$

Enfin, des calculs d'intégrales et des arguments liés à la parité de la Maxwellienne nous donnent le modèle de **Transport d'Énergie**:

$$\begin{aligned} \partial_t n + \nabla \cdot j_n &= 0, && (2.31)\\ \partial_t \mathcal{W} + \nabla \cdot j_{\mathcal{W}} + \nabla V \cdot j_n &= 0, && (2.32) \end{aligned}$$

$$\begin{aligned} j_n &= -\nabla \cdot \Pi - n \nabla V, && (2.33)\\ j_{\mathcal{W}} &= -\nabla \cdot \mathbb{Q} - (\mathcal{W}\mathrm{Id} + \Pi) \cdot \nabla V, && (2.34) \end{aligned}$$

$$\begin{aligned} \Pi &= \int f^0 (p \otimes p) dp = nT\mathrm{Id}, && (2.35)\\ \mathbb{Q} &= \int f^0 (p \otimes p) \frac{|p|^2}{2} dp = \frac{5}{2} nT^2 \mathrm{Id}, && (2.36) \end{aligned}$$

avec la relation

$$T = \frac{2}{3} \frac{\mathcal{W}}{n}. \tag{2.37}$$

La même méthode appliquée à l'équation de Boltzmann avec l'opérateur de collision Q_{di} nous donne le modèle isotherme de **Dérive-Diffusion**:

$$\begin{aligned} \partial_t n + \nabla \cdot j &= 0, && (2.38)\\ j &= -\nabla \cdot \Pi - n \nabla V, && (2.39)\\ \Pi &= \int f^0 (p \otimes p) dp = n\mathrm{Id}. && (2.40) \end{aligned}$$

2.2 Méthode pour le cas quantique

Il existe un grand nombre de traités dédiés à l'introduction de la théorie quantique dont nous pouvons citer [32, 8] pour un point de vue physique, et [39] pour une étude mathématique approfondie. Par ailleurs, concernant la dérivation des modèles fluides quantiques, nous conseillons vivement le lecteur de lire la section 2.1 (concernant le cas classique) avant d'aborder cette section. Nous ne donnons ici que les idées principales pour comprendre la dérivation des modèles étudiés dans cette thèse, le lecteur se référera à [14, 11] pour les détails.

2.2.1 Éléments de formalisme quantique

Commençons par considérer un système à une seule particule de masse m qui évolue en présence d'un potentiel V. L'équivalent quantique de l'équation de Newton est l'équation de Schrödinger (introduite en 1926 par l'Autrichien Erwin Schrödinger). La particule n'est plus décrite par sa position x et son impulsion p, mais par une fonction d'onde $\psi(x,t) \in L^2(\mathbb{R}^3)$ (espace des fonctions de carré sommable à valeur complexe) qui définit l'état de la particule au temps t. Cette fonction d'onde est régie par l'équation de Schrödinger qui s'écrit en prenant le même scaling que celui introduit dans la sous-section 2.1.2:

$$i\tilde{\hbar}\partial_t\psi = \mathcal{H}\psi = -\frac{\tilde{\hbar}^2}{2}\Delta\psi + V\psi, \tag{2.41}$$

où $\tilde{\hbar}$ est la constante de Planck adimensionnée égale à $\tilde{\hbar} = \frac{\lambda_{dB}}{L} = \frac{\hbar}{\sqrt{mk_BT_0L^2}}$ (on appelle $\lambda_{dB} = \frac{\hbar}{\sqrt{mk_BT_0}}$ la longueur d'onde de de Broglie). Ce nombre adimensionnel permet de "mesurer" le comportement quantique de la particule. En effet, plus $\tilde{\hbar}$ est grand, plus la particule va se comporter d'une manière quantique tandis que la limite $\tilde{\hbar} \to 0$ correspond à la limite semi-classique (voir la sous section 2.2.5). **Dans la suite de la thèse et pour des raisons de simplicité, nous noterons la constante de Planck adimensionnée $\hbar$.**

La quantité $|\psi(x,t)|^2$ représente la probabilité de présence de la particule et c'est pourquoi ψ est de norme 1 dans $L^2(\mathbb{R}^3)$: $\int |\psi|^2 dx = 1$. En mécanique quantique, tout "observable" (quantité physiquement mesurable) est obtenu comme la valeur moyenne sur la fonction d'onde ψ d'un opérateur symétrique O. Plus précisément, $< O >= (O\psi, \psi) = \int (O\psi)(x)\psi(x)dx$ donne l'espérance d'un ensemble de mesures de l'observable O effectuées sur un grand nombre de réalisations du système physique dont l'état est représenté par la fonction ψ.

Les opérateurs qui vont nous intéresser sont par exemple l'opérateur "position" X, l'opérateur "impulsion" P et l'opérateur "énergie totale" $\mathcal{H}$ (Hamiltonien). On a:

$$\begin{aligned} X\psi(x) &= x\psi(x), \\ P\psi(x) &= -i\hbar\nabla\psi(x), \\ \mathcal{H}\psi(x) &= \left(\frac{|P|^2}{2} + V(x,t)\right)\psi(x) = -\frac{\hbar^2}{2}\Delta\psi(x) + V\psi(x). \end{aligned}$$

Maintenant, si on regarde un système quantique à N particules, il faut introduire une fonction d'onde $\psi(x_1, x_2, ..., x_N, t)$ qui décrit l'état du système. Son évolution est régie par l'équation de Schrödinger suivante:

$$i\hbar\partial_t\psi = \sum_{i=1}^{N}(-\frac{\hbar^2}{2}\Delta_{x_i})\psi + V\psi. \tag{2.42}$$

Lorsque l'état dynamique d'un système quantique est incomplètement connu, on peut le décrire par un opérateur de densité ϱ (opérateur à classe hermitien et positif) sur $L^2(\mathbb{R}^3)$ tel que:

$$\text{Tr } \varrho = 1.$$

Puisque ϱ est un opérateur à trace, il est compact et possède un système complet de fonctions propres orthonormées $(\psi_s)_{s\in S}$ associées aux valeurs propres réelles ϱ_s. De

plus, la positivité de ϱ et sa propriété de trace impliquent:

$$0 \leq \varrho_s \leq 1, \quad \forall s \in S; \qquad \sum_{s\in S} \varrho_s = 1.$$

C'est pourquoi nous pouvons écrire l'action de ϱ sur n'importe quelle fonction $\varphi \in L^2(\mathbb{R}^3)$ par la relation:

$$\varrho\varphi = \sum_{s\in S} \varrho_s(\varphi, \psi_s)\psi_s, \tag{2.43}$$

où l'on note (φ, ψ_s) le produit scalaire de $L^2(\mathbb{R}^3)$ des deux fonctions φ et ψ_s.

L'interprétation physique de ϱ est assez naturelle: les fonctions propres ψ_s représentent les états possibles du système et les valeurs propres ϱ_s sont les probabilités associées à chaque état (c'est pourquoi la somme des ϱ_s vaut 1). Dans ce système, chaque état ψ_s évolue selon l'équation de Schrödinger. On peut alors vérifier que l'opérateur de densité évolue quant à lui en vérifiant l'équation de Liouville quantique suivante:

$$i\hbar\partial_t\varrho = [\mathcal{H}, \varrho], \tag{2.44}$$

où $\mathcal{H}$ est l'Hamiltonien décrit précédemment dans l'équation de Schrödinger (2.41), et les crochets désignent le commutateur $[\mathcal{H}, \varrho] = \mathcal{H}\varrho - \varrho\mathcal{H}$. Pour plus de détails, le lecteur pourra se référer au chapitre 8 section 4 (statistique quantique) du livre [32] par exemple.

2.2.2 Les équations de Wigner et de Wigner-Boltzmann

On veut maintenant pousser un peu plus loin la comparaison avec le cas classique et pour cela, il nous faut définir la transformée de Wigner (introduite en 1932 par l'Américain Eugene Wigner [42], voir [24] pour une étude mathématique très poussée). Soit $\underline{\varrho}(x, x')$ le noyau intégral de l'opérateur ϱ. L'application de ϱ sur une fonction quelconque $\varphi \in L^2(\mathbb{R}^3)$ se traduit alors par:

$$\varrho\varphi = \int \underline{\varrho}(x, x')\varphi(x')dx'.$$

D'après la relation (2.43), on peut donc exprimer $\underline{\varrho}$ comme suit:

$$\underline{\varrho}(x, x') = \sum_{s\in S} \varrho_s\psi_s(x)\overline{\psi_s(x')},$$

où $\overline{\psi_s(x')}$ est le conjugué complexe de $\psi_s(x')$.

La transformée de Wigner $W(\varrho)(x, p)$ de ϱ comme fonction dans l'espace des phases (x, p) est alors définie par:

$$W(\varrho)(x, p) = \int \underline{\varrho}\left(x - \frac{1}{2}\xi, x + \frac{1}{2}\xi\right) e^{i\xi\cdot p/\hbar}d\xi. \tag{2.45}$$

La transformée inverse, aussi nommée "quantification de Weyl" et parfois notée "Op", associe à chaque fonction $w(x, p)$ dans l'espace des phases un opérateur $\varrho = W^{-1}(f)$ agissant sur les fonctions de $L^2(\mathbb{R}^3)$ comme suit:

$$W^{-1}(w)\varphi = \frac{1}{(2\pi\hbar)^3}\int w\left(\frac{x+y}{2}, p\right)\varphi(y)e^{ip\cdot(x-y)/\hbar}dpdy. \tag{2.46}$$

Une propriété intéressante pour la suite est:

$$\mathrm{Tr}\ (\varrho\sigma^\dagger) = \int W(\varrho)\overline{W(\sigma)}\frac{dxdp}{(2\pi\hbar)^3}, \tag{2.47}$$

où $\sigma^\dagger$ est l'opérateur adjoint de σ.

On peut vérifier que si ϱ satisfait l'équation de Liouville quantique (2.44), alors $w = W(\varrho)$ vérifie l'équation de Wigner suivante:

$$\partial_t w + p\cdot\nabla_x w - \Theta^\hbar(V)w = 0, \tag{2.48}$$

où $\Theta^\hbar(V)$ est l'opérateur:

$$\Theta^\hbar(V)w = \frac{i}{(2\pi)^3\hbar}\int\left(V(x+\frac{\hbar}{2}\eta) - V(x-\frac{\hbar}{2}\eta)\right)w(x,p)e^{i\eta\cdot(p-q)}dpd\eta. \tag{2.49}$$

On remarquera que l'opérateur $\Theta^\hbar(V)$ converge vers $\nabla_x V\cdot\nabla_p$ quand $\hbar$ tend vers 0, ce qui nous montre la correspondance entre l'équation de Wigner et l'équation de Vlasov. Il faut cependant garder en mémoire le fait que w n'est pas forcément positive dans l'équation de Wigner.

Comme pour l'équation de Boltzmann, on peut ajouter un opérateur de collision pour prendre en compte l'interaction entre particules:

$$i\hbar\partial_t\varrho = [\mathcal{H},\varrho] + i\hbar\frac{\mathcal{Q}_L(\varrho)}{\varepsilon}, \tag{2.50}$$

avec $\varepsilon = \frac{\tau}{L}\sqrt{\frac{k_B T_0}{m}}$ le temps de relaxation adimensionné. Si maintenant ϱ satisfait l'équation de Liouville quantique avec opérateur de collision (2.50), alors $w = W(\varrho)$ vérifie l'équation de Wigner-Boltzmann suivante:

$$\partial_t w + p\cdot\nabla_x w - \Theta^\hbar(V)w = W\left(\frac{\mathcal{Q}_L(\varrho)}{\varepsilon}\right) = \frac{\mathcal{Q}(w)}{\varepsilon}. \tag{2.51}$$

On va maintenant, comme pour le cas classique, donner la forme des opérateurs de collision et utiliser la même méthodologie pour dériver les modèles fluides quantiques.

2.2.3 Opérateurs de collision et équilibres locaux quantiques

Équilibres locaux quantiques: Nous allons définir quatre équilibres locaux quantiques qui vont nous être utiles pour définir les quatres opérateurs de collision nécessaires à la dérivation des modèles fluides quantiques. Nous allons écrire ces équilibres locaux comme minimiseurs d'entropie mais contrairement au cas classique, on ne va pas prendre l'entropie de Boltzmann mais une entropie quelconque définie à partir d'une fonction convexe s. On pourrait écrire cette dérivation à partir de l'équation de Liouville avec le formalisme des opérateurs mais il est plus intuitif de le faire dans le formalisme de Wigner. Dans ce formalisme, les quantités macroscopiques qui nous intéressent s'expriment tout simplement en fonction des moments de w: la densité $n = \int w\frac{dp}{(2\pi\hbar)^3}$, le courant $nu = \int p\,w\frac{dp}{(2\pi\hbar)^3}$ et l'énergie $\mathcal{W} = \int\frac{p^2}{2}w\frac{dp}{(2\pi\hbar)^3}$. En revanche l'entropie ne s'exprime pas facilement avec le formalisme de Wigner et il est plus facile de l'exprimer avec le formalisme des opérateurs. Soit s une fonction convexe, l'entropie s'écrit:

$$S(\varrho) = \mathrm{Tr}\ (s(\varrho))\,. \tag{2.52}$$

Grâce à la propriété (2.47), cette entropie s'exprime dans le formalisme de Wigner comme:

$$S(w) = \int W\left(s\left(W^{-1}(w)\right)\right) \frac{dp\,dx}{(2\pi\hbar)^3}. \tag{2.53}$$

Maintenant on définit le problème suivant: Pour $(n, nu, \mathcal{W})$ donné, trouver

$$\min_w \left(S(w) / \int w \begin{pmatrix} 1 \\ p \\ \frac{|p|^2}{2} \end{pmatrix} \frac{dp}{(2\pi\hbar)^3} = \begin{pmatrix} n \\ nu \\ \mathcal{W} \end{pmatrix} \right). \tag{2.54}$$

Il a été démontré dans [14] que la solution, si elle existe, est donnée par l'équilibre local suivant:

$$w^{eq}_{n,nu,\mathcal{W}} = W\left((s')^{-1}\left(W^{-1}\left(-\frac{1}{2C}(p-B)^2 - A\right)\right)\right), \tag{2.55}$$

où $A(x)$ et $C(x)$ sont des fonctions scalaires, et $B(x)$ est une fonction vectorielle, toutes à valeurs réelles. On appellera les variables A, B et C respectivement le potentiel chimique généralisé, la vitesse moyenne généralisée et la température généralisée. Dans cette thèse on supposera l'existence et l'unicité de telles solutions. Dans le formalisme des opérateurs, l'équilibre local s'écrit plus simplement comme suit:

$$\varrho^{eq}_{n,nu,\mathcal{W}} = (s')^{-1}\left(-H(A,B,C)\right), \tag{2.56}$$

où l'on note $H(A,B,C)$ l'Hamiltonien suivant:

$$\begin{aligned} H(A,B,C) &= W^{-1}\left(\frac{1}{2C}(p-B)^2 + A\right) \\ &= -\hbar^2\left(\nabla\cdot(\frac{1}{2C}\nabla) + \frac{1}{4}\Delta\frac{1}{2C}\right) \\ &\quad + i\hbar\left(\frac{B}{C}\cdot\nabla + \frac{1}{2}(\nabla\cdot\frac{B}{C})\right) + A + \frac{B^2}{2C}. \end{aligned} \tag{2.57}$$

Remarquons que ces équilibres locaux $w^{eq}_{n,nu,\mathcal{W}}$ et $\varrho^{eq}_{n,nu,\mathcal{W}}$ ne s'expriment pas explicitement en fonction de $(n, nu, \mathcal{W})$ contrairement au cas classique. Ces équilibres locaux s'expriment en fonction de variables thermodynamiques intermédiaires (A, B, C) supposées uniques et fixées de telle manière que la densité, le courant et l'énergie de ces équilibres locaux soient égaux respectivement à n, nu et $\mathcal{W}$.

Maintenant définissons un autre équilibre local quantique avec un courant nul qui est solution de:

$$\min_w \left(S(w) / \int w \begin{pmatrix} 1 \\ \frac{|p|^2}{2} \end{pmatrix} \frac{dp}{(2\pi\hbar)^3} = \begin{pmatrix} n \\ \mathcal{W} \end{pmatrix} \right). \tag{2.58}$$

La solution est donnée par l'équilibre local suivant:

$$w^{eq}_{n,\mathcal{W}} = W\left((s')^{-1}\left(W^{-1}\left(-\frac{1}{2C}p^2 - A\right)\right)\right). \tag{2.59}$$

Enfin, pour dériver les modèles isothermes, nous devons définir l'entropie relative quantique (ou énergie libre quantique), qui s'exprime dans le formalisme des opérateurs comme:

$$G(\varrho) = E(\varrho) + S(\varrho) = \mathrm{Tr}\ \left(\mathcal{H}\varrho + s(\varrho)\right), \tag{2.60}$$

ou de manière équivalente

$$G(w) = E(w) + S(w) = \int \left(\frac{p^2}{2} + V\right) w + W\left(s\left(W^{-1}(w)\right)\right) \frac{dp\,dx}{(2\pi\hbar)^3}. \tag{2.61}$$

On définit ainsi un nouvel équilibre local solution de

$$\min_w \left(G(w) / \int w \begin{pmatrix} 1 \\ p \end{pmatrix} \frac{dp\,dx}{(2\pi\hbar)^3} = \begin{pmatrix} n \\ nu \end{pmatrix} \right). \tag{2.62}$$

La solution est donnée par l'équilibre local:

$$w^{eq}_{n,nu} = W\left((s')^{-1}\left(W^{-1}\left(-\frac{1}{2}(p-B)^2 - A\right)\right)\right). \tag{2.63}$$

Et enfin le dernier équilibre local est solution de

$$\min_w \left(G(w) / \int w\ \frac{dp\,dx}{(2\pi\hbar)^3} = n \right). \tag{2.64}$$

Cette solution est donnée par:

$$w^{eq}_{n} = W\left((s')^{-1}\left(W^{-1}\left(-\frac{p^2}{2} - A\right)\right)\right).$$

Opérateurs de collision: On peut à présent définir les opérateurs de collision dont on a besoin pour la dérivation des modèles macroscopiques quantiques. On définit quatre opérateurs analogues aux opérateurs classiques définis dans la sous-section 2.1.3 page 21: $\mathcal{Q}_h, \mathcal{Q}_{hi}, \mathcal{Q}_d$ et $\mathcal{Q}_{di}$. Pour avoir de bonnes propriétés physiques, chaque opérateur doit satisfaire 3 propriétés qui se dérivent facilement à partir du cas classique et que nous ne réécrivons pas. Pour les propriétés de décroissance de l'entropie, il faut bien évidemment changer la fonction $\log(\cdot)$ par la fonction $W(s'(W^{-1}(\cdot)))$.

Pour dériver les modèles de type hydrodynamique, on n'a pas besoin de connaître la forme exacte des opérateurs de collision (notons cependant que dans [13], des opérateurs de collision quantiques ont été écrits sous une forme proche de l'opérateur de Boltzmann classique). En revanche, pour dériver les modèles diffusifs, comme déjà remarqué pour le cas classique, il faut connaître la forme exacte des opérateurs de collision car les coefficients des matrices de diffusion en dépendent. Nous ne considérerons dans cette thèse que des opérateurs de type BGK qui sont de la forme:

$$\mathcal{Q}_d(w) = w^{eq}_{n,nu}(w) - w \quad ; \quad \mathcal{Q}_{di} = w^{eq}_{n}(w) - w. \tag{2.65}$$

2.2.4 Modèles macroscopiques

Pour obtenir les modèles macroscopiques, il suffit à présent de développer la même méthodologie que celle exposée dans la sous-section 2.1.4. Grâce aux propriétés de

l'opérateur $\Theta^{\hbar}(V)$ (nous renvoyons une fois de plus à [14] et [11] pour les détails), on obtient les modèles suivants qui vont être étudiés dans cette thèse.

Le modèle d'**hydrodynamique quantique**:

$$\begin{aligned} \partial_t n + \nabla \cdot nu &= 0, && (2.66)\\ \partial_t (nu) + \nabla \cdot \Pi &= -n\nabla V, && (2.67)\\ \partial_t \mathcal{W} + \nabla \cdot \Phi &= -nu \cdot \nabla V, && (2.68) \end{aligned}$$

avec

$$\begin{pmatrix} n \\ nu \\ \mathcal{W} \end{pmatrix} = \int w^{eq}_{n,nu,\mathcal{W}} \begin{pmatrix} 1 \\ p \\ \frac{|p|^2}{2} \end{pmatrix} \frac{dp}{(2\pi\hbar)^3}, \qquad (2.69)$$

et

$$\begin{aligned} \Pi &= \int w^{eq}_{n,nu,\mathcal{W}} (p \otimes p) \frac{dp}{(2\pi\hbar)^3}, && (2.70)\\ \Phi &= \int w^{eq}_{n,nu,\mathcal{W}} \frac{|p|^2}{2} p \frac{dp}{(2\pi\hbar)^3}. && (2.71) \end{aligned}$$

Le modèle d'**Euler quantique isotherme**:

$$\begin{aligned} \partial_t n + \nabla \cdot nu &= 0, && (2.72)\\ \partial_t (nu) + \nabla \cdot \Pi &= -n\nabla V, && (2.73) \end{aligned}$$

avec

$$\begin{pmatrix} n \\ nu \end{pmatrix} = \int w^{eq}_{n,nu} \begin{pmatrix} 1 \\ p \end{pmatrix} \frac{dp}{(2\pi\hbar)^3}, \qquad (2.74)$$

et

$$\Pi = \int w^{eq}_{n,nu} (p \otimes p) \frac{dp}{(2\pi\hbar)^3}. \qquad (2.75)$$

Le modèle de **transport d'énergie quantique**:

$$\begin{aligned} \partial_t n + \nabla \cdot j_n &= 0, && (2.76)\\ \partial_t \mathcal{W} + \nabla \cdot j_{\mathcal{W}} + \nabla V \cdot j_n &= 0, && (2.77) \end{aligned}$$

$$\begin{aligned} j_n &= -\nabla \cdot \Pi - n\nabla V, && (2.78)\\ j_{\mathcal{W}} &= -\nabla \cdot \mathbb{Q} - (\mathcal{W}\mathrm{Id} + \Pi) \cdot \nabla V + \frac{\hbar^2}{8} n \nabla(\Delta V), && (2.79) \end{aligned}$$

avec

$$\begin{pmatrix} n \\ \mathcal{W} \end{pmatrix} = \int w^{eq}_{n,\mathcal{W}} \begin{pmatrix} 1 \\ \frac{|p|^2}{2} \end{pmatrix} \frac{dp}{(2\pi\hbar)^3} \qquad (2.80)$$

et

$$\Pi = \int w^{eq}_{n,\mathcal{W}}(p \otimes p)\frac{dp}{(2\pi\hbar)^3}, \tag{2.81}$$

$$\mathbb{Q} = \int w^{eq}_{n,\mathcal{W}}(p \otimes p)\frac{|p|^2}{2}\frac{dp}{(2\pi\hbar)^3}. \tag{2.82}$$

Et enfin, le modèle de **Dérive-Diffusion Quantique**:

$$\partial_t n + \nabla \cdot j = 0, \tag{2.83}$$

$$j = -\nabla \cdot \Pi - n\nabla V, \tag{2.84}$$

avec

$$n = \int w^{eq}_n \frac{dp}{(2\pi\hbar)^3} \tag{2.85}$$

et

$$\Pi = \int w^{eq}_n (p \otimes p)\frac{dp}{(2\pi\hbar)^3}. \tag{2.86}$$

Notons que pour le modèle QDD, le terme $\nabla\cdot\Pi$ a été simplifié dans [12] en utilisant des calculs de commutateurs et il a été possible de l'écrire sous la forme $\nabla\cdot\Pi = -n\nabla A$, permettant d'écrire le courant sous la forme simplifiée:

$$j = n\nabla(A - V). \tag{2.87}$$

Cette remarque n'est pas anodyne car cette simplification a grandement facilité l'approche numérique (voir les chapitres I, II et III) concernant le modèle QDD. Par la suite, nous avons essayé de simplifier de la même manière les flux qui interviennent dans les autres modèles, cela a été possible pour le modèle d'Euler Quantique isotherme (voir le chapitre IV), mais la tâche a été plus difficile concernant les modèles non isothermes comme les modèles QHD et QET (voir le chapitre V).

2.2.5 Limite semi-classique

On sait depuis Madelung [26] que l'équation de Schrödinger 2.41 peut s'exprimer de manière équivalente avec une formulation fluide en utilisant la transformée de Madelung. Cela consiste à écrire la fonction d'onde dans sa forme WKB $\psi = \sqrt{n}e^{i\frac{S}{\hbar}}$ où n est la densité et S est la phase. En insérant cet ansatz dans l'équation de Schrödinger et en prenant la partie réelle et le gradient de la partie imaginaire, on obtient le système de Madelung qui a pour inconnues la densité n et le courant $nu = n\nabla S$:

$$\partial_t n + \nabla \cdot nu = 0, \tag{2.88}$$

$$\partial_t(nu) + \nabla \cdot (nu \otimes u) + n\nabla(V + V_B) = 0, \tag{2.89}$$

$$V^B = -\frac{\hbar^2}{2}\frac{\Delta\sqrt{n}}{\sqrt{n}}. \tag{2.90}$$

Ces équations sont les équations d'Euler sans pression auxquelles est ajouté un potentiel quantique appelé potentiel de Bohm V^B.

Cependant, ce modèle n'est valable que pour une seule particule, donc il n'y a pas d'effets de collisions ni d'effets liés à la température. En ce sens, le système de

Madelung est un modèle à température nulle (on montre formellement dans le chapitre IV que la limite d'Euler quantique quand la température tend vers 0 est ce système de Madelung).

Une limite opposée consiste à regarder ce qu'il se passe lorsque la constante de Planck adimensionnée $\hbar$ tend vers 0. Cette limite s'appelle la limite semi-classique et elle a un intérêt mathématique mais aussi physique puisque dans beaucoup de situations (en chimie quantique ou dans la physique des semiconducteurs par exemple), la constante de Planck adimensionnée $\hbar$ est petite. Beaucoup de travaux ont été dédiés à cette limite semi-classique dont on peut citer [17, 27, 28, 40]. Dans le chapitre VI, on propose des schémas asymptotiquement stables pour discrétiser le système de Madelung.

On peut aussi se demander ce qu'il se passe quand $\hbar$ tend vers 0 dans les modèles fluides quantiques étudiés dans cette thèse. Lorsqu'on choisit l'entropie quantique de Boltzmann $s(\varrho) = \varrho(\log \varrho - 1)$, l'équilibre local quantique $w^{eq}_{n,nu,\mathcal{W}}$ défini pour le modèle QHD dans la section 2.2.3 prend la forme (on l'appelle alors Maxwellienne quantique):

$$\mathcal{M}_{n,nu,\mathcal{W}} = \mathcal{E}\mathrm{xp}\left(-\frac{1}{2C}(p-B)^2 - A\right), \tag{2.91}$$

où l'exponentielle quantique d'un symbole $a(x,p)$ est définie comme $\mathcal{E}\mathrm{xp}(a)(x,p) = W(\exp W^{-1}(a(x,p)))$.

Il a été démontré dans [11] que l'on a formellement $\mathcal{E}\mathrm{xp}(a) \xrightarrow[\hbar\to 0]{} \exp(a)$. La Maxwellienne quantique tend donc vers la Maxwellienne classique et le modèle QHD converge donc vers le modèle d'hydrodynamique classique. Il est important de remarquer que la relation entre (A,B,C) et $(n,nu,\mathcal{W})$ n'est pas locale en espace dans le cas quantique contrairement au cas classique où l'on a tout simplement

$$A = -\log(n) + \frac{3}{2}\log\left(\frac{T}{2\pi\hbar^2}\right) \quad , \quad B = u \quad , \quad C = T \quad , \quad \mathcal{W} = \frac{1}{2}n|u|^2 + \frac{3}{2}nT. \tag{2.92}$$

De même, les autres modèles fluides quantiques étudiés dans cette thèse tendent vers leurs homologues classiques.

Par ailleurs, en utilisant du calcul pseudodifferentiel, il est possible de faire un développement limité de $\mathcal{E}\mathrm{xp}$ en puissances de $\hbar$ [11] et lorsqu'on garde les termes en $\hbar^2$, on trouve des modèles intermédiaires qui ne sont rien d'autres que les modèles classiques avec des corrections quantiques. Pour le modèle de dérive-diffusion quantique, on retrouve par exemple un modèle qui a beaucoup été étudié ces dernières années [2, 1, 36, 22, 5] et qui s'appelle Density Gradient. Ce modèle est constitué des équations de Dérive-Diffusion classique auxquelles on rajoute un potentiel qui n'est autre que $\frac{1}{3}V_B$.

3 Application au transport d'électrons dans les semiconducteurs

On peut penser à plusieurs domaines d'application des modèles fluides quantiques comme la chimie quantique [3], l'optique quantique, l'étude de la superfluidité, et surtout la modélisation du transport d'électrons dans les semiconducteurs. De nombreux ouvrages existent pour introduire la physique des semiconducteurs, on réfère par exemple à [41] pour une explication détaillée.

3.1 Quelques généralités sur les semiconducteurs

Un semiconducteur est un cristal (solide composé d'atomes arrangés de manière périodiques) dont la conductivité électrique se situe entre celle d'un conducteur et d'un isolant (on peut citer les 3 plus importants semiconducteurs que sont le germanium (Ge), le silicium (Si) et l'arséniure de gallium (GaAs)). Ce réseau cristallin crée un potentiel périodique V^{per} dont la période est de l'ordre de la taille d'une cellule du réseau L_{per} (typiquement de l'ordre de $10^{-10}m$). Dans cette thèse, on se place dans l'approximation de la masse effective, c'est à dire que si l'on considère un dispositif de taille caractéristique L avec $L_{per} << L$, on peut alors "oublier" le potentiel périodique à condition de remplacer la masse de l'électron m par sa masse effective m^*.

Par ailleurs, le réseau cristallin d'un semiconducteur n'est en général pas parfait. Il y a un grand nombre de sources d'imperfections mais la plus importante vient de la présence d'impuretés que sont d'autres atomes ou ions avec lesquels les électrons vont interagir. D'autre part, le réseau cristallin n'est pas fixe mais vibre. Ces vibrations peuvent être modélisées à l'aide de pseudoparticules que l'on appelle phonons et qui interagissent eux aussi avec les électrons. Ces interactions peuvent être modélisées au niveau cinétique grâce à des opérateurs de collision.

3.2 Domaine de validité des modèles fluides quantiques

L'utilisation des modèles fluides quantiques étudiés dans cette thèse est réservée à un domaine bien précis. Le dispositif que l'on veut modéliser doit être suffisamment petit pour que les effets quantiques soient importants, mais il doit par ailleurs être suffisamment grand pour que les collisions soient importantes et que le régime soit fluide. Essayons de préciser un peu ce domaine de validité. Lors de l'adimensionnement des équations de Wigner-Boltzmann (voir le scaling dans la sous-section 2.1.2), nous avons choisi deux valeurs de référence que sont la température T_0 et la longueur caractéristique du dispositif L.

Par ailleurs, deux paramètres adimensionnels apparaissent naturellement lors de la dérivation des modèles fluides quantiques: le temps de relaxation adimensionné ε qui mesure si l'ensemble de particules peut être décrit de manière fluide et la constante de Planck adimensionnée $\tilde{\hbar}$ (notée $\hbar$ dans cette thèse pour des raisons de simplicité) qui mesure l'importance des phénomènes quantiques. On rappelle qu'on a:

$$\begin{aligned} \varepsilon &= \tau\sqrt{\frac{k_B T_0}{mL^2}}, \\ \tilde{\hbar} &= \frac{\hbar}{\sqrt{m k_B T_0 L^2}}. \end{aligned}$$

On a donc

$$\tilde{\hbar} \sim L^{-1} T_0^{-1/2}. \tag{3.93}$$

D'autre part, le temps de relaxation τ qui apparaît dans le paramètre ε peut être déduit à partir de la mobilité des électrons grâce à la formule:

$$\tau = \frac{m^* \mu}{e}.$$

Pour les collisions avec les phonons, on a [41]

$$\mu_l \sim T_0^{-3/2}$$

et pour les collisions avec les impuretés, on a

$$\mu_i \sim T_0^{3/2}.$$

La mobilité combinée des deux type de collisions est donnée par

$$\mu = \left(\frac{1}{\mu_l} + \frac{1}{\mu_i}\right)^{-1}.$$

Pour l'arséniure de Gallium (GaAs), cette mobilité peut être approximée par $\mu \sim T_0^{1/2}$, ce qui nous donne

$$\varepsilon \sim L^{-1} T_0. \tag{3.94}$$

On en déduit dans la figure 2 les zones, en fonction de L et T_0 où l'on peut appliquer les modèles fluides quantiques. On devrait aussi partager par une ligne verticale les zones

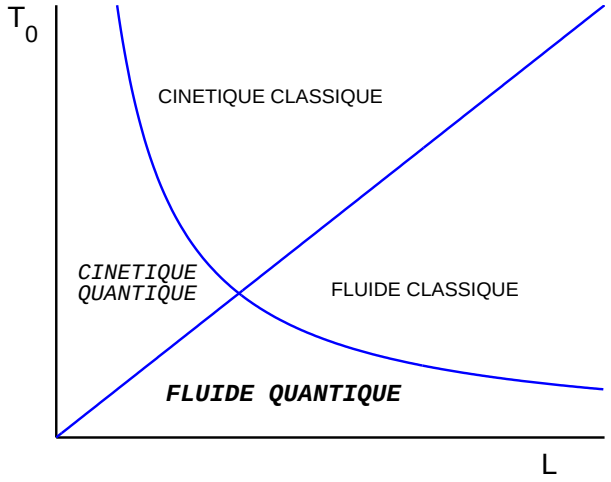

Figure 2: Domaine de validité des modèles fluides quantiques.

pour lesquelles l'approximation de la masse effective est valable (quand $\frac{L_{per}}{L} << 1$) ou non. La zone où les modèles fluides quantiques sont applicables est donc la zone qui se situe en bas à droite de ce graphique, lorsqu'on regarde un dispositif relativement petit à basse température.

3.3 Couplage à l'équation de Poisson

Pour l'instant, nous n'avons pas précisé comment le potentiel électrique V est déterminé. Ce potentiel peut provenir d'une différence de potentiel appliquée dans certaines zones de contact du semiconducteur, ou de l'emploi de différents matériaux à l'intérieur même du dispositif, et nous noterons ce potentiel extérieur V^{ext}. Par ailleurs, les électrons étant des particules chargées, ils interagissent avec eux même et les ions dopeurs éventuellement présents dans le semiconducteur. Ils créent ainsi un potentiel auto-consistant noté V^s et qui est solution de l'équation de Poisson:

$$-\varepsilon_0 \varepsilon_r \Delta V^s = e(n - n^d),$$

où n^d est la densité des ions dopants, e est la charge de l'électron et ε_0 et ε_r sont respectivement la permittivité du vide et la permittivité relative. Avec le même scaling

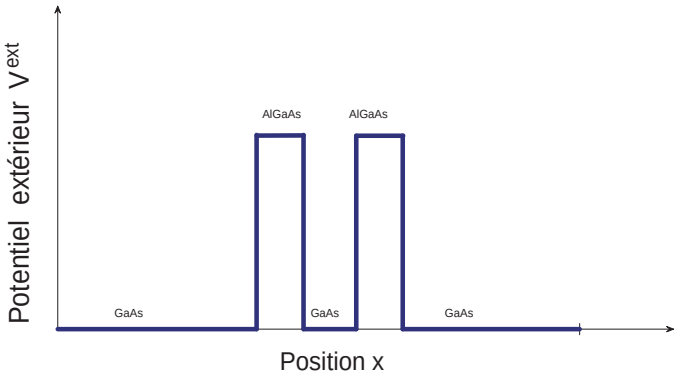

Figure 3: Double barrière de potentiel dans une diode à effet tunnel résonnant.

que celui proposé dans la sous-section 2.1.2, et en prenant pour densité de référence $\overline{n} = \sup n^d$ on obtient l'équation de Poisson adimensionnée:

$$-\alpha^2 \Delta V^s = n - n^d, \tag{3.95}$$

où $\alpha = \sqrt{\frac{\varepsilon_r \varepsilon_0 k_B T}{e^2 L^2 \overline{n}}} = \frac{\lambda_D}{L}$ avec λ_D la longueur caractéristique de Debye. Le paramètre adimensionnel α mesure donc les effets de charge d'espace.

3.4 La diode à effet tunnel résonnant

La diode à effet tunnel résonnant (en anglais "Resonant Tunneling Diode" ou RTD) a beaucoup été étudiée ces dernières années grâce à ses caractéristiques courant-tension non linéaires [7]. Ce dispositif montre en effet une résistance négative dans certaines plages de différence de potentiel qu'on lui applique, ce qui est intéressant pour beaucoup d'applications en logique électronique notamment. La diode est composée de deux réseaux cristallins: par exemple d'Arséniure de Gallium (GaAs) et de deux fines bandes d'Arséniure de Gallium et d'Aluminium (AlGaAs) qui créent une double barrière de potentiel dû au saut des bandes de conduction entre les deux matériaux (cf figure 3). A l'intérieur de cette double barrière, certains niveaux discrets d'énergie résonnante apparaissent et seuls les électrons avec une énergie proche de celle-ci peuvent passer la double barrière par effet tunnel. Appliquer une différence de potentiel aux bornes de la diode modifie l'énergie des électrons et c'est pourquoi augmenter la tension appliquée peut diminuer le courant. La taille de ces dispositifs ainsi que la possibilité de les simuler à l'aide de modèles 1D en font un très bon candidat pour tester les schémas numériques sur les modèles fluides quantiques développés dans cette thèse.

Nous allons maintenant présenter les résultats originaux que nous avons obtenus dans cette thèse.

4 Présentation des résultats

4.1 Chapitre I: Entropic discretization of the Quantum Drift-Diffusion model

Ce chapitre a pour but de proposer une discrétisation du modèle QDD (2.83)–(2.86) couplé à l'équation de Poisson (3.95) sur un domaine borné Ω avec des conditions fermées. Lors de la dérivation, on a choisi une entropie de Boltzmann de sorte que le modèle s'écrit:

$$\partial_t n + \nabla \cdot j = 0, \tag{4.96}$$
$$j = n\nabla(A - V), \tag{4.97}$$
$$-\alpha^2 \Delta V = n, \tag{4.98}$$
$$n = \int w_n^{eq} \frac{dp}{(2\pi\hbar)^3} = \int \mathcal{E}\mathrm{xp}\left(-\frac{p^2}{2} - A - V_{ext}\right) \frac{dp}{(2\pi\hbar)^3}. \tag{4.99}$$

Dans ce modèle, on appelle A le potentiel chimique quantique et on suppose que l'opérateur $H(A) = W\left(\frac{p^2}{2} + A + V^{ext}\right) = -\frac{\hbar^2}{2}\Delta + A + V^{ext}$ a un spectre discret de sorte que le lien entre n et A est donné par:

$$n = \sum_{p\geq 1} e^{-\lambda_p(A)} |\psi_p(A)|^2, \tag{4.100}$$

où $(\lambda_p(A), \psi_p(A))$ sont les éléments propres de $H(A)$. Pour des raisons de simplicité, on choisit le dopage n^d égal à zéro et pour des raisons techniques, on a choisi d'inclure le potentiel extérieur V^{ext} dans $H(A)$ plutôt que dans (4.97). Nous avons choisi pour conditions aux bords (la normale unitaire sortante est notée $\nu(x)$):

$$\nabla(A - V) \cdot \nu = 0, \quad V = 0, \quad \nabla\psi_p \cdot \nu = 0 \quad (\forall p \in \mathbb{N}) \qquad \text{sur } \partial\Omega.$$

Dans un premier temps on étudie un système semi-discrétisé. Soit $\Delta t > 0$ et $t^k = k\Delta t$ pour $k \in \mathbb{N}$. On introduit le système semi-discrétisé implicite suivant:

$$\frac{n^{k+1} - n^k}{\Delta t} + \nabla \cdot \left(n^k \nabla(A^{k+1} - V^{k+1})\right) = 0, \tag{4.101}$$
$$-\alpha^2 \Delta V^{k+1} = n^{k+1}, \tag{4.102}$$
$$n^{k+1} = \sum_p e^{-\lambda_p(A^{k+1})} |\psi_p(A^{k+1})|^2. \tag{4.103}$$

On démontre dans le théorème 3.1 que ce système est bien posé. En effet, on peut démontrer que ces trois équations sont exactement les équations d'Euler-Lagrange d'une fonctionnelle J définie comme suit. Soit n^k une fonction continue et strictement positive sur $\overline{\Omega}$. Pour tout $A \in H^1(\Omega), V \in H_0^1(\Omega)$, on pose:

$$J(A, V) = \frac{\Delta t}{2} \int n^k \left|\nabla(A - V)\right|^2 dx + \frac{\alpha^2}{2} \int |\nabla V|^2 \, dx + \sum_{p\geq 1} e^{-\lambda_p(A)} + \int n^k \, (A - V) \, dx.$$

Inspiré par les travaux de Nier [34], on peut montrer que cette fonctionnelle est strictement convexe et coercive ce qui démontre l'existence d'un unique couple minimiseur de J, et donc que l'on peut passer de manière unique de l'instant t^k à t^{k+1}. Nous

avons aussi démontré que ce système semi-discret conserve la masse et qu'il vérifie la même propriété de dissipation d'entropie que le modèle continu.

Dans un deuxième temps, on étudie le système complètement discrétisé (la variable d'espace est discrétisée par différences finies). Nous avons effectué une analyse numérique de ce schéma et démontré que ce schéma a de bonnes propriétés (la stricte positivité de la densité est garantie pour tout temps, la charge totale dans le domaine est conservée et une énergie libre discrète est décroissante au cours du temps). Comme pour le système semi-discret en temps, ce schéma numérique est complètement équivalent à la résolution d'un problème de minimisation convexe. Nous nous sommes appuyés sur cette propriété pour l'implémenter, via une méthode de Newton qui présente de bonnes propriétés de convergence. Par ailleurs, l'implémentation de ce schéma passe par la résolution de problèmes aux valeurs propres, dont la taille des matrices est la même que la grille spatiale. En réalité, il n'est pas nécessaire de calculer tous les éléments propres mais grâce à la statistique de Boltzmann en exponentielle, seules les valeurs propres les plus petites ont une contribution significative. Dans le programme, nous évaluons le nombre de valeurs propres à calculer (grâce à la formule de Weyl), et nous contrôlons a posteriori les approximations faites ainsi. Enfin, toutes les propriétés du schéma sont vérifiées par quelques illustrations numériques sur une diode à effet tunnel simplifiée.

Il convient à présent de tester ce modèle sur des cas tests physiques ainsi que de le comparer à des modèles existants, et pour cela il faut autoriser le passage d'un flux aux bords du domaine, c'est l'objet du chapitre II.

4.2 Chapitre II: An entropic Quantum Drift-Diffusion model for electron transport in resonant tunneling diodes

Ce chapitre a pour but de proposer une discrétisation du modèle QDD (2.83)–(2.86) couplé à l'équation de Poisson (3.95) sur un domaine borné Ω avec des conditions ouvertes et fermées, de tester le comportement du modèle sur un test physique, et de comparer le modèle avec d'autres modèles existants. Lors de la dérivation, on a choisi une entropie de Boltzmann de sorte que le modèle s'écrit (la dérivation est effectuée dans le formalisme des opérateurs dans l'appendice A):

$$\partial_t n + \nabla \cdot j = 0, \tag{4.104}$$

$$j = n\nabla(A - (V_s + V_{ext})), \tag{4.105}$$

$$-\alpha^2 \Delta V_s = n - n^d, \tag{4.106}$$

$$n = \int w_n^{eq} \frac{dp}{(2\pi\hbar)^3} = \int \mathcal{E} \exp\left(-\frac{p^2}{2} - A\right) \frac{dp}{(2\pi\hbar)^3}. \tag{4.107}$$

On suppose ici aussi que l'opérateur $H(A) = W\left(\frac{p^2}{2} + A\right) = -\frac{\hbar^2}{2}\Delta + A$ a un spectre discret de sorte que le lien entre n et A est donné par:

$$n = \sum_{p \geq 1} e^{-\lambda_p(A)} |\psi_p(A)|^2, \tag{4.108}$$

où $(\lambda_p(A), \psi_p(A))$ sont les éléments propres de $H(A)$.

Pour ne pas annuler la densité au bord et donc pour autoriser un flux d'électrons sur le bord $\partial\Omega$, on choisit des conditions de Neumann sur les fonctions propres

$$\forall p \geq 1 \quad \nabla\psi_p \cdot \nu = 0.$$

Par ailleurs, concernant les autres conditions aux bords, on propose deux types de conditions différentes:

- Des conditions isolantes en mettant des conditions de Neumann sur le potentiel électrochimique:
$$\nabla(A - (V_s + V_{ext})) \cdot \nu = 0 \quad \text{sur } \partial\Omega.$$
- Des conditions ouvertes en mettant des conditions de Dirichlet sur la densité:
$$n = \sum_{p \geq 1} e^{-\lambda_p(A)} |\psi_p(A)|^2 = n^d \quad \text{sur } \partial\Omega.$$

On propose un schéma semi-implicite en temps dont la variable d'espace est discrétisée par différence-finies. Ce schéma est résolu par la méthode de Newton. On s'assure que le schéma proposé vérifie bien numériquement certaines propriétés physiques du modèle, comme le fait que pour les systèmes fermés, l'énergie libre quantique décroît en fonction du temps et que la masse est bien conservée.

On montre par ailleurs que notre modèle est capable de capturer le comportement de la diode à effet tunnel résonnant. En effet, on montre que le modèle QDD peut produire des caractéristiques courant-tension ayant une résistance négative. Un paramètre qui semble avoir beaucoup d'influence sur la forme de ces caractéristiques est la masse effective des électrons. C'est pourquoi pour analyser un peu plus en détails cette influence, on a proposé un schéma où la masse effective est variable et il ressort que c'est la valeur de la masse effective à l'intérieur des doubles barrières qui a le plus d'importance, et c'est malheureusement là où l'approximation de la masse effective est la moins appropriée, puisque la taille d'une barrière n'est que de 50 Å, ce qui est de l'ordre de quelques mailles du réseau cristallin seulement.

On compare enfin notre modèle avec des modèles existant dans la littérature et qui ont un lien étroit avec le modèle QDD. Tout d'abord, le modèle de dérive-diffusion classique [31] et le modèle Density-Gradient (DG) [2, 1, 36, 22, 5] sont reliés au modèle QDD grâce à la limite semi-classique ($\hbar \to 0$). On montre que les modèles QDD et DG se comportent qualitativement de la même manière mais leurs résultats quantitatifs sont étonnamment éloignés, même pour des constantes de Planck adimensionnées $\hbar$ très faibles. Ce résultat peut s'expliquer par le fait que la limite semi-classique est obtenue pour des potentiels chimiques A très réguliers et que les hétérojonctions présentes dans la RTD créent des discontinuités qui faussent cette approximation. Remarquons au passage que les schémas numériques proposés dans ce chapitre concernant les modèles CDD et DG sont inspirés de la discrétisation du modèle QDD et sont originaux à notre connaissance. Le fait de choisir comme inconnue le logarithme de la densité et non la densité a pour avantage de garantir la positivité de la densité dans ces schémas.

Les modèles Schrödinger-Poisson Drift-Diffusion (SPDD) [37, 9] et Schrödinger-Poisson (SP) [34] sont reliés au modèle QDD en ce sens que les états stationnaires de QDD sont solutions de SP et que proche de cet équilibre, le potentiel électrochimique étant presque constant, on peut montrer que les modèles QDD et SPDD sont proches. Cette propriété est vérifiée une fois de plus numériquement.

Le modèle QDD semble donc être un bon candidat pour modéliser le transport diffusif dans les semiconducteurs, la prochaine étape est d'incorporer au modèle QDD un spectre continu pour l'Hamiltonien $H(A)$ en considérant des conditions transparentes sur les fonctions d'ondes, c'est l'objet du chapitre III.

4.3 Chapitre III: Transparent boundary conditions for the Quantum Drift-Diffusion model

Ce chapitre a pour but de prendre en compte des conditions transparentes pour le modèle de Dérive-Diffusion Quantique (QDD) couplé à l'équation de Poisson. Nous rappelons que pour le modèle QDD étudié dans les chapitres I et II, la matrice densité de l'équilibre local s'écrit comme une Maxwellienne quantique:

$$\varrho = \exp(-H(A)), \tag{4.109}$$

où $H(A)$ est l'Hamiltonien modifié suivant:

$$H(A) = -\frac{\hbar^2}{2}\Delta + A, \tag{4.110}$$

et où contrairement à l'Hamiltonien présent dans l'équation de Schrödinger, le potentiel chimique quantique A remplace le potentiel électrique V.

Dans les deux premiers chapitres et comme première approximation, on a considéré que le spectre de l'Hamiltonien $H(A)$ était discret (notons $(\lambda_k, \psi_k)_{k\in\mathbb{N}}$ les éléments propres) en mettant des conditions aux bords de type Neumann sur les fonctions propres ψ_k. Remarquons que pour le système de Schrödinger-Poisson étudié par exemple dans [35], de telles conditions annulent le courant qui est défini de manière microscopique par $j = \sum_k e^{-\lambda'_k} \mathcal{I}m\left(\overline{\psi'_k}\nabla\psi'_k\right)$ où $(\lambda'_k, \psi'_k)_{k\in\mathbb{N}}$ sont les éléments propres de l'Hamiltonian $\mathcal{H} = -\frac{\hbar^2}{2}\Delta + V$. Dans notre cas, le courant est défini macroscopiquement par

$$j = n\nabla(A - V), \tag{4.111}$$

de telle manière que de telles conditions aux bords autorisent un flux d'électrons sur les bords du domaine.

Cependant, mettre de telles conditions aux bords sur un dispositif ouvert n'a pas vraiment de sens physique et peut créer des couches limites indésirables sur la densité. Une meilleure approximation serait de considérer des conditions aux bords transparentes pour le spectre de l'Hamiltonien $H(A)$. Pour cela, on se place en une dimension et on suppose que le transport dans les réservoirs est principalement classique et que le potentiel chimique quantique correspond au potentiel chimique classique et est égal à

$$A(x) = A_0 = \log(n_0) - \log(n_0^d) \tag{4.112}$$

où n_0^d est le densité des ions dopants à droite et à gauche du domaine $\Omega = [0, 1]$ et $n_0 = (2\pi\hbar^2)^{1/2}$ est la densité d'état.

On obtient alors ce type de conditions sur ψ_p:

$$\hbar\psi'_p(1) + ip\psi_p(1) = 2ip \quad ; \quad \hbar\psi'_p(0) = ip\psi_p(0) \quad \text{pour } p < 0, \tag{4.113}$$

$$\hbar\psi'_p(0) + ip\psi_p(0) = 2ip \quad ; \quad \hbar\psi'_p(1) = ip\psi_p(1) \quad \text{pour } p > 0, \tag{4.114}$$

où ψ_p est solution de

$$-\frac{\hbar^2}{2}\psi''_p + A\psi_p = (\frac{p^2}{2} + A_0)\psi_p. \tag{4.115}$$

Remarquons bien que nous n'avons plus à résoudre un problème aux valeurs propres mais que les ψ_p sont solutions d'une infinité ($p \in \mathbb{R}$) d'équations de type Schrödinger. Nous montrons numériquement qu'il est important de considérer le spectre discret

de l'Hamiltonien dont les valeurs propres sont inférieures à A_0 de telle sorte que la densité s'écrit en fait:

$$n = \int_{-\infty}^{\infty} e^{-E_p} |\psi_p|^2 \, \frac{dp}{2\pi\hbar} + \sum_{\lambda_k < A_0} e^{-\lambda_k} |\psi_k|^2. \tag{4.116}$$

Beaucoup de travaux ont été effectués pour prendre en compte le spectre continu dans l'équation de Schrödinger couplée à l'équation de Poisson (citons un des plus récents [35]) et le but de ce chapitre est d'adapter ce travail pour le modèle QDD couplé à l'équation de Poisson, aussi bien pour le modèle stationnaire que pour le modèle dépendant du temps.

Pour résoudre le système stationnaire on propose d'utiliser une méthode de Gummel [18] qui a largement prouvé son efficacité, et pour résoudre le système instationnaire, on propose d'utiliser l'algorithme de Newton. Pour utiliser un tel algorithme, on doit calculer la dérivée de la densité par rapport au potentiel chimique quantique A et donc la dérivée des fonctions propres généralisées. On utilise pour cela des outils de théorie du scattering [39] comme l'équation de Lippmann-Schwinger en restant à un niveau formel. Des simulations numériques préliminaires sont présentées sur une diode avec une seule barrière de potentiel et sur une diode à effet tunnel résonnant. Le premier cas test qui ne comporte pas de résonances permet de tester que les schémas proposés fonctionnent bien et que l'on retrouve les résultats du modèle stationnaire (en particulier la valeur du courant) en laissant évoluer le modèle dépendant du temps. Concernant le deuxième cas test, on montre des résultats numériques pour des différences de potentiels appliquées faibles. Pour des potentiels appliqués plus grands, notre programme n'est pour l'instant pas capable de capturer suffisamment bien les résonances de la RTD pour tracer des caractéristiques courant-tension mais la prise en compte d'un pas d'impulsion adaptatif [35] ainsi que l'implémentation du code en Fortran (au lieu de Matlab) devrait permettre dans le futur de remédier à cela.

4.4 Chapitre IV: Isothermal Quantum Euler: derivation, asymptotic analysis and simulation

Dans ce chapitre, on étudie le modèle d'Euler quantique isotherme (2.72)–(2.75) et on a trois buts. Premièrement, comme cela a été fait pour le modèle QDD, on veut reformuler le modèle d'Euler quantique isotherme sous forme plus simple (différentielle). Pour cela, on redérive le modèle dans le formalisme des opérateurs et on utilise des calculs de commutateurs. Considérant que l'opérateur $H(A,B) = W\left(\frac{1}{2}(p-B)^2 + A\right) = \frac{1}{2}\left(i\hbar\nabla + B\right)^2 + A$ a un spectre discret, on obtient le système suivant:

$$\partial_t n + \nabla \cdot nu = 0, \tag{4.117}$$

$$\partial_t (nu) + \nabla \cdot (nu \otimes B) + n(\nabla B) \cdot (u - B) + n\nabla(V - A) = 0, \tag{4.118}$$

où (n, nu) est relié à (A, B) grâce à l'équation constitutive:

$$n = \sum_{p\in\mathbb{N}} (s')^{-1}\left(-\frac{\lambda_p}{T}\right) |\psi_p|^2, \qquad nu = \sum_{p\in\mathbb{N}} (s')^{-1}\left(-\frac{\lambda_p}{T}\right) \mathcal{I}m\left(\hbar\nabla\psi_p\,\overline{\psi_p}\right), \tag{4.119}$$

et où $(\lambda_p, \psi_p)_{p\in\mathbb{N}}$ sont les valeurs propres et les fonctions propres de l'Hamiltonien $H(A,B)$ (Comme on veut faire dans ce chapitre une limite à température nulle, on fait apparaître la température adimensionnée T dans ce modèle).

On montre par ailleurs plusieurs propriétés du modèle qui reposent sur une propriété d'invariance de jauge, ce qui permet d'écrire de grosses simplifications pour le modèle irrotationnel qui s'écrit (voir la proposition 2.8):

$$\partial_t n + \nabla \cdot nu = 0, \tag{4.120}$$
$$\partial_t (nu) + \nabla \cdot (nu \otimes u) + n\nabla(V - A) = 0, \tag{4.121}$$

où n est relié à A grâce à l'équation constitutive:

$$n = \sum_{p\in\mathbb{N}} (s')^{-1}\left(-\frac{\lambda_p}{T}\right) |\psi_p|^2, \tag{4.122}$$

et où $(\lambda_p, \psi_p)_{p\in\mathbb{N}}$ sont les valeurs propres et les fonctions propres de l'Hamiltonien $H(A,0) = -\frac{\hbar^2}{2}\Delta + A$. Cette propriété est intéressante car on démontre que si un fluide est irrotationnel au temps 0, alors il reste irrotationnel pour tout temps. Dans ce cas là, on fait donc disparaître l'inconnue B. Cette simplification est applicable au modèle en une dimension (par définition irrotationnel) ce qui facilitera grandement la création d'un schéma numérique par la suite.

Deuxièmement, on effectue plusieurs limites asymptotiques sur le modèle pour faire des liens avec des modèles existants: le modèle d'Euler isotherme en effectuant la limite semi-classique (on retrouve par ailleurs un modèle obtenu par Jüngel et Matthes [20] en gardant les termes en $\hbar^2$), le système de Madelung en effectuant la limite à température nulle et le modèle QDD en effectuant une limite diffusive. Cela montre l'intérêt du modèle d'Euler quantique qui crée un véritable pont entre les équations d'Euler classiques et l'équation de Schrödinger.

Troisièmement, on présente des simulations numériques préliminaires sur une diode à effet tunnel simplifiée, en prenant une statistique de Boltzmann et des conditions aux bords isolantes (on couple par ailleurs le modèle à l'équation de Poisson). Grâce aux simplifications obtenues pour les modèles irrotationnels, le problème de minimisation sous-jacent relie A à n comme pour le modèle QDD et le schéma proposé s'inspire grandement des schémas utilisés pour le modèle QDD dans les chapitres I et II.

Ces résultats concernant le modèle d'Euler quantiques sont prometteurs et nécessiteront une validation numérique plus poussée comme il a été fait au chapitre II pour QDD. Grâce aux simplifications obtenues pour le modèle 1D, on peut aussi imaginer qu'il sera relativement facile de rajouter le spectre continu de l'Hamiltonien $H(A)$ en considérant des conditions transparentes pour modéliser un système ouvert. Mais avant de faire cela, nous avons choisi d'étudier les modèles non isothermes, à savoir les modèles QHD et QET.

4.5 Chapitre V: On Quantum Hydrodynamic and Quantum Energy Transport Models

Le but de ce chapitre est d'étudier les modèles QHD (2.66)–(2.71) et QET (2.76)–(2.82) et d'essayer de les simplifier en vue d'une future discrétisation.

Tout d'abord, deux lemmes préliminaires nous donnent deux formules originales qui vont être utiles par la suite. La première formule (lemme 3.2) nous permet d'écrire, pour un équilibre local qui s'écrit $\varrho^{eq} = (s')^{-1}(-H)$ avec H un opérateur à spectre discret, ses moments ainsi que les dérivées de ses moments en fonction du spectre de H. En effet, soit $\alpha = (\alpha_1, \alpha_2, \alpha_3) \in \mathbb{N}^3$ et $\eta = (\eta_1, \eta_2, \eta_3) \in \mathbb{N}^3$ deux multi-indices, on

a (voir le lemme 3.1 pour les notations):

$$\partial_x^\eta \int p^\alpha W\left(\varrho^{eq}\right) \frac{dp}{(2\pi\hbar)^3} = (-i\hbar)^{|\alpha|} \sum_{p\in\mathbb{N}} (s')^{-1}(-\lambda_p) \times$$
$$\sum_{0\le\gamma\le\alpha} \begin{pmatrix} \alpha \\ \gamma \end{pmatrix} \left(-\frac{1}{2}\right)^{|\gamma|} \sum_{0\le\xi\le\gamma+\eta} \begin{pmatrix} \gamma+\eta \\ \xi \end{pmatrix} \left(\partial_x^{\alpha-\gamma+\xi}\psi_p\right) \left(\partial_x^{\gamma+\eta-\xi}\overline{\psi_p}\right). \quad (4.123)$$

Cette formule nous permet (dans les lemmes 4.1 et 5.1) d'écrire toutes les quantités qui apparaissent dans les modèles QHD et QET en fonction du spectre des Hamiltoniens

$$H(A,B,C) = W^{-1}\left(\frac{1}{2C}(p-B)^2 + A\right)$$
$$= -\hbar^2\left(\nabla\cdot(\frac{1}{2C}\nabla) + \frac{1}{4}\Delta\frac{1}{2C}\right) + i\hbar\left(\frac{B}{C}\cdot\nabla + \frac{1}{2}(\nabla\cdot\frac{B}{C})\right) + A + \frac{B^2}{2C} \quad (4.124)$$

et

$$\begin{aligned} H(A,0,C) &= W^{-1}\left(\frac{p^2}{2C} + A\right) \\ &= -\hbar^2\left(\nabla\cdot(\frac{1}{2C}\nabla) + \frac{1}{4}\Delta\frac{1}{2C}\right) + A. \end{aligned} \quad (4.125)$$

La deuxième formule (qui se trouve dans le lemme 3.4) nous permet quant à elle d'écrire une formule sur les commutateurs de deux opérateurs dont les symboles sont de la forme λp^α et μp^β, avec $\alpha = (\alpha_1,\alpha_2,\alpha_3) \in \mathbb{N}^3$ et $\beta = (\beta_1,\beta_2,\beta_3) \in \mathbb{N}^3$ deux multi-indices, $\lambda(x)$ et $\mu(x)$ étant deux fonctions régulières à valeur réelle ou complexe. En effet, si on note $[\lambda p^\alpha, \mu p^\beta]_\hbar$ le symbole associé aux commutateurs de $W^{-1}(\lambda p^\alpha)$ et $W^{-1}(\mu p^\beta)$, *i.e.* :

$$[\lambda p^\alpha, \mu p^\beta]_\hbar = W\left(\left[W^{-1}\left(\lambda p^\alpha\right), W^{-1}\left(\mu p^\beta\right)\right]\right), \quad (4.126)$$

on a la formule suivante:

$$[\lambda p^\alpha, \mu p^\beta]_\hbar = \sum_{k=0}^{\lfloor(|\alpha+\beta|-1)/2\rfloor} \hbar^{2k+1}[\lambda p^\alpha, \mu p^\beta]_{2k+1}, \quad (4.127)$$

avec

$$[\lambda p^\alpha, \mu p^\beta]_{2k+1} = i\left(-\frac{1}{4}\right)^k \sum_{\substack{0\le\gamma\le\alpha,\, 0\le\zeta\le\beta \\ |\gamma+\zeta|=2k+1}} (-1)^{|\gamma|} \begin{pmatrix} \alpha \\ \gamma \end{pmatrix} \begin{pmatrix} \beta \\ \zeta \end{pmatrix} \left(\partial_x^\zeta\lambda\right)\left(\partial_x^\gamma\mu\right) p^{\alpha+\beta-\gamma-\zeta}. \quad (4.128)$$

Cette formule est la base des théorèmes 4.2 et 5.2 qui donnent des contraintes différentielles qui lient les moments $(n, nu, \mathcal{W}, \Pi, \Phi, \mathbb{Q})$ aux quantités (A,B,C). Malheureusement, il n'est pas possible de sortir de ces contraintes des relations sur $\nabla\cdot\Pi, \nabla\cdot\Phi$ et $\nabla\cdot\mathbb{Q}$ pour simplifier les modèles comme il a été fait pour les modèles isothermes, même en supposant la température faiblement variable. En revanche, pour les modèles en une dimension, on peut écrire des modèles simplifiés, ce qui devrait faciliter

l'écriture de schémas numériques 1D. Notons que les simplifications pour le modèle QHD proviennent encore d'une invariance de jauge et nous permettent de nous débarrasser pour le modèle irrotationnel de l'inconnue B mais aussi du flux d'énergie Φ, et l'équilibre local s'écrit alors comme celui de QET. En revanche, on voit apparaître un terme dispersif $-\frac{\hbar^2}{8}\nabla\cdot(n\Delta u)$ dans l'équation sur l'énergie. Ce terme apparaît dans plusieurs autres modèles hydrodynamiques incluant des corrections quantiques en $\hbar^2$ [15, 16, 21]. Il a été noté dans [21] que ce terme semble stabiliser les schémas numériques.

4.6 Chapitre VI: An asymptotic preserving scheme for the Schrödinger equation in the semiclassical limit.

Le but de ce chapitre est d'écrire un schéma numérique asymptotiquement stable pour la limite semi-classique sur la formulation fluide de l'équation de Schrödinger, à savoir le système de Madelung (2.88)–(2.90). Ce système consiste en un modèle d'Euler sans pression où un terme quantique additionnel est ajouté: le potentiel de Bohm. Ces équations sont non linéaires contrairement à l'équation de Schrödinger mais leur avantage est que les inconnues macroscopiques ne développent pas d'oscillations d'ordre ε (dans ce chapitre, ε est la constante de Planck adimensionnée), ce qui est le cas de la fonction d'onde dans la formulation de Schrödinger. Ceci est un avantage sérieux dans la limite semi-classique où ε tend vers 0. Différentes stratégies de maillage ont été adoptées dans plusieurs articles sur des schémas pour l'équation de Schrödinger [29, 30, 3] mais même la meilleure méthode nécessite de prendre pour pas d'espace et de temps $\Delta x = o(\varepsilon)$ et $\Delta t = O(\varepsilon)$. Plus proche de cette note et en chimie quantique, des méthodes particulaires dans une formulation lagrangienne ont été employées pour résoudre le système de Madelung [6, 43].

Dans ce chapitre, nous proposons d'utiliser un schéma semi-implicite qui a le même coût que le schéma explicite pour résoudre le système de Madelung en formulation eulerienne et lagrangienne. Pour un potentiel extérieur nul, l'analyse du schéma pour le système linéarisé autour d'une densité constante et d'un courant nul montre qu'un critère de stabilité est donné par $\Delta t < \frac{\Delta x^2}{\varepsilon\pi^2}$. Pour palier l'hypothèse de faible courant et au vu de la même analyse linéaire, le système de Madelung en coordonnées lagrangiennes est discrétisé de manière analogue.

Les résultats numériques pour le schéma en formulation eulerienne et lagrangienne avec des potentiels extérieurs constants nous confirment que les schémas sont asymptotiquement stables et que pour un pas d'espace Δx fixé, on peut augmenter le pas de temps comme $1/\varepsilon$. L'inconvénient de ces schémas réside dans leur instabilité lorsque la densité est très proche de zéro. Par ailleurs le schéma en formulation eulerienne est instable lorsque le courant est trop fort alors que le schéma en formulation lagrangienne dont les coordonnées bougent avec le fluide reste stable. L'étude de problèmes plus complexes faisant intervenir l'apparition de caustiques et/ou faisant intervenir des potentiels extérieurs non constants est en cours.

General introduction (english version)

In this thesis, we are interested in some very special particle transport models: the quantum fluid models based on the entropy minimization principle. In this introduction, we are going to give first some motivations for studying such models, then we will remind how the models have been derived and for this purpose, we will summarize articles [14, 11, 12] which are the foundations of this thesis subject. Finally, we will introduce some notions on semiconductors which constitute a possible field of application of these models.

1 Motivations

Physics being not unified yet, there does not exist a universal theory which would allow to describe any particle system. Instead there exists some different theories which apply in certain particular domains. For instance, classical mechanics developed during the 17^{th} century by Newton is applicable only for particles with small velocities v compared to the speed of light c. Moreover, classical mechanics is only useful at relatively large space scales. In order to describe correctly particles with very high velocities, one should use relativistic mechanics developed by Einstein at the beginning of the 20^{th} century, and for very small space scales, one should use quantum mechanics developed by Bohr, Dirac, de Broglie, Heisenberg, Jordan, Pauli, Planck and Schrödinger in the first quarter of the 20^{th} century. Figure 1 is describing some theories and their links according to three constants which appear or not in the theories: the speed of light c, the gravitational constant G and the Planck constant $\hbar$. In this thesis, we are interested in the quantum theory and its links with the classical one according to what we call the semiclassical limit.

In addition, inside each theory, there exists different description scales. The most precise scale is the microscopic[1] (or particle) scale, the intermediate scale is the mesoscopic (or kinetic) scale, and the scale we are interested in in this thesis is the macroscopic (or fluid) scale. Of course, passing from one scale to another leads to a precision loss, but the modeling becomes less expensive from a numerical point of view.

[1] Be careful, words "microscopic", "mesoscopic" and "macroscopic" do not qualify necessarily the space scale, but the level of description that we choose. It is indeed possible to use a microscopic model in order to describe the planet movements inside the solar system, and we can use a macroscopic model in order to describe electron transport inside an integrated circuit!

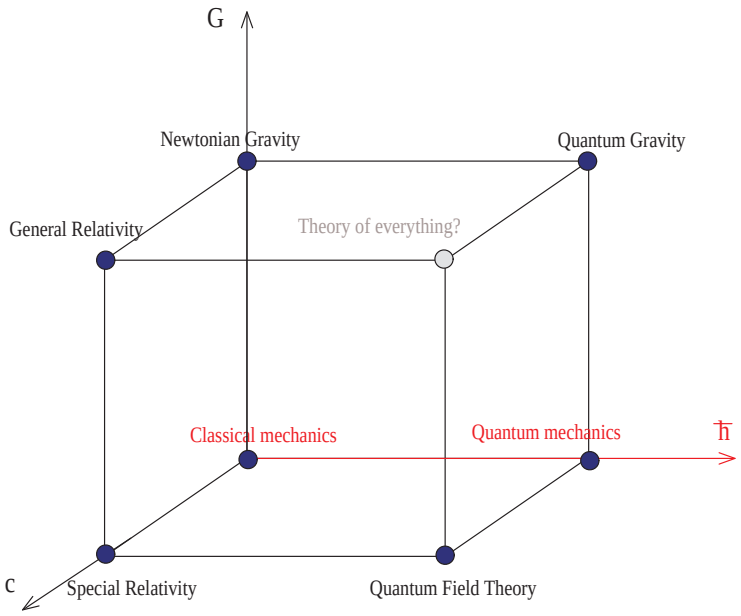

Figure 1: Different theories and their constants, c being the speed of light, G being the gravitational constant and $\hbar$ the Planck constant.

Fluid models in classical mechanics have been employed since a long time ago to describe huge particle systems, the most famous being probably the Navier-Stokes model which allows to model air movements in the atmosphere, ocean currents, water flows in a pipe, etc... In the semiconductor industry, the Drift-Diffusion model [10, 19, 31, 33] is widely used to model electron transport. However, the size of the devices being smaller and smaller (it can reach about 100 nanometers), this model is attaining its limits and quantum effects appear. Some devices (such the resonant tunneling diodes) behaviors are even based on effects that only quantum mechanics can explain. In order to model such devices, very few quantum fluid models exist and it is often compulsory to use microscopic models which are very expansive from a numerical point of view, and which do not take into account collisions. The only existing fluid models are often classical fluid models with additional quantum correction terms.

Models studied in this thesis have been derived in 2003 [14] by Degond and Ringhofer and in 2005 [11] by Degond, Méhats and Ringhofer and are fully quantum. Table 1 gives different classical and quantum models for particle transport at the three different scales described above. The four models studied in this thesis are quantum and macroscopic:

1. the Quantum Drift-Diffusion (QDD) model,
2. the Isothermal Quantum Euler model,
3. the Quantum Energy Transport(QET) model,
4. the Quantum Hydrodynamic (QHD) model.

The goal of this thesis is to study more in detail these models and to implement them numerically. Before giving the results obtained in this thesis, we are going to

	Classical	*Quantum*
Microscopic	Newton	Schrödinger
Mesoscopic	Vlasov/Boltzmann	Liouville/Wigner
Macroscopic	Drift-Diffusion	**Quantum Drift-Diffusion**
	Isothermal Euler	**Isothermal Quantum Euler**
	Energy Transport	**Quantum Energy Transport**
	Hydrodynamic	**Quantum Hydrodynamic**

Table 1: Some classical and quantum models describing particle systems at different scales.

remind how these models have been derived. To this aim, we are going to derive the macroscopic models from the microscopic ones in the classical setting first. This will introduce the hydrodynamic and diffusive limits and we will give then the derivation in the quantum setting which is based on the same method.

2 Derivation of the quantum fluid models

2.1 Method in the classical setting

2.1.1 From Newton's equations to Boltzmann equation

Let us start by considering a simple system of N particles of mass m evolving without collisions. At the fundamental level, we can describe this system according to Newton's laws of motion (these laws have been exposed for the first time in 1687 by Isaac Newton in "Philosophiae Naturalis Principia Mathematica"). Each particle denoted with a integer i is described by its position $x_i \in \mathbb{R}^3$ and its momentum (the product of mass and velocity) $p_i \in \mathbb{R}^3$ with $i = 1, ..., N$. We obtain the following system:

$$\partial_t x_i = \frac{p_i}{m}, \tag{2.1}$$

$$\partial_t p_i = F_i(x_1, ..., x_N), \tag{2.2}$$

where $F_i \in \mathbb{R}^3$ is the force applied on the particle number i by the other particles and by the external forces.

In practice, it is rare to know the exact number of particles contained in a given system, as well as their initial positions and momenta. Even if we knew these pieces of information, solving this system is often too expensive and useless. This is why it is common to use a less precise description level that we call mesoscopic or kinetic. At this scale, the system is described by a distribution function $f(x, p, t)$. This function represents a density in the phase space, meaning that $f(x, p, t)dxdp$ is the number of particles in the elementary volume $dxdp$ with position x and momentum p at time t.

In order to obtain the Vlasov equation, we write that all particles coming from the same point (x, p) in the phase space follow the same trajectory:

$$\partial_t X = \frac{P}{m} \quad ; \quad \partial_t P = F(X, t).$$

To obtain the equation satisfied by f, we write that the density is conserved along this trajectory:

$$\frac{d}{dt} f(X(t), P(t), t) = 0.$$

Using the chain rule, we obtain the following Vlasov equation:

$$\partial_t f + \frac{p}{m} \cdot \nabla_x f + F(x,t) \cdot \nabla_p f = 0. \tag{2.3}$$

If we want to take into account collisions, we have to introduce a collision operator noted $Q(f)$ which contains the physical properties of the system that we want to model. The Vlasov equation with a collision operator is called the Boltzmann equation (introduced by Ludwig Boltzmann at the end of the XIX$^{\text{th}}$ century):

$$\partial_t f + \frac{p}{m} \cdot \nabla_x f + F(x,t) \cdot \nabla_p f = \frac{Q(f)}{\tau},$$

where τ is the mean collision time. If the external force $F(x,t)$ is conservative, it is derived from a potential $V(x,t)$ according to $F(x,t) = -\nabla_x V(x,t)$, we obtain:

$$\partial_t f + \frac{p}{m} \cdot \nabla_x f - \nabla_x V \cdot \nabla_p f = \frac{Q(f)}{\tau}. \tag{2.4}$$

We can also write this equation in an hamiltonian form thanks to the Poisson bracket:

$$\partial_t f = \left\{ \hat{H}, f \right\} + \frac{Q(f)}{\tau}, \tag{2.5}$$

where $\hat{H}(x,p) = \frac{p^2}{2m} + V(x)$ is the Hamiltonian of the system and $\{a,b\}$ denotes the Poisson bracket:

$$\{a,b\} = \nabla_x a \cdot \nabla_p b - \nabla_x b \cdot \nabla_p a. \tag{2.6}$$

It is important to note that the insertion of the collision operator makes the Boltzmann equation time irreversible. It permits to reconciliate the Newton mechanisms, which are time reversible, with thermodynamics which is not. There is so much articles dedicated to the Boltzmann equation that we just give two references on the use of Boltzmann equation for semiconductors [23, 38].

2.1.2 Scaling of the Boltzmann equation

The two reference values that we choose are the reference length $\overline{x} = L$ and the reference temperature $\overline{T} = T_0$. We deduce the other reference values:

- Reference time: $\overline{t} = L\sqrt{\frac{m}{k_B T_0}}$,
- Reference momentum: $\overline{p} = \sqrt{k_B T_0 m}$,
- Reference potential: $\overline{V} = k_B T_0$,

with k_B the Boltzmann constant, and then we perform the following change of variable: $t' = \frac{t}{\overline{t}}, x' = \frac{x}{\overline{x}}, p' = \frac{p}{\overline{p}}, V' = \frac{V}{\overline{V}}$ and we omit the primes to obtain the following scaled Boltzmann equation:

$$\partial_t f + p \cdot \nabla_x f - \nabla_x V \cdot \nabla_p f = \frac{Q(f)}{\varepsilon}. \tag{2.7}$$

with ε the following scaled relaxation time[2]:

$$\varepsilon = \frac{\tau}{\bar{t}} = \frac{\lambda_{\text{mfp}}}{L}, \tag{2.8}$$

where $\lambda_{\text{mfp}} = \tau\sqrt{\frac{k_B T_0}{m}}$ denoted the mean free path.

2.1.3 Collision operators and Maxwellians

As the scaled relaxation time ε tends to zero (this corresponds to a system where collisions are predominant), the distribution function tends to a "local equilibrium" defined as the kernel of the collision operator. The Levermore approach [25] consists in defining this local equilibrium as the minimizer of an entropy under constraints on certain moments. This is indeed the entropy which describes the particles statistics. In this section, we are going to consider the Boltzmann entropy (in this case, we call "Maxwellian" the local equilibrium) and we will generalize with any entropy in the quantum case.

Maxwellians: We are going to define four Maxwellians which are going to be useful to define the four collision operators necessary for the derivation of the macroscopic models. First, the more general Maxwellian is defined as the minimizer of the entropy under constraint that its mass, momentum and energy are given. The notion of entropy, its definition and its name have been introduced in 1854 by Rudolf Clausius. Ludwig Boltzmann was the first to propose a microscopic interpretation of the entropy. In 1877, he linked this notion with a molecular disorder. He obtained the following expression for the entropy:

$$S(f) = \int f(\log f - 1)\, dp\, dx. \tag{2.9}$$

The macroscopic quantities that are going to be useful are expressed as moments of the distribution function f: the density of mass $n = \int f\, dp$, the current $nu = \int p\, f\, dp$ and the energy $\mathcal{W} = \int \frac{p^2}{2} f\, dp$. Now we can define the following minimization problem: for given $(n, nu, \mathcal{W})$, to find

$$\min_f \left(S(f) / \int f \begin{pmatrix} 1 \\ p \\ \frac{|p|^2}{2} \end{pmatrix} dp = \begin{pmatrix} n \\ nu \\ \mathcal{W} \end{pmatrix} \right). \tag{2.10}$$

The unique solution is given by the following Maxwellian:

$$M_{n,nu,\mathcal{W}} = \frac{n}{(2\pi T)^{3/2}} \exp\left(-\frac{1}{2T}(p-u)^2 \right), \tag{2.11}$$

with $T = \frac{2}{3}\frac{\mathcal{W}}{n} - \frac{1}{3}u^2$.

Now, we are going to define another Maxwellian carrying no current which is solution of:

$$\min_f \left(S(f) / \int f \begin{pmatrix} 1 \\ \frac{|p|^2}{2} \end{pmatrix} dp = \begin{pmatrix} n \\ \mathcal{W} \end{pmatrix} \right). \tag{2.12}$$

[2]For the Navier-Stokes equation, ε is called the Knudsen number and is denoted Kn.

The unique solution is given by the following Maxwellian:

$$M_{n,\mathcal{W}} = \frac{n}{(2\pi T)^{3/2}} \exp\left(-\frac{p^2}{2T}\right), \tag{2.13}$$

with $T = \frac{2}{3}\frac{\mathcal{W}}{n}$.

In this thesis, we are also interested in isothermal models, which means that the particles we are considering are in a "thermal bath" of a fixed temperature T_0 (so that once the equations are scaled, we have $T = 1$). This interaction does not conserve the energy of the particles and the good notion of entropy is given by the relative entropy (or free energy), defined as the sum of the total energy and the entropy:

$$G(f) = E(f) + S(f) = \int \hat{H} f + f(\log f - 1)\, dp\, dx, \tag{2.14}$$

with the Hamiltonian $\hat{H}(x,p) = \frac{p^2}{2} + V(x)$. We define a new Maxwellian solution of

$$\min_f \left(G(f) / \int f \begin{pmatrix} 1 \\ p \end{pmatrix} dp = \begin{pmatrix} n \\ nu \end{pmatrix} \right). \tag{2.15}$$

The unique solution is given by the following Maxwellian:

$$M_{n,nu} = \frac{n}{(2\pi)^{3/2}} \exp\left(-\frac{(p-u)^2}{2}\right). \tag{2.16}$$

Finally, the last Maxwellian is solution of

$$\min_f \left(G(f) / \int f\ dp = n \right). \tag{2.17}$$

The unique solution is given by the following Maxwellian:

$$M_n = \frac{n}{(2\pi)^{3/2}} \exp\left(-\frac{p^2}{2}\right).$$

Collision operators: We can now define the collision operators that we need for the derivation of the macroscopic models. We are interested in four operators: Q_h and Q_{hi} which will give respectively the hydrodynamic and the isothermal hydrodynamic models, Q_d and Q_{di} which will give respectively the diffusive and the isothermal diffusive models. In order to get good physical properties, each operator needs to satisfy 3 properties, the first concerning moments conservations, the second defining the local equilibrium as Maxwellians, and the third concerning entropy (or free energy) dissipation.
More precisely, Q_h has to satisfy the following properties:

1. $\forall f : \int Q_h(f) \begin{pmatrix} 1 \\ p \\ \frac{|p|^2}{2} \end{pmatrix} dp = 0,$
2. $Q_h(f) = 0 \Longleftrightarrow \exists (n, nu, \mathcal{W}) \ \mid \ f(x,p) = M_{n,nu,\mathcal{W}},$

3. $\int Q_h(f) \ln f dp \leq 0$.

In addition, Q_{hi} has to satisfy the following properties:

1. $\forall f : \int Q_{hi}(f) \begin{pmatrix} 1 \\ p \end{pmatrix} dp = 0$,
2. $Q_{hi}(f) = 0 \Longleftrightarrow \exists (n, nu) \ \mid \ f(x,p) = M_{n,nu}$,
3. $\int Q_{hi}(f)(\ln f + \hat{H}(x,p))dp \leq 0$.

The operator Q_d has to satisfy the following properties:

1. $\forall f : \int Q_d(f) \begin{pmatrix} 1 \\ \frac{p^2}{2} \end{pmatrix} dp = 0$,
2. $Q_d(f) = 0 \Longleftrightarrow \exists (n, \mathcal{W}) \ \mid \ f(x,p) = M_{n,\mathcal{W}}$,
3. $\int Q_d(f) \ln f dp \leq 0$.

Finally Q_{di} has to satisfy the following properties:

1. $\forall f : \int Q_{di}(f) dp = 0$,
2. $Q_{di}(f) = 0 \Longleftrightarrow \exists n \ \mid \ f(x,p) = M_n$,
3. $\int Q_{di}(f)(\ln f + \hat{H}(x,p))dp \leq 0$.

We do not need to know the exact form of the collision operators in order to derive the hydrodynamic models. In the other hand, we need to know the exact form of the collision operators in order to derive the diffusive models since the coefficients of the diffusive matrix depend on it. In this thesis, we will only consider BGK type operators (introduced by Bathnagar, Gross and Krook [4]):

$$Q_d(f) = M_{n,nu}(f) - f \ \ ; \ \ Q_{di} = M_n(f) - f, \tag{2.18}$$

where $M_{n,nu}(f)$ is the Maxwellian associated to f which has the same density and current as f, and $M_n(f)$ is the Maxwellian associated to f which has the same density as f. It is easy to check that these two operators satisfy the 3 properties defined above.

2.1.4 Macroscopic models

We are now able to show the link between the Boltzmann equation and the hydrodynamic and diffusive models thanks to the moment method defined by Levermore [25].

Hydrodynamic limit: We are going to consider the Boltzmann equation associated to the collision operator Q_h. In order to show the dependance of the solution on the parameter ε, we are going to denote the distribution function f^ε:

$$\partial_t f^\varepsilon + p \cdot \nabla_x f^\varepsilon - \nabla_x V \cdot \nabla_p f^\varepsilon = \frac{Q_h(f^\varepsilon)}{\varepsilon}. \tag{2.19}$$

The moment method consists in taking the moments of the Boltzmann equation (2.19), *i.e.* multiplying it by $\begin{pmatrix} 1 \\ p \\ \frac{|p|^2}{2} \end{pmatrix}$ and integrating it over p. Thanks to the conservation of mass, current and energy of the collision operator (property number 1 of Q_h), we obtain the following system:

$$\begin{aligned} \partial_t n^\varepsilon + \nabla \cdot n u^\varepsilon &= 0, \\ \partial_t (n u^\varepsilon) + \nabla \cdot \Pi^\varepsilon &= -n^\varepsilon \nabla V, \\ \partial_t \mathcal{W}^\varepsilon + \nabla \cdot \Phi^\varepsilon &= -n u^\varepsilon \cdot \nabla V, \end{aligned}$$

with the pressure tensor Π^ε and the energy flux Φ^ε given by:

$$\begin{aligned} \Pi^\varepsilon &= \int f^\varepsilon (p \otimes p)\, dp, \\ \Phi^\varepsilon &= \int f^\varepsilon \frac{|p|^2}{2} p\, dp. \end{aligned}$$

This system is not closed because Π^ε and Φ^ε cannot be expressed in function of n^ε, nu^ε and $\mathcal{W}^\varepsilon$. Now, if we look at a system where collisions are predominant, the scaled time of relaxation ε tends to zero so that equation (2.19) and property number 2 of Q_h imply $f^\varepsilon \overset{\varepsilon \to 0}{\longrightarrow} f^0 = M_{n^0, nu^0, \mathcal{W}^0}(f^0) = \frac{n^0}{(2\pi T^0)^{3/2}} \exp(-\frac{1}{2T^0}(p - u^0)^2)$.

At the limit $\varepsilon \to 0$, we obtain the following **hydrodynamic** model (after computation of the integrals):

$$\partial_t n + \nabla \cdot nu = 0, \tag{2.20}$$

$$\partial_t (nu) + \nabla \cdot (nu \otimes u) + \nabla (nT) = -n \nabla V, \tag{2.21}$$

$$\partial_t \mathcal{W} + \nabla \cdot (\mathcal{W} u) + \nabla \cdot (nuT) = -nu \cdot \nabla V. \tag{2.22}$$

The isothermal model is obtained through the same method by taking the collision operator Q_{hi} and considering only the first two moments. We obtain the following **isothermal Euler** model:

$$\partial_t n + \nabla \cdot nu = 0, \tag{2.23}$$

$$\partial_t (nu) + \nabla \cdot (nu \otimes u) + \nabla n = -n \nabla V. \tag{2.24}$$

$$\tag{2.25}$$

Diffusion limit: If we choose the same scaling of the Boltzmann equation for the diffusive limit and if we replace the collision operator Q_h by the operator Q_d, we obtain the Boltzmann equation:

$$\partial_t f^\varepsilon + p \cdot \nabla_x f^\varepsilon - \nabla_x V \cdot \nabla_p f^\varepsilon = \frac{Q_d(f^\varepsilon)}{\varepsilon}. \tag{2.26}$$

Now, if we integrate this equation against $\begin{pmatrix} 1 \\ p \\ \frac{|p|^2}{2} \end{pmatrix}$ we obtain:

$$\begin{aligned} \partial_t n^\varepsilon + \nabla \cdot nu^\varepsilon &= 0, \\ \partial_t (nu^\varepsilon) + \nabla \cdot \Pi^\varepsilon &= -n^\varepsilon \nabla V - \frac{nu^\varepsilon}{\varepsilon}, \\ \partial_t \mathcal{W}^\varepsilon + \nabla \cdot \Phi^\varepsilon &= -nu^\varepsilon \cdot \nabla V. \end{aligned}$$

If we make ε tend to 0, we have $f^\varepsilon \overset{\varepsilon \to 0}{\longrightarrow} f^0 = M_{n^0,\mathcal{W}^0}(f^0) = \frac{n^0}{(2\pi T^0)^{3/2}} \exp(-\frac{p^2}{2T^0})$ so that $nu^\varepsilon \overset{\varepsilon \to 0}{\longrightarrow} nu^0 = 0$. Since f^0 is even with respect to p, we have also $\Phi^0 = 0$ and we obtain the following system:

$$\begin{aligned} \partial_t n &= 0, \\ nu &= 0, \\ \partial_t \mathcal{W} &= 0, \end{aligned}$$

meaning nothing is moving! We have thus to change the time scale. We are going to take $\bar{t} = \varepsilon^{-1} \times L\sqrt{\frac{m}{k_B T_0}} = L^2 \frac{m}{\tau k_B T_0}$ instead of $\bar{t} = L\sqrt{\frac{m}{k_B T_0}}$. We have then:

$$\varepsilon \partial_t f^\varepsilon + p \cdot \nabla_x f^\varepsilon - \nabla_x V \cdot \nabla_p f^\varepsilon = \frac{Q_d(f^\varepsilon)}{\varepsilon}. \tag{2.27}$$

Again, if ε tends to 0, we have $f^\varepsilon \overset{\varepsilon \to 0}{\longrightarrow} f^0 = M_{n^0,\mathcal{W}^0}(f^0) = \frac{n^0}{(2\pi T^0)^{3/2}} \exp(-\frac{p^2}{2T^0})$. We introduce the following Chapman-Enskog expansion:

$$f^\varepsilon = M_{n,\mathcal{W}}(f^\varepsilon) + \varepsilon f_1^\varepsilon, \tag{2.28}$$

which defines f_1^ε in the following manner (we denote $\mathcal{T}$ the Transport operator $\mathcal{T} f^\varepsilon = p \cdot \nabla_x f^\varepsilon - \nabla_x V \cdot \nabla_p f^\varepsilon$):

$$f_1^\varepsilon = -\frac{1}{\varepsilon} Q(f^\varepsilon) = -\mathcal{T} f^\varepsilon - \varepsilon \partial_t f^\varepsilon. \tag{2.29}$$

At the limit, we have $f_1 = -\mathcal{T} f^0$. Then, we multiply (2.27) by $\begin{pmatrix} 1 \\ \frac{|p|^2}{2} \end{pmatrix}$ and integrate over p to get:

$$\partial_t \int f^\varepsilon \begin{pmatrix} 1 \\ \frac{|p|^2}{2} \end{pmatrix} dp + \frac{1}{\varepsilon} \int \mathcal{T} f^\varepsilon \begin{pmatrix} 1 \\ \frac{|p|^2}{2} \end{pmatrix} dp = 0, \tag{2.30}$$

and we make use of the expansion (2.28) to get:

$$\mathcal{T} f^\varepsilon = \mathcal{T} M_{n,\mathcal{W}}(f^\varepsilon) + \varepsilon \mathcal{T} f_1^\varepsilon.$$

The Maxwellian $M_{n,\mathcal{W}}(f^\varepsilon)$ being even with respect to p, it is easy to check that $\mathcal{T} M_{n,\mathcal{W}}(f^\varepsilon)$ is odd with respect to p. We have thus

$$\int \mathcal{T} M_{n,\mathcal{W}}(f^\varepsilon) \begin{pmatrix} 1 \\ \frac{|p|^2}{2} \end{pmatrix} dp = 0,$$

and at the limit $\varepsilon \to 0$:

$$\partial_t \int f^0 \begin{pmatrix} 1 \\ \frac{|p|^2}{2} \end{pmatrix} dp + \int \mathcal{T}\mathcal{T} f^0 \begin{pmatrix} 1 \\ \frac{|p|^2}{2} \end{pmatrix} dp = 0. \tag{2.31}$$

Finally, some integrals computations and parity arguments lead to the **Energy Transport** model:

$$\begin{aligned} \partial_t n + \nabla \cdot j_n &= 0, & (2.32)\\ \partial_t \mathcal{W} + \nabla \cdot j_{\mathcal{W}} + \nabla V \cdot j_n &= 0, & (2.33) \end{aligned}$$

$$\begin{aligned} j_n &= -\nabla \cdot \Pi - n\nabla V, & (2.34)\\ j_{\mathcal{W}} &= -\nabla \cdot \mathbb{Q} - (\mathcal{W}\mathrm{Id} + \Pi) \cdot \nabla V, & (2.35) \end{aligned}$$

$$\begin{aligned} \Pi &= \int f^0 (p \otimes p) dp = nT\mathrm{Id}, & (2.36)\\ \mathbb{Q} &= \int f^0 (p \otimes p) \frac{|p|^2}{2} dp = \frac{5}{2} nT^2 \mathrm{Id}, & (2.37) \end{aligned}$$

with

$$T = \frac{2}{3} \frac{\mathcal{W}}{n}. \tag{2.38}$$

The same method applied to the Boltzmann equation with the collision operator Q_{di} gives the **Drift-Diffusion** model:

$$\begin{aligned} \partial_t n + \nabla \cdot j &= 0, & (2.39)\\ j &= -\nabla \cdot \Pi - n\nabla V, & (2.40)\\ \Pi &= \int f^0 (p \otimes p) dp = n\mathrm{Id}. & (2.41) \end{aligned}$$

2.2 Method in the quantum setting

A huge literature is dedicated to the introduction of quantum theory. We can cite [32, 8] for a physical point of view and [39] for a deep mathematical analysis. Concerning the derivation of quantum fluid models, we advise the reader to read section 2.1 before reading this section. We give here only the main ideas to understand the derivation of the models studied in this thesis, we refer the reader to [14, 11] for the details.

2.2.1 Some quantum formalism

Let us start by considering a single particle system of mass m evolving in the presence of a potential V. The quantum equivalence of Newton's equations is the Schrödinger equation (introduced in 1926 by Erwin Schrödinger). The particle is no more described by its position x and its momentum p but by a wavefunction $\psi(x,t) \in L^2(\mathbb{R}^3)$ which describes the state of the particle at time t. This wavefunction is solution of the Schrödinger equation which reads (we take the same scaling as the one introduced in subsection 2.1.2):

$$i\tilde{\hbar}\partial_t \psi = \mathcal{H}\psi = -\frac{\tilde{\hbar}^2}{2}\Delta\psi + V\psi, \tag{2.42}$$

where $\tilde{\hbar}$ is the scaled Planck constant being equal to $\tilde{\hbar} = \frac{\lambda_{dB}}{L} = \frac{\hbar}{\sqrt{mk_BT_0L^2}}$ (we call $\lambda_{dB} = \frac{\hbar}{\sqrt{mk_BT_0}}$ the de Broglie wavelength). This number allows to "measure" the quantum behavior of the particle: if $\tilde{\hbar}$ is large enough, the behavior of the particle will be quantum whereas if $\tilde{\hbar}$ is small (see section 2.2.5 for an introduction to semiclassical limit), the behavior will be classical. **For simplicity reasons, the scaled Planck constant will be denoted $\hbar$ in the sequel of this thesis**.

The quantity $|\psi(x,t)|^2$ represents the probability density of the particle, this is why ψ is normalized in $L^2(\mathbb{R}^3)$: $\int |\psi|^2 dx = 1$. In quantum mechanics, every "observable" (quantity that we can physically measure) is obtained as the mean value on the wavefunction ψ of a symmetric operator O. More precisely, $\langle O \rangle = (O\psi, \psi) = \int (O\psi)(x)\psi(x)dx$ gives the expected value of a huge set of measures of the observable O realized on the physical system represented by the wavefunction ψ. The operators we are interested in are for example the "position" operator X, the "momentum" operator P and the "total energy" operator $\mathcal{H}$ (Hamiltonian). We have:

$$\begin{aligned} X\psi(x) &= x\psi(x), \\ P\psi(x) &= -i\hbar\nabla\psi(x), \\ \mathcal{H}\psi(x) &= \left(\frac{|P|^2}{2} + V(x,t)\right)\psi(x) = -\frac{\hbar^2}{2}\Delta\psi(x) + V\psi(x). \end{aligned}$$

Now if we look a quantum system of N particles, we have to introduce the wavefunction $\psi(x_1, x_2, ..., x_N, t)$. Its evolution is governed by the following Schrödinger equation:

$$i\hbar\partial_t\psi = \sum_{i=1}^{N}(-\frac{\hbar^2}{2}\Delta_{x_i})\psi + V\psi. \tag{2.43}$$

If the dynamical system is not completely known, we can describe it by a density operator ϱ (trace class hermitian operator) on $L^2(\mathbb{R}^3)$ such that:

$$\text{Tr } \varrho = 1.$$

The operator ϱ being trace class, it is compact and thus possesses a complete orthogonal system of eigenfunctions $(\psi_s)_{s\in S}$ associated to real eigenvalues ϱ_s. Moreover, the positivity of ϱ and its trace property give:

$$0 \leq \varrho_s \leq 1, \quad \forall s \in S; \qquad \sum_{s\in S} \varrho_s = 1.$$

This is why the ϱ act on any function $\varphi \in L^2(\mathbb{R}^3)$ according to:

$$\varrho\varphi = \sum_{s\in S} \varrho_s(\varphi, \psi_s)\psi_s, \tag{2.44}$$

where we denote (φ, ψ_s) the scalar product in $L^2(\mathbb{R}^3)$ of the two functions φ and ψ_s.

The physical interpretation of ϱ is quite natural: the eigenfunctions ψ_s represent the different possible states of the system and the eigenvalues ϱ_s are the probability associated to each state (this is why the sum of the ϱ_s is 1). In this system, each state ψ_s evolves according to the Schrödinger equation. We can check that the density operator evolves then according to the quantum Liouville equation:

$$i\hbar\partial_t\varrho = [\mathcal{H}, \varrho], \tag{2.45}$$

where $\mathcal{H}$ is the Hamiltonian defined in the Schrödinger equation (2.42), and the brackets denote the commutator $[\mathcal{H}, \varrho] = \mathcal{H}\varrho - \varrho\mathcal{H}$. For more details, the reader can refer to chapter 8 section 4 (quantum statistics) of the book [32] for instance.

2.2.2 The Wigner equation and the Wigner-Boltzmann equation

The formalism of density operators can be very useful but it is not very intuitive. In order to make it more intuitive, we are going to introduce the Wigner Transform (first used by Eugene Wigner in 1932 [42], see [24] for a mathematical study). Let $\underline{\varrho}(x, x')$ be the integral kernel of the operator ϱ. The action of ϱ on any function $\varphi \in L^2(\mathbb{R}^3)$ is given by:

$$\varrho\varphi = \int \underline{\varrho}(x, x')\varphi(x')dx'.$$

Thanks to relation (2.44), we can express $\underline{\varrho}$ in the following way:

$$\underline{\varrho}(x, x') = \sum_{s\in S} \varrho_s \psi_s(x)\overline{\psi_s(x')},$$

where $\overline{\psi_s(x')}$ is the complex conjugate of $\psi_s(x')$.

The Wigner Transform $W(\varrho)(x, p)$ of ϱ is a function in the phase space (x, p). It is defined by:

$$W(\varrho)(x, p) = \int \underline{\varrho}\left(x - \frac{1}{2}\xi, x + \frac{1}{2}\xi\right) e^{i\xi\cdot p/\hbar} d\xi. \tag{2.46}$$

The inverse Wigner Transform, called "Weyl quantification", associates each function $w(x, p)$ to an operator $\varrho = W^{-1}(f)$ acting on functions of $L^2(\mathbb{R}^3)$ in the following way:

$$W^{-1}(w)\varphi = \frac{1}{(2\pi\hbar)^3} \int w\left(\frac{x+y}{2}, p\right) \varphi(y) e^{ip\cdot(x-y)/\hbar} dp\, dy. \tag{2.47}$$

An interesting property is the following one:

$$\mathrm{Tr}\,(\varrho\sigma^\dagger) = \int W(\varrho)\overline{W(\sigma)} \frac{dx\, dp}{(2\pi\hbar)^3}, \tag{2.48}$$

where $\sigma^\dagger$ is the adjoint operator of σ.

We can check that if ϱ satisfies the quantum Liouville equation (2.45), then $w = W(\varrho)$ satisfies the following Wigner equation:

$$\partial_t w + p \cdot \nabla_x w - \Theta^\hbar(V)w = 0, \tag{2.49}$$

where $\Theta^\hbar(V)$ is the operator:

$$\Theta^\hbar(V)w = \frac{i}{(2\pi)^3\hbar} \int \left(V(x + \frac{\hbar}{2}\eta) - V(x - \frac{\hbar}{2}\eta)\right) w(x, p) e^{i\eta\cdot(p-q)} dp\, d\eta. \tag{2.50}$$

Note that the operator $\Theta^\hbar(V)$ converges formally to $\nabla_x V \cdot \nabla_p$ when $\hbar$ tends to zero, which shows the correspondance between the Wigner equation and the Vlasov equation.

Like for the Boltzmann equation, we can add a collision operator which takes into account collision phenomena:

$$i\hbar\partial_t\varrho = [\mathcal{H}, \varrho] + i\hbar\frac{\mathcal{Q}_L(\varrho)}{\varepsilon}, \tag{2.51}$$

where $\varepsilon = \frac{\tau}{L}\sqrt{\frac{k_B T_0}{m}}$ is the scaled relaxation time. If now ϱ satisfies the collisional quantum Liouville equation (2.51), then $w = W(\varrho)$ satisfies the Wigner-Boltzmann equation:

$$\partial_t w + p \cdot \nabla_x w - \Theta^{\hbar}(V) w = W\left(\frac{\mathcal{Q}_L(\varrho)}{\varepsilon}\right) = \frac{\mathcal{Q}(w)}{\varepsilon}. \tag{2.52}$$

As for the classical case, we are going to give the form of the collision operators and we are going to use the same methodology to derive the quantum fluid models.

2.2.3 Quantum collision operators and quantum local equilibria

Quantum local equilibria: We are going to define the four quantum local equilibria that we need to define the four collision operators necessary for the derivation of the quantum fluid models. We are going to define these local equilibria as minimizers of an entropy, but, by contrast with the classical case, we do not choose the Boltzmann entropy but any entropy defined thanks to a convex function s. We could write this derivation from the quantum Liouville equation in the operator formalism but it is more intuitive to perform it with the Wigner formalism. In this formalism, the quantities we are interested in are the density $n = \int w \frac{dp}{(2\pi\hbar)^3}$, the current $nu = \int p\, w \frac{dp}{(2\pi\hbar)^3}$ and the energy $\mathcal{W} = \int \frac{p^2}{2} w \frac{dp}{(2\pi\hbar)^3}$. On the other hand, the expression of the entropy is easier to write with the operator formalism:

$$S(\varrho) = \mathrm{Tr}\ \left(s(\varrho)\right). \tag{2.53}$$

Thanks to property (2.48), the expression of the entropy in the Wigner formalism is:

$$S(w) = \int W\left(s\left(W^{-1}(w)\right)\right) \frac{dp\, dx}{(2\pi\hbar)^3}. \tag{2.54}$$

Now we define the following problem: for given $(n, nu, \mathcal{W})$, to find

$$\min_w \left(S(w) / \int w \begin{pmatrix} 1 \\ p \\ \frac{|p|^2}{2} \end{pmatrix} \frac{dp}{(2\pi\hbar)^3} = \begin{pmatrix} n \\ nu \\ \mathcal{W} \end{pmatrix} \right). \tag{2.55}$$

It has been proved in [14] that the solution, if it exists, is given by the quantum local equilibrium:

$$w^{eq}_{n,nu,\mathcal{W}} = W\left((s')^{-1}\left(W^{-1}\left(-\frac{1}{2C}(p-B)^2 - A\right)\right)\right), \tag{2.56}$$

where $A(x)$ and $C(x)$ are scalar functions, and $B(x)$ is a vector function, all real valued. We will call the variables A, B and C respectively the generalized chemical potential, the generalized mean velocity and the generalized temperature. In this thesis, we will suppose the existence and uniqueness of such solutions. In the operator formalism, the local equilibrium reads:

$$\varrho^{eq}_{n,nu,\mathcal{W}} = (s')^{-1}\left(-H(A,B,C)\right), \tag{2.57}$$

where we denote $H(A,B,C)$ the following modified Hamiltonian:

$$\begin{aligned} H(A,B,C) &= W^{-1}\left(\frac{1}{2C}(p-B)^2+A\right) \\ &= -\hbar^2\left(\nabla\cdot(\frac{1}{2C}\nabla)+\frac{1}{4}\Delta\frac{1}{2C}\right) \\ &\quad +i\hbar\left(\frac{B}{C}\cdot\nabla+\frac{1}{2}(\nabla\cdot\frac{B}{C})\right)+A+\frac{B^2}{2C}. \end{aligned} \tag{2.58}$$

Note that by contrast with the classical case, we cannot express the local equilibria $w^{eq}_{n,nu,\mathcal{W}}$ and $\varrho^{eq}_{n,nu,\mathcal{W}}$ explicitly with respect to $(n,nu,\mathcal{W})$. This local equilibrium are written with respect to thermodynamic intermediate variables (A,B,C) that we suppose unique and fixed in such a way that the density, the current and the energy associated to these local equilibria are equal respectively to n, nu and $\mathcal{W}$.

Now we can define another quantum local equilibrium which carries no current and which is solution of:

$$\min_w\left(S(w)/\int w\begin{pmatrix}1\\ \frac{|p|^2}{2}\end{pmatrix}\frac{dp}{(2\pi\hbar)^3}=\begin{pmatrix}n\\ \mathcal{W}\end{pmatrix}\right). \tag{2.59}$$

The solution is given by the following quantum local equilibrium:

$$w^{eq}_{n,\mathcal{W}}=W\left((s')^{-1}\left(W^{-1}\left(-\frac{1}{2C}p^2-A\right)\right)\right). \tag{2.60}$$

Finally, in order to derive isothermal models, we need to define a quantum relative entropy (or quantum free energy) which is expressed in the operator formalism according to:

$$G(\varrho)=E(\varrho)+S(\varrho)=\text{Tr }\left(\mathcal{H}\varrho+s(\varrho)\right), \tag{2.61}$$

or equivalently

$$G(w)=E(w)+S(w)=\int\left(\frac{p^2}{2}+V\right)w+W\left(s\left(W^{-1}(w)\right)\right)\frac{dp\,dx}{(2\pi\hbar)^3}. \tag{2.62}$$

We define then a new quantum local equilibrium solution of:

$$\min_w\left(G(w)/\int w\begin{pmatrix}1\\ p\end{pmatrix}\frac{dp\,dx}{(2\pi\hbar)^3}=\begin{pmatrix}n\\ nu\end{pmatrix}\right). \tag{2.63}$$

The solution is given by the following quantum local equilibrium:

$$w^{eq}_{n,nu}=W\left((s')^{-1}\left(W^{-1}\left(-\frac{1}{2}(p-B)^2-A\right)\right)\right). \tag{2.64}$$

Finally, the last quantum local equilibrium is solution of:

$$\min_w\left(G(w)/\int w\,\frac{dp\,dx}{(2\pi\hbar)^3}=n\right), \tag{2.65}$$

and it is given by:

$$w^{eq}_{n}=W\left((s')^{-1}\left(W^{-1}\left(-\frac{p^2}{2}-A\right)\right)\right).$$

Collision operators: We are now able to define the collision operators that we need for the derivation of the quantum fluid models. We define four collision operators analogous to the classical ones defined in subsection 2.1.3 page 21: $\mathcal{Q}_h, \mathcal{Q}_{hi}, \mathcal{Q}_d$ and $\mathcal{Q}_{di}$. In order to be physically realistic, each operator has to satisfy 3 properties which are similar to the classical case and we do not rewrite them here. For the entropy decrease property, we have to replace the function $\log(\cdot)$ by $W(s'(W^{-1}(\cdot)))$.

Again, in order to derive the quantum hydrodynamic models, we do not need to know the exact form of the collision operators (however, note that in [13], quantum collision operators analogous to the classical Boltzmann collision operators have been written). In the other hand, we need to know the exact form of the collision operators in order to derive quantum diffusive models since the coefficients of the diffusive matrix depend on it. In this thesis, we will consider BGK type collision operators:

$$\mathcal{Q}_d(w) = w^{eq}_{n,nu}(w) - w \quad ; \quad \mathcal{Q}_{di} = w^{eq}_{n}(w) - w. \tag{2.66}$$

2.2.4 Macroscopic models

In order to derive quantum macroscopic models, it suffices to develop the same methodology as the one exposed in subsection 2.1.4. Thanks to the properties of the operator $\Theta^{\hbar}(V)$ (see [14] and [11] for more details), we obtain the following models that we are going to study in this thesis:

The **Quantum Hydrodynamic model**:

$$\begin{aligned} \partial_t n + \nabla \cdot nu &= 0, && (2.67)\\ \partial_t (nu) + \nabla \cdot \Pi &= -n\nabla V, && (2.68)\\ \partial_t \mathcal{W} + \nabla \cdot \Phi &= -nu \cdot \nabla V, && (2.69) \end{aligned}$$

with

$$\begin{pmatrix} n \\ nu \\ \mathcal{W} \end{pmatrix} = \int w^{eq}_{n,nu,\mathcal{W}} \begin{pmatrix} 1 \\ p \\ \frac{|p|^2}{2} \end{pmatrix} \frac{dp}{(2\pi\hbar)^3}, \tag{2.70}$$

and

$$\begin{aligned} \Pi &= \int w^{eq}_{n,nu,\mathcal{W}} (p \otimes p) \frac{dp}{(2\pi\hbar)^3}, && (2.71)\\ \Phi &= \int w^{eq}_{n,nu,\mathcal{W}} \frac{|p|^2}{2} p \frac{dp}{(2\pi\hbar)^3}. && (2.72) \end{aligned}$$

The **isothermal quantum Euler** model:

$$\begin{aligned} \partial_t n + \nabla \cdot nu &= 0, && (2.73)\\ \partial_t (nu) + \nabla \cdot \Pi &= -n\nabla V, && (2.74) \end{aligned}$$

with

$$\begin{pmatrix} n \\ nu \end{pmatrix} = \int w^{eq}_{n,nu} \begin{pmatrix} 1 \\ p \end{pmatrix} \frac{dp}{(2\pi\hbar)^3}, \tag{2.75}$$

and

$$\Pi = \int w_{n,nu}^{eq}(p \otimes p)\, \frac{dp}{(2\pi\hbar)^3}. \tag{2.76}$$

The **Quantum Energy Transport** model:

$$\partial_t n + \nabla \cdot j_n = 0, \tag{2.77}$$
$$\partial_t \mathcal{W} + \nabla \cdot j_{\mathcal{W}} + \nabla V \cdot j_n = 0, \tag{2.78}$$

$$j_n = -\nabla \cdot \Pi - n\nabla V, \tag{2.79}$$
$$j_{\mathcal{W}} = -\nabla \cdot \mathbb{Q} - (\mathcal{W}\mathrm{Id} + \Pi) \cdot \nabla V + \frac{\hbar^2}{8} n\nabla(\Delta V), \tag{2.80}$$

with

$$\begin{pmatrix} n \\ \mathcal{W} \end{pmatrix} = \int w_{n,\mathcal{W}}^{eq} \begin{pmatrix} 1 \\ \frac{|p|^2}{2} \end{pmatrix} \frac{dp}{(2\pi\hbar)^3} \tag{2.81}$$

and

$$\Pi = \int w_{n,\mathcal{W}}^{eq}(p \otimes p) \frac{dp}{(2\pi\hbar)^3}, \tag{2.82}$$
$$\mathbb{Q} = \int w_{n,\mathcal{W}}^{eq}(p \otimes p) \frac{|p|^2}{2} \frac{dp}{(2\pi\hbar)^3}. \tag{2.83}$$

And finally, the **Quantum Drift-Diffusion** model:

$$\partial_t n + \nabla \cdot j = 0, \tag{2.84}$$
$$j = -\nabla \cdot \Pi - n\nabla V, \tag{2.85}$$

with

$$n = \int w_n^{eq} \frac{dp}{(2\pi\hbar)^3} \tag{2.86}$$

and

$$\Pi = \int w_n^{eq}(p \otimes p) \frac{dp}{(2\pi\hbar)^3}. \tag{2.87}$$

Note that in [12], the term $\nabla \cdot \Pi$ has been simplified using commutators computations and they obtained $\nabla \cdot \Pi = -n\nabla A$, which allows to write the current in the simplified form:

$$j = n\nabla(A - V). \tag{2.88}$$

This remark is not insignificant because this simplification has made the numerical approach easier (see chapters I, II and III) for the QDD model. In the sequel, we have tried to simplify in the same way fluxes appearing in the other models, it has been successful for the isothermal quantum Euler model (see chapter IV) but the task has been more difficult with the non isothermal models QHD and QET (see chapter V).

2.2.5 Semiclassical limit

We know since Madelung [26] that the Schrödinger equation 2.42 can be reformulated in a fluid dynamical way thanks to the Madelung Transform. This consists in writing the wavefunction in WKB form $\psi = \sqrt{n}e^{i\frac{S}{\hbar}}$ where n is the density and S is the phase. Inserting this Ansatz in the Schrödinger equation, taking the real part and the gradient of the imaginary part, we obtain the Madelung system with unknown n (the density) and $nu = n\nabla S$ (the current):

$$\partial_t n + \nabla \cdot nu = 0, \tag{2.89}$$

$$\partial_t (nu) + \nabla \cdot (nu \otimes u) + n\nabla(V + V^B) = 0, \tag{2.90}$$

$$V^B = -\frac{\hbar^2}{2}\frac{\Delta\sqrt{n}}{\sqrt{n}}. \tag{2.91}$$

These equations are pressureless Euler equations with an additional quantum potential called the Bohm potential V^B.

This model concerns single particle systems, so there is no collisions nor temperature effects. In this sense, the Madelung system is a zero temperature model (we show formally in chapter IV that the quantum Euler model converges formally to the Madelung system as the temperature goes to 0).

An opposite limit consists in looking what happens when the scaled Planck constant $\hbar$ tends to 0: this limit is called the semiclassical limit. This limit is interesting from a mathematical as well as a physical point of view since in many applications (in quantum chemistry and semiconductors for instance), the scaled Planck constant $\hbar$ is small. A lot of works have been dedicated to the study of this limit and we can cite [17, 27, 28, 40]. We propose in chapter VI an asymptotically stable scheme for the Madelung system.

We can wonder what happens when $\hbar$ tends to 0 in the quantum fluid models studied in this thesis. If we choose the Boltzmann entropy $s(\varrho) = \varrho(\log\varrho - 1)$, the quantum local equilibrium $w^{eq}_{n,nu,\mathcal{W}}$ defined for the QHD model in section 2.2.3 takes the form (we call it quantum Maxwellian):

$$\mathcal{M}_{n,nu,\mathcal{W}} = \mathcal{E}\mathrm{xp}\left(-\frac{1}{2C}(p-B)^2 - A\right), \tag{2.92}$$

where the quantum exponential of a symbol $a(x,p)$ is defined as $\mathcal{E}\mathrm{xp}(a)(x,p) = W(\exp W^{-1}(a(x,p)))$.

It has been proved formally in [11] that $\mathcal{E}\mathrm{xp}(a) \xrightarrow[\hbar\to 0]{} \exp(a)$ so that the quantum Maxwellian tends to the classical one, and thus the QHD model converges to the classical hydrodynamic model. It is important to notice that the link between (A,B,C) and $(n,nu,\mathcal{W})$ is not local in the quantum case by contrast with the classical case where we have simply

$$A = -\log(n) + \frac{3}{2}\log\left(\frac{T}{2\pi\hbar^2}\right) \quad , \quad B = u \quad , \quad C = T \quad , \quad \mathcal{W} = \frac{1}{2}n|u|^2 + \frac{3}{2}nT. \tag{2.93}$$

In the same manner, the other quantum models converge to their classical counterparts as $\hbar$ tends to 0.

In addition, using pseudodifferential calculus, it is possible to perform an expansion of $\mathcal{E}\mathrm{xp}$ in power of $\hbar$ [11] and if we keep terms of order $\hbar^2$, we find intermediate models which are nothing else than the classical models with quantum corrections. For the

QDD model, we find for example the Density Gradient model [2, 1, 36, 22, 5]. This model is the classical Drift-Diffusion model where an additional quantum potential is added (and is equal to $\frac{1}{3}V_B$).

3 Application to electron transport in semiconductors

We can think about many fields of application for the quantum fluid models such as quantum chemistry [3], quantum optics, the study of superfluidity, and last but not least, electron transport in semiconductors. A lot of reference books deal with introduction to semiconductor physics, we refer the reader for instance to [41] for details.

3.1 Some statements on semiconductors

A semiconductor is a cristal (a solid in which atoms are packed in a regular order) whose electrical conductivity is in between that of a conductor and that of an insulator (the three most important semiconductors are the germanium (Ge), the silicium (Si) and the gallium arsenide (GaAs)). This cristal creates a periodic potential V^{per} which period length L_{per} is about one cell (typically of order $10^{-10}m$). In this thesis, we will make the effective mass approximation, meaning we will replace the mass of the electron m by its effective mass m^* so that we can "forget" this potential.

The cristal of a semiconductor is in general not perfect. There are a lot of imperfections sources but the most important one is due to the presence of impurities which are other atoms or ions with which electrons are interacting. In the other hand, the cristal is not fixed but vibrating. These vibrations can be modeled thanks to pseudoparticles that are called phonons and which also interact with electrons. These interactions can be modeled at a kinetic scale by collision operators.

3.2 Validity domain for the quantum fluid models

The use of quantum fluid models studied in this thesis is limited to a precise certain domain. The devices that we want to model have to be sufficiently small so that quantum effects are important, but they have to be sufficiently large so that collisions are predominant. Let us try to give more details about this validity domain. During the scaling of the Wigner-Boltzmann equation (see subsection 2.1.2 for the scaling), we have chosen two reference values: the reference temperature T_0 and the reference length of the device L.

In addition, two dimensionless parameters appear naturally during the derivation of quantum fluid models: the scaled relaxation time ε which measures the importance of the collisions (and the fact that we are in a fluid regime or not) and the scaled Planck constant $\tilde{\hbar}$ (denoted for simplicity $\hbar$ in this thesis) which measures the importance of quantum phenomena. We recall that we have:

$$\begin{aligned} \varepsilon &= \tau\sqrt{\frac{k_B T_0}{mL^2}}, \\ \tilde{\hbar} &= \frac{\hbar}{\sqrt{mk_B T_0 L^2}}. \end{aligned}$$

So that

$$\tilde{\hbar} \sim L^{-1}T_0^{-1/2}. \tag{3.94}$$

In the other hand, the relaxation time τ appearing inside the parameter ε can be calculated from the mobility of the electrons according to the following formula:

$$\tau = \frac{m^* \mu}{e}.$$

For collisions with phonons, we have [41]:

$$\mu_l \sim T_0^{-3/2}$$

and for collisions with impurities:

$$\mu_i \sim T_0^{3/2}.$$

The combined mobility is then

$$\mu = \left(\frac{1}{\mu_l} + \frac{1}{\mu_i} \right)^{-1}.$$

For the Gallium Arsenide (GaAs), this mobility can be approximated by $\mu \sim T_0^{1/2}$, which gives

$$\varepsilon \sim L^{-1} T_0. \tag{3.95}$$

We deduce from figure 2 the area, depending on L and T_0 where we can apply quantum fluid models. We should also split by a vertical line the areas where the effective mass

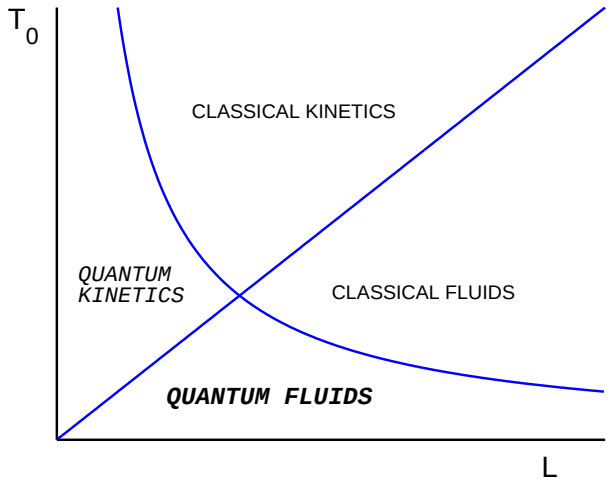

Figure 2: Validity domain of the quantum fluid models.

approximation is valid ($\frac{L_{per}}{L} << 1$) or not. The area where quantum fluid models are valid is therefore at the bottom right of this graph (relatively small devices at low temperatures).

3.3 The Poisson equation

For the moment, we have not given any details on how the electrical potential V is computed. This potential can come either from an external applied bias or from

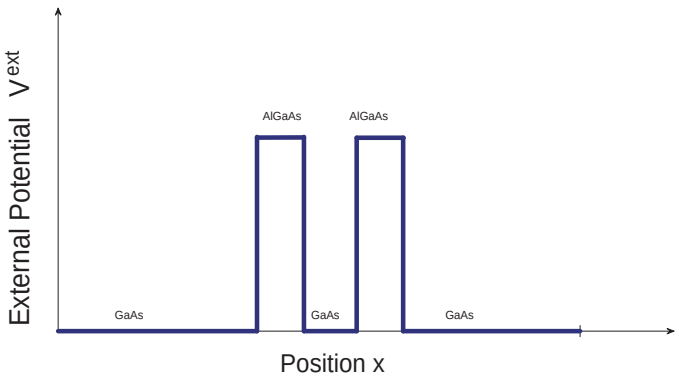

Figure 3: The double barrier potential in a resonant tunneling diode.

the use of different materials inside the device, and we will denote this potential V^{ext}. Electrons being charged particles, they interact with themselves and with doping ions. They create a self-consistant potential that we denote V^s and which is solution of the Poisson equation:

$$-\varepsilon_0\varepsilon_r\Delta V^s = e(n - n^d),$$

where n^d is the density of doping ions, e is the charge of an electron and ε_0, ε_r are respectively the vacuum permittivity and the relative permittivity. With the same scaling as the one proposed in subsection 2.1.2, and taking for reference density $\overline{n} = \sup n^d$, we obtain the scaled Poisson equation:

$$-\alpha^2\Delta V^s = n - n^d, \tag{3.96}$$

where $\alpha = \sqrt{\frac{\varepsilon_r\varepsilon_0 k_B T}{e^2 L^2 \overline{n}}} = \frac{\lambda_D}{L}$ with λ_D the Debye length. The dimensionless parameter α measures the space charge effects.

3.4 The Resonant Tunneling Diode (RTD)

The RTD has attracted a lot of interest due to its non linear current-voltage characteristics [7]. This device shows indeed a negative resistance for certain applied bias, which is interesting for many applications in electronics logic for instance. The RTD is composed of two crystals: for example the Gallium Arsenide (GaAs) and two small strips of Aluminium and Gallium Arsenide (AlGaAs) which create a double barrier potential due to the conduction band gap between the two materials (cf figure 3). Some discrete levels of resonant energies appear inside this double barrier and only electrons with energies sufficiently close to this resonant energies can go through this double barrier by tunneling effect. Applying an external bias on the RTD modifies electron energies this is why increasing the applied voltage can lower the current. The size of the RTD as well as the possibility to simulate it with 1D models are making of it a good candidate device to test the numerical schemes on the quantum fluid models developed in this thesis.

References

[1] M. G. Ancona, G. J. Iafrate, *Quantum correction of the equation of state of an electron gas in a semiconductor*, Phys. Rev. B **39** (1989), 9536–9540.

[2] , M. G. Ancona, H. F. Tiersten, *Macroscopic physics of the silicon inversion layer*, Pys. review, B **39** (1987), 7959–7965.

[3] W. Bao, S. Jin, P.A. Markowich, *On time-splitting spectral approximations for the Schrödinger equation in the semiclassical regime*, J. Comput. Phys. **175** (2002), 487–524.

[4] P. Bhatnagar, E. Gross, M. Krook, *A model for collision processes in gases. I. Small amplitude processes in charged and neutral one-component systems*, Phys. Review **94** (1954), 511–525.

[5] N. Ben Abdallah, A. Unterreiter, *On the stationary quantum driftdiffusion model*, Z. Angew. Math. Phys. **49** (1998), no. 2, 251–275.

[6] E. R. Bittner, *Quantum tunneling dynamics using hydrodynamic trajectories*, J. Chem. Phys. **112** (2000), no. 22, 9703–9710.

[7] L. L. Chang, L. Esaki and R. Tsu, *Resonant tunneling in semiconductor double barriers*, Appl. Phys. Lett. **24** (1974), 593–595.

[8] C. Cohen-Tannoudji, Mécanique Quantique, volumes 1 et 2, Hermann(1996).

[9] C. de Falco, E. Gatti, A. L. Lacaita, R. Sacco, *Quantum-corrected drift-diffusion models for transport in semiconductor devices*, J. Comput. Phys. **204** (2005), no. 2, 533–561.

[10] P. Degond, *Mathematical modelling of microelectronics semiconductor devices*, Proceedings of the Morningside Mathematical Center, Beijing, AMS/IP Studies in Advanced Mathematics, AMS Society and International Press, 2000, 77–109.

[11] P. Degond, F. Méhats, C. Ringhofer, *Quantum Energy-Transport and Drift-Diffusion models*, J. Stat. Phys. **118** (2005), no. 3-4, 625–665.

[12] P. Degond, F. Méhats, C. Ringhofer, *Quantum hydrodynamic models derived from entropy principle*, Contemp. Math. **371** (2005), 107–331.

[13] P. Degond, C. Ringhofer, *A note on binary quantum collision operators conserving mass, momentum and energy*, C. R. Acad. Sci. Paris **336**(2003), Ser I, 785–790.

[14] P. Degond, C. Ringhofer, *Quantum moment hydrodynamics and the entropy principle*, J. Stat. Phys. **112** (2003), no. 3-4, 587–628.

[15] C. Gardner, *Resonant tunneling in the quantum hydrodynamic model*, VLSI Design **3** (1995), 201–210.

[16] C. Gardner, C. Ringhofer, *The Chapman-Enskog Expansion and the Quantum Hydrodynamic Model for Semiconductor Devices*, VLSI Design **10** (2000), 415–435.

[17] P. Gérard, P. A. Markowich, N. J. Mauser, F. Poupaud, *Homogeneization limits and Wigner transforms*, Comm. Pure. Appl. Math. **50** (1997), 323–379.

[18] H. K. Gummel, *A self-consistent iterative scheme for one-dimensional steady state transistor calculations*, IEEE Trans. Electron. Devices, ED-11 (1964), 455–465.

[19] J. Jerome, Analysis of charge transport. A mathematical study of semiconductor devices, Springer, Berlin, New York, 1996.

[20] A. Jüngel, D. Matthes, *A derivation of the isothermal quantum hydrodynamic equations using entropy minimization*, Z. Angew. Math. Mech. **85** (2005), 806–814.

[21] A. Jüngel, D. Matthes, J.P. Milisic, *Derivation of new quantum hydrodynamic equations using entropy minimization*, SIAM J. Appl. Math. **67** (2006), 46–68.

[22] A. Jüngel, R. Pinnau, *A positivity preserving numerical scheme for a fourth-order parabolic equation*, SIAM J. Num. Anal. **39** (2001), no. 2, 385–406.

[23] S. E. Laux, M. V. Fischetti, *Semiconductor device physics and the modeling of small semiconductor devices*, Technical report, IBM.

[24] P. L. Lions, T. Paul, *Sur les mesures de Wigner*, Rev. Math. Iberoamericana **9** (1993), 553–618.

[25] C. D. Levermore, *Moment closure hierarchies for kinetic theories*, J. Stat. Phys., **83** (1996), no. 5-6, 1021–1065.

[26] E. Madelung, *Quantentheorie in hydrodynamischer Form*, Z. Physik **40** (1926), 322–326.

[27] P. A. Markowich, N.J. Mauser, *The classical limit of a self consistent quantum-Vlasov equation in 3D*, Math. Meth. Mod. **16** (1993), 409–442.

[28] P. A. Markowich, N.J. Mauser, F. Poupaud, *A Wigner function approach to semiclassical limits: electrons in a periodic potential*, J. Math. Phys **35** (1994), 1066-1094.

[29] P. A. Markowich, P. Pietra, and C. Pohl, *Numerical approximation of quadratic observables of Schrödinger type equations in the semi-classical limit*, Numer. Math. **81** (1999), 595–630.

[30] P. A. Markowich, P. Pietra, C. Pohl, H. P. Stimming, *A Wigner-measure analysis of the Dufort-Frankel scheme for the Schrödinger equation*, SIAM J. Numer. Anal. **40** (2002), 1281–1310.

[31] P. A. Markowich, C. Ringhofer, C. Schmeiser, Semiconductor Equations, Springer, 1990.

[32] A. Messiah, Mécanique Quantique, volumes 1 et 2, Dunod (1960).

[33] M. Mock, Analysis of Mathematical Models of Semiconductor Devices, Book Press, Dublin, 1983.

[34] F. Nier, *A variational formulation of Schrödinger-Poisson systems in dimension* $d \leq 3$, Comm. Partial Differential Equations **18** (1993), no. 7-8, 1125–1147.

[35] O. Pinaud, *Transient simulations of a resonant tunneling diode*, J. Appl. Phys. **92**(4) (2002), 1987–1994.

[36] R. Pinnau, A. Unterreiter, *The stationary current-voltage characteristics of the quantum drift-diffusion model*, SIAM J. Num. Anal. **37** (1999), no. 1, 211–245.

[37] A. Pirovano, A. Lacaita, A. Spinelli, *Two dimensional Quantum Effects in Nanoscale MOSFETs*, IEEE Trans. Electron. Dev. **49** (2002), no. 1, 25–31.

[38] F. Poupaud, C. Schmeider, *Charge transport in semiconductors with degeneracy effects*, Math. Meth. Appl. Sci. **14** (1991), 301–318.

[39] M Reed, B. Simon, Method of Modern Mathematical Physics, vol 1-4, Academic Press, San Diego, 1980.

[40] D. Robert, Autour de l'Approximation Semi-Classique, Birkhäuser, Boston, 1987.

[41] S.M. Sze, Physics of semiconductor devices.

[42] E. Wigner, *On the quantum correction for thermodynamic equilibrium*, Phys. Rev. **40** (1932), 749–759.

[43] R. E. Wyatt, C. L. Lopreore, G. Parlant *Electronic transitions with quantum trajectories*, J. Chem. Phys. **114** (2001), no. 12, 5113–5116.

Chapter I

Entropic discretization of the Quantum Drift-Diffusion model

This chapter has given an article written in collaboration with F. Méhats and published in the SIAM Journal on Numerical Analysis: *Entropic discretization of a quantum drift-diffusion model*, SIAM J. Numer. Anal. **43** (2005), no. 5, 1828–1849, and a note written in collaboration with F. Méhats and published in the Comptes Rendus de l'Académie des Sciences: *Numerical approximation of a quantum drift-diffusion model*, C. R. Math. Acad. Sci. Paris **339** (2004), no. 7, 519–524.

Abstract. This chapter is devoted to the discretization and numerical simulation of a new quantum drift-diffusion model that was recently derived. In a first step, we introduce an implicit semi-discretization in time which possesses some interesting properties: this system is well-posed, it preserves the positivity of the density, the total charge is conserved, and it is entropic (a free energy is dissipated). Then, after a discretization of the space variable, we define a numerical scheme which has the same properties and is equivalent to a convex minimization problem. These results are illustrated by some numerical simulations.

Key words. Quantum drift-diffusion, Schrödinger-Poisson, entropic scheme, convex minimization.

1 Introduction

Recently, Degond and Ringhofer [15, 16] have explored a new direction for quantum hydrodynamic models by extending Levermore's moment approach [33] to the context of quantum mechanics. Their strategy consists in defining a notion of "local" quantum equilibrium as the minimizer of an entropy functional under local moment constraints. Such equilibria are defined thanks to a relation between the thermodynamic quantities (such as the chemical potential or the temperature) and the extensive quantities (the densities) in a non local way. In [15], quantum hydrodynamic (QHD) models have been derived from quantum kinetic equations by moment expansions closed by these quantum equilibria. In this reference, Degond and Ringhofer have also sketched an important program related to these QHD models, including namely the setting up of a rigorous framework to this formal modeling, the inclusion of other quantum effects (Pauli exclusion principle, spin effects,...), or the numerical discretization and simulation. Following the same approach, these authors have then introduced in [17] a family of ad-hoc collision operators which decrease the quantum entropy and relax to the equilibria. Afterwards, this strategy was applied in [13] in order to derive quantum diffusive models: a quantum drift-diffusion model (QDD) and a quantum energy-transport model (QET). In a work in progress [8], other diffusive models of the type of the Spherical Harmonic Expansion (SHE) model are also constructed in the quantum framework.

All these fluid models are written as conservation laws coupled to constitutive equations. The quantum character of these models lies in these constitutive equations, which are non local in space and make these systems difficult to analyze (these papers [15, 13] remained at a formal level). However, an interesting property of these models is that –at least formally– a fluid entropy functional is dissipated. This feature gives an indication of the well-posedness of these systems; besides, it is interesting to recall that the entropic property is obtained as a by-product of the strategy of entropy minimization.

In this chapter, we are interested in the quantum drift-diffusion (QDD) model, with two objectives. Firstly, the present work is a first step in the rigorous analysis of this system, coupled to the Poisson equation. Secondly, we study the discretization of this system and its numerical simulation.

Let us now describe the main results of this chapter. The QDD system is given by (2.8)–(2.10). Actually, we are not able yet to answer the question of the well-posedness of this system. Nevertheless, we introduce, instead, and analyze rigourously a semi-discretized (in time) version of this model, defined by (3.21)–(3.23), and which presents the same entropy dissipation property as the QDD system. This first set of results is given in Theorem 3.1. Next, concerning the second objective of the chapter, the implicit numerical scheme (4.32)–(4.34) is defined. This scheme is well-posed and equivalent to a problem of convex minimization. Then, we show that this scheme is stable in the sense of a discrete entropy. These results concerning the numerical scheme are stated in Theorem 4.1.

We end this introduction with bibliographical notes on quantum transport modeling. The quantum drift-diffusion system applies to the modeling of nanoscale semiconductor devices. In the semiconductor industry, the classical drift-diffusion model has been a valuable tool for many years [11, 28, 35, 37, 48]. Currently, the ongoing miniaturization of electronic devices to the nanometer scale creates the need of models which take into account quantum effects. To this aim, two strategies can be followed.

The first approach, with a radical change in the level of description, consists in choosing full quantum models such as the Schrödinger equation, the von Neumann equation or the Wigner equation [4, 9, 12, 18, 19, 32, 38, 45, 46]. These models are well fitted for very small devices but they lead to the resolution of huge numerical systems at the intermediate scale which is currently considered by electronic engineers. Another reason why this approach is limited to very small devices is that the question of describing collisions in quantum transport models is extremely difficult and has not received a completely satisfactory answer yet. Therefore, full quantum models are still mainly reserved to ballistic transport in small devices.

The opposite strategy consists in introducing quantum correction terms in the classical drift-diffusion model. The most common quantum correction involves the Bohm potential, which naturally appears in quantum hydrodynamics, thanks to an analogy between the Schrödinger equation and the pressureless Euler system corrected with the Bohm potential. This analogy can be seen thanks to the Madelung transformation [34, 50], by considering the equations satisfied by the amplitude and the phase of a wavefunction solving the Schrödinger equation (see e.g. [13] for more details). Next, assuming that adding this Bohm potential enables to model quantum effects in classical macroscopic systems, several models with corrective terms have been written. In a fluid context, hydrodynamics models with quantum corrections have been studied in [22, 23, 24, 25, 26, 27, 29, 44, 51]. In a diffusive context, and closest to the QDD model studied in this chapter, one can find the drift-diffusion model corrected with the Bohm potential, called density-gradient model (it is also sometimes called quantum drift-diffusion model, but in this chapter we shall refer it as density-gradient model, in order to avoid any confusion with the QDD model presented here). This model was introduced in [1, 2], then mathematically and numerically studied in [3, 7, 29, 30, 41, 42]. An advantage of such an approach is that it takes into account collisions, at least heuristically. Another strength is that, as this method is based on an evolution of the classical drift-diffusion model, the numerical codes currently employed in semiconductor industry can be adapted by following this evolution. Nevertheless, one has to insist on the fact that the justification of these models is far from obvious in the case of statistical mixtures (several attempts were made to address this issue, see for instance [22, 23, 24, 27]). Moreover, quantum corrections involving the Bohm potential produce high order terms in these systems and make their resolution difficult, from the mathematical and from the numerical point of view. To conclude this description, one can also cite two other recent attempts to model quantum effects in diffusive models [6, 43]. The models presented in these works are different but both take the form of a drift-diffusion equation, coupled to the Poisson equation, and where the quantum phenomena are taken into account by a modification of the link between the density and the quasi-Fermi potential, via the resolution of a quasistatic Schrödinger equation.

As a compromise, the quantum drift-diffusion (QDD) model studied in the present chapter tries to conciliate these two approaches: this model is really quantum and non local, while the length scales are macroscopic and collisions are modeled. Indeed, as it is shown in Section 2.3, the steady states of the QDD model solve the Schrödinger-Poisson system studied in [31, 39, 40]: this shows the quantum character of this model. Besides, it has been shown in [13] that, at least formally, the limit of the QDD model as $\hbar$ goes to zero is the classical drift-diffusion model, while the leading order correction term in an $\hbar$ expansion is the Bohm potential: this shows a clear link between the QDD model and the density-gradient model described above.

The chapter is organized as follows: in Section 2, we write a formulation of the QDD model in a bounded domain and give some of its properties. Then, in Section 3, we define the semi-discretization in time of the QDD system and show that this new system is well-posed and entropic. In Section 4, the numerical scheme is constructed and we analyze its properties (well-posedness, stability). Finally, in Section 5 we illustrate these properties by some numerical simulations.

2 The quantum drift-diffusion model

This section is devoted to the presentation of the quantum drift-diffusion model (QDD). It is not clear which precise functional framework would be adapted to a rigorous analysis of this system. Nevertheless, we can still state some properties satisfied by any smooth solution of this system. This enables to put into perspective the results of Section 3. Indeed, we shall see in Section 3 that similar properties are satisfied by the solutions of the semi-discretized QDD system (3.21)–(3.23), whereas their existence can be rigourously proved.

2.1 Notations: the QDD model on a bounded domain

Let us first give a formulation of the quantum drift-diffusion model in the case of bounded domains. This model, which describes the evolution of a quantum system of electrons, was derived in [13] and a most convenient equivalent form of this model was written in the review paper [14]. The first equation is the equation of mass conservation:

$$\partial_t n + \nabla \cdot j = 0. \tag{2.1}$$

The second equation of the model is the constitutive equation which gives the expression of the current:

$$j = n\nabla(A - V). \tag{2.2}$$

In this equation, $V(t,x)$ is the selfconsistent potential (modeling the interactions between the electrons) and $A(t,x)$ is the *quantum chemical potential*, linked to the density by a relation which is non local in space and which is the key of this quantum model. In order to make this relation explicit, let us introduce the operator

$$H(A) = -\frac{\tilde{\hbar}^2}{2}\Delta + A + V^{ext},$$

whose domain $D(H)$ will be specified below and where $\tilde{\hbar}$ is the dimensionless Planck constant:

$$\tilde{\hbar} = \frac{\hbar}{(m^* L^2\, kT)^{1/2}},$$

m^* being the effective mass, L a characteristic length of the device and T the temperature. For simplicity, we will denote $\hbar$ the dimensionless Planck constant in the sequel. Here, $V^{ext}(x)$ is an external potential applied to the system (assumed independent of time for simplicity). In the QDD model, the electron system is at any time in a *local quantum equilibrium* (see [15, 13]) and its density matrix is

$$\varrho = \exp\left(-H(A)\right), \tag{2.3}$$

where exp denotes here the exponential of the operator. Remark that when the chemical potential A differs from the electrical potential, the operator $H(A)$ is not

the Hamiltonian and ϱ is not the density matrix of a global quantum equilibria as defined usually [5]. A consequence of this formula (2.3) is the relation between the density and the chemical potential, given in a weak sense by:

$$\forall \phi \in L^\infty \qquad \int n\,\phi\,dx = \mathrm{Tr}\ \left(\exp\left(-H(A)\right)\ \phi\right). \tag{2.4}$$

Here we used the usual convention where, for any test function ϕ, $\mathrm{Tr}\ (\exp(-H(A))\,\phi)$ denotes the trace of the composition of the exponential of the operator $-H(A)$ with the operator of multiplication by ϕ. Finally, the last equation of the model is the Poisson equation, which links the density and the selfconsistent potential:

$$-\alpha^2 \Delta V = n. \tag{2.5}$$

In this equation, α^2 is a dimensionless parameter, proportional to the square of the Debye length of the system; more precisely, if ε_0 and ε_r denote the vacuum permittivity and the relative permittivity of the material, if $\overline{n}$ denotes a characteristic density and if e denotes the elementary charge, we have

$$\alpha^2 = \frac{\varepsilon_0\,\varepsilon_r\,kT}{e^2\,L^2\,\overline{n}}.$$

A given background charge density may be taken into account in this model, for instance, by a modification of the external potential V^{ext} and a shift of the chemical potential A.

Let $\Omega \subset \mathbb{R}^d$ be a regular bounded domain ($d \leq 3$). Its boundary is denoted by $\partial\Omega$ and $\nu(x)$ is the outward unit normal vector at $x \in \partial\Omega$. All the unknowns of the system $n(t,x)$, $j(t,x)$, $A(t,x)$, $V(t,x)$ are defined for $t \geq 0$ and $x \in \Omega$. Now we need to precise the boundary conditions for this system. The most simple ones, that will be studied in this chapter, prescribe a vanishing current at the boundary. This no-flux boundary condition takes the form of the Neumann condition:

$$\nabla(A - V)\cdot\nu = 0 \qquad \text{on } \partial\Omega$$

(recall that we assume A and V smooth enough to give sense to this Neumann condition; for the semi-discretized model analyzed in Section 3, the $W^{2,p}$ regularity obtained in Theorem 3.1 is enough). For the selfconsistent potential, we consider a Dirichlet boundary condition

$$V = 0 \qquad \text{on } \partial\Omega.$$

It remains to fix the domain of the Hamiltonian $H(A)$. In the Note [21], the QDD model was written with Dirichlet boundary conditions for the wavefunctions, as well as its discrete version. Here, for technical reasons which will be explained further (we need to ensure the positivity of the density on $\overline{\Omega}$: see the beginning of the proof of Theorem 3.1), Neumann boundary conditions are chosen:

$$D(H) = \left\{\phi \in H^2(\Omega)\ :\ \nabla\phi\cdot\nu = 0 \qquad \text{on } \partial\Omega\right\}. \tag{2.6}$$

Hence, if A belongs to –say– $L^2(\Omega)$, then the operator $H(A)$ is bounded from below and has a compact resolvent. Let us denote by $(\psi_p(A))_{p=1,\cdots,\infty}$ an orthogonal basis of eigenfunctions, associated to the eigenvalues $\lambda_1(A) \leq \lambda_2(A) \leq \cdots \leq \lambda_p(A) \leq \cdots$. The non local relation (2.4) between n and A takes a more explicit form:

$$n(A) = \sum_{p\geq 1} e^{-\lambda_p(A)}\,|\psi_p(A)|^2. \tag{2.7}$$

To summarize this part, one can write the quantum drift-diffusion model including self-consistent effects as follows:

$$\partial_t n + \nabla \cdot (n \nabla (A - V)) = 0, \tag{2.8}$$

$$-\alpha^2 \Delta V = n, \tag{2.9}$$

$$n = \sum_p e^{-\lambda_p(A)} |\psi_p(A)|^2, \tag{2.10}$$

where $(\lambda_p(A), \psi_p(A))_p$ denote the eigenvalues and the eigenfunctions of the Hamiltonian $H(A) = -\frac{\hbar^2}{2}\Delta + A + V^{ext}$ whose domain is $D(H) = \{\Psi \in H^2(\Omega) \, : \, \partial_\nu \Psi = 0\}$. The unknowns of this system are subject to the following no-flux boundary conditions on $\partial\Omega$:

$$V = 0 \quad ; \quad \partial_\nu (A - V) = 0 \qquad\qquad (\partial\Omega) \tag{2.11}$$

and to a Cauchy datum $n^0(x)$.

In this chapter, the assumptions on the data will be the following ones:

Assumption 2.1 *The initial datum n^0 is continuous and positive on $\overline{\Omega}$.*

Assumption 2.2 *The external potential V^{ext} is nonnegative and belongs to $L^\infty(\Omega)$.*

2.2 Technical lemmas: the relation between n and A

In this subsection, we gather some technical lemmas that are used in this chapter. The first lemma, which is given without proof, is directly adapted from [40] (the only difference lies in the domain $D(H)$; in [40], a Dirichlet boundary condition was considered instead of our Neumann boundary condition).

Lemma 2.3 *Let $A \in H^1(\Omega)$ and let $n(A)$ be defined by*

$$n(A) = \sum_{p \geq 1} e^{-\lambda_p(A)} |\psi_p(A)|^2,$$

where $\lambda_p(A)$ and $\psi_p(A)$ are the spectral elements of

$$H(A) = -\frac{\hbar^2}{2}\Delta + A + V^{ext},$$

whose domain $D(H)$ is defined by (2.6). Then $n(A)$ is a continuous function on $\overline{\Omega}$. Moreover, the map F defined by

$$A \in H^1(\Omega) \mapsto F(A) := \mathrm{Tr}\left(e^{-H(A)}\right) = \int n(A)\, dx \tag{2.12}$$

is well-defined, Fréchet C^∞ and strictly convex. Its first derivative in the direction $\phi \in H^1(\Omega)$ reads

$$d_A F \cdot \phi = -\mathrm{Tr}\left(e^{-H(A)}\, \phi\right) = -\int n(A)\, \phi\, dx \tag{2.13}$$

and its second derivative reads

$$d_A^2 F \cdot \phi \cdot \phi = -\sum_{p=1}^{\infty} \sum_{q=1}^{\infty} \frac{e^{-\lambda_p(A)} - e^{-\lambda_q(A)}}{\lambda_p(A) - \lambda_q(A)} \left| \int \phi\, \psi_p\, \overline{\psi_q}\, dx \right|^2, \tag{2.14}$$

where $\frac{e^{-\lambda_p(A)} - e^{-\lambda_q(A)}}{\lambda_p(A) - \lambda_q(A)}$ conventionally equals $-e^{-\lambda_p(A)}$ if $\lambda_p(A) = \lambda_q(A)$.

Remark that this lemma gives a sense to the formula (2.7) as soon as A belongs to $H^1(\Omega)$.

Lemma 2.4 *Let A and $\widetilde{A}$ belong to $H^1(\Omega)$ and, using the notations of the previous lemma 2.3, let*

$$n = n(A) = \sum_{p\geq 1} e^{-\lambda_p(A)} |\psi_p(A)|^2, \qquad \widetilde{n} = n(\widetilde{A}) = \sum_{p\geq 1} e^{-\lambda_p(\widetilde{A})} |\psi_p(\widetilde{A})|^2.$$

Then we have

$$\int \Big(n(A-\widetilde{A}) + n - \widetilde{n} \Big)\, dx \leq 0. \tag{2.15}$$

Proof. The functional $F(A)$ defined in Lemma 2.3 is convex, thus we have the inequality:

$$F(\widetilde{A}) - F(A) \geq d_A F \cdot (\widetilde{A} - A).$$

The desired result is a consequence of the expression (2.13) of $d_A F$. □

2.3 Steady states and entropy dissipation

The steady states of the QDD system are well-known: these are the solutions of the Schrödinger-Poisson system studied by Nier in [40]. Following this reference, the following Proposition can be proved (its proof is left to the reader):

Proposition 2.5 *Let $N > 0$ and let (n, A, V) be a steady state of (2.8)–(2.10) such that $\int n(x)\, dx = N$. Assume that n is continuous and positive on $\overline{\Omega}$. Then there exists a constant ϵ_F such that $A = V - \epsilon_F$ and (n, V, ϵ_F) is the unique solution of the Schrödinger-Poisson system under a constraint of total charge:*

$$\begin{cases} -\dfrac{\hbar^2}{2}\Delta\psi_p + (V + V^{ext})\,\psi_p = \lambda_p\,\psi_p \qquad (p = 1, \cdots, \infty) \\ \psi_p \in D(H) \quad ; \quad \displaystyle\int \psi_p\,\overline{\psi_q} = \delta_{pq}\,, \end{cases} \tag{2.16}$$

$$-\alpha^2 \Delta V = n = \sum_p e^{\epsilon_F - \lambda_p} |\psi_p|^2, \qquad V \in H^1_0(\Omega), \tag{2.17}$$

$$\int n(x)\, dx = N. \tag{2.18}$$

Next, the following formal result shows that the QDD system coupled with the Poisson equation is entropic:

Proposition 2.6 *Let (n, A, V) be a smooth solution of (2.8)–(2.10). Then the following properties hold:*
(i) The following free energy $S(t)$ is a decreasing function of time and is bounded from below (by a negative constant depending only on Ω and $\hbar$):

$$S(t) = -\int n\,(A+1)\, dx + \frac{\alpha^2}{2}\int |\nabla V|^2\, dx.$$

(ii) If $(n^\infty, A^\infty, V^\infty)$ *is the solution of* (2.16)–(2.18) *corresponding to* $N = \int n(0,x)\,dx$, *then the following relative entropy* $\Sigma(t)$ *is the sum of two nonnegative terms and is a decreasing function of time:*

$$\Sigma(t) = -\int \left(n\,(A - A^\infty) + n - n^\infty\right) dx + \frac{\alpha^2}{2}\int |\nabla(V - V^\infty)|^2 dx.$$

Proof. By applying (2.15) with $\widetilde{A} \equiv 0$, we get

$$-\int n\,(A+1) \geq -\int n(0)\,dx.$$

Assumption 2.2 gives $V^{ext} \geq 0$. Hence, by the min-max formula, the eigenvalues $\lambda_p(0)$ of $H(0) = -\frac{\hbar^2}{2}\Delta + V^{ext}$ satisfy $\lambda_p(0) \geq \lambda_p^\Delta$, where λ_p^Δ are the eigenvalues of $-\frac{\hbar^2}{2}\Delta$ with Neumann boundary conditions on $\partial\Omega$. Thus we have

$$\int n(0)\,dx \leq \sum_p e^{-\lambda_p^\Delta}$$

and S is bounded from below by a constant which depends only on Ω and $\hbar$.

Let us now remark that, due to the no-flux boundary conditions (2.11), an integration of the first equation of (2.8)–(2.10) yields the conservation of the total charge:

$$\forall t \geq 0 \qquad \int n(t,x)\,dx = \int n(0,x)\,dx. \tag{2.19}$$

Independently, by differentiating with respect to time the functional $F(A)$ defined by (2.12), and recalling that V^{ext} is independent of time, we get

$$\frac{d}{dt}\int n(t,x)\,dx = \frac{d}{dt}F(A(t)) = d_A F \cdot \partial_t A = -\int n(t,x)\,\partial_t A(t,x)\,dx,$$

thus we have

$$\frac{d}{dt}\int n\,(A+1)\,dx = \int (\partial_t n) A\,dx.$$

To prove Item *(i)*, it remains to remark that the Poisson equation with Dirichlet boundary conditions yields

$$\frac{d}{dt}\frac{\alpha^2}{2}\int |\nabla V|^2\,dx = \int (\partial_t n)\,V\,dx.$$

Consequently we obtain

$$\frac{d}{dt}S(t) = -\int (\partial_t n)(A - V)dx = -\int n\,|\nabla(A - V)|^2\,dx \leq 0, \tag{2.20}$$

which proves *(i)*. Let us now prove *(ii)*. The fact that the first term of $\Sigma(t)$ is nonnegative stems from (2.15). Besides, since we have $A^\infty = V^\infty - \epsilon_F$, we deduce the equivalent expression:

$$\begin{aligned}\Sigma(t) \quad &= -\int \left(n\,(A + \epsilon_F) + n - n^\infty\right) dx \\ &\quad +\alpha^2 \int \nabla V \cdot \nabla V^\infty\,dx + \frac{\alpha^2}{2}\int |\nabla(V - V^\infty)|^2 \\ &= S(t) - \epsilon_F \int n\,dx + \int n^\infty\,dx + \frac{\alpha^2}{2}\int |\nabla V^\infty|^2\,dx,\end{aligned}$$

where we used the Poisson equation $-\alpha^2 \Delta V = n$. Therefore, by using (2.19), we deduce

$$\frac{d}{dt}\Sigma(t) = \frac{d}{dt}S(t) \leq 0.$$

□

Remark 2.7 *Eq. (2.20) gives the expression of the entropy dissipation. This term indicates that, in long time, $A - V$ should converge towards a constant. Thus any transient solution of the QDD model should converge to the (unique) corresponding steady state. In order to prove rigourously this convergence, we need to control n from below; this is an open problem.*

3 Semi-discretization in time

This section is devoted to the study of a semi-discrete version of (2.8)–(2.10), which appears as a first step towards the numerical scheme that is presented in Section 4. Let $\Delta t > 0$ be the time step. For $k \in \mathbb{N}$, the semi-discretized model is written:

$$\frac{n^{k+1} - n^k}{\Delta t} + \nabla \cdot \left(n^k \nabla (A^{k+1} - V^{k+1}) \right) = 0, \tag{3.21}$$

$$-\alpha^2 \Delta V^{k+1} = n^{k+1}, \tag{3.22}$$

$$n^{k+1} = \sum_p e^{-\lambda_p(A^{k+1})} |\psi_p(A^{k+1})|^2, \tag{3.23}$$

subject to the boundary conditions

$$V^{k+1} = 0 \quad ; \quad \partial_\nu (A^{k+1} - V^{k+1}) = 0. \tag{3.24}$$

Recall that, in this system, $\lambda_p(\cdot)$ and $\psi_p(\cdot)$ denote the whole sequence of eigenvalues and eigenfunctions of the operator $H(\cdot)$ defined in Section 2.1 by

$$H(A) = -\frac{\hbar^2}{2}\Delta + A + V^{ext}.$$

The unknowns are the density $n^k(x)$, the quantum chemical potential $A^k(x)$ and the selfconsistent potential $V^k(x)$, for $k \in \mathbb{N}^*$. For $k = 0$, the density n^0 is given satisfying Assumption 2.1. Then the Poisson equation enables to define V^0. Concerning the initial chemical potential A^0, since it is not clear whether (2.7) can be inverted, we choose to let A^0 undetermined. Remark that A^0 is not required in this model to compute (n^k, A^k, V^k) for $k \geq 1$. An alternative choice for the initial conditions would be to take an initial datum A^0, then to deduce n^0 by (2.7) and V^0 by the Poisson equation. However, it seems more interesting, for physical reasons, to start from an initial density n^0.

The main result of this section is the

Theorem 3.1 *Under Assumptions 2.1 and 2.2, we have the following properties:*
(i) The semi-discretized model (3.21)–(3.23) is well-posed. For all $k \in \mathbb{N}^*$, the functions $A^k \in W^{2,p}(\Omega)$, $V^k \in W^{2,p}(\Omega)$ (for any $p < \infty$) and $n^k \in C(\overline{\Omega})$ are uniquely

defined and, for all k, we have $n^k > 0$ on $\overline{\Omega}$.
(ii) The total charge is conserved:

$$\forall k \in \mathbb{N} \qquad \int n^k \, dx = \int n^0 \, dx \tag{3.25}$$

and the following free energy S^k, defined for $k \geq 1$, is bounded from below and decreases as k increases:

$$S^k = -\int n^k \left(A^k + 1\right) dx + \frac{\alpha^2}{2} \int |\nabla V^k|^2 \, dx.$$

(iii) If $(n^\infty, A^\infty, V^\infty)$ is the solution of the Schrödinger-Poisson system (2.16)–(2.18) corresponding to $N = \int n^0 \, dx$, then the following relative entropy Σ^k is the sum of two nonnegative terms and decreases as k increases:

$$\Sigma^k = -\int \left(n^k \left(A^k - A^\infty\right) + n^k - n^\infty\right) dx + \frac{\alpha^2}{2} \int |\nabla (V^k - V^\infty)|^2.$$

Proof. *(i)* Let us first give the outline of this proof. We shall proceed by induction: for any function n^k, positive and continuous on $\overline{\Omega}$, we will show that there exists a unique pair $(A^{k+1}, V^{k+1}) \in H^1(\Omega) \times H^1_0(\Omega)$ satisfying

$$\frac{n(A^{k+1}) - n^k}{\Delta t} + \nabla \cdot \left(n^k \nabla (A^{k+1} - V^{k+1})\right) = 0 \tag{3.26}$$

and

$$-\alpha^2 \Delta V^{k+1} = n(A^{k+1}), \tag{3.27}$$

with the boundary condition (3.24), where we recall the notation

$$n(A^{k+1}) = \sum_p e^{-\lambda_p(A^{k+1})} \, |\psi_p(A^{k+1})|^2.$$

Then, as soon as (A^{k+1}, V^{k+1}) is defined, it suffices to set $n^{k+1} = n(A^{k+1})$ and (3.21)–(3.23) is satisfied. Moreover, the first part of Lemma 2.3 shows that n^{k+1} is continuous on $\overline{\Omega}$. Hence, (3.21)–(3.23) and standard elliptic regularity estimates imply that for any $p < \infty$ we have $V^{k+1} \in W^{2,p}(\Omega)$ and $A^{k+1} \in W^{2,p}(\Omega)$. By Sobolev embeddings, we deduce that $A^{k+1} \in L^\infty(\Omega)$, which is enough to apply Krein-Rutman's theorem [10]: the choice of Neumann boundary conditions for the eigenfunction ψ_p (see (2.6)) ensures the fact that ψ_1^{k+1} does not vanish on the closed domain $\overline{\Omega}$. Consequently n^{k+1} is itself positive and continuous on $\overline{\Omega}$, and can be used to initiate the next step of the induction: we are then able to construct $(A^{k+2}, V^{k+2}, n^{k+2})$. Finally, thanks to Assumption 2.1 on the initial density n^0, all the sequence $(A^k, V^k, n^k)_{k \geq 1}$ can be constructed by induction.

Let us now prove the claim: for any given positive and continuous function n^k, one can construct a unique corresponding (A^{k+1}, V^{k+1}) satisfying (3.26), (3.27). This proof, inspired by [39, 40], is based on a variational argument. We introduce the following functional, defined for $A \in H^1(\Omega)$ and $V \in H^1_0(\Omega)$:

$$J(A, V) = \frac{\Delta t}{2} \int n^k \, |\nabla (A - V)|^2 \, dx + \frac{\alpha^2}{2} \int |\nabla V|^2 \, dx + F(A) + \int n^k \left(A - V\right) dx,$$

where $F(A)$ is defined by

$$F(A) = \mathrm{Tr}\, \left(e^{-H(A)}\right) = \sum_{p \geq 1} e^{-\lambda_p(A)}.$$

Note that this functional J depends on n^k. By Lemma 2.3, this functional is continuous, Fréchet differentiable, and its derivative is given by

$$\begin{aligned} d_{A,V}J\cdot(\delta A,\delta V) = \quad & \Delta t\int n^k\,\nabla(A-V)\cdot\nabla(\delta A-\delta V)\,dx \\ & +\alpha^2\int\nabla V\cdot\nabla\delta V\,dx \\ & -\int n(A)\,\delta A\,dx+\int n^k\,(\delta A-\delta V)\,dx, \end{aligned}$$

where $\delta A\in H^1(\Omega)$, $\delta V\in H^1_0(\Omega)$ and we recall the notation

$$n(A)=\sum_p e^{-\lambda_p(A)}\,|\psi_p(A)|^2.$$

Therefore it is readily seen that the critical points of J satisfy (3.21)–(3.23), (3.24). To prove the existence and uniqueness of A^{k+1} and V^{k+1}, it suffices to show that J is strictly convex and coercive, since its unique minimizer will be (A^{k+1},V^{k+1}). The strict convexity is a consequence of Lemma 2.3 (which states that F is strictly convex), of the strict convexity of the functional

$$V\in H^1_0(\Omega)\longmapsto\int|\nabla V|^2\,dx$$

and of the convexity of the functional

$$(A,V)\in H^1(\Omega)\times H^1_0(\Omega)\longmapsto\int n^k\,|\nabla(A-V)|^2\,dx.$$

It remains to prove the coercivity with respect to $A\in H^1(\Omega)$ and $V\in H^1_0(\Omega)$. Let $(A^\varepsilon,V^\varepsilon)$ be a sequence in $H^1(\Omega)\times H^1_0(\Omega)$, parameterized by $\varepsilon>0$, such that $J(A^\varepsilon,V^\varepsilon)$ has an upper bound independent of ε. To prove the coercivity of J, it suffices to show that $\|A^\varepsilon\|_{H^1}+\|V^\varepsilon\|_{H^1}$ can be bounded independently of ε.

Setting $a^\varepsilon=\frac{1}{|\Omega|}\int A^\varepsilon\,dx$ (where $|\Omega|$ denotes the measure of Ω), we introduce the function $B^\varepsilon=A^\varepsilon-a^\varepsilon$. We have

$$\begin{aligned} J(A^\varepsilon,V^\varepsilon) = \quad & \frac{\Delta t}{2}\int n^k\,|\nabla(B^\varepsilon-V^\varepsilon)|^2\,dx+\frac{\alpha^2}{2}\int|\nabla V^\varepsilon|^2\,dx \\ & +e^{-a^\varepsilon}\sum_p e^{-\lambda_p(B^\varepsilon)}+\int n^k\,(B^\varepsilon-V^\varepsilon)\,dx+a^\varepsilon\int n^k\,dx\le C, \end{aligned}$$

where C does not depend on ε. We recall that there exist two constants $\underline{n}>0$ and $\overline{n}>0$, independent of ε, such that

$$\underline{n}\le n^k(x)\le\overline{n}\qquad\text{on }\overline{\Omega}.$$

Hence the Cauchy-Schwarz inequality gives

$$\begin{aligned} \frac{\Delta t}{2}\,\underline{n}\int|\nabla(B^\varepsilon-V^\varepsilon)|^2\,dx+\frac{\alpha^2}{2}\int|\nabla V^\varepsilon|^2\,dx-\overline{n}\,|\Omega|^{1/2}\left(\|B^\varepsilon\|_{L^2(\Omega)}+\|V^\varepsilon\|_{L^2(\Omega)}\right) \\ +e^{-a^\varepsilon}\sum_p e^{-\lambda_p(B^\varepsilon)}+a^\varepsilon\int n^k\,dx\le J(A^\varepsilon,V^\varepsilon)\le C. \end{aligned} \tag{3.28}$$

Besides, denoting by $\widetilde{H^1}(\Omega)$ the space of $H^1(\Omega)$ functions which have a vanishing integral on Ω, a classical compactness argument shows that, for any $a_1 > 0$ and $a_2 > 0$, the norm

$$(B,V) \in \widetilde{H^1}(\Omega) \times H^1_0(\Omega) \quad \longmapsto \quad \Big(a_1 \|\nabla(B-V)\|^2_{L^2(\Omega)} + a_2 \|\nabla V\|^2_{L^2(\Omega)}\Big)^{1/2}$$

is equivalent on this space $\widetilde{H^1}(\Omega) \times H^1_0(\Omega)$ to the standard $H^1(\Omega) \times H^1(\Omega)$ norm. Hence there exist two constants $C_0 > 0$ and $C_1 > 0$ independent of ε such that

$$\frac{\Delta t}{2}\,\underline{n} \int |\nabla(B^\varepsilon - V^\varepsilon)|^2\,dx + \frac{\alpha^2}{2}\int |\nabla V^\varepsilon|^2\,dx - \overline{n}\,|\Omega|^{1/2}\left(\|B^\varepsilon\|_{L^2(\Omega)} + \|V^\varepsilon\|_{L^2(\Omega)}\right)$$
$$\geq C_0\|B^\varepsilon\|^2_{H^1(\Omega)} + C_0\|V^\varepsilon\|^2_{H^1(\Omega)} - C_1$$

thus (3.28) gives

$$C_0\|B^\varepsilon\|^2_{H^1(\Omega)} + C_0\|V^\varepsilon\|^2_{H^1(\Omega)} + e^{-a^\varepsilon}\sum_p e^{-\lambda_p[B^\varepsilon)} + a^\varepsilon \int n^k\,dx \leq C. \tag{3.29}$$

Let us now recall that the first eigenvalue of $H(B^\varepsilon)$ is defined by

$$\lambda_1(B^\varepsilon) = \min_{\substack{\phi \in H^1(\Omega) \\ \|\phi\|_{L^2(\Omega)} = 1}} \left(\frac{\hbar^2}{2}\int |\nabla\phi|^2\,dx + \int (B^\varepsilon + V^{ext})\,\phi^2\,dx\right).$$

By choosing the test function $\phi(x) \equiv 1/\sqrt{|\Omega|}$ in this formula, we deduce from $\int B^\varepsilon\,dx = 0$ that

$$\lambda_1(B^\varepsilon) \leq \frac{1}{|\Omega|}\int V^{ext}\,dx.$$

There exists consequently a constant $C_2 > 0$ independent of ε such that

$$e^{-a^\varepsilon}\sum_p e^{-\lambda_p(B^\varepsilon)} \geq C_2\,e^{-a^\varepsilon}$$

and (3.29) implies

$$C_0\|B^\varepsilon\|^2_{H^1(\Omega)} + C_0\|V^\varepsilon\|^2_{H^1(\Omega)} + C_2 e^{-a^\varepsilon} + a^\varepsilon \int n^k\,dx \leq C.$$

Since $\int n^k\,dx > 0$, it is clear then that $\|B^\varepsilon\|_{H^1(\Omega)}$, $\|V^\varepsilon\|_{H^1(\Omega)}$ and $|a^\varepsilon|$ are bounded independently of ε. Thus $\|A^\varepsilon\|_{H^1(\Omega)}$ is bounded, which completes the proof of coercivity.

(ii) The conservation of mass (3.25) can be easily shown by an integration of (3.21) on Ω, which gives, thanks to the boundary conditions (3.24):

$$\int n^{k+1}\,dx = \int n^k\,dx. \tag{3.30}$$

To prove the decay of the free energy, let us adapt to the semi-discrete case the proof of Proposition 2.6. By using Lemma 2.4, we have

$$\int \left(n^k(A^k - A^{k+1}) + n^k - n^{k+1}\right)\,dx \leq 0,$$

thus

$$\begin{aligned} -\int (n^{k+1}\,A^{k+1} - n^k\,A^k + n^{k+1} - n^k)\,dx &= -\int (n^{k+1} - n^k)\,A^{k+1}\,dx \\ &\quad + \int \left(n^k (A^k - A^{k+1}) + n^k - n^{k+1} \right) dx \\ &\leq -\int (n^{k+1} - n^k)\,A^{k+1}\,dx. \end{aligned} \tag{3.31}$$

Besides, by using the Poisson equation (3.22), we obtain

$$\begin{aligned} \frac{\alpha^2}{2} \int \left(|\nabla V^{k+1}|^2 - |\nabla V^k|^2 \right) dx &= \frac{1}{2} \int (n^{k+1}\,V^{k+1} - n^k\,V^k)\,dx \\ &= \frac{1}{2} \int (n^{k+1} - n^k)\,V^{k+1}\,dx + \frac{1}{2} \int n^k (V^{k+1} - V^k)\,dx \\ &= \frac{1}{2} \int (n^{k+1} - n^k)\,V^{k+1}\,dx + \frac{1}{2} \int V^k (n^{k+1} - n^k)\,dx. \end{aligned}$$

By remarking that

$$0 \leq \alpha^2 \int |\nabla (V^{k+1} - V^k)|^2 dx = \int (n^{k+1} - n^k)(V^{k+1} - V^k),$$

we deduce that

$$\frac{1}{2} \int V^k (n^{k+1} - n^k)\,dx \leq \frac{1}{2} \int V^{k+1} (n^{k+1} - n^k)\,dx$$

and get

$$\frac{\alpha^2}{2} \int \left(|\nabla V^{k+1}|^2 - |\nabla V^k|^2 \right) dx \leq \int V^{k+1} (n^{k+1} - n^k)\,dx.$$

By combining this inequality and (3.31), we obtain

$$\begin{aligned} S^{k+1} - S^k &\leq -\int (n^{k+1} - n^k)(A^{k+1} - V^{k+1})\,dx \\ &= \Delta t \int (A^{k+1} - V^{k+1})\,\nabla \cdot \left(n^k \nabla (A^{k+1} - V^{k+1}) \right) dx, \end{aligned}$$

thanks to (3.21). An integration by parts, using (3.24), gives finally

$$S^{k+1} - S^k \leq -\Delta t \int n^k\,|\nabla (A^{k+1} - V^{k+1})|^2\,dx \leq 0.$$

This proves *(ii)*. Finally, to prove *(iii)*, it suffices to remark as for Proposition 2.6 that

$$\Sigma^{k+1} - \Sigma^k = S^{k+1} - S^k \leq 0.$$

□

4 The fully discretized system: construction and analysis

We complete the construction of a numerical scheme for the QDD model (2.8)–(2.10) by now discretizing the system (3.21)–(3.23) with respect to the space variable. In the following section, we construct the scheme and give in Theorem 4.1 its main properties: well-posedness, charge conservation and entropy dissipation. These properties are proved in Section 4.2. Section 4.3 is devoted to the particular question of the initial step: it is shown in Proposition 4.4 that, at the discrete level, there exists a unique chemical potential A corresponding to each positive density n.

4.1 Notations and main results

For simplicity, the space dimension is now $d = 1$. The domain is $\Omega = (0,1)$ and the space gridstep is $\Delta x = 1/(N+1)$. The grid is composed of the points $x_i = i\Delta x$ for $i = 0, \cdots, N+1$, where $N \in \mathbb{N}$. In order to write the fully discretized finite difference numerical scheme, let us introduce the following $N \times N$ matrices of discrete derivative:

$$D^- = \frac{1}{\Delta x}\begin{pmatrix} 0 & 0 & \cdots & \\ -1 & 1 & 0 & \cdots \\ 0 & \ddots & \ddots & 0 \\ \vdots & 0 & -1 & 1 \end{pmatrix}, \qquad D^+ = \frac{1}{\Delta x}\begin{pmatrix} -1 & 1 & 0 & \dots \\ 0 & -1 & 1 & \cdots \\ 0 & \ddots & \ddots & 1 \\ \vdots & \cdots & 0 & 0 \end{pmatrix},$$

$$\widetilde{D^-} = \frac{1}{\Delta x}\begin{pmatrix} 1 & 0 & \cdots & \\ -1 & 1 & 0 & \cdots \\ 0 & \ddots & \ddots & 0 \\ \vdots & 0 & -1 & 1 \end{pmatrix}, \qquad \widetilde{D^+} = \frac{1}{\Delta x}\begin{pmatrix} -1 & 1 & 0 & \dots \\ 0 & -1 & 1 & \cdots \\ 0 & \ddots & \ddots & 1 \\ \vdots & \cdots & 0 & 1 \end{pmatrix},$$

$$\Delta_{Dir} = \frac{1}{\Delta x^2}\begin{pmatrix} -2 & 1 & 0 & \dots \\ 1 & -2 & \ddots & 0 \\ 0 & \ddots & \ddots & 1 \\ \vdots & \cdots & 1 & -2 \end{pmatrix}, \qquad \Delta_{Neu} = \frac{1}{\Delta x^2}\begin{pmatrix} -1 & 1 & 0 & \dots \\ 1 & -2 & \ddots & 0 \\ 0 & \ddots & \ddots & 1 \\ \vdots & \cdots & 1 & -1 \end{pmatrix}.$$

Remark that $\Delta_{Neu} = \widetilde{D^-}D^+ = \widetilde{D^+}D^-$. The unknowns are the following sequences of vectors in $\mathbb{R}^N$: $n^k = (n_i^k)_{1\le i\le N}$, $A^k = (A_i^k)_{1\le i\le N}$, $V^k = (V_i^k)_{1\le i\le N}$ and the scheme is written:

$$\frac{n^{k+1}-n^k}{\Delta t} + \frac{1}{2}\widetilde{D^-}\left(n^k\, D^+(A^{k+1}-V^{k+1})\right) + \frac{1}{2}\widetilde{D^+}\left(n^k\, D^-(A^{k+1}-V^{k+1})\right) \tag{4.32}$$

$$-\alpha^2\,\Delta_{Dir}V^k = n^k, \tag{4.33}$$

$$n^k = \sum_p \exp\left(-\ell_p(A^k)\right)(X_p(A^k))^2 \tag{4.34}$$

for $k \in \mathbb{N}$ (here and in the sequel, for any $(X,Y) \in \mathbb{R}^N \times \mathbb{R}^N$, XY denotes the direct product $(X_iY_i)_{1\le i\le N}$). In this discretized system, the definitions of $\ell_p(A)$ and $X_p(A)$ are the discrete analogue of those of $\lambda_p(A)$, $\psi_p(A)$ for the continuous problem.

These quantities are the eigenvalues and the normalized eigenvectors of the discretized Hamiltonian with Neumann boundary conditions:

$$M(A) = -\frac{\hbar^2}{2}\Delta_{Neu} + \mathrm{Diag}(A + V^{ext}),$$

where $\mathrm{Diag}(A)$ denotes the diagonal matrix of coefficients $(A_i)_{1\le i\le N}$ and where the components of the vector V^{ext} are $V_i^{ext} = \frac{1}{\Delta x}\int_{x_{i-1/2}}^{x_{i+1/2}} V^{ext}(x)\,dx$. Of course, the index p of the eigenvalues and eigenvectors belongs now to $\{1, \cdots, N\}$. Moreover, the eigenvectors are normalized with respect to the euclidean norm $\|\cdot\|_N$ associated to the scalar product on $\mathbb{R}^N$:

$$(U, V)_N = \Delta x \sum_{i=1}^{N} U_i\, V_i\,.$$

Remark that the boundary conditions are already taken into account in this scheme, the values of the unknowns for $i = 0$ or $i = N + 1$ being implicitly defined. To complete (4.32)–(4.34), it suffices to add an initial condition. If a Cauchy data for the continuous problem n^0 is given, the vector $n^0 \in \mathbb{R}^N$ is chosen as follows:

$$n_i^0 = \frac{1}{\Delta x}\int_{x_{i-1/2}}^{x_{i+1/2}} n^0(x)\,dx \qquad \text{for } i = 1, \cdots, N. \tag{4.35}$$

The numerical scheme (4.32)–(4.34) is clearly consistent with the QDD system (2.8)–(2.11). Its properties are listed in the following Theorem, whose proof is developed in the three next subsections:

Theorem 4.1 *If Assumptions 2.1 and 2.2 are satisfied, the numerical scheme (4.32)–(4.35) is consistent with (2.8)–(2.11) and has the following properties:*
(i) (well-posedness) *For all $k \in \mathbb{N}$, its numerical solution (n^k, A^k, V^k) is uniquely defined. Moreover, for all $k \in \mathbb{N}$, (A^{k+1}, V^{k+1}) is the unique minimizer of the strictly convex and coercive functional*

$$\begin{aligned}\widehat{J}(A, V) = \;& \frac{\Delta t\,\Delta x}{4}\sum_{i=1}^{N} n_i^k\,(D^+(A - V))_i^2 + \frac{\Delta t\,\Delta x}{4}\sum_{i=1}^{N} n_i^k\,(D^-(A - V))_i^2 \\ & + \frac{\alpha^2\,\Delta x}{2}\sum_{i=1}^{N}(D^+V)_i^2 + \frac{\alpha^2}{2\,\Delta x}(V_1)^2 + \frac{\alpha^2}{2\,\Delta x}(V_N)^2 \\ & + \sum_{p=1}^{N}\exp\left(-\ell_p(A)\right) + \Delta x\sum_{i=1}^{N} n_i^k\,(A_i - V_i)\,.\end{aligned} \tag{4.36}$$

(ii) (charge conservation) *For all k and for all i we have $n_i^k > 0$ and the (discrete) total charge is conserved:*

$$\forall k \in \mathbb{N} \qquad \Delta x\sum_{i=1}^{N} n_i^k = \Delta x\sum_{i=1}^{N} n_i^0\,. \tag{4.37}$$

(iii) (entropy dissipation) *The sequence of (discrete) free energies defined by*

$$S^k = -\Delta x\sum_{i=1}^{N} n_i^k\,(A_i^k + 1) + \frac{\alpha^2\Delta x}{2}\sum_{i=1}^{N}(D^+V^k)_i^2 + \frac{\alpha^2}{2\,\Delta x}(V_1^k)^2 + \frac{\alpha^2}{2\,\Delta x}(V_N^k)^2 \tag{4.38}$$

is decreasing and belongs to ℓ^∞. Moreover there exists a constant $C > 0$ (depending only on Ω and $\hbar$) such that, for any $K \in \mathbb{N}$, we have

$$\begin{aligned} -C \leq S^K + \frac{\Delta t \Delta x}{2} \sum_{k=1}^{K} \sum_{i=1}^{N} n_i^{k-1} \left(D^+(A^k - V^k)\right)_i^2 \\ + \frac{\Delta t \Delta x}{2} \sum_{k=1}^{K} \sum_{i=1}^{N} n_i^{k-1} \left(D^-(A^k - V^k)\right)_i^2 \leq S^0. \end{aligned} \tag{4.39}$$

4.2 Proof of well-posedness and entropy dissipation

For the sake of conciseness, we shall only sketch the proof of Theorem 4.1. Indeed, it suffices to adapt to the discrete case the proof of Theorem 3.1. These results are based on formulas of discrete integration by parts and on technical results concerning matrix analysis which are the discrete equivalents of the technical results stated in Section 2.2, and that we have listed in Lemma 4.2 below.

It is worthwhile to precise that the similarity between the functional $J(A, V)$, introduced in the proof of Theorem 3.1, and the functional $\widehat{J}(A, V)$ of this Theorem 4.1 is due to two useful formulas of discrete integration by parts: for any pair of vectors $(U, V) \in \mathbb{R}^N \times \mathbb{R}^N$, we have

$$\begin{aligned} -\left(\Delta_{Neu} U, V\right)_N &= -\left(\widetilde{D^-} D^+ U, V\right)_N = \left(D^+ U, D^+ V\right)_N \\ &= -\left(\widetilde{D^+} D^- U, V\right)_N = \left(D^- U, D^- V\right)_N \end{aligned} \tag{4.40}$$

and

$$-\left(\Delta_{Dir} U, V\right)_N = \left(D^+ U, D^+ V\right)_N + \frac{U_1 V_1 + U_N V_N}{\Delta x}. \tag{4.41}$$

Next, we gather in the following lemma some classical but useful technical results on matrices:

Lemma 4.2 *Let $A \in \mathbb{R}^N$. Then the eigenvalues $\ell_p(A)$ of the matrix $M(A) = -\frac{\hbar^2}{2}\Delta_{Neu} + \mathrm{Diag}(A + V^{ext})$ are simple. (Up to a multiplication by -1), its first eigenvector $X_1(A)$ has positive components. The derivatives of the eigenvalues and eigenvectors of $M(A)$ with respect to A, in the direction δA, are given by*

$$d\ell_p(A) \cdot \delta A = \left(\delta A\, X_p(A), X_p(A)\right)_N,$$

$$dX_p(A) \cdot \delta A = \sum_{q \neq p} \frac{1}{\ell_p(A) - \ell_q(A)} \left(\delta A\, X_p(A), X_q(A)\right)_N X_q(A).$$

Proof. The simplicity of the eigenvalues of $M(A)$ is a general classical result for Hessenberg matrices [49], *i.e* matrices $M = (m_{i,j})_{1 \leq i,j \leq N}$ such that

$$m_{i,j} = 0 \text{ for } j < i - 1 \qquad \text{and} \qquad m_{i,i-1} \neq 0 \text{ for } 2 \leq i \leq N.$$

This simplicity enables to differentiate ℓ_p and $X_p(A)$ by using classical perturbation theory.

Let $\lambda = 1 + \max_i |A_i|$. Then it is clear that the matrix $M(A) + \lambda I$ is invertible and satisfies the discrete maximum principle:

$$\forall Y \in \mathbb{R}^N \backslash \{0\} \qquad Y \geq 0 \quad \Longrightarrow \quad \left(M(A) + \lambda I\right)^{-1} Y > 0,$$

where, for any vector $X \in \mathbb{R}^N$, the notation $X \geq 0$ (resp. $X > 0$) stands for $X_i \geq 0$ (resp. $X_i > 0$), for all $i = 1, \cdots, N$. Hence Perron-Frobenius theorem (see [49]) applies to the matrix $(M(A) + \lambda I)^{-1}$: the spectral radius of this matrix is an eigenvalue and, up to a multiplication by -1, the corresponding eigenvector has positive components. This vector is the ground state $X_1(A)$ of $M(A)$. □

Remark 4.3 *A special care has to be taken for the initial step of the scheme. In the semi-discrete case of system (3.21)–(3.23), the question of the initial step was left unsolved: for a given initial density $n^0(x)$, can we define a unique corresponding chemical potential A^0 such that (3.23) holds ? In the fully discrete case, this question finds a positive answer, as stated in Theorem 4.1,* (i). *Section 4.3 is devoted to this particular point of the theorem.*

4.3 Initialization of the chemical potential

As noted above in Remark 4.3, one question has not been addressed yet concerning the numerical scheme (4.32)–(4.35): the computation of the initial chemical potential A^0 corresponding to the initial data n^0. While, in the continuous problem, we do not know whether (or in which functional framework) the non local relation (2.7) linking n to A is invertible, this operation is possible with its discrete analogous (4.34). The aim of this section is to establish this property: we show that this problem is again equivalent to a convex minimization problem. Remark that this enables to deduce a practical method to solve numerically this problem, by writing an algorithm for this optimization problem (see [20] for details). Note also that the possibility of inverting the constitutive relation $A \mapsto n(A)$, interesting for itself, is not mandatory for the other steps of the scheme (see Theorem 4.1 *(i)*): the minimization of J for the computation of (A^{k+1}, V^{k+1}) does not require the knowledge of A^k. The following Proposition is the main result of this subsection:

Proposition 4.4 *Let $n \in (\mathbb{R}_+^*)^N$. Then there exists a unique $A \in \mathbb{R}^N$ such that*

$$n = \sum_{p=1}^{N} \exp\left(-\ell_p(A)\right) \left(X_p(A)\right)^2, \tag{4.42}$$

where $\ell_p(A)$ and $X_p(A)$ are the eigenvalues and the eigenvectors of the discrete Hamiltonian $M(A) = -\frac{\hbar^2}{2}\Delta_{Neu} + \mathrm{Diag}(A + V^{ext})$.

Proof. Consider the functional

$$\Phi(A) = \sum_{p} \exp\left(-\ell_p(A)\right) + (n, A)_N \,. \tag{4.43}$$

Straightforward calculations using Lemma 4.2 lead to the expression of its first and second derivatives:

$$d\Phi_A \cdot \delta A = \left(n - \sum_{p} \exp(-\ell_p(A)) \left(X_p(A)\right)^2, \delta A \right)_N$$

and

$$d^2\Phi_A \cdot \delta A \cdot \delta A = \sum_{p=1}^{N} \exp(-\ell_p(A)) \, (\delta A \, X_p(A) \, , \, X_p(A))_N^2 \\ - \sum_p \sum_{q \neq p} \frac{\exp(-\ell_p(A)) - \exp(-\ell_q(A))}{\ell_p(A) - \ell_q(A)} \, (\delta A \, X_p(A) \, , \, X_q(A))_N^2 \, .$$

It is clear then that this functional Φ is strictly convex and that its unique minimizer satisfies (4.42). To prove the existence of a solution to the problem, the major task is to prove the coercivity of this functional.

Recall that

$$\ell_1(A) = \min_{\|\phi\|_N = 1} \left((-\frac{\hbar^2}{2} \Delta_{Neu} \phi, \phi)_N + (\mathrm{Diag}(A + V^{ext})\phi, \phi)_N \right) . \tag{4.44}$$

Let $i_0 \in \{1, \cdots, N\}$ (arbitrary). By choosing the i_0-th normalized basis vector as ϕ in (4.44) (*i.e.* $\phi_i = \delta_{i,i_0}/\sqrt{\Delta x}$), we obtain

$$\ell_1(A) \leq A_{i_0} + \frac{\hbar^2}{\Delta x^2} + V_{i_0}^{ext} \, . \tag{4.45}$$

Hence, there exists a constant $C > 0$ depending only on Δx, $\hbar$ and V^{ext} such that

$$\Phi(A) \geq C \sum_i \exp\left(-A_i\right) + \Delta x \sum_i n_i \, A_i \, . \tag{4.46}$$

Since for all i we have $n_i > 0$, it is clear that

$$\lim_{\|A\| \to \infty} \Phi(A) = +\infty.$$

This proves the coercivity of Φ. □

5 Numerical results

In order to simulate the quantum drift-diffusion model, the numerical scheme (4.32)–(4.34) has been implemented by minimizing the functional $\widehat{J}$ defined by (4.36). Each strictly convex unconstrained minimization problem is solved by a Newton method (note that the Hessian matrix is explicit and always positive definite). The computation of the eigenelements of the discrete Hamiltonian $M(A)$ is performed by using the matlab function `eigs` [36]. For details concerning the practical implementation of the scheme, one can refer to [20].

The external potential is a discontinuous function playing the role of a double barrier structure potential and the initial density n^0 is concentrated on the left of the double barrier (see Figure I.1). The initial step involves the inversion of the formula (4.42), *i.e.* the computation of the initial chemical potential A^0 corresponding to n^0. The calculation of A^0 is done by minimizing the strictly convex functional Φ defined in (4.43). Recall that A^0 is not used in the sequel of the algorithm.

On Figures I.1, I.2, I.3, I.4 and I.5, we have represented, as functions of x, the density n, the total potential $V + V^{ext}$ and the electrochemical potential $A - V$ at the

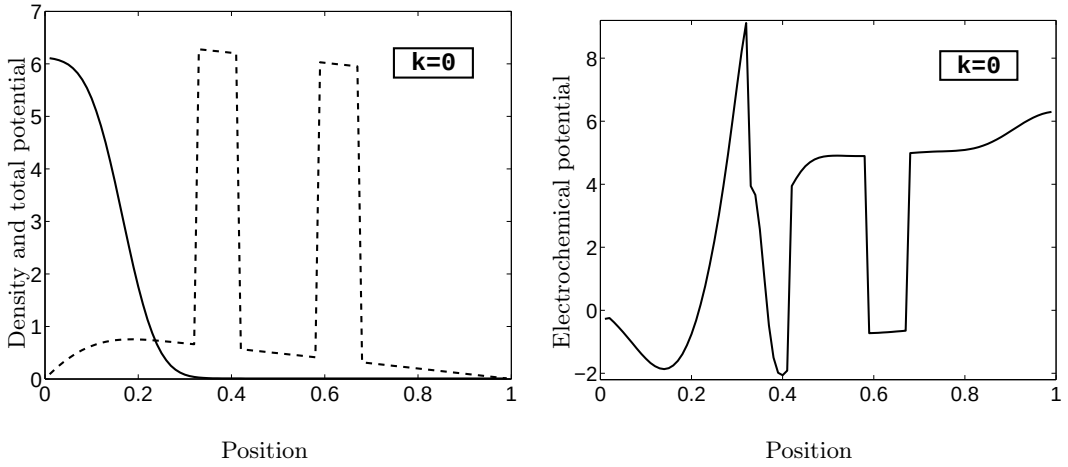

Figure I.1: Numerical solution of the QDD model: initial step. Left: the density $n(x)$ (solid line) and the total potential $(V+V^{ext})(x)$(dashed line) as functions of the position x. Right: the electrochemical potential $(A-V)(x)$.

initial step and at different time steps: $k = 3$, 20, 100, 500. The parameters of these computations are the following ones:

Δx	Δt	$\hbar^2$	α^2
0.01	0.005	0.04	0.1

On the right side of these figures, one can check that the electrochemical potential converges to a constant: at time $t = 500\Delta t$, one can consider that the system has converged to a steady state, which solves a discrete Schrödinger-Poisson system. On Figure I.6, we show the evolution of the free energy S^k defined by (4.38) and check that it is a decreasing function, converging to a constant. In these simulations, the initial total charge is equal to 1 and this quantity is conserved during the evolution, up to a relative error of 10^{-4} %.

6 Conclusion

We have introduced a semi-discrete (in time) version (3.21)–(3.23) of the quantum drift-diffusion model (2.8)–(2.10). We have proved that this system is well-posed and that its resolution amounts to minimizing a convex functional. Moreover, this semi-discrete model has the following interesting properties: it preserves the total charge and the positivity of the density and it dissipates the free energy. Then we have defined the numerical scheme (4.32)–(4.34) by discretizing the space variable in this system. As a consequence, this scheme possesses the same properties as the semi-discrete model. Finally, we have given some results of numerical simulations which have been performed with this scheme.

A lot of open questions arise naturally. Let us list a few of them. By passing formally to the limit in the semi-discrete model as Δt goes to zero, one obtains a solution of the initial QDD model. To make this statement rigorous, one of the most difficult points to be solved seems to find a bound from below for the density. Studying

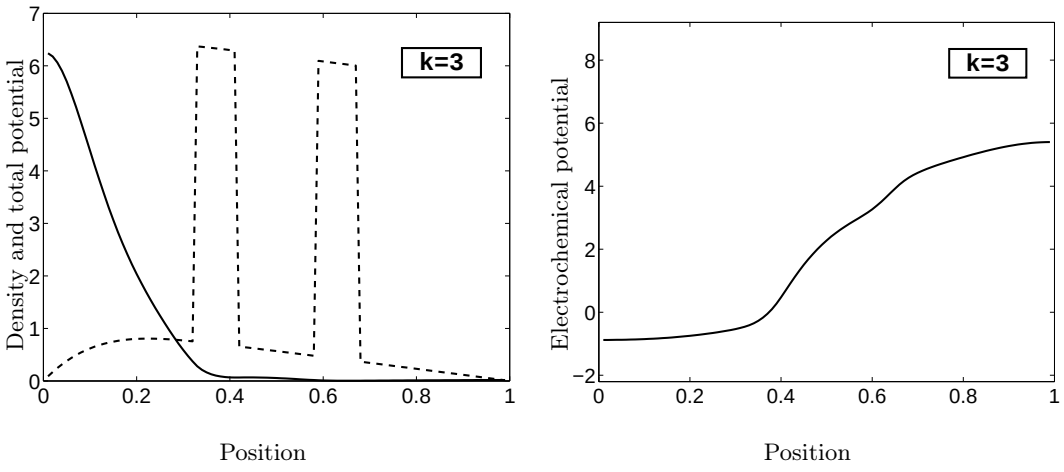

Figure I.2: Numerical solution of the QDD model, after 3 iterations. The same quantities as on Fig. I.1 are represented.

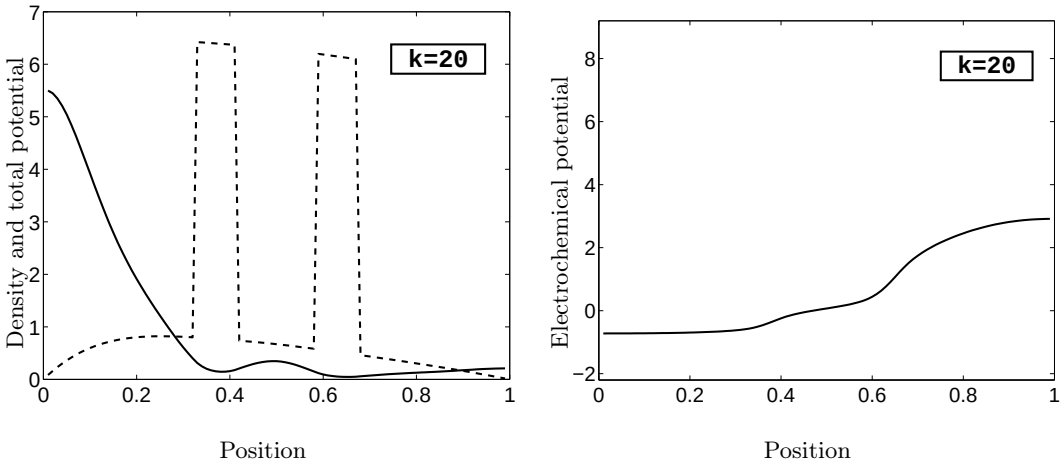

Figure I.3: Numerical solution of the QDD model, after 20 iterations. The same quantities as on Fig. I.1 are represented.

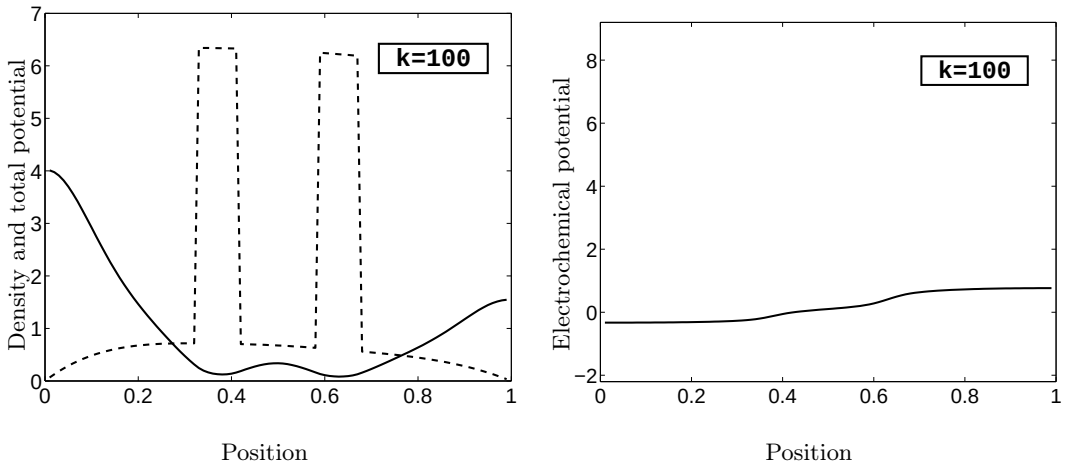

Figure I.4: Numerical solution of the QDD model, after 100 iterations. The same quantities as on Fig. I.1 are represented.

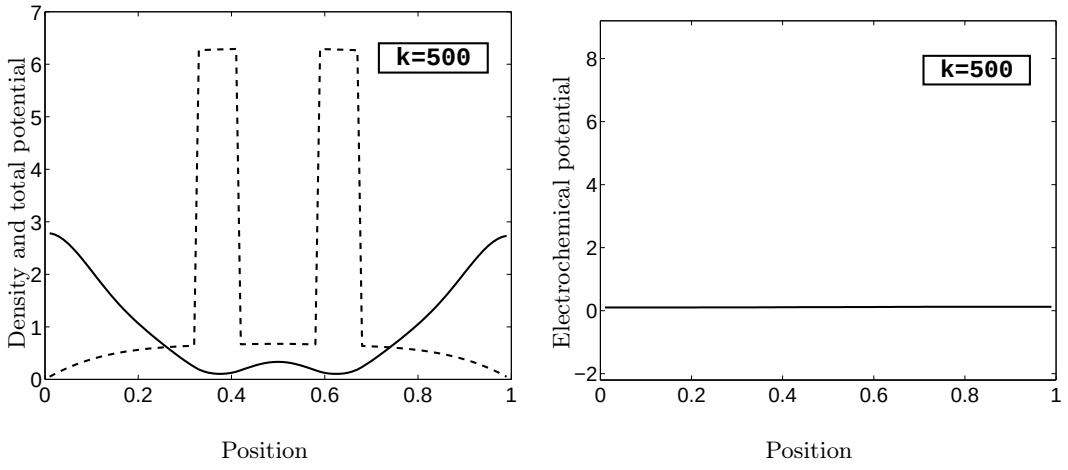

Figure I.5: Numerical solution of the QDD model, after 500 iterations. The same quantities as on Fig. I.1 are represented.

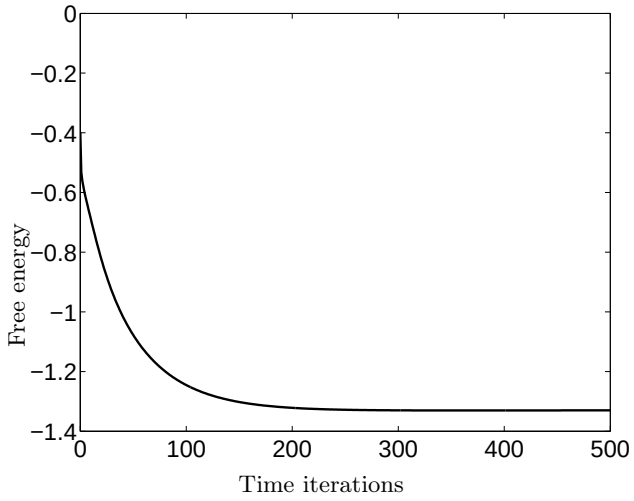

Figure I.6: Free energy S^k as a function of the time step k

the long-time behavior of the semi-discrete model or the continuous model is also an interesting challenge: do their solutions converge to the solution of the Schrödinger-Poisson system studied in [39, 40] ? Another important question is concerned with boundary conditions. We have chosen no-flux boundary conditions, but for practical use it is necessary to enable a current flow through the boundary. This issue will be investigated in next chapter.

References

[1] M. G. Ancona, *Diffusion-Drift modeling of strong inversion layers*, COMPEL **6** (1987), 11–18.

[2] M. G. Ancona, G. J. Iafrate, *Quantum correction of the equation of state of an electron gas in a semiconductor*, Phys. Rev. B **39** (1989), 9536–9540.

[3] M. G. Ancona, Z. Yu, R. W. Dutton, P. J. Voorde, M. Cao, D. Vook, *Density-gradient analysis of MOS tunneling*, IEEE Trans. Electron. Dev. **47** (2000), 2310–2319.

[4] A. Arnold, J.L. Lopez, P.A. Markowich, J. Soler, *An Analysis of Quantum Fokker-Planck Models: A Wigner Function Approach*, Rev. Mat. Iberoamericana. **20** (2004), no. 3, 771–814.

[5] R. Balian, From microphysics to macrophysics, Springer, 1982.

[6] N. Ben Abdallah, F. Méhats, N. Vauchelet, *Analysis of a Drift-Diffusion-Schrödinger-Poisson system*, C. R. Acad. Sci. Paris, Ser. **I** 335 (2002), 1007-1012.

[7] N. Ben Abdallah, A. Unterreiter, *On the stationary quantum drift-diffusion model*, Z. Angew. Math. Phys., **49** (1998), no. 2, 251–275.

[8] J.-P. Bourgade, F. Méhats, C. Ringhofer, *Phonon collision operators consistent with quantum entropy relaxation and quantum Spherical Harmonics Expansion models*, in preparation.

[9] S. Datta, *Nanoscale device modeling: the Green's function method*, Superlattices and Microstructures **28** (2000), no. 4, 253–278.

[10] R. Dautray, J.-L. Lions, Analyse mathématique et calcul numérique pour les sciences et les techniques, Vol. 5, *Spectre des opérateurs*, INSTN: Collection Enseignement, Masson, Paris, 1988.

[11] P. Degond, *Mathematical modelling of microelectronics semiconductor devices*, Proceedings of the Morningside Mathematical Center, Beijing, AMS/IP Studies in Advanced Mathematics, AMS Society and International Press, 2000, 77–109.

[12] P. Degond, A. El Ayyadi, *A coupled Schrödinger Drift-Diffusion model for quantum semiconductor device simulations*, J. Comput. Phys. **181** (2002), no. 1, 222–259.

[13] P. Degond, F. Méhats, C. Ringhofer, *Quantum Energy-Transport and Drift-Diffusion models*, J. Stat. Phys. **118** (2005), no. 3-4, 625–665.

[14] P. Degond, F. Méhats, C. Ringhofer, *Quantum hydrodynamic models derived from entropy principle*, Contemp. Math. **371** (2005), 107–331.

[15] P. Degond, C. Ringhofer, *Quantum moment hydrodynamics and the entropy principle*, J. Stat. Phys. **112** (2003), no. 3-4, 587–628.

[16] P. Degond, C. Ringhofer, *A note on quantum moment hydrodynamics and the entropy principle*, C. R. Acad. Sci. Paris, Ser I **335** (2002),no. 11, 967–972.

[17] P. Degond, C. Ringhofer, *Binary quantum collision operators conserving mass momentum and energy*, C. R. Acad. Sci. Paris, Ser I **336** (2003), no. 9, 785–790.

[18] M. V. Fischetti, *Theory of electron transport in small semiconductor devices using the Pauli Master equation*, J. Appl. Phys. **83** (1998), 270–291.

[19] W. R. Frensley, *Boundary conditions for open quantum systems driven far from equilibrium*, Rev. Mod. Phys. **62** (1990), 745–791.

[20] S. Gallego, *Étude théorique et numérique du modèle de dérive-diffusion quantique*, rapport de stage de DEA, Toulouse, 2004.

[21] S. Gallego, F. Méhats, *Numerical approximation of a quantum drift-diffusion model*, C. R. Acad. Sci. Paris, Ser. I **339** (2004), 519–524.

[22] C. Gardner, *The quantum hydrodynamic model for semiconductor devices*, SIAM J. Appl. Math. **54** (1994), no. 2, 409–427.

[23] C. Gardner, C. Ringhofer, *The smooth quantum potential for the hydrodynamic model*, Phys. Rev. E **53** (1996), 157–167.

[24] C. Gardner, C. Ringhofer, *The Chapman-Enskog Expansion and the Quantum Hydrodynamic Model for Semiconductor Devices*, VLSI Design **10** (2000), 415–435.

[25] I. Gasser and A. Jüngel, *The quantum hydrodynamic model for semiconductors in thermal equilibrium*, Z. Angew. Math. Phys. **48** (1997), no. 1, 45–59 .

[26] I. Gasser, P. A. Markowich, *Quantum Hydrodynamics, Wigner Transforms and the Classical Limit*, Asympt. Analysis, **14** (1997), no. 2, 97-116.

[27] I. Gasser, P. Markowich and C. Ringhofer, *Closure conditions for classical and quantum moment hierarchies in the small temperature limit*, Transp. Th. Stat. Phys. **25** (1996), no. 3-5, 409–423.

[28] J. Jerome, Analysis of charge transport. A mathematical study of semiconductor devices, Springer, Berlin, New York, 1996.

[29] A. Jüngel, Quasi-hydrodynamic semiconductor equations, Progress in Nonlinear Differential Equations, Birkhäuser, 2001.

[30] A. Jüngel, R. Pinnau, *A positivity preserving numerical scheme for a fourth-order parabolic equation*, SIAM J. Num. Anal. **39** (2001), no. 2, 385–406.

[31] H.-C. Kaiser, J. Rehberg, *About a stationary Schrödinger-Poisson system with Kohn-Sham potential in a bounded two- or three-dimensional domain*, Nonlinear Analysis **41** (2000), 33–72.

[32] N. C. Kluksdahl, A. M. Kriman, D. K. Ferry, and C. Ringhofer, *Self-consistent study of the resonant-tunneling diode*, Phys. Rev. B **39** (1989), 7720–7735.

[33] C. D. Levermore, *Moment closure hierarchies for kinetic theories*, J. Stat. Phys., **83** (1996), no. 5-6, 1021–1065.

[34] E. Madelung, *Quantentheorie in hydrodynamischer Form*, Z. Physik **40** (1926), 322–326.

[35] P. A. Markowich, C. Ringhofer, C. Schmeiser, Semiconductor Equations, Springer, 1990.

[36] Matlab Documentation: the `eigs` function, 1994-2004 The MathWorks, Inc., available at `http://www.mathworks.com/access/helpdesk/help/techdoc/ref/eigs.html`.

[37] M. Mock, Analysis of Mathematical Models of Semiconductor Devices, Book Press, Dublin, 1983.

[38] P. Mounaix, O. Vanbésien and D. Lippens, *Effect of cathode spacer layer on the current voltage characteristics of resonant tunneling diodes*, App. Phys. Let. **57** (1990), no. 15, 1517–1519.

[39] F. Nier, *A Stationary Schrödinger-Poisson System Arising from the Modelling of Electronic Devices*, Forum Math. **2** (1990), no. 5, 489–510.

[40] F. Nier, *A variational formulation of Schrödinger-Poisson systems in dimension* $d \leq 3$, Comm. Partial Differential Equations **18** (1993), no. 7-8, 1125–1147.

[41] R. Pinnau, A. Unterreiter, *The Stationary Current-Voltage Characteristics of the Quantum Drift-Diffusion Model*, SIAM J. Numer. Anal. **37** (1999), no. 1, 211-245.

[42] R. Pinnau. *The Linearized Transient Quantum Drift-Diffusion Model - Stability of Stationary States*, ZAMM Z. Angew. Math. Mech. **80** (2000), no. 5, 327-344.

[43] A. Pirovano, A. Lacaita, A. Spinelli, *Two dimensional Quantum Effects in Nanoscale MOSFETs*, IEEE Trans. Electron. Dev. **49** (2002), no. 1, 25–31.

[44] C. Pohl, *On the Numerical Treatment of Dispersive Equations*, PhD thesis, TU Berlin, 1998.

[45] E. Polizzi, *Modélisation et simulations numériques du transport quantique balistique dans les nanostructures semi-conductrices*, PhD thesis, INSA Toulouse, (2001)

[46] E. Polizzi, N. Ben Abdallah, *Self-consistent three dimensional models for quantum ballistic transport in open systems*, Phys. Rev B **66** (2002), 245301.

[47] M. Reed, B. Simon, Methods of Modern Mathematical Physics *Vol. 4. Analysis of Operators*, Academic Press, New York, San Francisco and London, 1978.

[48] S. Selberherr, Analysis and simulation of semiconductor devices, Springer, 1984.

[49] D. Serre, Matrices. Theory and applications, translated from the 2001 French original, Grad. Texts in Math., 216, Springer-Verlag, New York, 2002.

[50] E. Wigner, *On the quantum correction for thermodynamic equilibrium*, Phys. Rev. **40** (1932), 749–759.

[51] J. R. Zhou, D. Ferry, *Modeling of quantum effects in ultrasmall HEMT devices*, IEEE Trans. Electron. Dev. **40** (1993), no. 2, 421–427.

Chapter II

An entropic Quantum Drift-Diffusion model for electron transport in resonant tunneling diodes

This chapter has given an article written in collaboration with P. Degond and F. Méhats, and published in the Journal of Computational Physics: *An entropic Quantum Drift-Diffusion model for electron transport in resonant tunneling diodes*, J. Comput. Phys. **221** (2007), 226–249.

Abstract. We present an entropic Quantum Drift-Diffusion model (QDD) and show how it can be derived on a bounded domain as the diffusive approximation of the Quantum Liouville equation with a quantum BGK operator. Some links between this model and other existing models are exhibited, especially with the Density Gradient (DG) model and the Schrödinger-Poisson Drift-Diffusion model (SPDD). Then a finite difference scheme is proposed to discretize the QDD model coupled to the Poisson equation and we show how this scheme can be slightly modified to discretize the other models. Numerical results show that the properties listed for the QDD model are checked, as well as the model captures important features concerning the modeling of a resonant tunneling diode. To finish, some comparisons between the models stated above are realized.

Key words. entropic Quantum Drift-Diffusion, density matrix, Quantum Liouville, Density-Gradient, Schrödinger-Poisson Drift-Diffusion, resonant tunneling diode, current-voltage characteristics.

1 Introduction

Miniaturization of semiconductor devices to the nanometer scale increases the role of quantum effects in electron transport. Moreover, new classes of devices operate on the basis of these quantum effects. This is the case for the resonant tunneling diode (RTD) which has attracted and continues to attract interest due to its highly nonlinear static current-voltage characteristic. This device exhibits a negative and non monotonous resistance in a certain range of applied biases, which is interesting in many applications to logic electronics. The RTD conduction band involves a double potential barrier with one or several resonant energy levels within the well inside the two barriers. Only electrons with energies close to the resonant energy can pass through the double barrier thanks to tunneling effects. Changing the applied bias changes the energy of the incident electrons and increasing the bias can lower the current [10].

The Classical Drift-Diffusion model has been a valuable tool for many years in the semiconductor industry [33] but it is not adapted to the modeling of such devices. In order to capture tunneling effects, one has to use a quantum model. At the microscopic scale, one can use the Schrödinger or the Wigner equation as it is done in [30, 35, 40, 36, 38, 4]. But these models are ballistic quantum models and taking into account collisions in this context is a difficult task. In RTDs, the electron transport in the vicinity of the double barriers can be expected to be quantum and collisionless while transport in the access zone is mainly classical and collisional. This is why a class of hybrid models was developed [6, 13, 5, 28] but the coupling methodology is far from obvious.

An alternative way for modeling quantum effects is by adding quantum corrections terms to classical macroscopic models. The most common quantum correction involves the Bohm potential, which naturally appears in quantum hydrodynamics. In a fluid context, such models were studied in [20, 22, 23, 24, 25, 26, 27]. In a diffusive context, one can find the energy transport model corrected with the Bohm potential [11] and, closer to the QDD model studied in this chapter, the Drift-Diffusion model corrected with the Bohm potential, called Density-Gradient (DG) model (also "Quantum Drift-Diffusion model" in the literature). This model was derived in [2, 1] and studied in [42, 29, 9]. But the Bohm potential has the disadvantage of bringing higher order differential terms which are difficult to handle numerically and mathematically. To conclude this description, one can also cite another recent attempt to include quantum effects in a diffusive model: the Schrödinger-Poisson Drift-Diffusion model (SPDD) derived in [39] and implemented in [12]. This model takes into account the discrete spectrum of energy states for the electrons inside the expression of the density.

In this chapter, we propose to use the entropic Quantum Drift-Diffusion (QDD) model. This model was derived following the moment closure approach developed in [32] and extending it to the context of Quantum mechanics. The strategy consists in defining the notion of "local" quantum equilibrium as the minimizer of an entropy functional under local moment constraints. Such equilibria are defined thanks to a relation between the thermodynamic quantities (such as the chemical potential) and the extensive quantities (density, current,...) in a non local way. In [17], quantum hydrodynamic (QHD) models were derived from the Wigner equation by moment expansions closed by these quantum equilibria. In this reference, new directions related to these QHD models were sketched, including namely the setting up of a rigorous framework to this formal modeling, the inclusion of other quantum effects (Pauli

exclusion principle, spin effects,...), or the numerical discretization and simulation. Following the same approach, a family of ad-hoc collision operators which decrease the quantum entropy and relax to the equilibria were introduced in [16]. Afterwards, this strategy was applied in [14] in order to derive the QDD model and the Quantum Energy-Transport (QET) model. The QDD model was written in a more convenient way in the review article [15]. The first attempt to study the model mathematically and numerically was achieved in [18, 19]. The non local relation between the chemical potential and the density makes the model difficult to analyze. The question of the well posedness of the model has not been answered yet but a semidiscretized (in time) version of this model was proposed and rigorously analyzed, as well as a fully discretized version.

The model properties are listed briefly. By construction, the QDD model takes into account collisions. In [15, 19], we have shown that steady states of this model are solutions of the stationary Schrödinger-Poisson system (studied in [37] for example). Moreover, it is built in order to be consistent with entropy dissipation and the density is always nonnegative (provided the solution exists). Some links were exhibited in [14] between the QDD model and two other models stated above: the Classical Drift-Diffusion model on the one hand and the Density-Gradient model on the other hand. Indeed, the limit of the QDD model as the dimensionless Planck constant goes to zero is the Classical Drift-Diffusion model, while the leading order correction term is the Bohm potential.

The aim of this chapter is to propose a discretization of the QDD model on a bounded domain and to check that the above stated properties are numerically verified. We also show that the model can capture the main features of a resonant tunneling diode and compare the QDD model with the SPDD model and the DG model.

The chapter is organized as follows. In section 2, the QDD model is presented (which is justified in Appendix A by applying formally a diffusive limit to the collisional Quantum Liouville equation). Then links between the QDD model and the other existing models are briefly given. In section 3, we discretize the models using finite-differences and we perform numerical experiments in section 4. The QDD model and the SPDD model are compared one to each other on an isolated RTD while the QDD model and the DG model are compared on a RTD connected to reservoirs, allowing us to compute current-voltage characteristics.

2 Presentation of the models

In this section, we present the entropic Quantum Drift-Diffusion model on a bounded domain (the derivation of this model can be found in appendix A) and we give some links with other existing models. For the sake of readability, parameters like the effective mass, the permittivity and the mobility are supposed constant throughout the device. The reader should refer to appendix B where the models are written with variable parameters.

2.1 The entropic Quantum Drift-Diffusion model (QDD)

2.1.1 Presentation

In this subsection, the entropic Quantum Drift-Diffusion model is presented on a bounded domain (the boundary conditions will be given in subsection 2.1.3). Let Ω

be a regular domain of $\mathbb{R}^d$ ($d = 1, 2$ or 3) . The QDD model is a quantum fluid model describing the evolution of the electron density $n(t, x)$ subject to the electrical potential $V(t, x)$ and interacting with a thermal bath of fixed temperature T. The first equation is the equation of mass conservation and reads:

$$e\partial_t n - \nabla \cdot j = 0, \tag{2.1}$$

where e is the positive electron charge and j is the current defined as follows:

$$j = e\mu n \nabla(A - V). \tag{2.2}$$

In this equation, μ is the electron mobility. We call $A(t, x)$ the quantum chemical potential which is linked to the density of electrons by a relation which is non local in space and which is the key of this quantum model:

$$n(A) = \sum_{p\geq 1} \exp(-\frac{\lambda_p(A)}{k_B T})|\psi_p(A)|^2. \tag{2.3}$$

Here k_B is the Boltzmann constant and $(\lambda_p, \psi_p)_{p\geq 1}$ are the eigenvalues and the normalized eigenfunctions of the following modified Hamiltonian (where the electrical potential is replaced by the quantum chemical potential):

$$H(A) = -\frac{\hbar^2}{2m}\Delta - eA, \tag{2.4}$$

where $\hbar$ is the Planck constant and m is the effective mass of an electron.

The electrical potential V can be split into a given external potential V_{ext} (assumed independent of time for simplicity) and a self consistent potential V_s created by the difference between a given doping density n^d and the electron density n according to the following Poisson equation:

$$-\varepsilon\Delta V_s = e(n^d - n), \tag{2.5}$$

where ε is the permittivity of the semiconductor.

2.1.2 Scaling

Before introducing the other models, it is useful to rewrite the QDD model in a scaled form. We take for reference density $\overline{n}$, the maximum value of the doping profile throughout the device: $\overline{n} = \max|n^d|$. We assume that the device has a characteristic length $\overline{x} = L$ and voltages are scaled with respect to the thermal potential: $\overline{V} = \frac{k_B T}{e}$. Finally, we take the following reference values for the time and the current: $\overline{t} = \frac{L^2 e}{\mu k_B T}$ and $\overline{j} = \frac{\mu k_B T \overline{n}}{Le}$. Then we write the following dimensionless quantities:

$$n' = \frac{n}{\overline{n}} \ ; \ x' = \frac{x}{\overline{x}} \ ; \ j' = -\frac{j}{\overline{j}} \ ; \ t' = \frac{t}{\overline{t}} \ ; \ V' = -\frac{V}{\overline{V}} \ ; \ A' = -\frac{A}{\overline{V}} + \log\overline{n} \ ;$$

and obtain the QDD model coupled with the Poisson equation (forgetting the primes):

$$\partial_t n + \nabla \cdot j = 0, \tag{2.6}$$

$$j = n\nabla(A - (V_s + V_{ext})), \tag{2.7}$$

$$-\alpha^2\Delta V_s = n - n^d, \tag{2.8}$$

$$n = \sum_{p\geq 1} e^{-\lambda_p(A)}|\psi_p(A)|^2, \tag{2.9}$$

where $(\lambda_p(A), \psi_p(A))$ are the eigenvalues and eigenfunctions of the Hamiltonian $H(A) = -\frac{\tilde{\hbar}^2}{2}\Delta + A$, α and $\tilde{\hbar}$ being the scaled Debye length and the scaled de Broglie length (will denote $\hbar$ this constant in the sequel):

$$\alpha = \sqrt{\frac{\varepsilon k_B T}{e^2 L^2 \overline{n}}} = \frac{\lambda_D}{L}, \tag{2.10}$$

$$\tilde{\hbar} = \sqrt{\frac{\hbar^2}{m L^2 k_B T}} = \frac{\lambda_{dB}}{L}. \tag{2.11}$$

2.1.3 Boundary conditions

Boundary conditions for the potentials. In this work, two classes of boundary conditions will be studied:

- Insulating boundary conditions. The total number of particles in the domain is enforced to be constant by putting Neumann boundary conditions on the electrochemical potential (and thus the current vanishes on the boundary):

  $$\nabla(A - (V_s + V_{ext})) \cdot \nu = 0 \ \text{ on } \partial\Omega.$$

  Moreover, no bias is applied on the device, which is translated by the following Dirichlet conditions on the electrical potential:

  $$V_s = 0 \ \text{ on } \partial\Omega.$$

- Open boundary conditions. In order to allow a current flow at the boundary, non homogeneous Dirichlet conditions are applied on the density:

  $$n = \sum_{p \geq 1} e^{-\lambda_p(A)} |\psi_p(A)|^2 = n^d \ \text{ on } \partial\Omega,$$

  and non homogeneous Dirichlet conditions on the electrical potential V_s:

  $$V_s = V_0 \ \text{ on } \partial\Omega.$$

  The function $V_0(x)$ permits to control the bias applied on the device.

Boundary conditions for the wave functions. We have chosen for the wave functions Neumann boundary conditions permitting to define a density which does not vanish on the boundary as we need to allow a current flow to exist:

$$\forall p \geq 1 \ \ \nabla\psi_p \cdot \nu = 0 \ \text{ on } \partial\Omega, \tag{2.12}$$

where the boundary is denoted by $\partial\Omega$ and $\nu(x)$ is the outward unit normal vector at $x \in \partial\Omega$. These boundary conditions can be seen as an approximation of boundary conditions that would consider the exterior domain as an homogeneous medium with a constant chemical potential. The next step should be the use of transparent boundary conditions for the wave functions (and a continuous spectrum for the modified Hamiltonian) which is a work in progress.

2.1.4 Properties of the isolated system

Entropy dissipation. An important property of the QDD model coupled to the Poisson equation is that, if we choose boundary conditions isolating the domain Ω, the macroscopic quantum free energy G defined by

$$G = \int_\Omega -n(A - V_{ext}) + \frac{\alpha^2}{2}|\nabla V_s|^2 \, dx$$

is a decreasing function of time:

$$\frac{d}{dt}G = -\int_\Omega n|\nabla(A - (V_s + V_{ext}))|^2 \, dx \;\leq\; 0.$$

This property is a consequence of the method of the model derivation (see appendix A) where the density matrix is chosen to minimize the microscopic quantum free energy and thus the system is at any time in a local equilibrium.

Steady states. Another interesting property of the QDD model with insulating boundary conditions is that steady states are solutions of the Schrödinger-Poisson model (SP). Let (n, A, V_s) be a steady state of (2.6)-(2.9) such that $\int_\Omega n(x)dx = N$, then there exists a constant ϵ_F (the quantum quasi Fermi level) such that $A - (V_s + V_{ext}) = \epsilon_F$ and (n, V_s, ϵ_F) is the unique solution of the Schrödinger-Poisson model under a constraint of total charge:

$$-\alpha^2 \Delta V_s = n - n^d, \tag{2.13}$$

$$n = \sum_{p\geq 1} e^{\epsilon_F - \lambda_p}|\psi_p|^2, \tag{2.14}$$

$$\int_\Omega n(x)dx = N, \tag{2.15}$$

where (λ_p, ψ_p) are the eigenvalues and the normalized eigenfunctions of the Hamiltonian: $\mathcal{H} = H(V_s + V_{ext}) = -\frac{\hbar^2}{2}\Delta + (V_s + V_{ext})$.

2.2 Links with other existing models

2.2.1 The Classical Drift-Diffusion model (CDD)

Presentation. We are going to present now the classical counterpart of the QDD model. The CDD model coupled to the Poisson equation can be written with the same dimensionless parameter α and is independent of the scaled Planck constant $\hbar$:

$$\partial_t n + \nabla \cdot j = 0, \tag{2.16}$$

$$j = n\nabla(-\log n - (V_s + V_{ext})), \tag{2.17}$$

$$-\alpha^2 \Delta V_s = n - n^d. \tag{2.18}$$

The term $n\nabla \log n = \nabla n$ is the diffusion term of the current and $n\nabla(V_s + V_{ext})$ is the drift term. The same boundary conditions as for the QDD model can be used: Neumann conditions on $-\log n - (V_s + V_{ext})$ permit to isolate the device while Dirichlet conditions on the density n allow a current at the boundary (the conditions for the electrical potential are unchanged).

Link with the QDD model. In order to display a link between the QDD model (2.6)-(2.9) and the CDD model (2.16)-(2.18), it is possible to expand the density for

the QDD model (2.9) in powers of the scaled Planck constant $\hbar$ (see [14]). Let A be a smooth function of x, then:

$$n(A) = \sum_{p\geq 1} e^{-\lambda_p(A)}|\psi_p(A)|^2 = n_0 e^{-A} + \mathcal{O}(\hbar^2), \tag{2.19}$$

where $n_0 = (2\pi\hbar^2)^{d/2}$ is the effective density of states. This gives:

$$A = -\log n + \log n_0 + \mathcal{O}(\hbar^2). \tag{2.20}$$

Putting this relation in (2.7), we find the expression of the current for the CDD model (2.17). The difference between the QDD model and the CDD model being of order $\hbar^2$, we will note formally:

$$\text{QDD} - \text{CDD} = \mathcal{O}(\hbar^2).$$

2.2.2 The Density Gradient model (DG)

Presentation. The difference between the DG model and the CDD model lies in a term of order $\hbar^2$ (called the Bohm potential) that is added in the current expression (only equation (2.17) changes and is replaced by equation (2.22)):

$$\partial_t n + \nabla \cdot j = 0, \tag{2.21}$$

$$j = n\nabla(-\log n - (V_s + V_{ext} + \frac{1}{3}V_B)), \tag{2.22}$$

$$-\alpha^2 \Delta V_s = n - n^d, \tag{2.23}$$

$$V_B = -\frac{\hbar^2}{2}\frac{\Delta\sqrt{n}}{\sqrt{n}}. \tag{2.24}$$

Since this is a fourth order parabolic system, we need an additional boundary condition. The most standard choice consists in an homogeneous Dirichlet conditions on the Bohm potential, assuming there is no quantum effect on the boundary (see [29]):

$$V_B = 0 \quad \text{on } \partial\Omega. \tag{2.25}$$

Link with the QDD model. We want to show a link between the QDD model (2.6)-(2.9) and the DG model (2.21)-(2.24). If the terms of order $\hbar^2$ are explicitly written in the expansion (2.19), one obtains:

$$n(A) = \sum_{p\geq 1} e^{-\lambda_p(A)}|\psi_p(A)|^2 = n_0 e^{-A}\left(1 + \frac{\hbar^2}{24}(-2\Delta A + |\nabla A|^2)\right) + \mathcal{O}(\hbar^4). \tag{2.26}$$

Using relation (2.20), it follows:

$$A = -\log n + \log n_0 + \frac{\hbar^2}{6}\frac{\Delta\sqrt{n}}{\sqrt{n}} + \mathcal{O}(\hbar^4). \tag{2.27}$$

Putting this relation in (2.7), we find the expression of the current for the DG model (2.22).

The difference between the QDD model and the DG model being of order $\hbar^4$, we will note formally:

$$\text{QDD} - \text{DG} = \mathcal{O}(\hbar^4).$$

2.2.3 The Schrödinger-Poisson Drift-Diffusion model (SPDD)

Presentation: The simplified version of the Schrödinger-Poisson Drift-Diffusion model introduced in [39] is very close to the QDD model, except that the expression of the density is different. In the SPDD model, electron density can be expressed as:

$$n(x) = \int_0^\infty g(\epsilon) e^{-A-\epsilon}\, d\epsilon, \tag{2.28}$$

where $g(\epsilon)$ is the density of states corresponding to the energy ϵ. In a classical model, we would have $g(\epsilon) = \frac{2}{\sqrt{\pi}} n_0 \sqrt{\epsilon}$ while in the SPDD model, we have:

$$g(\epsilon) = \sum_{p\geq 1} \delta(\epsilon - \lambda_p(V_s + V_{ext}) + (V_s + V_{ext}))\ |\psi_p(V_s + V_{ext})|^2,$$

where δ is the Dirac delta function and $\lambda_p(V_s + V_{ext})$ and $\psi_p(V_s + V_{ext})$ are the eigen elements of the Hamiltonian $\mathcal{H} = H(V_s + V_{ext}) = -\frac{\hbar^2}{2}\Delta + (V_s + V_{ext})$. This gives the following system (only equation (2.9) changes in the QDD model and is replaced by (2.32)):

$$\partial_t n + \nabla \cdot j = 0, \tag{2.29}$$
$$j = n\nabla(A - (V_s + V_{ext})), \tag{2.30}$$
$$-\alpha^2 \Delta V_s = n - n^d, \tag{2.31}$$
$$n = \sum_{p\geq 1} e^{-\lambda_p - A + (V_s + V_{ext})} |\psi_p|^2. \tag{2.32}$$

Link with the QDD model. Both models can be linked in the case where we take insulating boundary conditions. The SPDD model can then be seen as an intermediate model between the QDD model and the stationary Schrödinger-Poisson system (2.13)-(2.15) in a situation close to the equilibrium.

Indeed, if the current $j = n\nabla(A - V)$ is small, this means that the electrochemical potential $\varphi(x) = A(x) - V(x)$ is slowly variable. Then the commutator between the Hamiltonian $\mathcal{H} = H(V) = -\frac{\hbar^2}{2}\Delta + V$ and $\varphi(x)$ is small and a "space-adiabatic" approximation can be performed in the expression of the density given by the QDD model:

$$\begin{aligned} n^{\text{QDD}} &= \sum_{p\geq 1} e^{-\lambda_p(V+\varphi)} |\psi_p(V+\varphi)|^2 \\ &\sim \sum_{p\geq 1} e^{-\lambda_p(V)-\varphi} |\psi_p(V)|^2 = n^{\text{SPDD}}. \end{aligned}$$

For a discussion on space adiabatic approximation in the context of Born-Oppenheimer approximation in molecular dynamics, one can refer for instance to [41].

2.2.4 Summary

We can summarize the links between the QDD model and the other models with the following diagram:

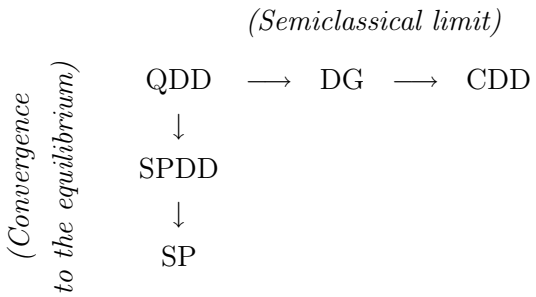

3 Numerical Methods

3.1 Numerical scheme for the QDD model

The space dimension is now $d = 1$ so that the domain Ω is $(0, 1)$. Parameters such as the mobility, the permittivity and the effective mass are now variable (the reader should refer to appendix B where the models are written with variable parameters). The QDD model is discretized in time using a semi implicit Euler scheme in order to preserve the quantum free energy dissipation. We discretize the space variable using finite-differences (Note here that for simplicity, the space discretization is not symmetric compared to what we have done in [19]; But both versions of the discretization appear to be stable, independently of the direction of the transport). Let $\Delta t > 0$ be the time step and $\Delta x = \frac{1}{N+1}$ the space gridstep. The grid is composed of the points $x_i = i\Delta x$ for $i = 0 \cdots N + 1$, where $N \in \mathbb{N}$. The unknowns are the chemical potential A_i^k and the self consistent electrical potential $V_{s,i}^k$ at the point x_i and at the time $t_k = k\Delta t$. For the sake of readability, we use the auxiliary variables n_i^k for the density and j_i^k for the current.

The fully discretized scheme for the QDD model coupled to the Poisson equation reads for $i = 1 \cdots N$:

$$\frac{n_i^{k+1} - n_i^k}{\Delta t} + \frac{j_i^{k+1} - j_{i-1}^{k+1}}{\Delta x} = 0, \tag{3.33}$$

$$j_i^{k+1} = \mu_i n_i^k \frac{(A_{i+1}^{k+1} - (V_{ext,i+1} + V_{s,i+1}^{k+1})) - (A_i^{k+1} - (V_{ext,i} + V_{s,i}^{k+1}))}{\Delta x}, \tag{3.34}$$

$$-\frac{\alpha^2}{\Delta x^2}(\varepsilon_i(V_{s,i+1}^{k+1} - V_{s,i}^{k+1}) - \varepsilon_{i-1}(V_{s,i}^{k+1} - V_{s,i-1}^{k+1})) = n_i^{k+1} - n_i^d, \tag{3.35}$$

$$n_i^{k+1} = \sum_{p\geq 1} \exp(-\lambda_p(A^{k+1}))|\psi_{p,i}(A^{k+1})|^2, \tag{3.36}$$

where $(\lambda_p(A^{k+1}), \psi_p(A^{k+1}))_{p\geq 1}$ is the whole sequence of eigenvalues and eigenvectors of the $(N+2)\times(N+2)$ tridiagonal matrix H^{k+1} discretizing the modified Hamiltonian $H\left(A(t_{k+1}, x)\right)$. This tridiagonal matrix H^{k+1} is defined by (for $i = 1 \cdots N$):

$$\begin{aligned} H_{i,i-1}^{k+1} &= -\frac{\hbar^2}{2\Delta x^2}\frac{1}{m_i}, \\ H_{i,i}^{k+1} &= \frac{\hbar^2}{2\Delta x^2}\left(\frac{1}{m_{i+1}} + \frac{1}{m_i}\right) + A_i^{k+1}, \\ H_{i,i+1}^{k+1} &= -\frac{\hbar^2}{2\Delta x^2}\frac{1}{m_{i+1}}, \end{aligned}$$

and the other components $H_{i,j}^{k+1}$ with $j \notin \{i-1, i, i+1\}$ are zero. For each i, the vector component m_i of the effective mass is defined by:

$$m_i = \frac{1}{\Delta x} \int_{x_{i-1/2}}^{x_{i+1/2}} m(x)dx$$

The vectors defining the mobility of the electrons (μ), the permittivity of the semiconductor (ε) as well as the doping profile (n^d) are calculated in the same way.

Boundary conditions. The Neumann conditions on the eigenfunctions ψ give for the matrix H:

$$H_{0,0}^{k+1} = \frac{\hbar^2}{2\Delta x^2}\frac{1}{m_0} + A_0^{k+1} \quad , \quad H_{0,1}^{k+1} = -\frac{\hbar^2}{2\Delta x^2}\frac{1}{m_1},$$
$$H_{N+1,N}^{k+1} = -\frac{\hbar^2}{2\Delta x^2}\frac{1}{m_N} \quad , \quad H_{N+1,N+1}^{k+1} = \frac{\hbar^2}{2\Delta x^2}\frac{1}{m_{N+1}} + A_{N+1}^{k+1}.$$

In order to complete the scheme, we prescribe boundary conditions on the potentials:

- Insulating boundary conditions: We put homogeneous Dirichlet conditions on the electrical potential V_s:

  $$V_{s,0} = 0 \quad ; \quad V_{s,N+1} = 0.$$

  The Neumann conditions on the electrochemical potential give:

  $$\begin{aligned}(A_1^{k+1} - (V_{ext,1} + V_{s,1}^{k+1})) - (A_0^{k+1} - (V_{ext,0} + V_{s,0}^{k+1})) &= 0,\\ (A_{N+1}^{k+1} - (V_{ext,N+1} + V_{s,N+1}^{k+1})) - (A_N^{k+1} - (V_{ext,N} + V_{s,N}^{k+1})) &= 0.\end{aligned}$$

- Open boundary conditions: We prescribe non homogeneous Dirichlet conditions on the electrical potential, V_r being the parameter permitting to control the applied bias:

  $$V_{s,0} = 0 \quad ; \quad V_{s,N+1} = V_r.$$

  The non homogeneous Dirichlet conditions on the density give:

  $$\begin{aligned}n_0^{k+1} &= \sum_{p\geq 1} e^{-\lambda_p(A^{k+1})}|\psi_{p,0}(A^{k+1})|^2 = n_0^d;\\ n_{N+1}^{k+1} &= \sum_{p\geq 1} e^{-\lambda_p(A^{k+1})}|\psi_{p,N+1}(A^{k+1})|^2 = n_{N+1}^d.\end{aligned}$$

Algorithm. Given an initial positive density n^0 we solve the scheme for each time step using Newton algorithm implemented with Matlab (for more details, in particular the expression of the derivative of n with respect to A, one can refer to [19]). It is well known that the efficiency of the Newton method depends on the initial guess of the variables. For all time steps $k \geq 2$, it is natural to initialize the electrical potential with V_s^{k-1} and the chemical potential with A^{k-1}. For the first time step, it is easy to solve the Poisson equation to find the electrical potential V_s^0 corresponding to the density n^0 and thus we have a good initial guess. It is a little bit more difficult to initialize the chemical potential A^0. We have proved in [19] the existence and uniqueness of the quantum chemical potential A^0 corresponding to n^0. It has been shown to be the solution of a minimization problem which is easy to implement. Nevertheless,

when $\hbar$ is very small (high temperature), we can also initialize A by considering the semiclassical limit $n \approx \frac{\sqrt{m}}{\sqrt{2\pi\hbar^2}} e^{-A}$, giving $A^0 = -\log n^0 + \frac{1}{2}\log m - \frac{1}{2}\log 2\pi\hbar^2$. On the contrary, if $\hbar$ is large, we can consider the limit (near the zero temperature) where the expression of the density is given by $n \approx e^{-\lambda_1}|\psi_1|^2$. This gives (we recognize the Bohm potential appearing with a factor 3) $A^0 = -\log\left(\int_\Omega n^0\ dx\right) + \frac{\hbar^2}{2}\frac{\partial_x^2\sqrt{n^0}}{\sqrt{n^0}}$.

Note that we have to solve an eigenvalue problem for each Newton iteration which is numerically expensive (we use the Matlab function `eigs`). Hopefully, the dependence on the eigenvalues is exponential and we need only the few lowest ones. In fact, (3.36) is replaced by:

$$n_i^{k+1} = \sum_{p=1}^{p_{\max}} \exp(-\lambda_p(A^{k+1}))|\psi_{p,i}(A^{k+1})|^2.$$

The value of $p_{\max}$ is chosen such that $N\exp(-\lambda_{p_{\max}})$ is below a small given tolerance value; note that for this prediction we use the asymptotic formula: $\lambda_p \sim \frac{\hbar^2}{2}p^2\pi^2$ (valid for large p's).

3.2 Numerical schemes for the other models

The DG and CDD schemes. For the discretization of the DG and CDD model, we employ an exponential change of variable which permits to define a scheme very similar to the one of the QDD model. Let us note $n = e^{-u}$, so that we can rewrite the DG model as follows (here, we still assume that m, ε and μ are independent of x for simplicity):

$$\begin{aligned}
&\partial_t n + \nabla\cdot j = 0,\\
&j = n\nabla(u - (V_s + V_{ext} + \frac{1}{3}V_B)),\\
&-\alpha^2\Delta V_s = n - n^d,\\
&V_B = -\frac{\hbar^2}{8}(-2\Delta u + |\nabla u|^2),\\
&n = e^{-u}.
\end{aligned}$$

Now the unknowns for the scheme are the u_i^k and $V_{s,i}^k$ at the point x_i and at the time $t_k = k\Delta t$. The scheme reads for $i = 1\cdots N$:

$$\begin{aligned}
&\frac{n_i^{k+1} - n_i^k}{\Delta t} + \frac{j_i^{k+1} - j_{i-1}^{k+1}}{\Delta x} = 0,\\
&j_i^{k+1} = \mu_i n_i^k \frac{(u_{i+1}^{k+1} - (V_{ext,i+1} + V_{s,i+1}^{k+1} + \frac{1}{3}V_{B,i+1}^{k+1})) - (u_i^{k+1} - (V_{ext,i} + V_{s,i}^{k+1} + \frac{1}{3}V_{B,i}^{k+1}))}{\Delta x},\\
&-\frac{\alpha^2}{\Delta x^2}(\varepsilon_i(V_{s,i+1}^{k+1} - V_{s,i}^{k+1}) - \varepsilon_{i-1}(V_{s,i}^{k+1} - V_{s,i-1}^{k+1})) = n_i^{k+1} - n_i^d,\\
&n_i^{k+1} = e^{-u_i^{k+1}},\\
&V_{B,i}^k = -\frac{\hbar^2}{8\Delta x^2}\left(-\frac{2}{m_i}(u_{i+1}^k - u_i^k) + \frac{2}{m_{i-1}}(u_i^k - u_{i-1}^k) + \frac{1}{m_i}\left|u_{i+1}^k - u_i^k\right|^2\right).
\end{aligned}$$

The boundary conditions can be easily deduced from the one applied for the QDD scheme and we add homogenous Dirichlet conditions on the Bohm potential (see subsection 2.2.2):

$$V_{B,0} = V_{B,N+1} = 0. \tag{3.37}$$

For the CDD model, we use the same scheme but $V_{B,i} = 0$ for $i = 0 \cdots N+1$.

Remark that fixing the density on the boundary (in the case of open boundary conditions) automatically fixes the unknown u_i^k on the boundary. For the QDD model, the relation between the quantum chemical potential A and the density n being non local, the unknown A is not a priori fixed on the boundary.

The SPDD scheme. For the SPDD model, the only difference with the scheme for the QDD model lies in the expressions of the density and the Hamiltonian which are modified in consequence:

$$n_i^{k+1} = \sum_{p\geq 1} \exp(-\lambda_p(V_s^{k+1} + V_{ext}) - A_i^{k+1} + V_{s,i}^{k+1} + V_{ext,i}) \ |\psi_{p,i}(V_s^{k+1} + V_{ext})|^2,$$

where $(\lambda_p(V_s^{k+1} + V_{ext}), \psi_p(V_s^{k+1} + V_{ext}))$ are the eigen elements of the tridiagonal matrix $\mathcal{H}^{k+1}$ defined by (for $i = 1 \cdots N$):

$$\begin{aligned}
\mathcal{H}_{i,i-1}^{k+1} &= -\frac{\hbar^2}{2\Delta x^2}\frac{1}{m_i}, \\
\mathcal{H}_{i,i}^{k+1} &= \frac{\hbar^2}{2\Delta x^2}(\frac{1}{m_{i+1}} + \frac{1}{m_i}) + V_{s,i}^{k+1} + V_{ext,i}, \\
\mathcal{H}_{i,i+1}^{k+1} &= -\frac{\hbar^2}{2\Delta x^2}\frac{1}{m_{i+1}}.
\end{aligned}$$

To complete the scheme, we add boundary conditions that can be easily deduced from the one applied for the QDD scheme. All the schemes are solved using the Newton algorithm.

4 Numerical results

Our aim is to check the properties stated for the QDD model in the two kinds of situations: with insulating or open boundary conditions. We also want to compare the QDD model with the SPDD model and the DG model. For the numerical investigations, the devices that we have chosen are resonant tunneling diodes (RTD). For the use of the open boundary conditions, the structure of the studied RTD is depicted in figure II.1. It consists of two 5nm barriers of $Al_{0.3}Ga_{0.7}As$ separated by a 5nm well of $GaAs$. The double barrier is sandwiched between two 5nm spacer layers and two 25nm $GaAs$ highly doped access zones (doping density equal to $10^{24}m^{-3}$), while the channel is moderately doped (doping density equal to $10^{21}m^{-3}$). For the use of the insulating boundary conditions, the RTD is chosen with a doping profile equal to 0. The schemes which have been developed in the previous sections have been implemented in Matlab and the time and space steps are taken equal to 5×10^{-3} in the dimensionless units.

4.1 Insulating boundary conditions

4.1.1 The QDD model

The parameters are all chosen independent of x in this case and are given in table II.1. The corresponding dimensionless parameters have values equal to $\alpha = 1.7061$ and $\hbar = 0.0884$. The initial density is concentrated to the left of the double barrier

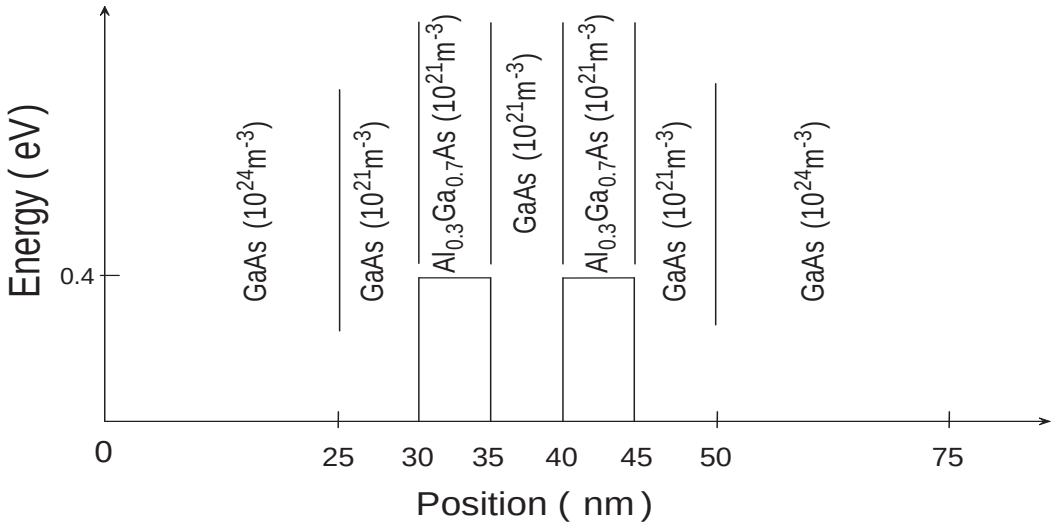

Figure II.1: The double barrier resonant tunneling structure.

and figure II.2 shows the evolution of electrons for the QDD model under insulating boundary conditions. Steady state is achieved at about $6000fs$ as confirmed by the next figure (figure II.3) which demonstrates that the quantum free energy is no more evolving (the figure shows also clearly that the quantum free energy is a decreasing function of time). Figure II.4 displays the evolution of the electrochemical potential $\varphi(x) = A(x) - (V_s(x) + V_{ext}(x))$ and we can see that it is constant at $t = 10000\ fs$ (and equal to $0.0623V$). At equilibrium, the density (which is a solution of the Schrödinger-Poisson (SP) model) is perfectly symmetric and the mass has been conserved up to a relative error of $10^{-4}\%$.

Effective mass m (kg)	Mobility μ $(m^2V^{-1}s^{-1})$	Permittivity ε (Fm^{-1})	Temperature T (K)
$0.067 \times 9.11e-31$	0.85	$11.44 \times 8.85e-12$	300

Table II.1: Parameters used for the modeling of an isolated RTD.

4.1.2 Comparison between the QDD model and the SPDD model

Figure II.5 permits to compare the QDD model, the SPDD model and the stationary SP model. The dashed line shows the evolution of the relative difference (in L^2 norm) between the densities for the QDD model and the SPDD model while the solid line shows the evolution of the relative difference between the densities for the QDD model and the SP model. The QDD and the SPDD model are closer than the QDD and the SP models (as suggested in section 2.2) but the relative difference between the densities decreases with the same rate.

The QDD model and the SPDD model with insulating boundary conditions seem very close but if we apply open boundary conditions and if the applied bias is too high, it appears that the SPDD model is not as stable as the QDD model. The current

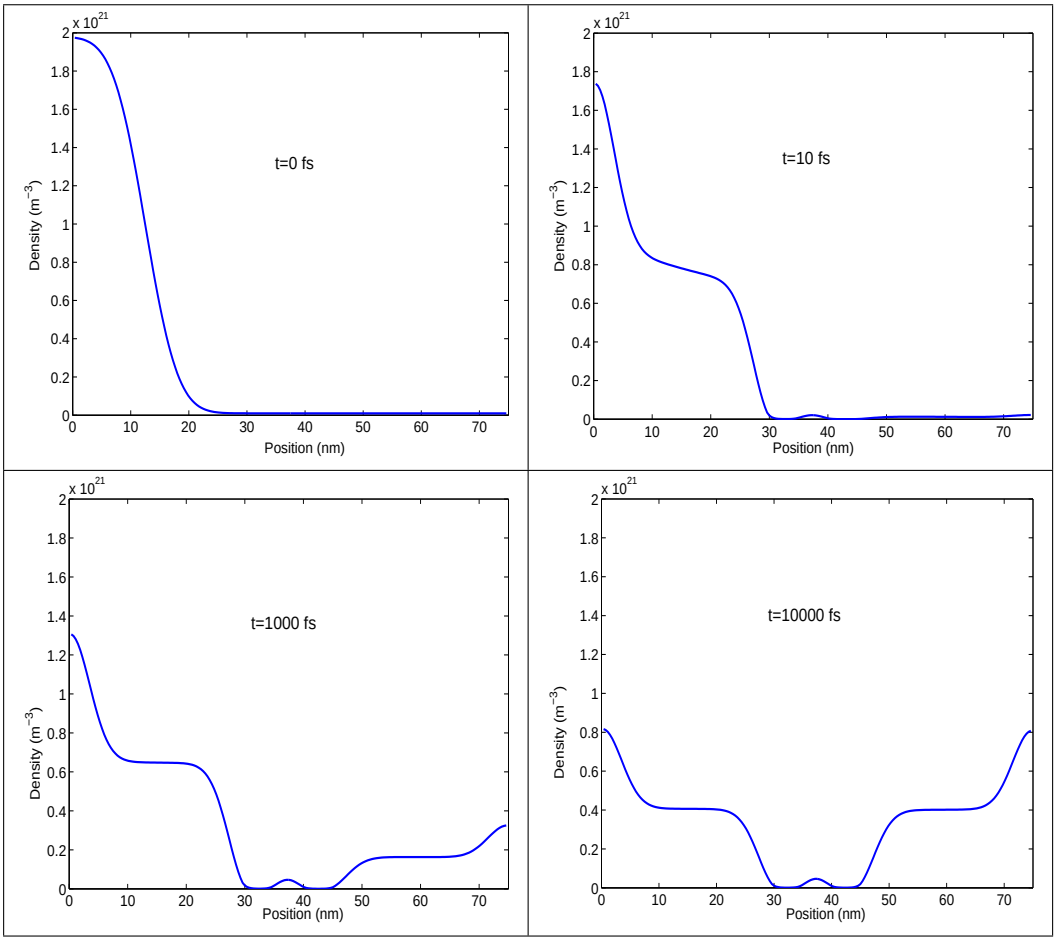

Figure II.2: Electron density at different times ($t = 0, 10, 1000$ and $10000\ fs$) for the QDD model.

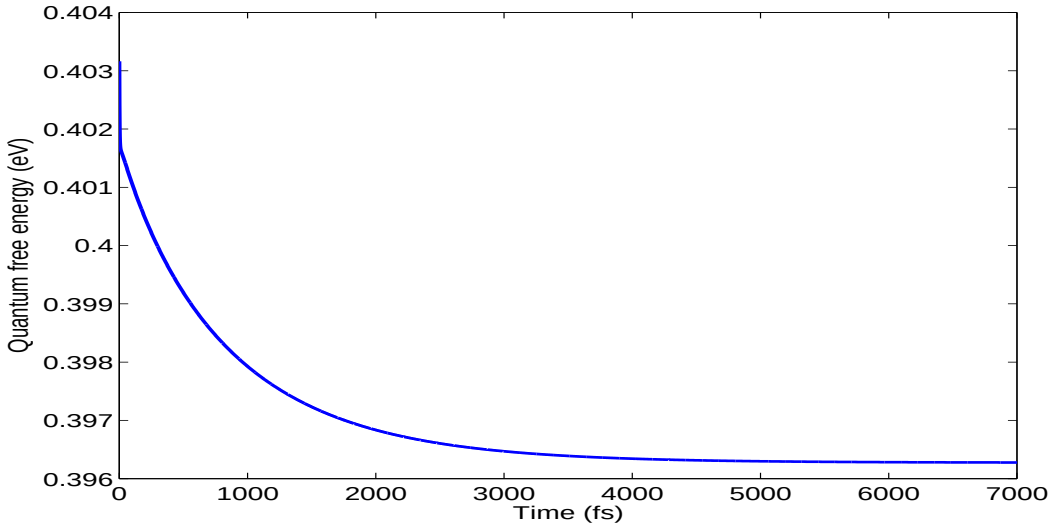

Figure II.3: Evolution of the Quantum free energy.

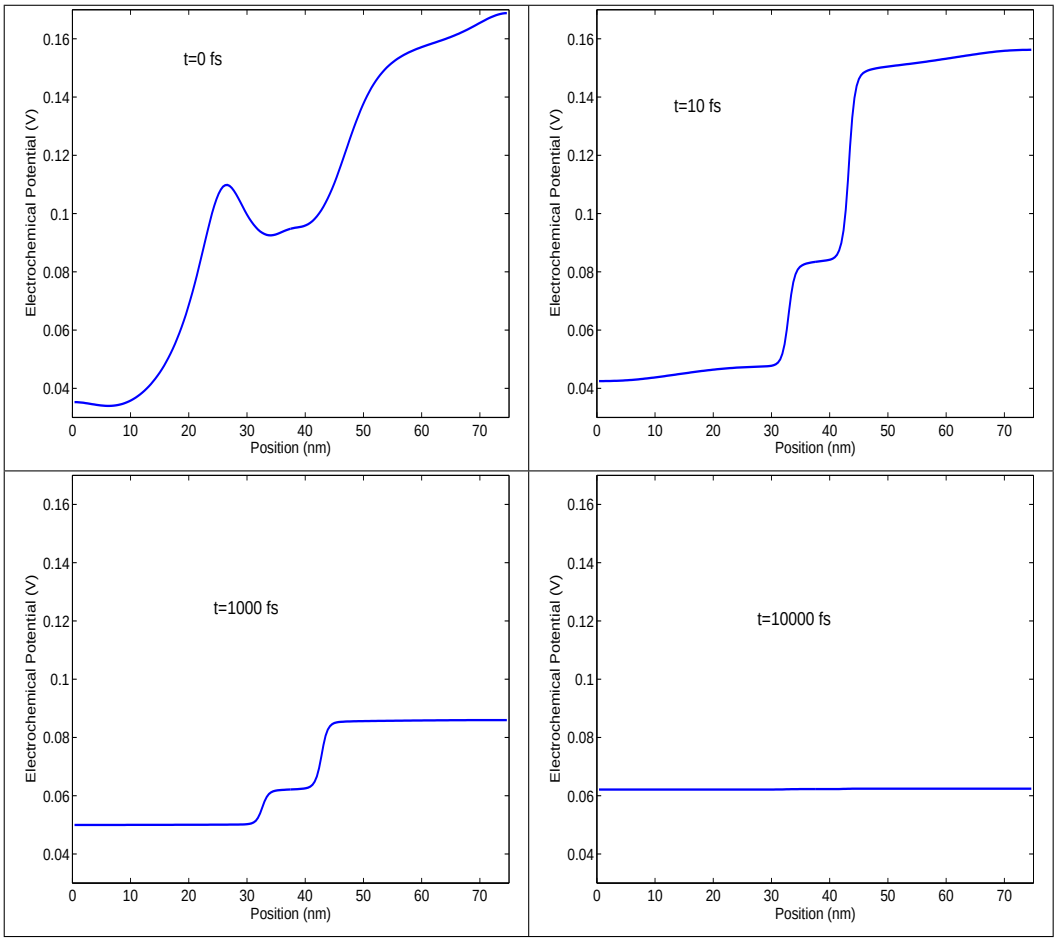

Figure II.4: Electrochemical potential ($\varphi(x) = A - (V_s + V_{ext})$) at different times ($t = 0, 10, 1000$ and $10000\ fs$).

oscillates and does not stabilize. This is why we have not been able to plot current-voltage characteristics for the SPDD model. This is perhaps due to the fact that the SPDD model is not entropic. However, we have been able to compare IV curves for the QDD model and the DG model (see next section).

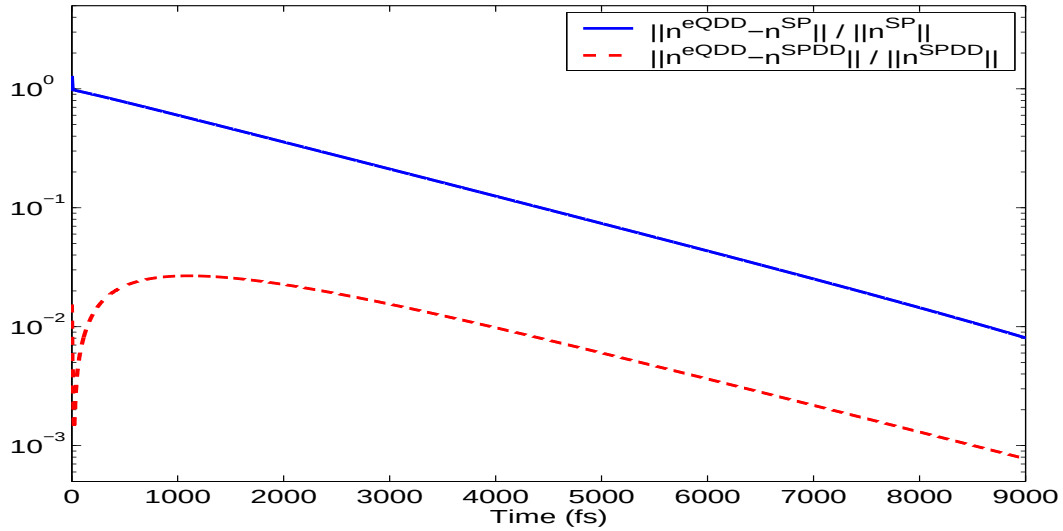

Figure II.5: Comparison between the QDD model and the SPDD model (dashed line), and between the QDD model and the SP model (solid line).

4.2 Open boundary conditions

4.2.1 The QDD model

The goal of this subsection is to check if the QDD model captures some properties of a RTD and to analyse the influence of the effective mass on the current-voltage characteristics. For each bias V_r applied on the diode, we find the stationary state and we record the corresponding current $j(V_r)$. We consider that the stationary state is achieved when $\frac{\max(j)-\min(j)}{\text{mean}(j)} \leq 10^{-2}$ (this constant was fixed heuristically).

Let us first analyze the influence of the effective mass on the shape of the IV curve. The temperature is chosen equal to $77K$ and the mobility is supposed to be constant and equal to 0.85 $m^2V^{-1}s^{-1}$. The permittivity is also supposed to be constant and equal to 11.44 ε_0. Figure II.6 shows four different IV curves with different values of the effective mass inside and outside the double barriers. As pointed out in [34], this parameter appears to be critical to obtain resonance with the DG model and it seems to be the same for the QDD model. To be more precise, an interesting feature that can be seen on figure II.6 is that the IV curve is much more sensitive on m_2 (the effective mass inside the AlGaAs barriers) than on m_1 (the effective mass in the GaAs, outside the barriers). Note that with the most realistic physical values ($m_1 = 0.067m_e$ and $m_2 = 0.092m_e$), the IV curve does not show negative resistance and we need to artificially increase the effective masses to see such phenomenon appear. This problem has been also reported for the DG model in [34, 42]. An explanation to this phenomenon could be that the approximation of effective mass is unappropriate for small distances (one barrier is only 50Å long). We can also see that as expected,

increasing the effective mass lowers the current.

Figure II.7 shows the time evolution of the density from the peak to the valley when the effective mass is $m_2 = 1.5 \times 0.092 m_e$ inside the barriers and $m_1 = 1.5 \times 0.067 m_e$ outside it (corresponding to the IV curve at the bottom right of figure II.6). To obtain this figure, we apply a voltage of $0.25V$ and wait for the electrons to achieve the stationary state. Then we suddenly change the value of the applied bias to $0.29V$ and we record the evolution of the density. As expected, the density inside the well grows significantly and the stationary state is achieved at about $1500fs$.

A small density depletion can be observed on the edge, which does not seems physical. It may be due to the choice in our model of Neumann boundary conditions for the wave functions whereas open (or transparent) boundary conditions should be preferable. However, because this "boundary layer" appears inside the doped region, it does not seem to affect the current, but this question requires more investigations.

The next two figures (fig. II.8 and fig. II.9) display the details of the reconstruction of the density from the eigenstates ψ_p (for $p = 1 \cdots 6$) of the modified Hamiltonian $H(A)$. The density $e^{-\lambda_p}|\psi_p|^2$ corresponding to each eigenstate is plotted for two values of the applied bias, respectively corresponding to the current peak (fig.II.8) and to the valley (fig.II.9). Table 4.2.1 shows the values of the corresponding energies λ_p. Some interesting features can be pointed out. First, the eigenstates split in three categories: three of them ($p = 1, 3, 6$) correspond to wave functions which give rise to the density of incident electrons (on the left hand side of the double barrier), one and only one ($p = 4$) describes the electrons inside the well and two wavefunctions ($p = 2, 5$) correspond to electrons on the right hand side of the double barrier. Table 4.2.1 shows clearly that the voltage shift has no incidence on the energies corresponding to the incident electrons while the energies of the electrons on the right hand side of the double barriers increase. An important change concerns the energy corresponding to electrons which are trapped inside the well, starting with an energy of $2.03eV$ and finishing with an energy of $1.70eV$, explaining the density increase in this region.

Lastly, figure II.10 shows the transient current at the left contact ($x = 0$). As we switch at time $t = 0$ out of the equilibrium state ($j = 0$), we can observe that the current suffers one oscillation before achieving its equilibrium state at the valley. Oscillations were also reported in [38] for example where a transient Schrödinger Poisson model was used for the simulation. The current was highly oscillatory because of the ballistic effects. Here, because of the diffusion effects, we cannot expect the same behavior. Note that the behavior of the QDD model is again qualitatively similar to the DG model, the same phenomenon having been reported in [29].

	λ_1	λ_2	λ_3	λ_4	λ_5	λ_6	λ_7
Peak	0.87	1.05	1.56	2.03	2.28	3.03	4.47
Valley	0.87	1.11	1.57	1.70	2.54	3.05	5.03

Table II.2: Eigenvalues (Energies [eV]) of the modified Hamiltonian $H(A)$ at the Peak and at the Valley.

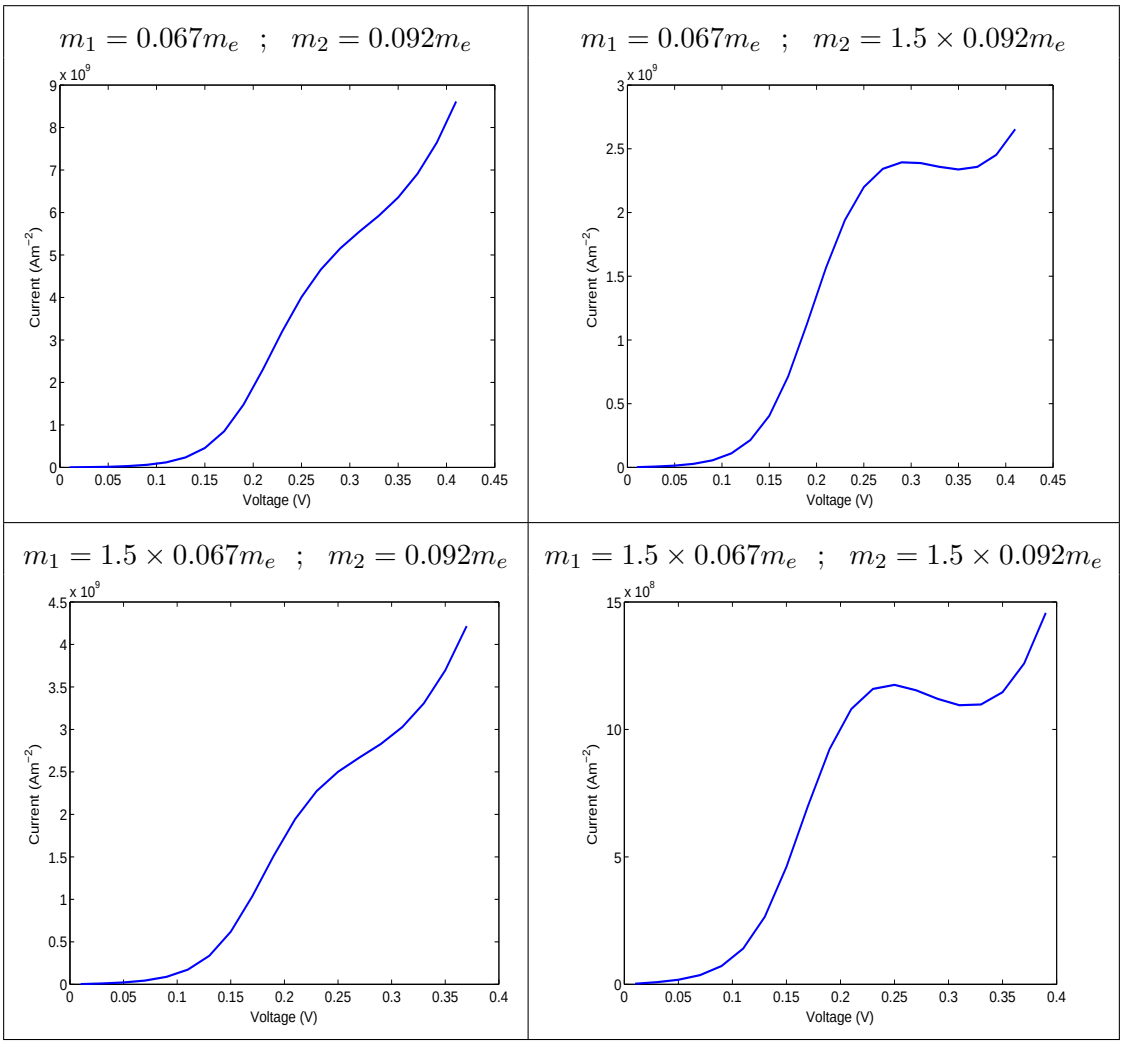

Figure II.6: Influence of the effective mass on the IV curve, m_1 being the mass outside the barriers, and m_2 being the mass inside.

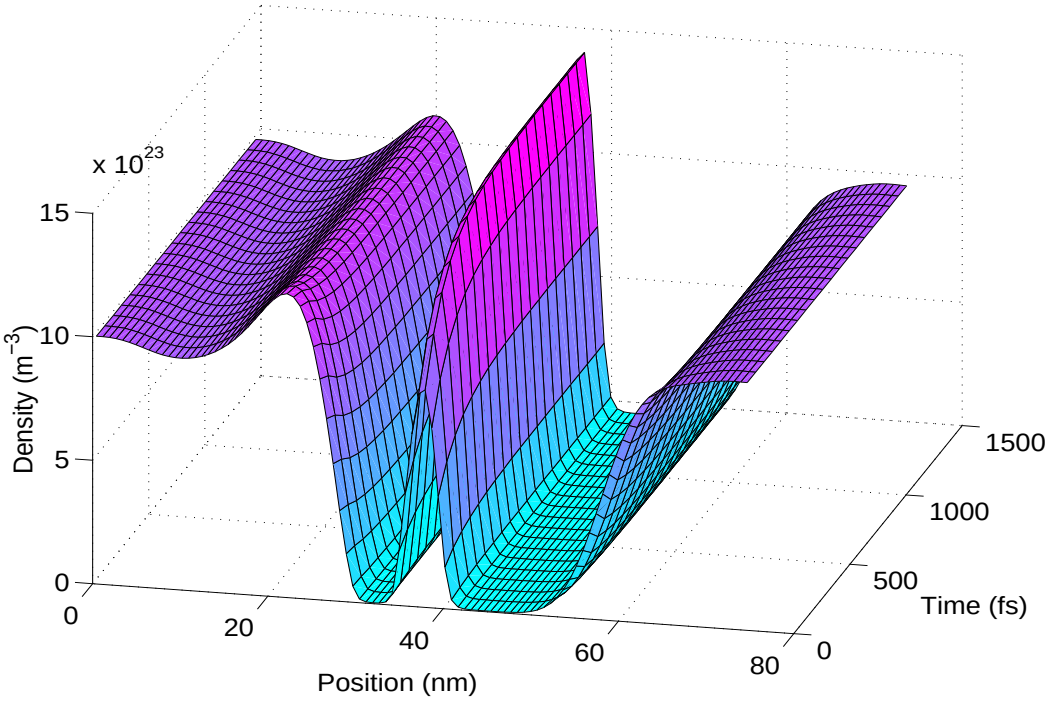

Figure II.7: Evolution of the density from the peak (applied bias: 0.25V) to the valley (applied bias: 0.31V).

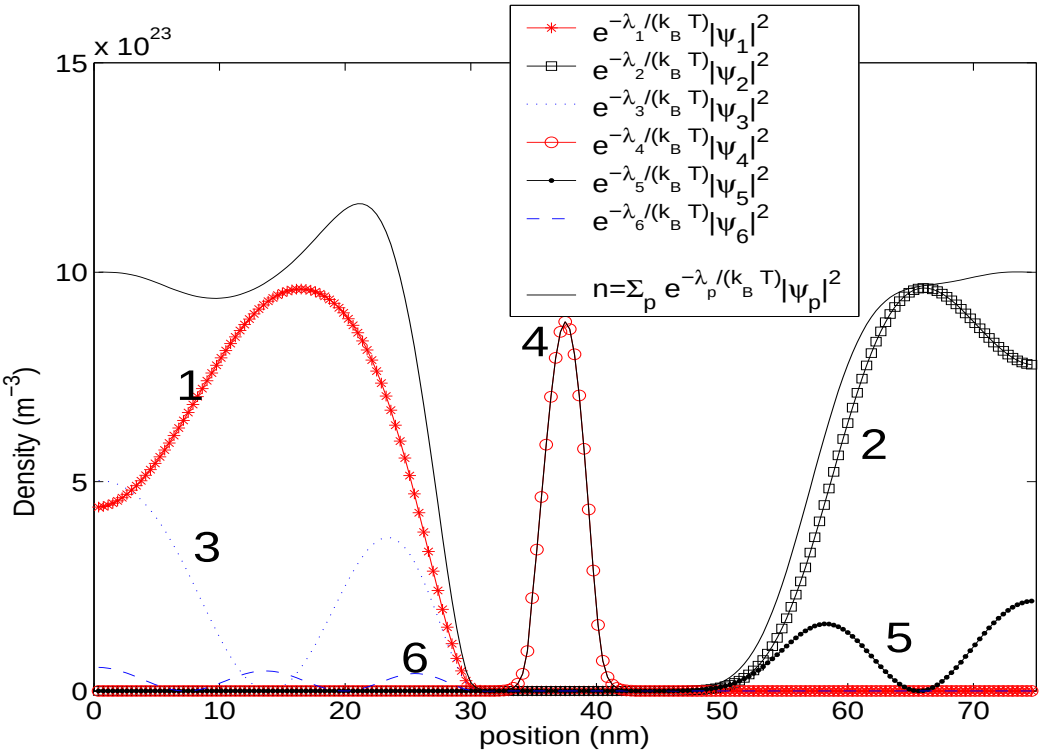

Figure II.8: Density at the peak (Applied bias: 0.25V).

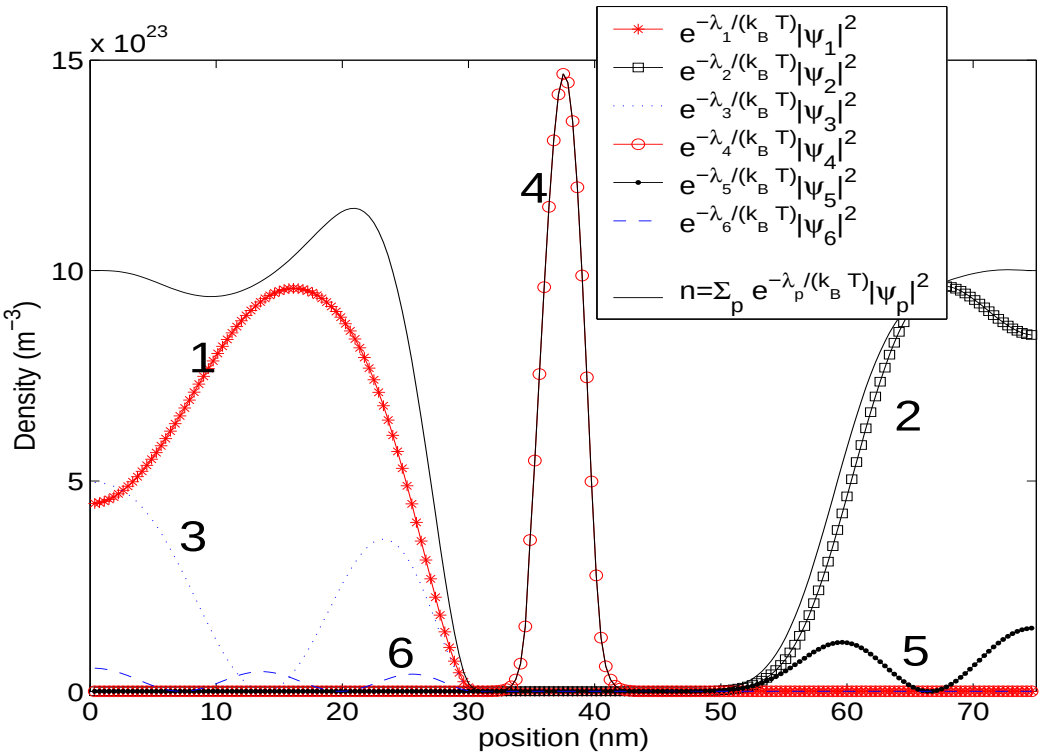

Figure II.9: Density at the valley (Applied bias: 0.31V).

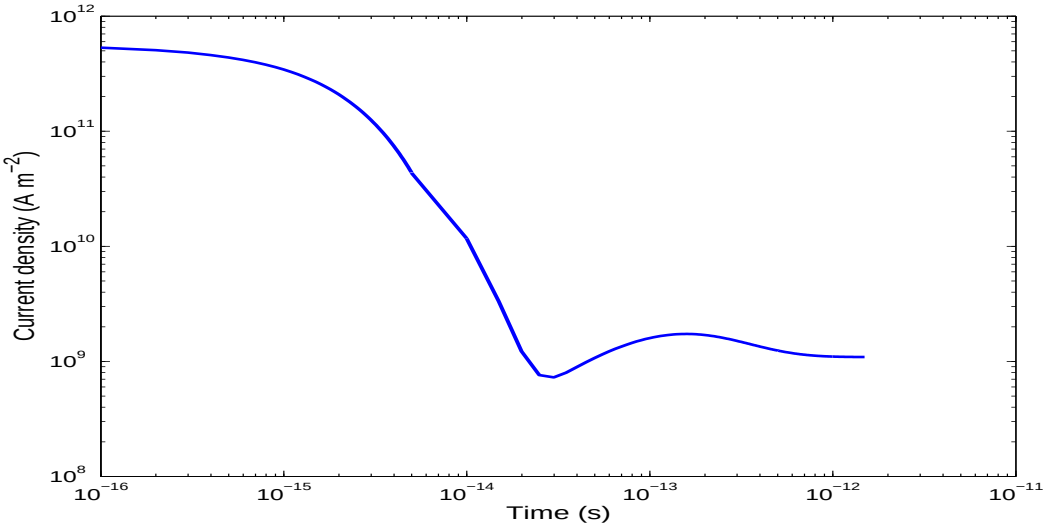

Figure II.10: Transient Current density.

4.2.2 Comparison between the QDD model and the DG model

In Figure II.11, we show the results obtained with the Density Gradient model using the same parameters as defined for the QDD model. As we can see, results are qualitatively similar but differ significantly even if the fourth power of the scaled Planck constant $\hbar^4$ is between 10^{-6} and 10^{-4} depending on the value of the effective mass. The current is much smaller for the DG model and the peak-to-valley ratios are more important. This may be due to the fact that the heterojunctions of the RTDs create discontinuities not only on the external potential, but also on the quantum chemical potential and so the error estimate made in (2.26) may not be valid because the quantum chemical potential is not a smooth function. This is not surprising then that these two models give different results on such a device. Even with a smoother external potential (replacing the two step functions by two gaussians), it appears that the current-voltage characteristics are still different for the two models as suggested by figure II.12. In order to avoid any confusion induced by the variable mass (the link between both models having been written for a constant effective mass), we take a mass constant and equal to $0.067 \times me$. A parameter which seems important for the models to fit is the height of the double barriers. Indeed, even with a smooth external potential, if the height of the barriers is important, it appears that the density varies a lot, creating a Bohm potential which is not small (in $\hbar^2$) as needed for the error estimate (2.27) to be valid.

We have observed that we can fit the results obtained with the QDD model and the DG model dividing the effective mass (which is equivalent to multiplying the Bohm potential) by an appropriate constant in the DG model. Astonishingly, not only the stationary current fits but also the time behavior of the density and the current, but we do not yet explain this fact which does not seem to be a coincidence. Moreover, we have not found any convincing physical explanation for this similarity. To finish, figure II.13 shows the role of the temperature on the current for an applied bias of $0.2V$ and for the three models QDD, DG and CDD with a constant mass equal to $0.067m_e$. For fairly large temperatures, the currents seem to converge to the same

limit, due to the high thermoionic effects. Moreover, the DG model seems closer from the QDD model than from the CDD model as discussed in section 2.2 (note that $\hbar$ is small when T is large). We refer to appendix C for comparisons of the QDD model with the mixed state Schrödinger model, the NEMO simulator and the Smooth QHD model.

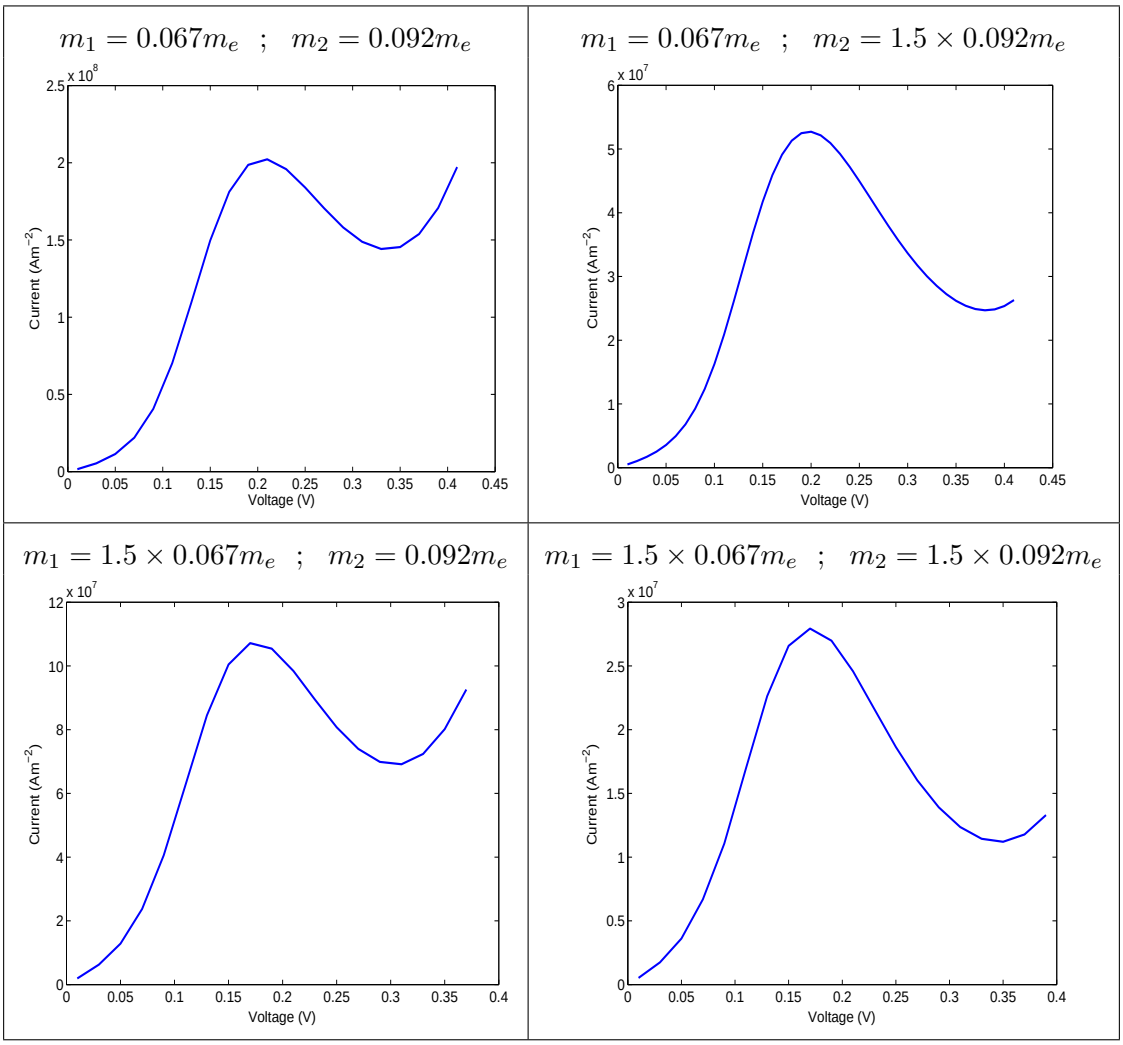

Figure II.11: IV curves obtained with the DG model (m_1 being the mass outside the barriers, and m_2 being the mass inside).

5 Summary and Conclusion

An entropic Quantum Drift-Diffusion model for transport in nanostructures has been presented on a bounded domain. A discretization has been proposed and numerical results have permitted to check the main properties of the model such as entropy dissipation, mass conservation, and convergence to the stationary Schrödinger-Poisson model. The QDD model captures also some interesting features of the resonant tunneling diode, such as the resonance peak on the IV curve, characteristic of such a device. The model seems to be quite sensitive to the value of the effective mass inside the double barrier. The QDD model has also been compared to the Schrödinger

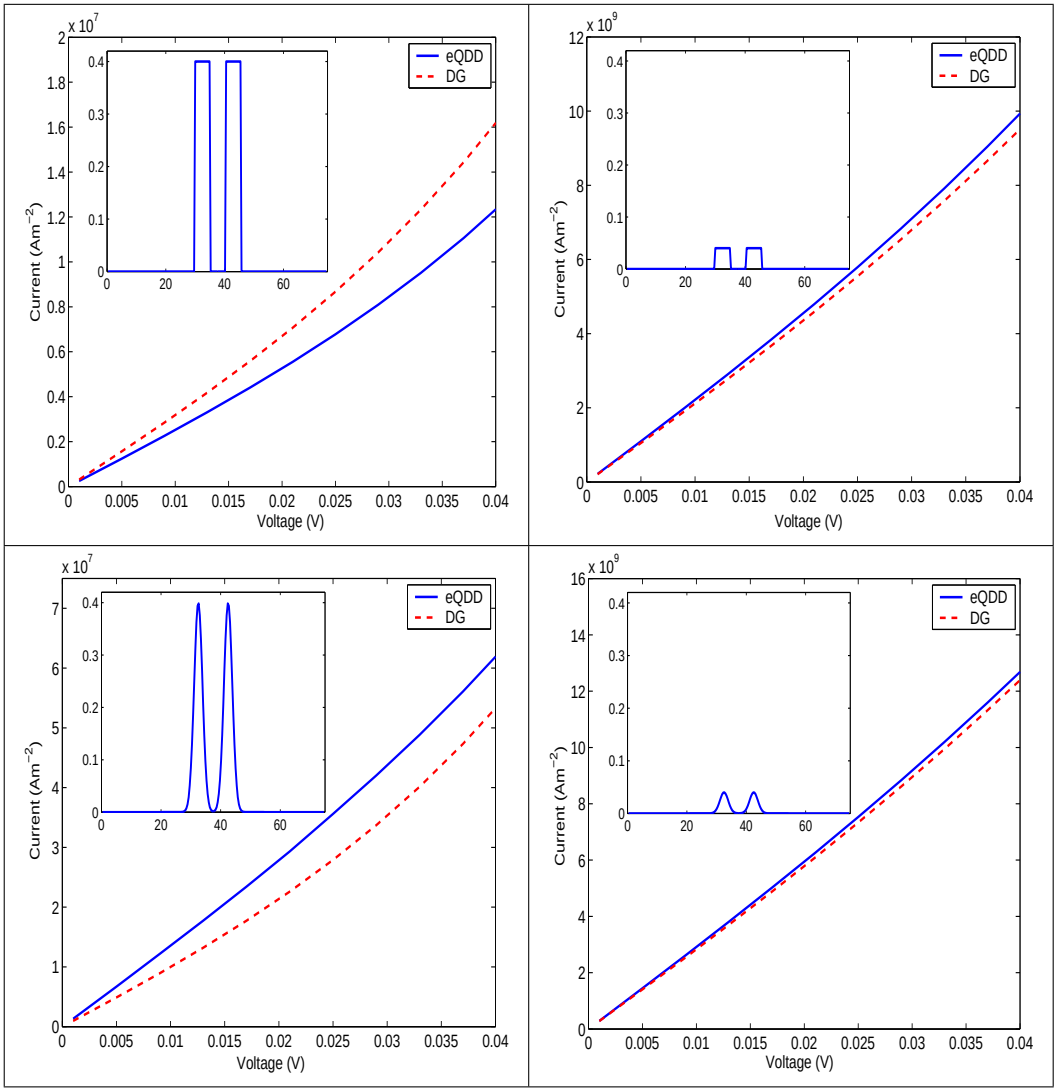

Figure II.12: Influence of the shape and the height of the double barrier on the Current-Voltage characteristics for the QDD and DG models.

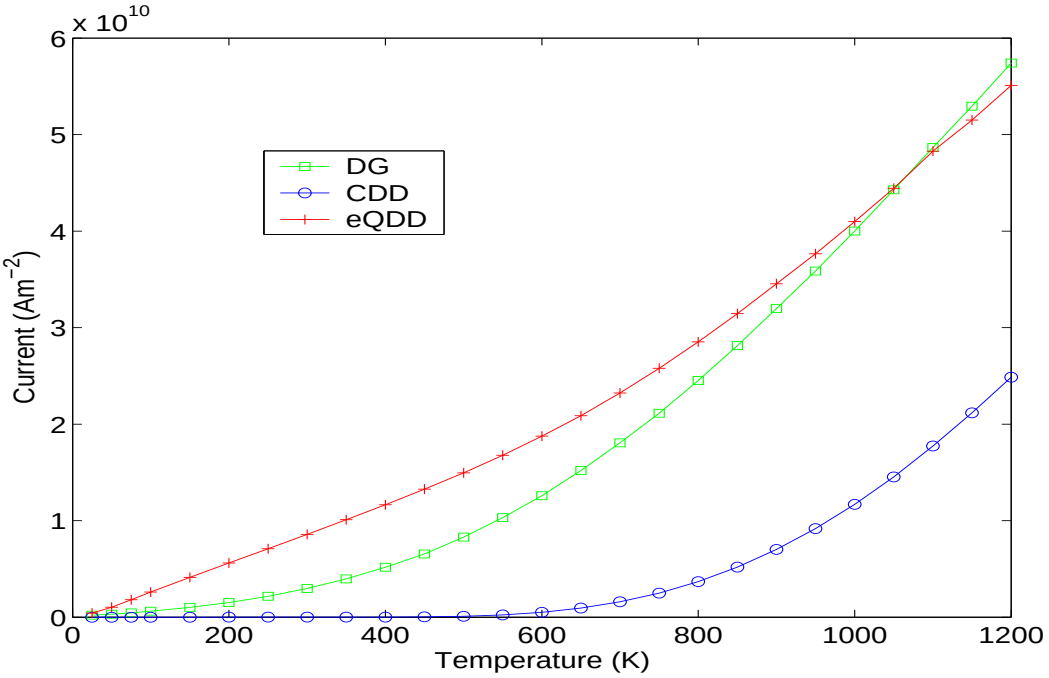

Figure II.13: Current-Temperature curve (applied bias: $0.2V$).

Poisson Drift-Diffusion model on the one hand and the Density Gradient model on the other hand, showing interesting differences: The QDD model is very close to the SPDD model near the equilibrium but seem to be more stable far from the equilibrium (this is probably because it dissipates free energy). For quantum devices such as RTDs with heterojunctions, the QDD model and the DG model are not so close quantitatively because of the discontinuity of the potentials but they exhibit similar qualitative behavior. In the next chapter, we are going to incorporate to the QDD model the continuous spectrum of the modified Hamiltonian H by considering transparent boundary conditions for the wave functions, adapting the work done for the Schrödinger equation in [3, 8, 7, 38, 31].

Appendix

A Derivation of the QDD model

In order to understand why this model dissipates quantum entropy, we are going to recall how it can be derived from the Quantum Liouville equation applying a diffusive limit. In article [14], the diffusive limit is performed on the unbounded domain of dimension d ($\mathbb{R}^d$) using the Wigner transform. Here, we adapt this work to derive the QDD model in the density matrix formulation, which enables to work on a arbitrary set $\Omega \subset \mathbb{R}^d$ (bounded or not) with a characteristic size L. For the sake of simplicity we are going to suppose that the effective mass m is constant in Ω, but all the following calculations can be extended to the case of a variable effective mass.

Derivation of the model. A quantum particle system can be described by a density operator ρ which is a positive hermitian, trace-class operator satisfying the collisional Liouville equation:

$$i\hbar\partial_t\rho = [\mathcal{H}, \rho] + i\hbar\mathcal{Q}(\rho), \tag{A.38}$$

where $[\mathcal{H}, \rho] = \mathcal{H}\rho - \rho\mathcal{H}$ is the commutator of the Hamiltonian $\mathcal{H} = -\frac{\hbar^2}{2m}\Delta - eV$ and the density operator and $\mathcal{Q}(\rho)$ is a collision operator describing the interactions between particles and a thermal bath at temperature T. The density of particles $n(x)$ is defined weakly by:

$$\forall\phi \quad \int_\Omega n(x)\phi(x)dx = \mathrm{Tr}\ (\rho\phi)\,, \tag{A.39}$$

where on the right hand side, we interpret ϕ as the multiplication operator by the function $\phi(x)$. In order to define this collision operator, we have to introduce the quantum free energy and the Quantum Maxwellians. The microscopic quantum free energy of a system is defined by:

$$G(\rho) = E(\rho) - TS(\rho), \tag{A.40}$$

where E is the energy of the system and S is the quantum entropy. The entropy is given by:

$$S(\rho) = -k_B\mathrm{Tr}\ (\rho\log\rho)\,, \tag{A.41}$$

and the energy is defined by:

$$E(\rho) = \mathrm{Tr}\ (\rho\mathcal{H})\,. \tag{A.42}$$

We obtain the following expression for the microscopic quantum free energy:

$$G(\rho) = \mathrm{Tr}\ \left(\rho k_B T(\log\rho + \frac{\mathcal{H}}{k_B T})\right). \tag{A.43}$$

Now, we consider the problem of minimizing the quantum free energy G under the constraint of given density $n(x)$:

$$\min\{G(\rho) \mid \forall\phi \quad \int n(x)\phi(x)dx = \mathrm{Tr}\ (\rho\phi)\}. \tag{A.44}$$

Assuming that this minimization problem has a solution, this solution is given by [17, 14]:

$$\rho(A) = \exp(-\frac{H(A)}{k_B T}),$$

where $H(A)$ is the modified Hamiltonian defined in relation (2.4) and $A = A(x)$ is a quantum chemical potential which is determined in such a way that the density constraint in (A.44) is satisfied. We note $\mathcal{M}_\rho = \exp(-\frac{H(A)}{k_B T})$ the quantum Maxwellian which has the same density as ρ (*i.e* Tr $(\mathcal{M}_\rho \phi)$ = Tr $(\rho\phi)$ $\forall \phi$). Now, we define the collision operator as follows:

$$\mathcal{Q}(\rho) = \frac{\mathcal{M}_\rho - \rho}{\tau}. \tag{A.45}$$

where τ is the relaxation time of the collision operator which can be found from the mobility of the material: $\tau = \frac{m\mu}{e}$. We expect that, as in the classical setting, this simple collision operator of BGK type provides a simple relaxation model with similar features as physically more realistic operators. Now we want to perform a diffusive limit on the quantum Liouville equation. For this purpose, we start by doing the same scaling as in section 2.1.2 on the quantum Liouville equation and we obtain (omitting the primes):

$$i\varepsilon \partial_t \rho^\varepsilon = \frac{1}{\hbar}[\mathcal{H}, \rho^\varepsilon] + i\frac{\mathcal{M}_{\rho^\varepsilon} - \rho^\varepsilon}{\varepsilon}, \tag{A.46}$$

where $\mathcal{H} = -\frac{\hbar^2}{2}\Delta + V$. The dimensionless parameter $\hbar$ is the scaled Planck constant and the dimensionless parameter ε is the scaled mean free path defined by:

$$\varepsilon = \sqrt{\frac{k_B T}{m}}\frac{\tau}{L} = \frac{\lambda_{\text{mfp}}}{L}.$$

A typical value of ε is $\varepsilon \sim 0.5$ at $T \sim 77K$. In smaller temperatures, ε can be estimated to be small and the limit $\varepsilon \to 0$ can be investigated. Even if ε is not small, the limit $\varepsilon \to 0$ can be believed to at least provides a reasonable approximation of the problem.

Therefore, we are interested in the limit $\varepsilon \to 0$. We assume that $\rho^\varepsilon \to \rho^0$ as $\varepsilon \to 0$. Then at leading order, we have $\mathcal{Q}(\rho^0) = 0$ which means that ρ^0 belongs to the null space of the collision operator Q. Thus, we deduce that there exists a function $A(x,t)$ such that

$$\rho^0 = e^{-H(A)}, \tag{A.47}$$

with $H(A)$ the modified scaled Hamiltonian:

$$H(A) = -\frac{\hbar^2}{2}\Delta + A.$$

Now we introduce the following Chapman-Enskog expansion:

$$\rho^\varepsilon = \mathcal{M}_{\rho^\varepsilon} + \varepsilon \rho_1^\varepsilon. \tag{A.48}$$

Then, clearly:

$$\frac{\mathcal{M}_{\rho^\varepsilon} - \rho^\varepsilon}{\varepsilon} = -\rho_1^\varepsilon.$$

Inserting this expression into equation (A.46) and taking the limit $\varepsilon \to 0$ we get:

$$\rho_1^0 = -\frac{i}{\hbar}[\mathcal{H}, \rho^0]. \tag{A.49}$$

Now, we compose equation (A.46) with the multiplication by a test function ϕ and we take the trace. We use that, by definition, Tr $((\mathcal{M}_\rho - \rho)\phi) = 0$ and we get:

$$\text{Tr } (i\partial_t \rho^\varepsilon \phi) - \frac{1}{\hbar\varepsilon}\text{Tr } ([\mathcal{H}, \rho^\varepsilon]\phi) = 0. \tag{A.50}$$

We can simplify this equation by noticing that:

$$\text{Tr } ([\mathcal{H}, \mathcal{M}_{\rho^\varepsilon}]\phi) = 0.$$

Indeed, $\mathcal{H} = H(A^\varepsilon) - (A^\varepsilon - V)$ where A^ε is such that $\mathcal{M}_{\rho^\varepsilon} = e^{-H(A^\varepsilon)}$, so that $[\mathcal{H}, \mathcal{M}_{\rho^\varepsilon}] = [H(A^\varepsilon), \mathcal{M}_{\rho^\varepsilon}] - [A^\varepsilon - V, \mathcal{M}_{\rho^\varepsilon}]$. The first commutator is equal to zero because the commutator between an operator and its exponential is zero. The trace of the second commutator multiplied by ϕ is equal to zero because of the cyclicity of the trace. We remind that $\forall(a, b, c)$, we have Tr $([a, b]c) =$ Tr $(a[b, c]) =$ Tr $([c, a]b)$ so that Tr $([A^\varepsilon - V, \mathcal{M}_{\rho^\varepsilon}]\phi) =$ Tr $([\phi, A^\varepsilon - V]\mathcal{M}_{\rho^\varepsilon}) = 0$ (ϕ and $A^\varepsilon - V$ being operators of multiplication by functions). Equation (A.50) becomes:

$$\text{Tr } (i\partial_t \rho^\varepsilon \phi) - \frac{1}{\hbar}\text{Tr } ([\mathcal{H}, \rho_1^\varepsilon]\phi) = 0$$

At the limit $\varepsilon \to 0$ and using (A.49), we obtain:

$$\text{Tr } \left(i\partial_t \rho^0 \phi\right) + \frac{1}{\hbar^2}\text{Tr } \left(i[\mathcal{H}, [\mathcal{H}, \rho^0]]\phi\right) = 0.$$

We again use the fact that the commutator between an operator and its exponential is zero, so

$$[\mathcal{H}, \rho^0] = -[A - V, \rho^0].$$

Also using the cyclicity of the trace, we find that

$$\text{Tr } \left([\mathcal{H}, [A - V, \rho^0]]\phi\right) = \text{Tr } \left([-\frac{\hbar^2}{2}\Delta, [A - V, \rho^0]]\phi\right)$$

and we obtain:

$$\text{Tr } \left(i\partial_t \rho^0 \phi\right) - \frac{1}{\hbar^2}\text{Tr } \left(i[-\frac{\hbar^2}{2}\Delta, [A - V, \rho^0]]\phi\right) = 0.$$

Now, we can prove that

$$\text{Tr } \left([-\frac{\hbar^2}{2}\Delta, [A - V, \rho^0]]\phi\right) = \hbar^2 \text{Tr } \left(\rho^0 \nabla\phi \cdot \nabla(A - V)\right).$$

Indeed, using the cyclicity of the trace, we first see that Tr $\left([-\Delta, [A - V, \rho^0]]\phi\right) =$ Tr $\left(\rho^0[[\Delta, \phi], A - V]\right)$, and second, a direct computation of the double commutator leads to the fact that $[[\Delta, \phi], A - V] = 2\nabla\phi \cdot \nabla(A - V)$. The density being weakly defined by:

$$\forall\phi \quad \int_\Omega n\phi dx = \text{Tr } \left(\rho^0 \phi\right), \tag{A.51}$$

we finally obtain the following equality being true for every test function ϕ:

$$\int_\Omega (\partial_t n\phi - n\nabla(A - V) \cdot \nabla\phi) dx = 0,$$

which gives after an integration by parts the dimensionless version of the QDD model (2.6)-(2.7) in a weak formulation.

Entropic character of the model. We are now able to prove that the QDD model dissipates the quantum free energy. The scaled microscopic quantum free energy reads:

$$G(\rho) = \text{Tr } (\rho(\log \rho + \mathcal{H})),$$

so that

$$\frac{d}{dt}G(\rho) = \mathrm{Tr}\ ((\log\rho + \mathcal{H} + \mathrm{Id})\partial_t\rho)\,.$$

This identity is not obvious and uses a formula for the derivative of G with respect to ρ which can be found in [17] or [14]. Using the Liouville equation (A.46), we obtain:

$$\frac{d}{dt}G(\rho^\varepsilon) = \mathrm{Tr}\ \left((\log\rho^\varepsilon + \mathcal{H} + \mathrm{Id})(-i\frac{[\mathcal{H},\rho^\varepsilon]}{\hbar^2\varepsilon} + \frac{\mathcal{M}_{\rho^\varepsilon} - \rho^\varepsilon}{\hbar^2\varepsilon^2})\right).$$

But using the cyclicity of the trace, we find:

$$\mathrm{Tr}\ \left((\log\rho^\varepsilon + \mathcal{H} + \mathrm{Id})(-i\frac{[\mathcal{H},\rho^\varepsilon]}{\hbar^2\varepsilon})\right) = 0,$$

and using the convexity of the quantum free energy, we have the inequality:

$$G'(\rho^\varepsilon)(\mathcal{M}_{\rho^\varepsilon} - \rho^\varepsilon) = \mathrm{Tr}\ ((\log\rho^\varepsilon + \mathcal{H} + \mathrm{Id})(\mathcal{M}_{\rho^\varepsilon} - \rho^\varepsilon)) \leq G(\mathcal{M}_{\rho^\varepsilon}) - G(\rho^\varepsilon).$$

Because $\mathcal{M}_{\rho^\varepsilon}$ is chosen to minimize G, we finally have:

$$\frac{d}{dt}G(\rho^\varepsilon) \leq 0.$$

This inequality is true at the limit $\varepsilon \to 0$, giving the dissipation of the macroscopic quantum free energy:

$$G(n) = \int_\Omega -n(A - V)\ dx.$$

Relation between the density and the quantum chemical potential. Note that if A belongs to $L^2(\Omega)$ and if we choose for $H(A)$ a domain such that $H(A)$ has a compact resolvent (putting Neumann conditions on the wave functions for example), $H(A)$ possesses an orthogonal basis of eigenfunctions $(\psi_p(A))_{p=1\cdots\infty}$ associated with the eigenvalues $\lambda_1(A) \leq \lambda_2(A) \leq ....$ The relation (A.51) between n and A takes a more explicit form:

$$n(A) = \sum_{p\geq 1} \exp(-\lambda_p(A))|\psi_p(A)|^2, \tag{A.52}$$

where the ψ_p are normalized:

$$\int_\Omega \psi_p\psi_q = \delta_{pq}.$$

Indeed, we can write:

$$\begin{aligned}
\forall\phi \quad \int_\Omega n\phi\ dx &= \mathrm{Tr}\ \left(e^{-H(A)}\phi\right) \\
&= \sum_{p\geq 1}\left(\phi e^{-H(A)}\psi_p, \psi_p\right)_{L^2(\Omega)} \\
&= \sum_{p\geq 1}\int_\Omega \phi e^{-\lambda_p}|\psi_p|^2\ dx \\
&= \int_\Omega (\sum_{p\geq 1} e^{-\lambda_p}|\psi_p|^2)\phi\ dx,
\end{aligned}$$

defining weakly the density.

B The dimensionless models in dimension 1 with variable parameters

In this section, for the sake of completeness, the dimensionless models with variable mass, permittivity and mobility are written.

The QDD model. The entropic Quantum Drift-Diffusion model coupled with the Poisson equation is written:

$$\begin{aligned}
&\partial_t n + \partial_x j = 0,\\
&j = n\mu(x)\partial_x(A - (V_s + V_{ext})),\\
&-\alpha^2(\partial_x \varepsilon(x)\partial_x V_s) = n^d - n,\\
&n = \sum_{p\geq 1} e^{-\lambda_p}|\psi_p|^2,
\end{aligned}$$

where (λ_p, ψ_p) are the eigenvalues and eigenfunctions of $H(A) = -\frac{\tilde{\hbar}^2}{2}\partial_x(\frac{1}{m(x)}\partial_x) + A$, with α and $\hbar$ the scaled Debye length and the scaled de Broglie length:

$$\begin{aligned}
\alpha &= \sqrt{\frac{\overline{\varepsilon} k_B T}{e^2 L^2 \overline{n}}} = \frac{\lambda_D}{L},\\
\tilde{\hbar} &= \sqrt{\frac{\hbar^2}{2\overline{m} L^2 k_B T}} = \frac{\lambda_{dB}}{L}.
\end{aligned}$$

The reference values for the mobility $\overline{\mu}$,the effective mass $\overline{m}$ and the permittivity $\overline{\varepsilon}$ are chosen as follows:

$$\overline{\mu} = \max|\mu(x)| \;\; ; \;\; \overline{m} = \max|m(x)| \;\; ; \;\; \overline{\varepsilon} = \max|\varepsilon(x)|$$

The DG model and the CDD model. The Density Gradient model coupled with the Poisson equation is written:

$$\begin{aligned}
&\partial_t n + \partial_x j = 0,\\
&j = n\mu(x)\partial_x(-\log n - (V_s + V_{ext} + \frac{1}{3}V_B)) = 0,\\
&-\alpha^2\partial_x(\varepsilon(x)\partial_x V_s) = n - n^d,\\
&V_B = -\frac{\hbar^2}{2}\frac{\partial_x(\frac{1}{m}\partial_x\sqrt{n})}{\sqrt{n}}.
\end{aligned}$$

For the Classical Drift-Diffusion model, we take $V_B = 0$.

The SPDD model. The Schrödinger-Poisson Drift-Diffusion model coupled with the Poisson equation is written:

$$\begin{aligned}
&\partial_t n + \partial_x j = 0,\\
&j = n\mu(x)\partial_x(A - (V_s + V_{ext})) = 0,\\
&-\alpha^2\partial_x\varepsilon(x)\partial_x V_s = n^d - n,\\
&n = \sum_{p\geq 1} e^{-\lambda_p - A + (V_s + V_{ext})}|\psi_p|^2,
\end{aligned}$$

where (λ_p, ψ_p) are the eigenvalues and eigenfunctions of the Hamiltonian $\mathcal{H} = H\,(V_s + V_{ext}) = -\frac{\hbar^2}{2}\partial_x(\frac{1}{m(x)}\partial_x) + (V_s + V_{ext})$.

C ADDENDUM: Comparisons of the QDD model with the mixed state Schrödinger model, the NEMO simulator and the Smooth QHD model

We propose in this addendum to compare the QDD model with the mixed state Schrödinger model studied in [38], the NEMO simulator and the Smooth QHD model that have been compared in [21].

Figures 14, 15 and 16 compare current-voltage characteristics obtained with the mixed-state Schrödinger model with those obtained with the QDD model at $77K$ and $300K$. As it can be seen, the curves obtained with QDD do not exhibit negative resistances and currents are much higher than those obtained with the mixed-state Schrödinger model (by an order 30 to 40). The same conclusion holds when comparing QDD with NEMO or Smooth QHD (figures 17 and 18). As already noticed for the Density-Gradient model, the QDD model is probably too diffusive and in order to obtain negative resistances, one has to artificially increase the effective mass as it has been done in this chapter.

There is a hope that the isothermal quantum Euler model studied in the fourth chapter of this thesis gives more realistic results on RTDs. We can see on figure 19 different IV curves obtained on the same RTD as the one studied in this chapter. We first see that as the scaled relaxation time τ tends to zero, the IV curves tend to the one obtained with QDD. Secondly, we see that the greater the relaxation time is, the smaller is the current and the bigger is the peak-to-valley ratio.

Non isothermal models involving higher moments (studied in the fifth chapter of this thesis) should give better IV curves because electrons cool dramatically as they penetrate potential barriers. Implementation of such models and simulation on RTDs is clearly one of the perspectives of this thesis.

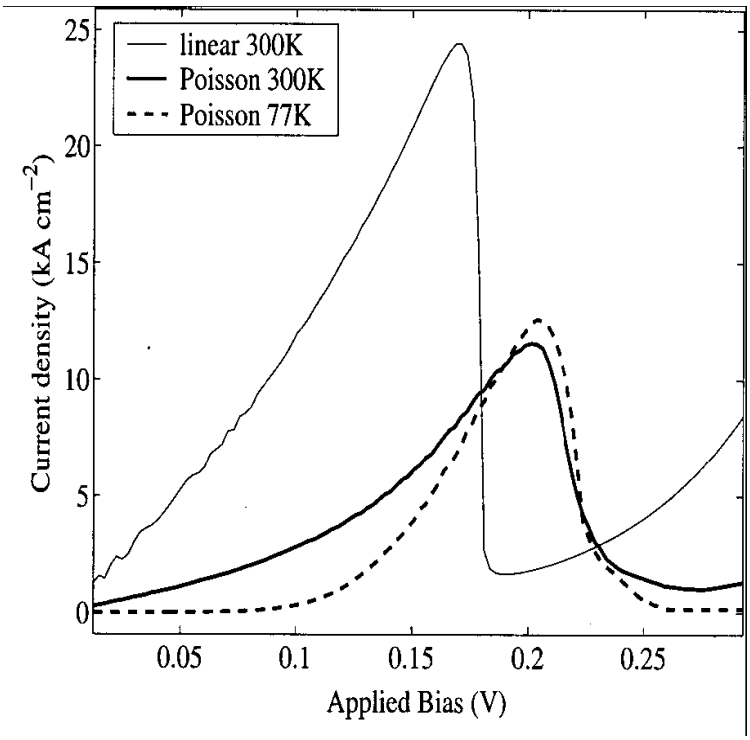

Figure 14: IV curves obtained in [38] with the mixed state SP model. The solid and dash dot lines represent the IV cuves of a model including self-consistent effects at 300K and 77K, the dash line represents a model without self-consistent effects at 300K.

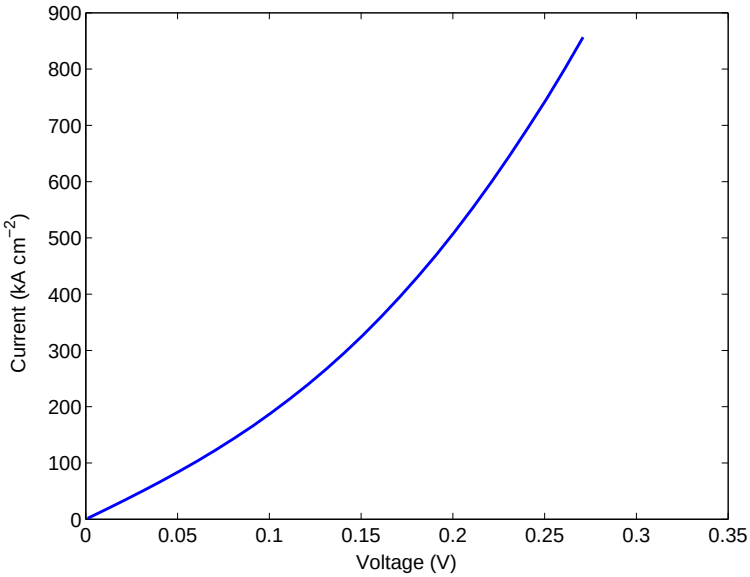

Figure 15: IV curve obtained with QDD coupled to Poisson at 300K with the same RTD as in [38].

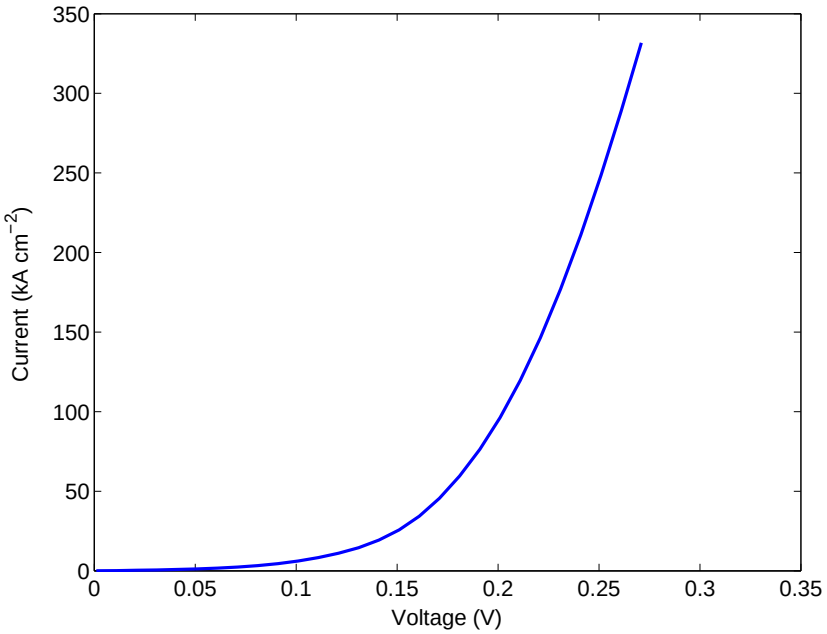

Figure 16: IV curve obtained with QDD coupled to Poisson at 77K with the same RTD as in [38].

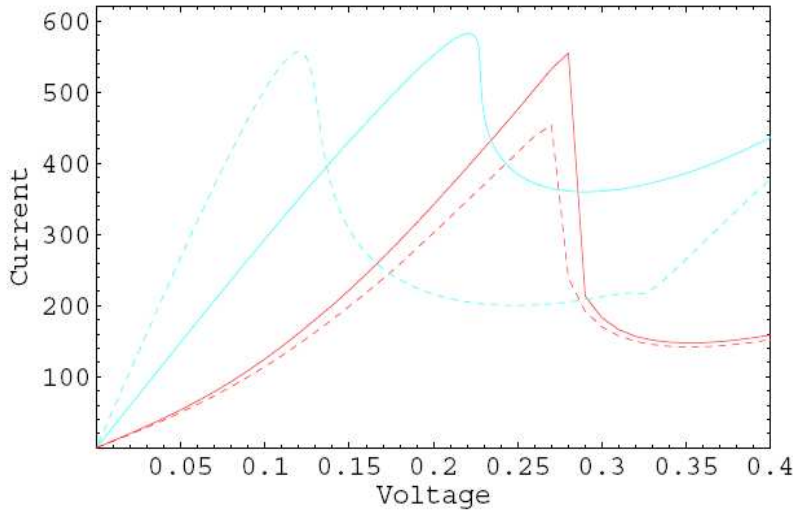

Figure 17: IV curves obtained with NEMO and smooth QHD in [21] at 300K: NEMO (red, dark), NEMO plus drift-diffusion (dotted red, dotted dark) in the contacts, smooth QHD with $\mu_{n0} = 1000cm^2/(Vs)$ (cyan, light) in the contacts, smooth QHD with $\mu_{n0} = 2000cm2/(Vs)$ (dotted cyan, dotted light) in the contacts.

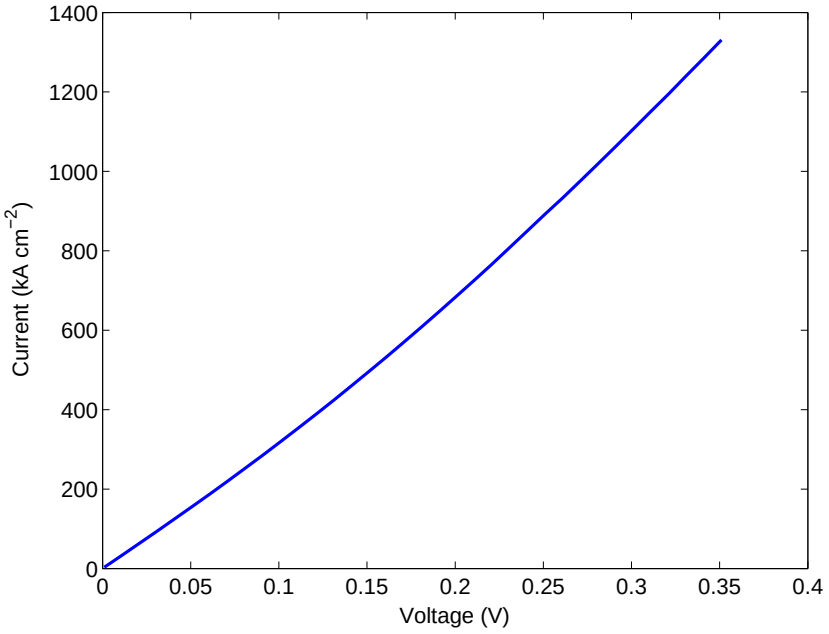

Figure 18: IV curve obtained with QDD at 300K with the same RTD as in [21] ($\mu_{n0} = 1000cm^2/(Vs)$).

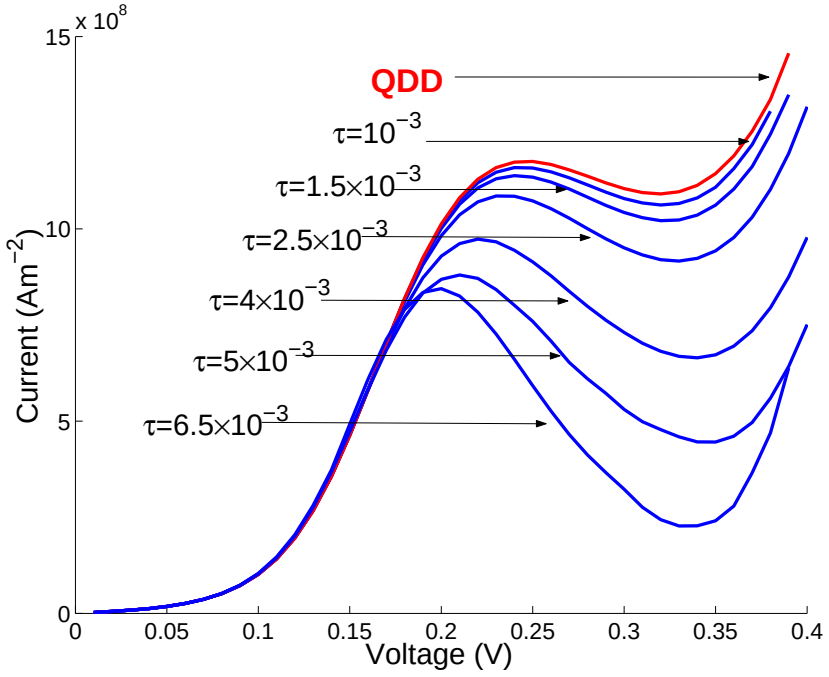

Figure 19: IV curves obtained with th isothermal Quantum Euler model (studied in chapter IV) for different scaled relaxation time (τ) (the same RTD as the one studied in this chapter is used).

References

[1] M. G. Ancona, G. J. Iafrate, *Quantum correction of the equation of state of an electron gas in a semiconductor*, Phys. Rev. B **39** (1989), 9536–9540.

[2] , M. G. Ancona, H. F. Tiersten, *Macroscopic physics of the silicon inversion layer*, Pys. review, B **39** (1987), 7959–7965.

[3] A. Arnold, *Mathematical concepts of open boundary conditions*, Phys. Lett., **30** (2001), 561–584.

[4] A. Arnold, F. Nier, *The two-dimensional Wigner-Poisson problem for an electron gas in the charge neutral case*, Math. Methods Appl. Sci. **14** (1991), no. 9, 595–613.

[5] M. Baro, N. Ben Abdallah, P. Degond, A. El Ayyadi, *A 1d coupled Schrödinger drift-diffusion model including collisions*, J. Comput. Phys. **203** (2005), 129–153.

[6] N. Ben Abdallah, *A hybrid kinetic-quantum model for stationary electron transport in a resonant tunneling diode*, J. Stat. Phys. **90** (1998), 627–662.

[7] N. Ben Abdallah, *On a multidimensional Schrödinger-Poisson scattering model for semiconductors*, J. Math. Phys. **41** (2000), 4241–4261.

[8] N. Ben Abdallah, P. Degond, P. A. Markowich, *On a one-dimensional Schrödinger-Poisson scattering model*, Z. Angew. Math. Phys. **48** (1997), 135–155.

[9] N. Ben Abdallah, A. Unterreiter, *On the stationary quantum driftdiffusion model*, Z. Angew. Math. Phys. **49** (1998), no. 2, 251–275.

[10] L. L. Chang, L. Esaki, R. Tsu, *Resonant tunneling in semiconductor double barriers*, Appl. Phys. Lett. bf 24 (1974), 593–595.

[11] R.-C. Chen, J.-L. Liu, *A quantum corrected energy-transport model for nanoscale semiconductor devices*, J. Comput. Phys. **204** (2005), 131–156.

[12] C. de Falco, E. Gatti, A. L. Lacaita, R. Sacco, *Quantum-corrected drift-diffusion models for transport in semiconductor devices*, J. Comput. Phys. **204** (2005), no. 2, 533–561.

[13] P. Degond, A. El Ayyadi, *A coupled Schrödinger drift-diffusion model for quantum semiconductor devices*, J. Comput. Phys. **181** (2002), 222–259.

[14] P. Degond, F. Méhats, C. Ringhofer, *Quantum Energy-Transport and Drift-Diffusion models*, J. Stat. Phys. **118** (2005), no. 3-4, 625–665.

[15] P. Degond, F. Méhats, C. Ringhofer, *Quantum hydrodynamic models derived from the entropy principle*, Contemp. Math. **371** (2005), 107–331.

[16] P. Degond, C. Ringhofer, *Binary quantum collision operators conserving mass momentum and energy*, C. R. Acad. Sci. Paris, Ser I **336** (2003), no. 9, 785–790.

[17] P. Degond, C. Ringhofer, *Quantum moment hydrodynamics and the entropy principle*, J. Stat. Phys. **112** (2003), no. 3-4, 587–628.

[18] S. Gallego, F. Méhats, *Numerical approximation of a quantum drift-diffusion model*, C. R. Acad. Sci. Paris, Ser. I **339** (2004), 519–524.

[19] S. Gallego, F. Méhats, *Entropic discretization of a quantum drift-diffusion model*, SIAM J. Numer. Anal. **43** (2005), no. 5, 1828–1849.

[20] C. Gardner, *The quantum hydrodynamic model for semiconductor devices*, SIAM J. Appl. Math. **54** (1994), no. 2, 409–427.

[21] C. L. Gardner, G. Klimeck, C. Ringhofer *Smooth Quantum Hydrodynamic Model vs. NEMO Simulation of Resonant Tunneling Diodes*, Journal of Computational Electronics **3** (2004) 95–102.

[22] C. Gardner, C. Ringhofer, *The smooth quantum potential for the hydrodynamic model*, Phys. Rev. E **53** (1996), 157–167.

[23] C. Gardner, C. Ringhofer, *The Chapman-Enskog Expansion and the Quantum Hydrodynamic Model for Semiconductor Devices*, VLSI Design **10** (2000), 415–435.

[24] I. Gasser, A. Jüngel, *The quantum hydrodynamic model for semiconductors in thermal equilibrium*, Z. Angew. Math. Phys. **48** (1997), no. 1, 45–59.

[25] I. Gasser, P. A. Markowich, *Quantum Hydrodynamics, Wigner Transforms and the Classical Limit*, Asympt. Analysis **14** (1997), no. 2, 97–116.

[26] I. Gasser, P. Markowich and C. Ringhofer, *Closure conditions for classical and quantum moment hierarchies in the small temperature limit*, Transp. Th. Stat. Phys. **25** (1996), no. 3-5, 409–423.

[27] A. Jüngel, *Quasi-hydrodynamic semiconductor equations*, Progress in Nonlinear Differential Equations, Birkhäuser, 2001.

[28] A. Jüngel, A. El Ayyadi, *Semiconductor simulations using a coupled quantum drift-diffusion Schrödinger-Poisson model*, SIAM J. Appl. Math. **66** (2005), no. 2, 554–572.

[29] A. Jüngel, R. Pinnau, *A positivity preserving numerical scheme for a fourth-order parabolic equation*, SIAM J. Num. Anal. **39** (2001), no. 2, 385–406.

[30] N. C. Kluksdahl, A. M. Kriman, D. K. Ferry, and C. Ringhofer, *Self-consistent study of the resonant-tunneling diode*, Phys. Rev. B **39** (1989), 7720–7735.

[31] C. S. Lent, D. J. Kirkner, *The quantum transmitting boundary method*, J. Appl. Phys. **67** (1990), 6353–6359.

[32] C. D. Levermore, *Moment closure hierarchies for kinetic theories*, J. Stat. Phys. **83** (1996), 1021–1065.

[33] P. A. Markowich, C. Ringhofer, C. Schmeiser, *Semiconductor Equations*, Springer, 1990.

[34] S. Micheletti, R. Sacco, P. Simioni, *Numerical simulation of resonant tunnelling diodes with a quantum-drift-diffusion model*, Scientific Computing in Electrical Engineering, Lecture Notes in Computer Science (2004), Springer-Verlag, 313–321.

[35] P. Mounaix, O. Vanbťesien, D. Lippens, *Effect of cathode spacer layer on the current voltage characteristics of resonant tunneling diodes*, App. Phys. Let. **2** (1990), no. 5, 489–510.

[36] F. Nier, *A stationary Schrödinger-Poisson system arising from the modeling of electronic devices*, Forum Math. **2** (1990), no. 5, 489–510.

[37] F. Nier, *A variational formulation of Schrödinger-Poisson systems in dimension* $d \leq 3$, Comm. Partial Differential Equations **18** (1993), no. 7-8, 1125–1147.

[38] O. Pinaud, *Transient simulations of a resonant tunneling diode*, J. Appl. Phys. **92**(4) (2002), 1987–1994.

[39] A. Pirovano, A. Lacaita, A. Spinelli, *Two dimensional Quantum Effects in Nanoscale MOSFETs*, IEEE Trans. Electron. Dev. **49** (2002), no. 1, 25–31.

[40] E. Polizzi, N. Ben Abdallah, *Self-consistent three dimensional models for quantum ballistic transport in open systems*, Phys. Rev. B, **66** (2002), 245–301.

[41] S. Teufel, *Adiabatic Perturbation Theory in Quantum Dynamics*, Springer-Verlag, 2003.

[42] A. Unterreiter, R. Pinnau, *The stationary current-voltage characteristics of the quantum drift-diffusion model*, SIAM J. Num. Anal. **37** (1999), no. 1, 211–245.

Chapter III

Transparent boundary conditions for the Quantum Drift-Diffusion model

Abstract. This chapter is devoted to the derivation and numerical implementation of transparent boundary conditions for the Quantum Drift-Diffusion model (QDD) coupled to the Poisson equation, both in the stationary case and in the transient case. In the stationary case, we propose to use a Gummel algorithm while in the transient case, we propose to use the Newton algorithm. Some preliminary numerical simulations on a single barrier diode and a resonant tunneling diode are shown to test the algorithms.

Key words. entropic Quantum Drift-Diffusion, density matrix, Transparent boundary conditions, continuous spectrum, Gummel Algorithm, Resonant tunneling diode.

1 Introduction

Recently, the entropic quantum drift-diffusion model (QDD) has been derived in [8], studied numerically in [9] and application to the modeling of a resonant tunneling diode (RTD) has been performed in [7]. This model consists in an equation for the conservation of mass:

$$\partial_t n + \nabla \cdot j = 0, \tag{1.1}$$

where n is the density of mass and j is the current which is the product of the density and the gradient of the electrochemical potential:

$$j = n\nabla(A - V), \tag{1.2}$$

V being the electrical potential and A being the quantum chemical potential. The key of the QDD model is the quantum constitutive equation linking the density to the quantum chemical potential. To understand this link, one has to understand the notion of quantum Maxwellian, which is defined as the minimiser of a relative quantum entropy under constraint. In the QDD model, the quantum Maxwellian takes the form of the following density matrix:

$$\varrho = \exp(-H(A)), \tag{1.3}$$

where $H(A)$ is the following modified Hamiltonian:

$$H(A) = -\frac{\hbar^2}{2}\Delta + A, \tag{1.4}$$

with $\hbar$ the scaled Planck constant. Note that by contrast with the usual Hamiltonian, the quantum chemical potential A replaces the electrical potential V.

As a first approximation, we have considered that the spectrum of this Hamiltonian is discrete (we note $(\lambda_k, \psi_k)_{k\in\mathbb{N}}$ the discrete eigenelements), putting Neumann boundary conditions on the eigenfunctions ψ_k. Note that for the Schrödinger-Poisson system studied for example in [14], such conditions annihilate the current which is defined microscopically according to $j = \sum_k e^{-\lambda'_k} \mathcal{I}m\left(\overline{\psi'_k}\nabla\psi'_k\right)$, where $(\lambda'_k, \psi'_k)_{k\in\mathbb{N}}$ are the eigenelements of the Hamiltonian $\mathcal{H} = -\frac{\hbar^2}{2}\Delta + V$. In our case, the current is defined macroscopically according to equation (1.2) so that such conditions allow a macroscopic current to exist.

Nevertheless, putting such boundary conditions on a open device has no real physical meanings and can create "boundary layers" on the density. A better approximation would be to consider transparent boundary conditions for the spectrum of the modified Hamiltonian $H(A)$. With such boundary conditions, the spectrum is no more discrete but continuous and we have to deal with what we call generalized eigenfunctions. A lot of work has been performed on such transparent boundary conditions for the Schrödinger equation. On can cite for instance [2, 4, 3, 14, 11]. The goal of this chapter is to propose numerical schemes for the QDD model coupled to the Poisson equation in the stationary case as well as in the transient case with such transparent boundary conditions. This chapter is organized as follows: In the first part, we derive the transparent boundary conditions for the QDD model. Then we propose some numerical schemes for the QDD model coupled to the Poisson equation in the stationary case, the most interesting one being based on a Gummel method [10]. We test this scheme on the Resonant tunneling diode (RTD) studied in [14] and on a single-barrier

diode. Finally, we deal with the transient model in the third section. We propose to use a Newton algorithm which requires to compute the derivative of the density with respect to the quantum chemical potential. To this aim, we use scattering theory tools such as the Lippman-Schwinger equation [15] and we give preliminary numerical results on a single barrier diode.

2 Derivation of the transparent boundary conditions

The density matrix for the QDD model on the real line $\mathbb{R}$ is defined according to:

$$\varrho = \exp\left(-H(A)\right), \tag{2.5}$$

where $H(A)$ is the following Hamiltonian:

$$H(A) = -\frac{\hbar^2}{2}\partial_x^2 + A. \tag{2.6}$$

Consider that the chemical potential A is regular enough such that the Hamiltonian $H(A)$ possesses no eigenvalues imbedded in the continuous spectrum. Then, the density can be written:

$$n(x) = \int_{-\infty}^{\infty} e^{-E_p}|\psi_p|^2 \ \frac{dp}{2\pi\hbar} + \sum_{\lambda_k} e^{-\lambda_k}|\psi_k|^2, \tag{2.7}$$

where E_p is the energy corresponding to the momentum p of the injected electrons (E_p will be defined later) and ψ_p are the wave functions satisfying the modified Schrödinger equation on the real line:

$$-\frac{\hbar^2}{2}\psi_p'' + A(x)\psi_p = E_p\psi_p. \tag{2.8}$$

The couples (λ_k, ψ_k) are the discrete eigenvalues and normalized eigenfunctions of the Hamiltonian $H(A)$.

The goal is to write an equivalent formulation of the density on a bounded domain with appropriate boundary conditions on the spectrum. Let consider that the device can be represented by the spatial interval $\Omega = [0, 1]$ and is connected to two reservoirs (figure III.1) where electron transport is mainly classical and where the density of electrons is constant and equal to the doping profile. For the sake of simplicity, we take:

$$n(x) = n_0 e^{-A(x)} = n_0^d \ \text{ on }]-\infty, 0] \cup [1, \infty[, \tag{2.9}$$

where n_0^d is the doping profile on the left and on the right of the domain Ω and $n_0 = (2\pi\hbar^2)^{1/2}$ is the density of states. It implies that the chemical potential is constant inside the reservoirs and equal to:

$$A(x) = A_0 = \log(n_0) - \log(n_0^d) \ \text{ on }]-\infty, 0] \cup [1, \infty[. \tag{2.10}$$

Then, it is possible to solve exactly equation (2.8) inside the reservoirs.

- If $p > 0$: We consider the case where a wave function is entering the device via the left reservoir. E_p is equal to $\frac{p^2}{2} + A_0$ and the solution on $]-\infty, 0]$ can be written:

$$\psi_p = 1e^{ipx/\hbar} + R_p e^{-ipx/\hbar},$$

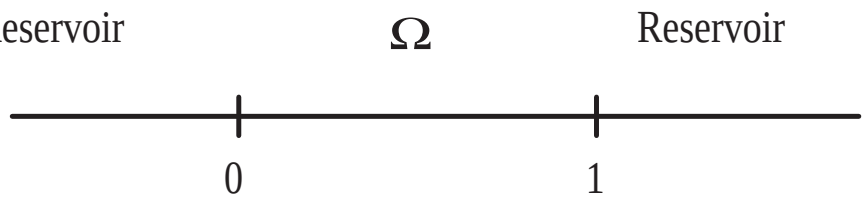

Figure III.1: The device.

where R_p is the reflection coefficient (unknown). the solution on $]1,\infty]$ can be written:

$$\psi_p = T_p e^{ip(x-1)/\hbar},$$

where T_p is the transmission coefficient (also unknown). It is then possible to eliminate the coefficients R_p and T_p by a simple algebraic manipulation which gives:

$$\begin{aligned} \hbar\psi_p'(0) + ip\psi_p(0) &= 2ip, & (2.11)\\ \hbar\psi_p'(1) &= ip\psi_p(1). & (2.12) \end{aligned}$$

- If $p < 0$: We consider the case where a wave function is entering the device via the right reservoir. We obtain the following boundary conditions:

$$\begin{aligned} \hbar\psi_p'(1) + ip\psi_p(1) &= 2ip, & (2.13)\\ \hbar\psi_p'(0) &= ip\psi_p(0). & (2.14) \end{aligned}$$

Suppose now that the chemical potential A is regular enough so that the Hamiltonian $H(A)$ possesses no eigenvalues imbedded in the continuous spectrum. Then, all the eigenvalues λ_k are smaller than A_0. For the corresponding eigenfunctions, it does not seem possible to derive transparent boundary conditions. We know that the eigenfunctions are of the form $K_0 e^{\sqrt{A_0-\lambda_k}x/\hbar}$ on $]-\infty,0]$ and $K_1 e^{-\sqrt{A_0-\lambda_k}(x-1)/\hbar}$ on $[1,\infty[$. That is why we can enlarge the domain taking $\Omega' = [0-l, 1+l]$ with $l \sim 2\hbar/\Delta p$ where Δp is the momentum step that we have chosen to discretize p for the continuous spectrum. Then we can choose for example for the boundary conditions of ψ_k on Ω' homogeneous Dirichlet boundary conditions:

$$\psi_k(0-l) = \psi_k(1+l) = 0 \quad (\forall k \in \mathbb{N}). \qquad (2.15)$$

3 The stationary QDD model with transparent boundary conditions

The stationary QDD model (coupled to the Poisson equation) with transparent boundary conditions is written on $\Omega = [0, 1]$:

$$\partial_x(n\partial_x(A - (V_s + V_{ext}))) = 0, \tag{3.16}$$
$$-\alpha^2 V_s'' = n - n^d, \tag{3.17}$$
$$n = \int_{-\infty}^{\infty} e^{-E_p}|\psi_p|^2 \frac{dp}{2\pi\hbar} + \sum_{\lambda_k < A_0} e^{-\lambda_k}|\psi_k|^2, \tag{3.18}$$
$$-\frac{\hbar^2}{2}\psi_p'' + A\psi_p = (\frac{p^2}{2} + A_0)\psi_p, \tag{3.19}$$
$$-\frac{\hbar^2}{2}\psi_k'' + A\psi_k = \lambda_k\psi_k. \tag{3.20}$$

with the following boundary conditions:

$$A(0) = A_0 = \ ; \quad A(1) = A_0; \tag{3.21}$$
$$V_s(0) = V_0 \ ; V_s(1) = V_1; \tag{3.22}$$
$$\hbar\psi_p'(1) + ip\psi_p(1) = 2ip \ ; \quad \hbar\psi_p'(0) = ip\psi_p(0) \quad \text{for } p < 0, \tag{3.23}$$
$$\hbar\psi_p'(0) + ip\psi_p(0) = 2ip \ ; \quad \hbar\psi_p'(1) = ip\psi_p(1) \quad \text{for } p > 0, \tag{3.24}$$
$$\psi_k(0 - l) = \psi_k(1 + l) = 0, \tag{3.25}$$

and where V_0 and V_1 allow to control the applied bias on the device, V_s is the selfconsistant potential and V_{ext} is the external potential.

3.1 Numerical method

3.1.1 First Approach

A "natural" first try to solve 3.16-3.20 is the following iterative algorithm: given a density n^{k-1}, do the following loop:

1) Compute V_s^k by $-\alpha^2\partial_x^2 V_s^k = n^{k-1} - n^d$,
↓
2) Compute A^k by $\partial_x(n^{k-1}\partial_x(A^k - (V_s^k + V_{ext}))) = 0$,
↓
3) Compute n^k by $n^k = \int_{-\infty}^{\infty} e^{-E_p}|\psi_p|^2 \frac{dp}{2\pi\hbar} + \sum_{\lambda_k < A_0} e^{-\lambda_k}|\psi_k|^2$.

Steps number 1 and 2 are performed using a usual finite-differences scheme. For the step number 3, one has to solve many (depending on the discretization of p) ordinary differential equations (3.19) with boundary conditions (3.23) and (3.24). It is possible to rewrite the ordinary differential equations as initial value problems, that we can solve with a Runge Kutta algorithm:

- $p > 0$:

$$\begin{aligned} &-\frac{\hbar^2}{2}u_p'' + Au_p = (\frac{p^2}{2} + A_0)u_p, \\ &\hbar u_p'(1) = ip, \\ &u_p(1) = 1. \end{aligned}$$

We obtain ψ_p normalizing u_p by $\frac{2ip}{\hbar u_p'(0)+ipu_p(0)}$.

- $p < 0$:

$$\begin{aligned} &-\frac{\hbar^2}{2}\psi_p'' + A\psi_p = (\frac{p^2}{2} + A_1)\psi_p, \\ &\hbar u_p'(0) = ip, \\ &u_p(1) = 1. \end{aligned}$$

We obtain ψ_p normalizing u_p by $\frac{2ip}{\hbar u_p'(1)+ipu_p(1)}$.

3.1.2 Second Approach: relaxation algorithm

It appears that the first algorithm is unstable for certain initial densities. An oscillating regime is observed. A high density generates high potentials which decrease the density, generating low potentials which increase the density and so on... A solution to this problem can be to include two relaxation parameters ε_1 and ε_2 in the two first steps. Given $n^{k-1}, V^{k-1}, A^{k-1}$, this algorithm reads:

1) Compute V_s^* by $-\alpha^2\partial_x^2 V_s^* = n^{k-1} - n^d$,
   Then, compute V_s^k by $V_s^k = \varepsilon_1 V_s^* + (1-\varepsilon_1)V_s^{k-1}$,
   $\downarrow$
2) Compute A^* by $\partial_x(n^{k-1}\partial_x(A^* - (V_s^k + V_{ext}))) = 0$,
   Then, compute A^k by $A^k = \varepsilon_2 A^* + (1-\varepsilon_2)A^{k-1}$,
   $\downarrow$
3) Compute n^k by $n^k = \displaystyle\int_{-\infty}^{\infty} e^{-E_p}|\psi_p|^2 \frac{dp}{2\pi\hbar} + \sum_{\lambda_k < A_0} e^{-\lambda_k}|\psi_k|^2$.

This algorithm is more stable but the convergence time is large because of the smallness of the parameters ε_1 and ε_2 (~ 0.05).

3.1.3 Third Approach: the Gummel algorithm

In order to accelerate the algorithm, we use the Gummel method [10]. The Gummel method permits to take into account the exponential dependence of the density on the potentials. Writing $n^k = n(V_s^k) = n(V_s^{k-1} + \delta V_s^k) \approx n^{k-1}e^{-\delta V_s^k} \approx n^{k-1}(1 - \delta V_s^k)$ and inserting this expression in the step 1 (replacing n^{k-1}), we obtain the following

algorithm:

$$\begin{aligned}
&1) \quad \text{Compute } V_s^k \text{ by } -\alpha^2\partial_x^2 V_s^k + n^{k-1}V_s^k = n^{k-1}(1+V_s^{k-1}) - n^d,\\
&\qquad\qquad \downarrow\\
&2) \quad \text{Compute } A^k \text{ by } \partial_x(n^{k-1}\partial_x(A^k - (V_s^k + V_{ext}))) = 0,\\
&\qquad\qquad \downarrow\\
&3) \quad \text{Compute } n^k \text{ by } n^k = \int_{-\infty}^{\infty} e^{-E_p}|\psi_p|^2 \,\frac{dp}{2\pi\hbar} + \sum_{\lambda_k<A_0} e^{-\lambda_k}|\psi_k|^2.
\end{aligned}$$

We can also replace the first step by the non linear partial differential equation:

$$1)\text{Compute } V_s^k \text{ by } -\alpha^2\Delta V_s^k = n^{k-1}(e^{-V_s^k+V_s^{k-1}}) - n^d$$

and solve it with the Newton algorithm. In this case, this method is called the non-linear Gummel algorithm.

This algorithm is much faster but it seems unstable for large applied biases as noticed in subsection 3.3.

3.2 Why is it necessary to include the discrete spectrum in the model?

In the literature, when the Schrödinger equation is used with transparent boundary conditions, the discrete spectrum is often neglected. We try to show numerically why it can be necessary to include it.

3.2.1 Numerical illustration for the need of both the continuous and the discrete spectrum

Let us fix $\hbar \ll 1$ ($\hbar = 0.01$) and a quantum chemical potential A. We are going to reconstruct the density using three different formulas:

$$n_1 = n_0 e^{-A}, \tag{3.26}$$

$$n_2 = \sum_k e^{-\lambda_k}|\psi_k|^2, \tag{3.27}$$

$$n_3 = \int_{-\infty}^{\infty} e^{-E_p}|\psi_p|^2 \,\frac{dp}{2\pi\hbar}. \tag{3.28}$$

The density n_1 corresponds to the classical density while n_2 and n_3 are quantum. The density n_2 corresponds to the density used in the last two chapters while the density n_3 corresponds to the continuous spectrum derived in this chapter with transparent boundary conditions. Normally, the three densities should be close. As we knew, we can see on figures III.2-III.5 that the reconstruction with the discrete spectrum creates an unwanted 'boundary layer' which is of order $\hbar$ (here 0.06). We can see on figures III.2 and III.3 that the reconstruction with the continuous spectrum is giving satisfactory results for a concave and constant density but problems arise on figures III.4 and III.5 where the chemical potential is convex or sinusoidal.

In order to reconstruct the density for such chemical potentials, we have to take into account the discrete spectrum. Now we perform the same experiment but we take n_3 as following:

$$\int_{-\infty}^{\infty} e^{-E_p}|\psi_p|^2 \,\frac{dp}{2\pi\hbar} + \sum_{\lambda_k<A_0} e^{-\lambda_k}|\psi_k|^2.$$

Figure *III.6* and *III.7* show that now the problem is corrected taking 4 eigenelements (corresponding to eigenvalues smaller than $A(0)$).

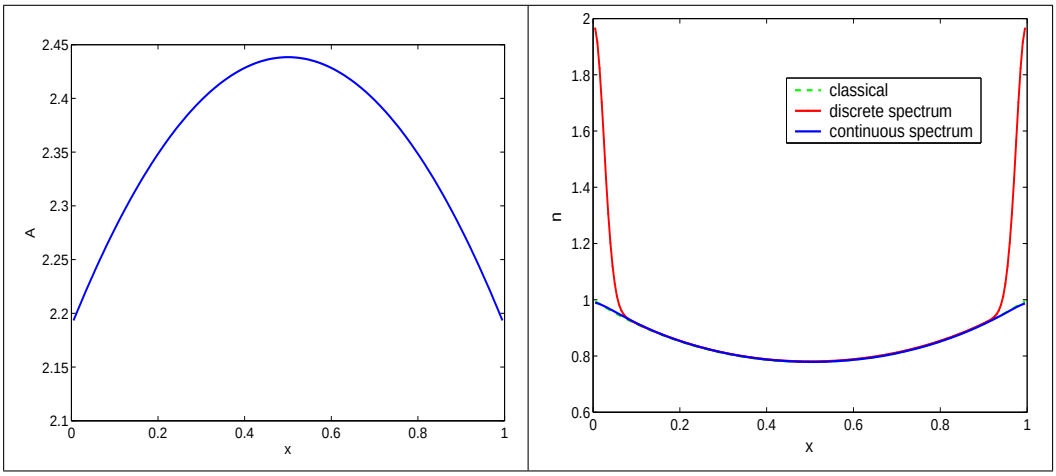

Figure III.2: Reconstruction of the density for a convex chemical potential.

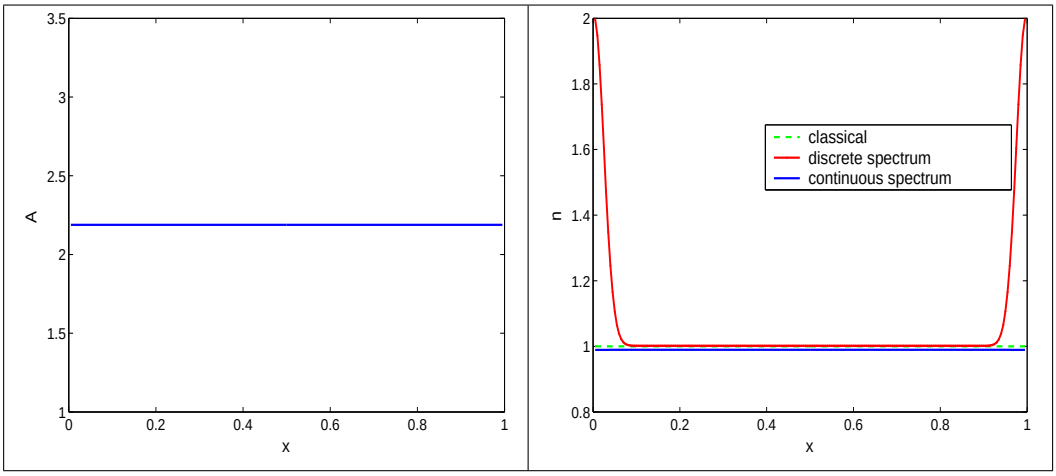

Figure III.3: Reconstruction of the density for a constant chemical potential.

3.2.2 What is happening inside the Gummel iterations

We have not found for the moment a steady states with a concave chemical potential which creates a discrete spectrum for the Hamiltonian. But when starting from any initial point, step number 2 can generate a chemical potential A with a small depletion. If we do not take into account the discrete spectrum, the density generated in step number 3 will show a depletion instead of a "bump". In this very place, we will have $n - n^d < 0$, giving $V_s'' > 0$. So the electrical potential computed in step number 1 will be convex and so will be the chemical potential A computed in step number 2, increasing the depletion, and thus increasing the depletion on the density, etc, etc... and the algorithm will diverge. Adding the discrete spectrum as proposed in this chapter cures this problem.

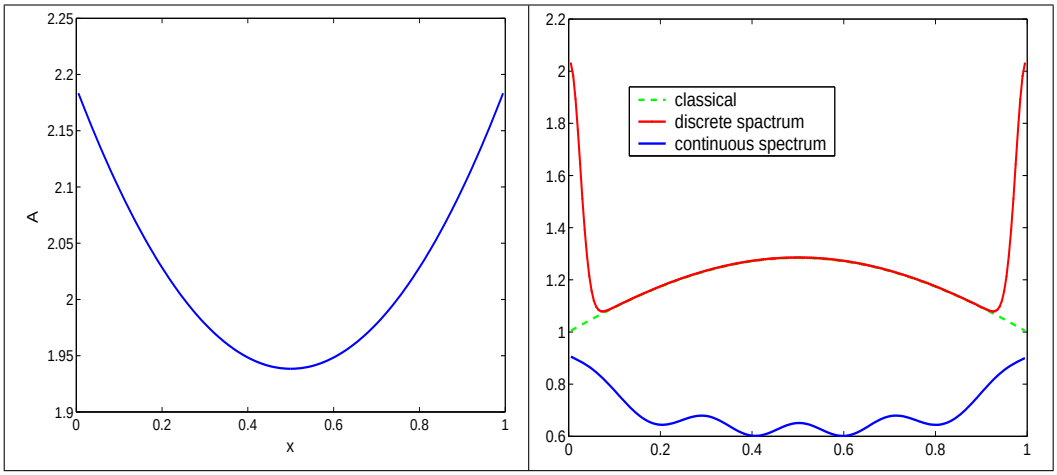

Figure III.4: Reconstruction of the density for a concave chemical potential.

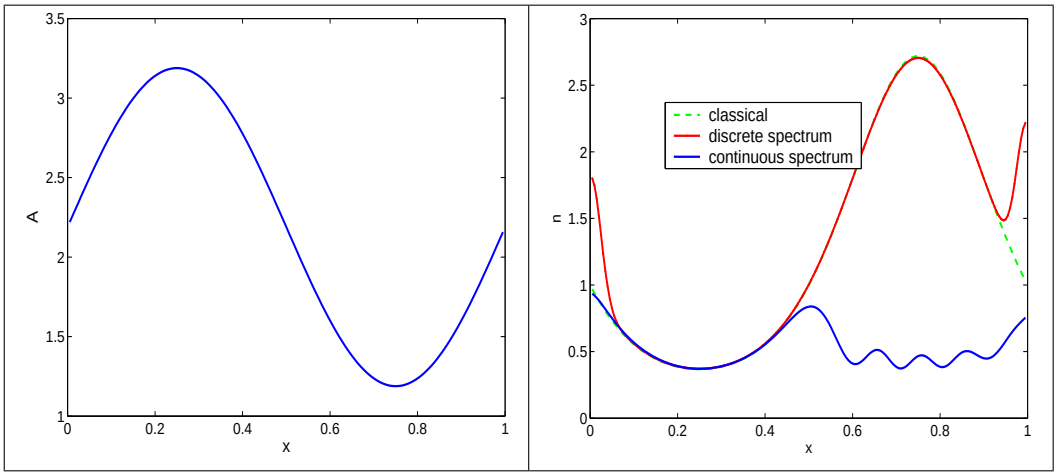

Figure III.5: Reconstruction of the density for a sinusoidal chemical potential.

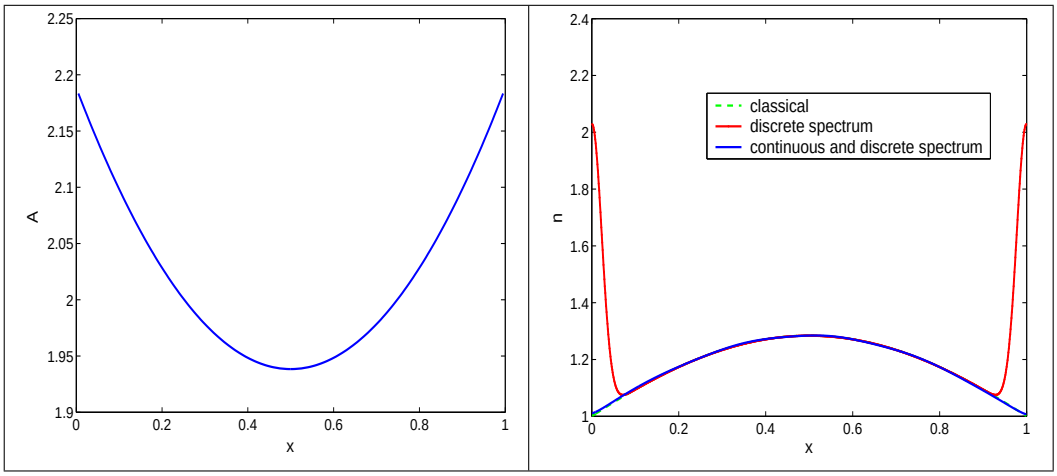

Figure III.6: Reconstruction of the density for a sinusoidal chemical potential (bis).

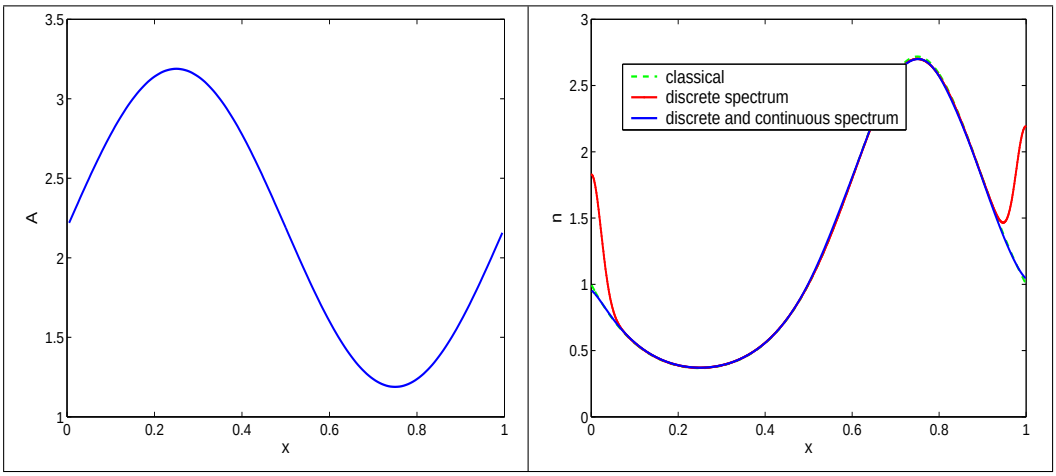

Figure III.7: Reconstruction of the density for a sinusoidal chemical potential (bis).

3.3 Numerical results

We take the same resonant tunneling diode as the one studied in [14]. This RTD length is 135 nm, including 2 access zones of 50 nm and doped at 10^{18} cm^{-3}, and a 35 nm active region including 2 barriers of 5nm separated by a well of 5 nm. This active zone includes a spacer layer of 10 nm doped at 5×10^{15} cm^{-3}. We take the effective mass equal to $m^* = 0.067 m_e$, the permittivity $\varepsilon_r = 11.44$, the mobility $\mu = 0.85 m^2 V^{-1} s^{-1}$ and the temperature $T = 300K$.

In order to test the numerical schemes on a simple device (with no resonance effects) we take as a first test case a single barrier diode (we consider that the first barrier height is 0.3 eV and we suppress the second one). We take as scaled mesh size $\Delta x = 0.005$ (x being in [0,1]) and as scaled momentum step $\Delta p = 0.04$, (p being in [-4,4]). We use the non linear Gummel algorithm and we initialize V_s to 0 and A to $A(x) = \log(n_0) - \log(n^d(x))$ if $n^d(x) \neq 0$, $A(x) = \log(n_0) - \log(0.1)$ otherwise. We apply a bias of 0.05 V and we consider that the algorithm has converged when $\|A^{k+1} - A^k\|/\|A^k\| + \|V_s^{k+1} - V_s^k\|/\|V_s^k\| < 10^{-8}$ which takes about 20 iterations. The current is equal to $j = 1.4524 A m^{-2}$. Figure III.8 shows the density, the total electrical potential and the chemical potential. Figure III.9 shows the square norm of the generalized eigenfunctions $\psi_p(x)$. As we can see, there is no resonance, meaning that the momentum p can be discretized with a large step size. This figure can be compared to figure III.11 which concerned the second test case of a double barrier (the two barriers heights are 0.3 V). We have plotted the square norm of the generalized eigenfunctions ψ_p for $x = 67.5$ nm (middle of the well) and we can see two resonant peaks which are thin and high, which means that the momentum p must be discretized with a very small step size. We have chosen $\Delta p = 0.004$, meaning that we have to solve 2000 Schrödinger equations for each iteration. On figure III.8, we can see the density and potentials for an applied bias of 0.05V. Unfortunately, we have not been able to plot current voltage characteristics because for higher biases, the Gummel algorithm does not converge any more. We have not been able to find a cure for this ill-behavior yet.

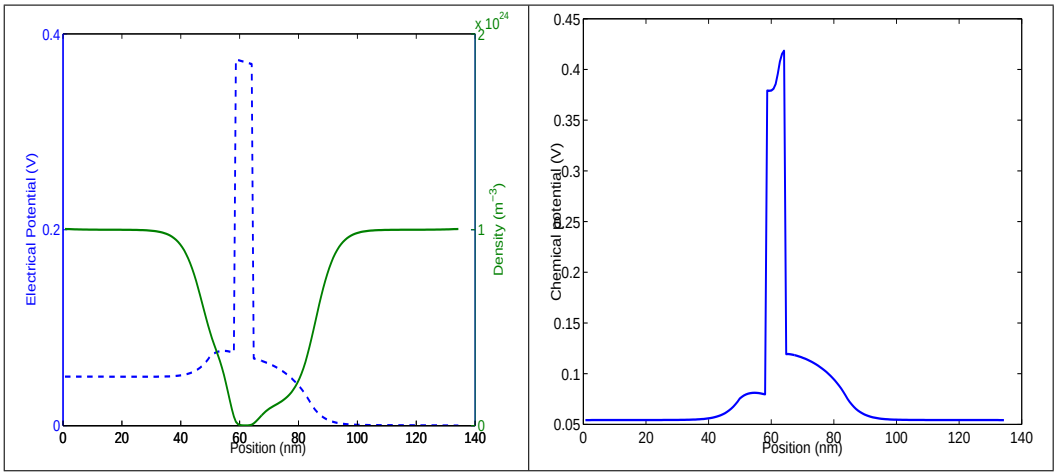

Figure III.8: Density and potentials for the first test case (single barrier) for an applied bias of 0.05V.

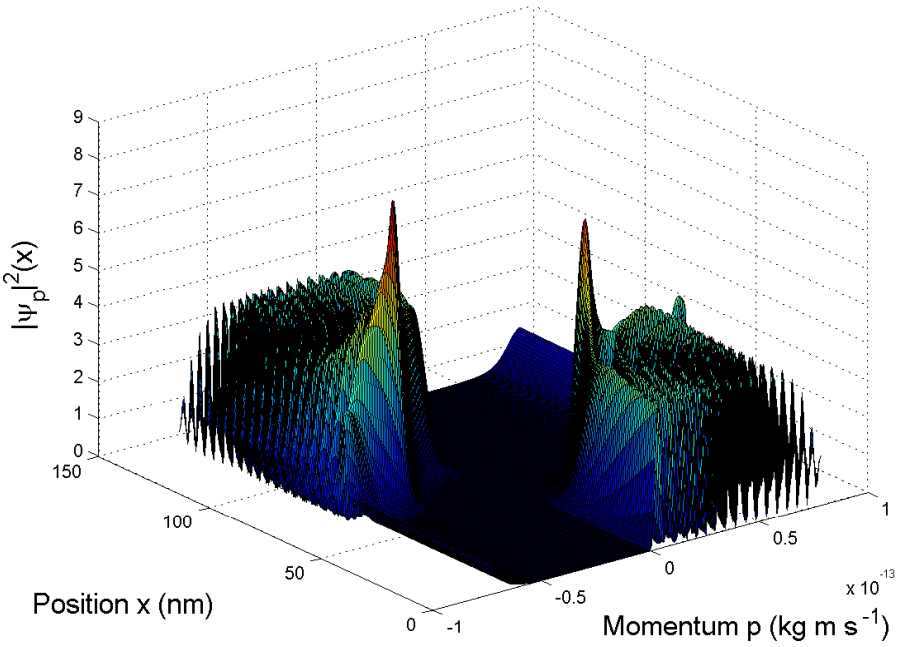

Figure III.9: Square norm of the generalized eigenfunctions $\psi_p(x)$ for the first test case (single barrier) for an applied bias of 0.05V : we can see there is no resonance meaning the momentum p can be discretized with a big step size.

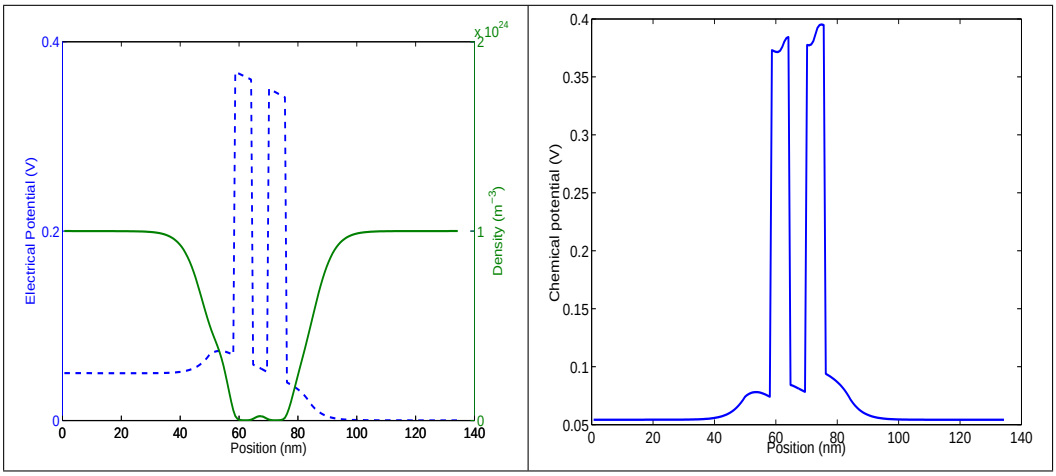

Figure III.10: Density and potentials for the second test case (double barrier) for an applied bias of 0.05V

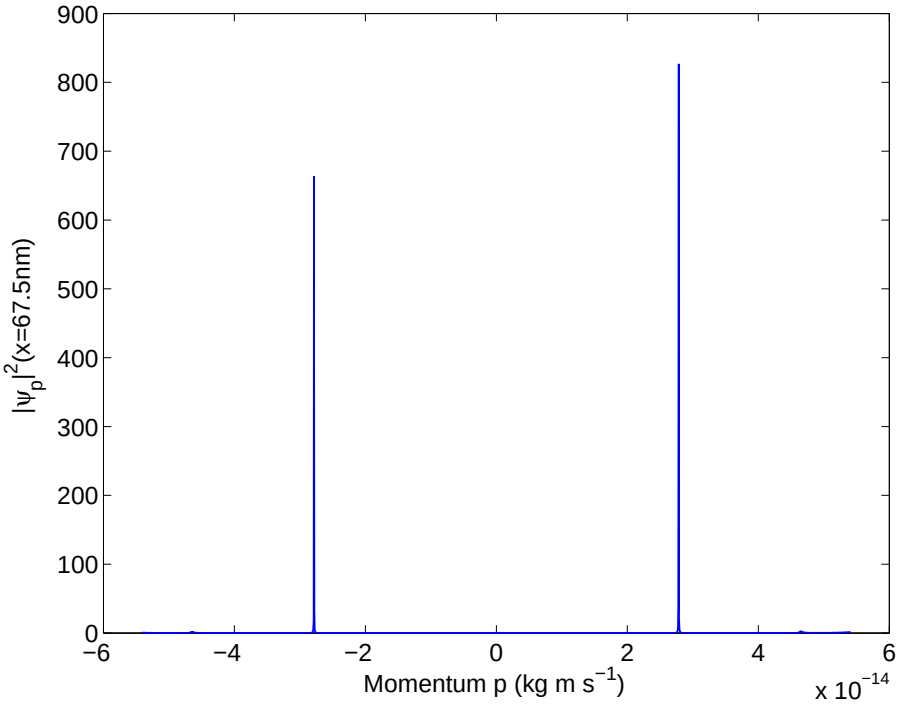

Figure III.11: Square norm of the generalized eigenfunctions ψ_p for the second test case (double barrier) for an applied bias of 0.05V and for $x = 67.5$ nm (middle of the well): we can see two resonant peaks which are thin and high, which means the momentum p must be discretized with a very small step size.

4 The transient QDD model

We could choose to adapt the Gummel algorithm to the transient model. We have chosen instead to use the Newton algorithm which is a new approach concerning the continuous spectrum to our knowledge. We propose to use exactly the same scheme as [7] (the reader can refer to it for the details about the time and space discretizations) except that we add the continuous spectrum in the expression of the density.

4.1 Derivative of the density with respect to the potential

In order to implement the Newton algorithm, we need to differentiate the density with respect to the chemical potential A in equation (2.7). And for this purpose, we need to differentiate the generalized eigenfunctions ψ_p with respect to A. We are going to use formally scattering theory tools. Scattering theory for the Schrödinger equation is widely studied, and one can refer to [12, 5] for a physical point of view, and to [15, 16, 6] for mathematical aspects.

4.1.1 Derivative of the density when the Hamiltonian has a discrete spectrum only

Let us remind briefly the result obtained when we take for the domain of the Hamiltonian the following one:

$$D(H) = \{H^2(0,1), \psi_k'(0) = \psi_k'(1) = 0\}. \tag{4.29}$$

With such a domain, the Hamiltonian possesses a sequence of eigenvalues $\lambda_1 < \lambda_2 < ...$ associated to an orthogonal basis of eigenfunctions ψ_k. We can calculate the following derivatives (see for instance [13]):

$$d\lambda_k(A)\cdot\delta A = \int_0^1 |\psi_k|^2 \delta A \, dx, \tag{4.30}$$

$$d\psi_k(A)\cdot\delta A = \sum_{k\neq q} \frac{1}{\lambda_k - \lambda_q}\left(\int_0^1 \psi_k\psi_q\delta A \, dx\right)\psi_q. \tag{4.31}$$

This gives the following derivative of the density $n = \sum_k e^{-\lambda_k}|\psi_k|^2$:

$$dn(A)\cdot\delta A = \sum_{k,q} \frac{e^{-\lambda_k} - e^{-\lambda_q}}{\lambda_k - \lambda_q}\int_0^1 \psi_k\psi_q\delta A \, dx\psi_k\psi_q, \tag{4.32}$$

where $\frac{e^{-\lambda_k}-e^{-\lambda_q}}{\lambda_k-\lambda_q}$ conventionally equals $e^{-\lambda_k}$ if $k = q$.

4.1.2 Derivative of the wavefunctions

We use the Lippmann-Schwinger equation [6] in order to compute formally the derivative of the wave functions ψ_p.

First, we are going to compute the derivative of ψ_p when the potential is equal to zero. The Lippmann-Schwinger equation reads:

$$\psi_p^\varepsilon(x) = \psi_{p,0} - R_0^-\left(\frac{p^2}{2}\right)\left(\varepsilon\delta A(\cdot)\psi_p^\varepsilon(\cdot)\right)(x), \tag{4.33}$$

where R_0 is the resolvent of the operator $H_0 = -\frac{\hbar^2}{2}\partial_x^2$, we denote $R_0^-(\lambda)\phi = \lim_{\eta\downarrow 0} R_0(\lambda - i\eta)\phi$, $\psi_{p,0}$ are the wavefunctions solutions of the Schrödinger equation with a null potential and ψ_p^ε are the wave functions solutions to the following Schrödinger equation:

$$-\frac{\hbar^2}{2}\psi_p^{\varepsilon\prime\prime} + \varepsilon\delta A\psi_p^\varepsilon = \frac{p^2}{2}\psi_p^\varepsilon. \tag{4.34}$$

Firstly, we see with this equation that $\psi_p^\varepsilon = \psi_{p,0} + O(\varepsilon)$, and secondly, we see that

$$\lim_{\varepsilon\to 0}\frac{\psi_p^\varepsilon(x) - \psi_{p,0}}{\varepsilon} = d\psi_p(0)\cdot\delta A = -R_0^-\left(\frac{p^2}{2}\right)(\delta A(\cdot)\psi_{p,0}(\cdot))(x).$$

Here, the derivative can be computed explicitly using the Fourier Transform. We have indeed

$$\begin{aligned}
-R_0^-(\frac{p^2}{2})(\delta A(\cdot)\psi_{p,0}(\cdot))(x) &= -\mathcal{F}^{-1}\mathcal{F}(R_0^-(\frac{p^2}{2})(\delta A(\cdot)\psi_{p,0}(\cdot))(x)) \\
&= -\mathcal{F}^{-1}\left(\frac{2}{\hbar^2\xi^2 - p^2 + i0}\mathcal{F}\delta A\psi_{0,p}\right) \\
&= -\mathcal{F}^{-1}\left(\frac{2}{\hbar^2\xi^2 - p^2 + i0}\right) * (\delta A\psi_{0,p}) \\
&= -\int\frac{2}{\xi^2 - p^2 + i0}e^{ix\xi/\hbar}\frac{d\xi}{2\pi\hbar} * (\delta A\psi_{0,p}).
\end{aligned}$$

Now, we can try to compute the derivative of ψ_p for a potential $A \neq 0$. For the sake of simplicity, we choose A(0)=A(1)=0. The Lippman-Schwinger equation reads:

$$\psi_p^\varepsilon(x) = \psi_p - R_A^-\left(\frac{p^2}{2}\right)\left(\varepsilon\delta A(\cdot)\psi_p^\varepsilon(\cdot)\right)(x), \tag{4.35}$$

where R_A is the resolvent of the operator $H(A) = -\frac{\hbar^2}{2}\partial_x^2 + A$, ψ_p are the wavefunctions solutions of the Schrödinger equation with a potential A and ψ_p^ε are the wave functions solution to the following Schrödinger-like equation:

$$-\frac{\hbar^2}{2}\psi_p^{\varepsilon\prime\prime} + (A + \varepsilon\delta A)\psi_p^\varepsilon = \frac{p^2}{2}\psi_p^\varepsilon. \tag{4.36}$$

Now, we have

$$\lim_{\varepsilon\to 0}\frac{\psi_p^\varepsilon(x) - \psi_p}{\varepsilon} = d\psi_p(A)\cdot\delta A = -R_A^-\left(\frac{p^2}{2}\right)(\delta A(\cdot)\psi_p(\cdot))(x).$$

We need to use the Generalized Fourier transform (or Agmon Transform [1]) defined as follows for each function f in $L^2(\mathbb{R})_{ac}$ (the space of absolutely continuous functions of $L^2(\mathbb{R})$):

$$\mathcal{F}_- f = \frac{1}{\sqrt{2\pi\hbar}}\lim_{N\to\infty}\int_{|x|<N} f(x)\overline{\psi_p(x)}dx. \tag{4.37}$$

Here, unfortunately, the derivative cannot be computed explicitly using the Generalized Fourier inverse Transform. But the Generalized Fourier Transform of the derivative, which is going to be useful, is given by:

$$\mathcal{F}_-(d\psi_p(A)\cdot\delta A)(\xi) = \frac{2}{p^2 - \xi^2 - i0}\mathcal{F}_-(\delta A\psi_p(A))(\xi). \tag{4.38}$$

Note that here, we suppose that $d\psi_p(A)\cdot\delta A$ is in $L^2(\mathbb{R})_{ac}$. We will give at the end the general case where $d\psi_p(A)\cdot\delta A$ is in $L^2(\mathbb{R})$.

4.1.3 Derivative of the density

In order to obtain the derivative of the density, we start by assuming that $H(A)$ has no discrete spectrum so that :

$$n(A) = \int_{-\infty}^{+\infty} e^{-\frac{p^2}{2}} |\psi_p|^2 \ \frac{dp}{2\pi\hbar}.$$

Then, we have for any test function ϕ:

$$\begin{aligned}
\int_{-\infty}^{+\infty} dn(A)\cdot\delta A\phi \ dx &= 2\mathrm{Re}\int_{-\infty}^{+\infty}\int_{-\infty}^{+\infty} e^{-\frac{p^2}{2}}\overline{\psi_p} d\psi_p(A)\cdot\delta A\phi \ \frac{dp}{2\pi\hbar}\ dx \\
&= 2\mathrm{Re}\int_{-\infty}^{+\infty} e^{-\frac{p^2}{2}} \left(d\psi_p(A)\cdot\delta A, \phi\psi_p\right)_{L^2} \ \frac{dp}{2\pi\hbar} \\
&= 2\mathrm{Re}\int_{-\infty}^{+\infty} e^{-\frac{p^2}{2}} \left(\mathcal{F}_-(d\psi_p(A)\cdot\delta A), \mathcal{F}_-(\phi\psi_p)\right)_{L^2} \ \frac{dp}{2\pi\hbar} \\
&= 2\mathrm{Re}\int_{-\infty}^{+\infty} e^{-\frac{p^2}{2}} \left(\frac{2}{p^2-\xi^2-i0}\mathcal{F}_-(\psi_p\delta A), \mathcal{F}_-(\psi_p\phi)\right)_{L^2} \ \frac{dp}{2\pi\hbar} \\
&= 2\mathrm{Re}\int_{-\infty}^{+\infty} e^{-\frac{p^2}{2}} \int_{-\infty}^{+\infty}\left(\int_{-\infty}^{+\infty}\overline{\psi_p(x)}\psi_\xi(x)\phi(x)\ dx\right) \\
&\quad \frac{2}{p^2-\xi^2-i0}\left(\int_{-\infty}^{+\infty}\psi_p(y)\overline{\psi_\xi(y)}\delta A(y)\ dy\right)\ \frac{d\xi\, dp}{(2\pi\hbar)^2}.
\end{aligned}$$

This gives the following expression for the derivative of the density in a weak sense:

$$\begin{aligned}
dn(A)\cdot\delta A &= 2\mathrm{Re}\int_{-\infty}^{+\infty}\int_{-\infty}^{+\infty} \frac{e^{-\frac{p^2}{2}}}{\frac{p^2}{2}-\frac{\xi^2}{2}-i0}\left(\int_{-\infty}^{+\infty}\psi_p(y)\overline{\psi_\xi(y)}\delta A(y)\ dy\right)\overline{\psi_p(x)}\psi_\xi(x)\ \frac{d\xi\, dp}{(2\pi\hbar)^2} \\
&= \mathrm{Re}\int_{-\infty}^{+\infty}\int_{-\infty}^{+\infty} \frac{e^{-\frac{p^2}{2}}-e^{-\frac{\xi^2}{2}}}{\frac{p^2}{2}-\frac{\xi^2}{2}}\left(\int_{-\infty}^{+\infty}\psi_p(y)\overline{\psi_\xi(y)}\delta A(y)\ dy\right)\overline{\psi_p(x)}\psi_\xi(x)\ \frac{d\xi\, dp}{(2\pi\hbar)^2}.
\end{aligned}$$

We can see that this expression is very similar to the one obtained for the discrete spectrum (4.32), except that the discrete sums are replaced by integrals. In the case where the density is composed of discrete and continuous spectrum, and where $A(0)\neq 0$ the derivative reads:

$$\begin{aligned}
dn(A)\cdot\delta A &= \mathrm{Re}\int_{-\infty}^{+\infty}\int_{-\infty}^{+\infty} \frac{e^{-E_p}-e^{-E_\xi}}{E_p-E_\xi}\left(\int_{-\infty}^{+\infty}\psi_p(y)\overline{\psi_\xi(y)}\delta A(y)\ dy\right)\overline{\psi_p(x)}\psi_\xi(x)\ \frac{d\xi\, dp}{(2\pi\hbar)^2} + \\
&\quad 2\mathrm{Re}\int_{-\infty}^{+\infty}\sum_k \frac{e^{-E_p}-e^{-\lambda_k}}{E_p-\lambda_k}\left(\int_{-\infty}^{+\infty}\psi_p(y)\psi_k(y)\delta A(y)\ dy\right)\overline{\psi_p(x)}\psi_k(x)\frac{dp}{2\pi\hbar} + \\
&\quad \sum_{k,q}\frac{e^{-\lambda_k}-e^{-\lambda_q}}{\lambda_k-\lambda_q}\int_{-\infty}^{\infty}\psi_k(y)\psi_q(y)\delta A(y)\ dx\psi_k\psi_q.
\end{aligned}$$

4.2 Numerical results

We use exactly the same scheme as [7] (the reader can refer to it for the details about the time and space discretizations) except we add the continuous spectrum in the expression of the density. Figures III.12–III.14 show the evolution of the density

n, the total electrical potential $V_s + V_{ext}$ and the current j for the first test case of a single barrier described in subsection 3.3 (we use the same parameters and a scaled time step $\Delta t = 0.002$). The model converges to the same stationary state as found with the stationary Gummel method, we can see indeed on the last figure that the current converges to a constant equal to $1.4524 \times 10^9 Am^{-2}$. Unfortunately, the momentum step needed to capture the resonance of the second test case (the RTD) is too small to allow us to run our program, which is written currently with Matlab. The calculation of the derivative is numerically expensive because of the double integral (which becomes a double sum when discretized). Each sum having around 2000 terms with a sufficiently small momentum step, the total of terms is equal to $2000 \times 2000 = 4 \times 10^6$ for each derivative calculation. Several attempts have been made to lower this cost but with no result yet. We have good hope to solve this problem by using an adaptative mesh size for the momentum (see for instance [14]) and programming the algorithm in Fortran.

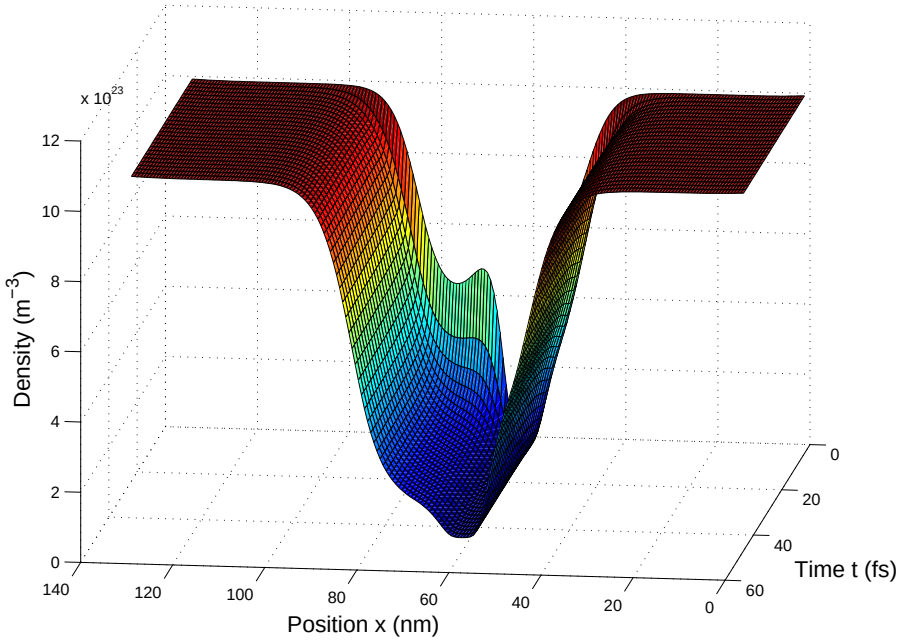

Figure III.12: Density n as function of the position and time for the first test case (single barrier).

5 Conclusion and perspectives

In this chapter, we have proposed numerical methods to deal with the continuous spectrum arising from the use of transparent boundary conditions for the quantum drift-diffusion model coupled to the Poisson equation. For the stationary case, we propose a Gummel method while for the transient case, we adapt the Newton algorithm used on the scheme proposed in [7]. We show preliminary numerical results on a single and a double barrier diode. The numerical cost of adding the continuous spectrum is important and it is difficult yet to deal with a realistic RTD which possesses a sharp

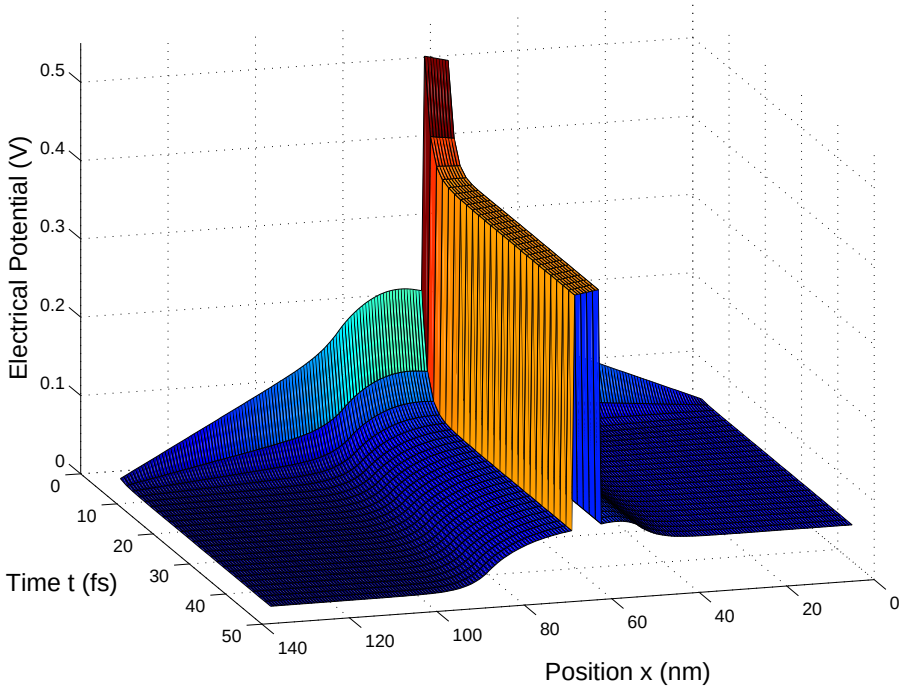

Figure III.13: Total electrical potential $V_s + V_{ext}$ as function of the position and time for the first test case (single barrier)

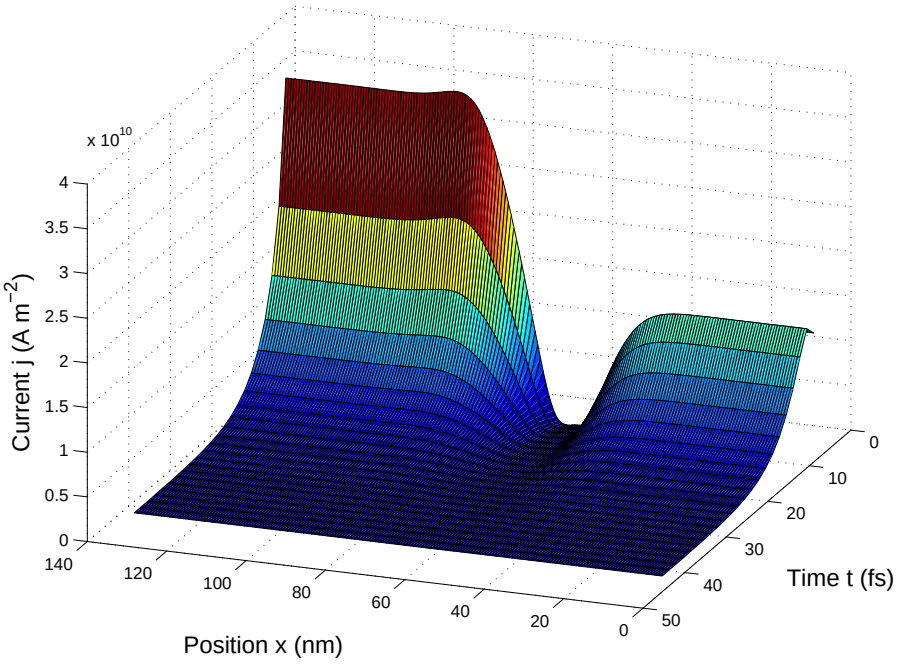

Figure III.14: Current j as function of the position and time for the first test case (single barrier)

resonance. Optimization of the scheme and the code (especially using an adaptative meshing strategy for the momentum and coding with Fortran) should allow in the future to perform tests and to see if it is really necessary to use such transparent boundary conditions, or if the use of Neumann boundary conditions on the spectrum does not affect significantly the results.

References

[1] S. Agmon, *Spectral properties of Schrödinger operators and scattering theory*, Ann. Scuola Norm. Sup. Pisa Cl. Sci., **II**, 2(1975), 679–684.

[2] A. Arnold, *Mathematical concepts of open boundary conditions*, Phys. Lett., **30** (2001), 561–584.

[3] N. Ben Abdallah, *On a multidimensional Schrödinger-Poisson scattering model for semiconductors*, J. Math. Phys. **41** (2000), 4241–4261.

[4] N. Ben Abdallah, P. Degond, P. A. Markowich, *On a one-dimensional Schrödinger-Poisson scattering model*, Z. Angew. Math. Phys. **48** (1997), 135–155.

[5] C. Cohen-Tannoudji, *Mécanique Quantique*, volumes 1 et 2, Hermann(1996).

[6] P. Degond, *Introduction à la théorie quantique*, notes d'un cours enseigné dans le cadre du DEA de Mathématiques Appliquées de l'Université Paul Sabatier.

[7] P. Degond, S. Gallego, F. Méhats, *An entropic Quantum Drift-Diffusion model for electron transport in resonant tunneling diodes*, J. Comput. Phys. **221** (2007), 226–249.

[8] P. Degond, F. Méhats, C. Ringhofer, *Quantum Energy-Transport and Drift-Diffusion models*, J. Stat. Phys. **118** (2005), no. 3-4, 625–665.

[9] S. Gallego, F. Méhats, *Entropic discretization of a quantum drift-diffusion model*, SIAM J. Numer. Anal. **43** (2005), no. 5, 1828–1849.

[10] H. K. Gummel, *A self-consistent iterative scheme for one-dimensional steady state transistor calculations*, IEEE Trans. Electron. Devices, ED-11 (1964), 455–465.

[11] C. S. Lent, D. J. Kirkner, *The quantum transmitting boundary method*, J. Appl. Phys. **67** (1990), 6353–6359.

[12] A. Messiah, *Mécanique Quantique*, volumes 1 et 2, Dunod (1960).

[13] F. Nier, *A variational formulation of Schrödinger-Poisson systems in dimension* $d \leq 3$, Comm. Partial Differential Equations **18** (1993), no. 7-8, 1125–1147.

[14] O. Pinaud, *Transient simulations of a resonant tunneling diode*, J. Appl. Phys. **92**(4) (2002), 1987–1994.

[15] M Reed, B. Simon, *Method of Modern Mathematical Physics, vol 3, Scattering Theory*, Academic Press, San Diego, 1980.

[16] D. R. Yafaev, *Mathematical scattering Theory, general theory*, Translations of mathematical monographs vol 105, AMS, Providence, 1992.

Chapter IV

Isothermal quantum Euler: derivation, asymptotic analysis and simulation

This chapter has given an article written in collaboration with P. Degond and F. Méhats, and published in SIAM Multiscale Modeling and Simulation: *Isothermal quantum hydrodynamics: derivation, asymptotic analysis and simulation*, SIAM Multiscale Model. Simul. **6** (2007), no. 1, 246–272.

Abstract. This chapter is devoted to the reformulation of an isothermal version of the quantum hydrodynamic model (QHD) derived by Degond and Ringhofer in J. Stat. Phys. **112** (2003), 587–628 (which will be referred to as the quantum Euler system). We write the model under a simpler (differential) way. The derivation is based on an appropriate use of commutators. Starting from the quantum Liouville equation, the system of moments is closed by a density operator which minimizes the quantum free energy. Some properties of the model are then exhibited and most of them rely on a gauge invariance property of the system. Several simplifications of the model are also written for the special case of irrotational flows. The second part of the chapter is devoted to a formal analysis of the asymptotic behavior of the quantum Euler system in three situations: at the semiclassical limit, at the zero-temperature limit and at a diffusive limit. The remarkable fact is that in each case we recover a known model: respectively the isothermal Euler system, the Madelung equations and the entropic quantum drift-diffusion model. Finally, we give in the third part some preliminary numerical simulations.

Key words. density matrix, quantum Liouville equation, quantum moment hydrodynamics, local equilibria, entropy minimization, quantum Euler, asymptotic analysis, Madelung equations, entropic quantum drift-diffusion, numerical simulations.

1 Introduction

Various works have been devoted in the past decade to the derivation of quantum hydrodynamic models for semiconductors in order to simulate nanoscale devices such as tunneling diodes or lasers. The interest in such models comes from the fact that they are supposed to describe quantum transport in highly collisional situations and to be computationally less expensive than corresponding quantum microscopic models, such as the Schrödinger equation or the Wigner equation [1, 6, 22, 23, 24]. It is known since Madelung [21] that the Schrödinger equation can be reformulated in a fluid dynamic way. Indeed, using WKB wave functions $\psi = \sqrt{n}e^{iS/\hbar}$ enables us to obtain a system on the density $n(t,x)$ and the velocity $u = \nabla S(t,x)$ which is formally equivalent to the Schrödinger equation and takes the form of a pressureless Euler system, with an additional term involving the so-called Bohm potential proportional to $\Delta(\sqrt{n})/\sqrt{n}$ (see (3.71), (3.72)). Unfortunately, this approach is essentially devoted to pure-state quantum mechanics, since it is difficult to adapt it in order to take into account many-body effects and statistical mechanics. In this sense, one can say that the Madelung equations are the zero-temperature quantum hydrodynamic equations.

To design quantum hydrodynamic models with temperature effects, the route which has been usually followed consists in incorporating to classical fluid models some "quantum" correction terms, based on the Bohm potential [12, 13, 14, 15, 16, 18]. However, such approaches are not obvious to justify from physical principles. Moreover, quantum corrections involving the Bohm potential produce high order terms in these systems and make their resolution difficult, from the mathematical and numerical points of view.

In 2003, Degond and Ringhofer [10] proposed a different manner to derive quantum hydrodynamic models, by closing the systems of moments thanks to a quantum entropy minimisation principle. This systematic approach, which is an extension of Levermore's moment method [20] to the framework of quantum mechanics, seems very fruitful, although it is still formal. Following this first paper, an entropic quantum drift-diffusion model has been derived in [9] and after reformulation thanks to elementary algebra in [8], it has been possible to go further in its analysis and to discretize it numerically in [11]. Numerical comparisons of this model with existing quantum transport models in [7] showed that it is a good candidate model for quantum device simulations in diffusive regimes. Here, we are interested in the hydrodynamic regime with a quantum Euler system, which is nothing but an isothermal version of the quantum hydrodynamic model derived in [10]. Let us shortly present this model (more detail can be found in Section 2, where the derivation of this system is revisited). From the Wigner equation, integrations with respect to the momentum variable $p \in \mathbb{R}^d$ (d being the dimension of the momentum space, $d = 3$ in this chapter) enable to obtain equations for the first two moments $n(t,x)$ (the mass density) and $n(t,x)u(t,x)$ (the current density), both densities being functions of the space variable $x \in \mathbb{R}^3$ and the time variable $t \in \mathbb{R}$:

$$\partial_t n + \nabla \cdot nu = 0, \tag{1.1}$$

$$\partial_t (nu) + \nabla \cdot (nu \otimes u + \mathbb{P}) + n\nabla V = 0, \tag{1.2}$$

where V denotes an applied potential. Of course, this system of equations is not closed, since the pressure tensor $\mathbb{P}$ is still expressed in terms of the microscopic Wigner

function $w(t,x,p)$:

$$\mathbb{P} = \int_{\mathbb{R}^d} (p-u)(p-u)\, w(t,x,p)\, \frac{dp}{(2\pi\hbar)^d}, \tag{1.3}$$

where $\hbar$ is the dimensionless Planck constant. The quantum Euler model is thus complete only as soon as the closure assumption is made precise. We close the system by replacing the expression (1.3) of $\mathbb{P}$ by another one in terms of n and nu:

$$\mathbb{P} = \int_{\mathbb{R}^d} (p-u)(p-u)\, w^{eq}_{n,nu}\, \frac{dp}{(2\pi\hbar)^d}, \tag{1.4}$$

where $w^{eq}_{n,nu}$ is the so-called local equilibrium, depending only on n and nu in a non local (and non explicit) way. It is precisely defined in Section 2 as follows: $w^{eq}_{n,nu} = W\left(\varrho^{eq}_{n,nu}\right)$, where W is the Wigner transform and $\varrho^{eq}_{n,nu}$ is the local equilibrium density operator obtained thanks to an entropy minimization principle. The Wigner transform W and the equilibrium density operator $\varrho^{eq}_{n,nu}$ will be precisely defined in the next section.

Needless to say, presented in this manner, this quantum Euler model (1.1), (1.2), (1.4) is rather involved and not easy to handle numerically. The aim of this chapter is threefold. First, as it was done for the entropic quantum drift-diffusion model in [8], we reformulate (in Section 2) this system in a simpler (differential) and more tractable way, and we prove directly a few properties of this model. Note that, to do this, we rederive the model thanks to the entropy minimization principle without using the Wigner formalism, which has in itself an interest since this approach is easily adaptable to systems set on bounded domains (subject to adequate boundary conditions). We also show some properties of the model, which, for most of them, rely on a gauge invariance property of the system and we write several simplifications of the model for the special case of irrotational flows.

Second, we investigate in Section 3 several asymptotic limits for this model, which enable us to make some links with other models: the isothermal Euler system at the semiclassical limit in section 3.1 (during this asymptotics, we also recover a model obtained by Jüngel and Matthes in [19]), the Madelung equations at the zero-temperature limit (section 3.2) and the entropic quantum drift-diffusion model of [9] at the diffusive limit (section 3.3). Note also that, in this section 3.3, we consider the quantum Euler model with a relaxation term and suggest that this additional term drives the system to global quantum equilibria.

Third, we present as preliminary results in section 4 some numerical simulations to illustrate the model on a simple device. A future article will be devoted to the study of the numerical scheme employed here and comparisons with other models will be performed.

The main results of this chapter are thus Theorem 2.5, reformulating the quantum Euler system, Proposition 2.8, dealing with the special case of irrotational flows, and Theorems 3.3, 3.5, 3.8 and 3.9 dealing with its asymptotic approximations. We wish to specify that the arguments presented in this article are formal. A precise mathematical framework in which this analysis could be made rigorous is still to be found.

We finish this introduction by giving some possible applications of the Quantum Euler model. We first have in mind the semiconductor industry where engineers have first introduced Hydrodynamics models with $\hbar^2$ quantum corrections in order to simulate nanoscale devices. One nanoscale device of interest is the so-called Resonant

Tunneling Diode [4]. The use of these models have permitted to exhibit interesting features of RTD such as negative resistance or hysteresis [5, 17]. The Quantum Euler model could be also used in quantum chemistry [3], or other areas of physics such as quantum optics, the study of superfluidity, etc...

2 Derivation of the model and main properties

In this section, we recall how the strategy of Degond and Ringhofer [10] enables to derive a closed system of moment equations with a constant temperature. The key ingredient is a free energy (instead of an entropy) minimization principle. It gives rise to the notion of local equilibrium microscopic state which is chosen in order to close the system of moments. This argument is shortly presented in subsection 2.2 and in the beginning of subsection 2.3. The quantum Euler system is then rewritten under a simplified form in Theorem 2.5, which gathers the main new result of this section.

2.1 Notations

By a density operator, we shall always mean a positive, Hermitian, trace-class operator acting on $L^2(\mathbb{R}^3)$. Let us define the first moments of a density operator ϱ, *i.e.* the mass density n and the current density nu, by duality, considering scalar test functions ϕ and vector ones Φ. We set

$$\forall \phi \in C_0^\infty(\mathbb{R}^3) \qquad \int n\phi \, dx = \mathrm{Tr}\ (\varrho\phi)\,, \tag{2.5}$$

$$\forall \Phi \in C_0^\infty(\mathbb{R}^3)^3 \qquad \int nu\cdot\Phi \, dx = \mathrm{Tr}\ \left(\varrho W^{-1}\left(p\cdot\Phi\right)\right) = -i\hbar\mathrm{Tr}\ \left(\varrho\left(\Phi\cdot\nabla + \frac{1}{2}(\nabla\cdot\Phi)\right)\right) \tag{2.6}$$

(in the right-hand sides, ϕ, Φ and $\nabla\cdot\Phi$ are the multiplication operators). Note that an immediate consequence of (2.5) and (2.6) is the following property which will be useful later:

$$\forall \Phi \qquad -\frac{i}{\hbar}\mathrm{Tr}\ (\varrho(\Phi\cdot\nabla)) = \int nu\cdot\Phi \, dx + \frac{i\hbar}{2}\int n\ \nabla\cdot\Phi \, dx. \tag{2.7}$$

In (2.6), W^{-1} denote the inverse Wigner transform (or Weyl quantization). For the sake of completeness, let us recall the definitions of the Wigner transform and the inverse Wigner transform. The Wigner transform maps operators on $L^2(\mathbb{R}^3)$ onto symbols, *i.e.* $L^2(\mathbb{R}^3\times\mathbb{R}^3)$ functions of the classical position and momentum variables $(x,p)\in\mathbb{R}^3\times\mathbb{R}^3$. More precisely, one defines the integral kernel of the operator ϱ to be the distribution $\underline{\varrho}(x,x')$ such that ϱ operates on any function $\psi(x)\in L^2(\mathbb{R}^3)$ as follows:

$$\varrho\psi(x) = \int \underline{\varrho}(x,x')\psi(x')dx'.$$

Then, the Wigner transform $W(\varrho)(x,p)$ is defined by:

$$W(\varrho)(x,p) = \int \underline{\varrho}\left(x-\frac{1}{2}\eta, x+\frac{1}{2}\eta\right)e^{\frac{i\eta\cdot p}{\hbar}}d\eta. \tag{2.8}$$

The Wigner transform can be inverted and its inverse is defined for any function $w(x,p)$ as the operator acting on $\psi(x)\in L^2(\mathbb{R}^3)$ as:

$$W^{-1}(w)\psi(x) = (2\pi\hbar)^{-3}\int w\left(\frac{x+y}{2},p\right)\psi(y)e^{\frac{ip(x-y)}{\hbar}}\,dp\,dy. \tag{2.9}$$

We end this section by expressing a few commutator identities that are used in the remainder of this article. Let $\phi(x)$, $\psi(x)$, $\Phi(x)$, $\Psi(x)$ be test functions (the capital letters are used for vector functions while the lower case letters are used for scalar ones). Then, the following equalities hold:

$$[\phi, \psi] = 0, \tag{2.10}$$

$$[\phi, \Psi \cdot \nabla] = -\Psi \cdot \nabla\phi, \tag{2.11}$$

$$[\Phi \cdot \nabla, \Psi \cdot \nabla] = ((\Phi \cdot \nabla)\Psi - (\Psi \cdot \nabla)\Phi) \cdot \nabla, \tag{2.12}$$

$$[\phi, \Delta] = -\Delta\phi - 2\nabla\phi \cdot \nabla. \tag{2.13}$$

We also recall the cyclicity of the trace, where a, b, c are three operators:

$$\text{Tr } ([a, b]c) = \text{Tr } ([c, a]b) = \text{Tr } ([b, c]a)\,.$$

2.2 Local equilibria via entropy minimization

Let s be a strictly convex continuously differentiable function on $\mathbb{R}^+$. We define the quantum entropy by:

$$S(\varrho) = \text{Tr } (s(\varrho))\,. \tag{2.14}$$

We intend to describe the effect of the interaction of a quantum system, subject to a potential V, with a thermal bath at temperature T. To this aim, it is convenient to introduce the quantum free energy defined by:

$$G(\varrho) = TS(\varrho) + E(\varrho) = \text{Tr } (Ts(\varrho) + \mathcal{H}\varrho)\,. \tag{2.15}$$

where $\mathcal{H} = -\frac{\hbar^2}{2}\Delta + V$ is the Hamiltonian.

The main assumption concerning the interaction between the system and the thermal bath is that the first two moments n and nu are conserved during these interactions. According to this statement, we now claim the quantum free energy minimization principle in the following definition (the reader can refer to [10] for details):

Definition 2.1 *Let the functions n and nu be given. Consider the following constrained minimization problem:*

$$\min \{G(\varrho) \text{ such that } \varrho \text{ is a density operator satisfying (2.5) and (2.6)}\}\,. \tag{2.16}$$

The solution, if it exists, is called the local equilibrium density operator associated to n and nu. Lagrange multiplier theory for the constrained problem (2.16) (see [10]) shows that there exist a scalar function A and a vector function B, both real valued and defined on $\mathbb{R}^3$, such that this local equilibrium density operator takes necessarily the form:

$$\varrho^{eq}_{n,nu} = (s')^{-1}\left(-\frac{1}{T}\,H(A, B)\right), \tag{2.17}$$

where $H(A, B)$ is the following modified Hamiltonian:

$$H(A, B) = W^{-1}\left(\frac{1}{2}(p - B)^2 + A\right) = \frac{1}{2}\,(i\hbar\nabla + B)^2 + A. \tag{2.18}$$

This definition is obviously incomplete if no assumption is made on n and nu. In fact, this result has to be understood only at a formal level. Several crucial questions remain open: in which functional spaces n and nu have to be chosen, in which spaces A and B have to be sought, or the question of existence and uniqueness of A and B. Throughout this chapter, we shall postpone this delicate question of realizability of moments, assuming that, as soon as the minimization problem (2.16) has to be solved, n and nu are such that the associate functions A and B are uniquely defined. In fact, since we are dealing with trace-class operators, the mass and current densities n and nu vanish at the infinity and it seems reasonable to assume that the modified Hamiltonian $H(A,B)$ has always a compact resolvent and thus a discrete spectrum $(\lambda_p(A,B))_{p\in\mathbb{N}}$ and a complete set of (normalized) eigenfunctions denoted by $(\psi_p(A,B))_{p\in\mathbb{N}}$. According to these assumptions, one can rewrite the mass density and the current density associated to $\varrho^{eq}_{n,nu}$ in terms of the eigen-elements of $H(A,B)$:

$$n(A,B) = \sum_{p\in\mathbb{N}} (s')^{-1}\left(-\frac{\lambda_p(A,B)}{T}\right)|\psi_p(A,B)|^2, \tag{2.19}$$

$$(nu)(A,B) = \sum_{p\in\mathbb{N}} (s')^{-1}\left(-\frac{\lambda_p(A,B)}{T}\right)\mathcal{I}m\left(\hbar\nabla\psi_p(A,B)\,\overline{\psi_p(A,B)}\right). \tag{2.20}$$

Remark 2.2 (Towards a numerical method to compute A and B) *The constitutive equations (2.19)–(2.20) provide no explicit relation between the extensive quantities (n,nu) and the associate intensive quantities (A,B). Nevertheless, we can provide a practical method to compute A^0 and B^0 associated to given n^0 and n^0u^0.*

Consider the change of variable $\tilde{A} = -A - B^2/2$ and $\tilde{B} = B$ so that the following Hamiltonian $\tilde{H}(\tilde{A},\tilde{B})$ is now linear in $(\tilde{A},\tilde{B})$:

$$\tilde{H}(\tilde{A},\tilde{B}) = H(A,B) = -\frac{\hbar^2}{2}\Delta + i\hbar\tilde{B}\cdot\nabla + i\hbar/2\,\nabla\cdot\tilde{B} - \tilde{A},$$

and consider the following functional:

$$\tilde{\Sigma}(\tilde{A},\tilde{B}) = T\mathrm{Tr}\left(s^*(-\frac{1}{T}\tilde{H}(\tilde{A},\tilde{B}))\right) := \Sigma(A,B), \tag{2.21}$$

where s^* is the convex conjugate function of s defined such that $(s^*)' = (s')^{-1}$ (note that this functional, called the Massieu-Planck potential, is in fact the Legendre dual of the quantum free energy [2]). The Gâteaux derivative of $\tilde{\Sigma}$ can be computed (using a formula which can be found for instance in [10] or [9]) and gives:

$$\frac{\delta\tilde{\Sigma}}{\delta\tilde{A}} = n(A,B) \quad ; \quad \frac{\delta\tilde{\Sigma}}{\delta\tilde{B}} = (nu)(A,B). \tag{2.22}$$

Let define now the following functional:

$$J(\tilde{A},\tilde{B}) = \Sigma(A,B) - \int n^0\tilde{A}\,dx - \int n^0u^0\cdot\tilde{B}\,dx, \tag{2.23}$$

so that the Gâteaux derivative of J is given by:

$$\frac{\delta J}{\delta\tilde{A}} = n(A,B) - n^0 \quad ; \quad \frac{\delta J}{\delta\tilde{B}} = (nu)(A,B) - n^0u^0. \tag{2.24}$$

We deduce that if J admits a critical point $(\tilde{A}^0, \tilde{B}^0)$, then the functions $A^0 = -\tilde{A}^0 - (\tilde{B}^0)^2/2$ and $B^0 = \tilde{B}^0$ are associated to n^0 and n^0u^0 according to Definition 2.1. Note that the functional J is strictly convex due to the fact that s^* is strictly convex, that $\tilde{H}(\tilde{A}, \tilde{B})$ is linear in $(\tilde{A}, \tilde{B})$, and that the two integrals are linear in $(\tilde{A}, \tilde{B})$. This remark allows us to elaborate a numerical method based on a minimization algorithm to compute A^0 and B^0 corresponding to given n^0 and n^0u^0.

Lemma 2.3 (Gauge invariance) *Let $S(x)$ be a smooth function. Then, we have:*

$$\exp\left(\frac{iS}{\hbar}\right) H(A,B) \exp\left(-\frac{iS}{\hbar}\right) = H(A, B + \nabla S). \tag{2.25}$$

As a consequence we have the following identities:

$$n(A, B+\nabla S) = n(A,B) \ ; \ (nu)(A, B+\nabla S) = (nu)(A,B) + n(A,B)\nabla S, \tag{2.26}$$

which relates the density and velocity for two values of B differing by a gradient.

Proof. To prove identity (2.25), we remark that

$$\exp\left(\frac{iS}{\hbar}\right) (i\hbar\nabla + B) \exp\left(-\frac{iS}{\hbar}\right) = i\hbar\nabla + B + \nabla S.$$

Hence

$$\exp\left(\frac{iS}{\hbar}\right) \left(\frac{1}{2}(i\hbar\nabla + B)^2 + A\right) \exp\left(-\frac{iS}{\hbar}\right) = \frac{1}{2}(i\hbar\nabla + B + \nabla S)^2 + A,$$

which is (2.25).

As a consequence, the eigenvalues of $H(A,B)$ and $H(A, B+\nabla S)$ are the same. Also, if two operators are conjugate, any function of these two operators is also conjugate by the same conjugation operator. This implies that:

$$\exp\left(\frac{iS}{\hbar}\right) s^*\left(-\frac{1}{T}H(A,B)\right) \exp\left(-\frac{iS}{\hbar}\right) = s^*\left(-\frac{1}{T}H(A, B+\nabla S)\right), \tag{2.27}$$

where s^* is the convex conjugate function of s defined such that $(s^*)' = (s')^{-1}$. Therefore, the eigenvalues of $s^*\left(-\frac{1}{T}H(A,B)\right)$ and $s^*\left(-\frac{1}{T}H(A, B+\nabla S)\right)$ are the same and we have the following equality for the functional Σ defined in (2.21):

$$\Sigma(A, B+\nabla S) = \Sigma(A,B), \tag{2.28}$$

and in particular, we have:

$$\frac{\delta\Sigma}{\delta A}(A, B+\nabla S) = \frac{\delta\Sigma}{\delta A}(A,B) \ \ ; \ \ \frac{\delta\Sigma}{\delta B}(A, B+\nabla S) = \frac{\delta\Sigma}{\delta B}(A,B). \tag{2.29}$$

Using the formula of the Gâteaux derivative of Σ given in (2.22) and the chain rule leads to:

$$\frac{\delta\Sigma}{\delta A} = -n \ \ ; \ \ \frac{\delta\Sigma}{\delta B} = nu - nB, \tag{2.30}$$

where n and nu shortly denote here $n(A,B)$ and $(nu)(A,B)$, so that identities (2.26) stem directly from (2.29) and (2.30). □

We end this subsection by giving a lemma which will be needed in the proof of the main result (Theorem 2.5) of the next subsection. This lemma expresses the very strong result that u and B are not equal but differ by a vector field which is a curl divided by the density.

Lemma 2.4 *Let n, nu, A, B be given according to Definition 2.1. Then we have*

$$\nabla \cdot nu = \nabla \cdot nB. \tag{2.31}$$

Proof. The proof of this lemma is a direct consequence of (2.28) and (2.30). We have indeed for any test function $S(x)$:

$$\begin{aligned} \lim_{t\to 0} \left(t^{-1}(\Sigma(A, B + t\nabla S) - \Sigma(A, B))\right) &= 0 \\ &= \int \frac{\delta \Sigma}{\delta B} \cdot \nabla S \, dx \\ &= \int (nu - nB) \cdot \nabla S \, dx, \end{aligned}$$

meaning that $\nabla \cdot (nu - nB) = 0$ almost everywhere. □

2.3 The quantum Euler system

At the microscopic scale, a quantum system evolving in $\mathbb{R}^3$ and subject to a potential $V(t, x)$ can be described by a time-dependent density operator satisfying the quantum Liouville equation:

$$i\hbar \partial_t \varrho = [\mathcal{H}, \varrho] + i\hbar \mathcal{Q}(\varrho), \tag{2.32}$$

where $[\mathcal{H}, \varrho] = \mathcal{H}\varrho - \varrho\mathcal{H}$ is the commutator of the Hamiltonian $\mathcal{H} = -\frac{\hbar^2}{2}\Delta + V$ with the density operator ϱ and $\hbar$ is the scaled Planck constant. In the right-hand side of this equation, we have introduced a collision term $\mathcal{Q}(\varrho)$. The precise form of this operator will not play an important role in this article. The key property that we request is that it drives the system to the local equilibria defined in the previous section. This is a consequence of the two following assumptions:

(i) mass and momentum are conserved during collision, *i.e.* for any density operator ϱ we have

$$\forall \varphi, \Phi \qquad \mathrm{Tr}\ (\mathcal{Q}(\varrho)\varphi) = 0 \quad \text{and} \quad \mathrm{Tr}\left(\mathcal{Q}(\varrho)\left(\Phi \cdot \nabla + \frac{1}{2}(\nabla \cdot \Phi)\right)\right) = 0. \tag{2.33}$$

(ii) the quantum free energy is dissipated, except for the density operator in the kernel of $\mathcal{Q}$, which is explicitly described as follows:

$$\mathcal{Q}(\varrho) = 0 \text{ iff } \exists (A,\ B) \text{ such that } \varrho = (s')^{-1}\left(-\frac{1}{T}\left(\frac{1}{2}(i\hbar\nabla + B)^2 + A\right)\right). \tag{2.34}$$

For $\varrho(t)$ solving (2.32), let us write the equations satisfied by the corresponding moments n and nu. To this aim, we first take the trace of the Liouville equation (2.32) against a test function ϕ. Using (2.33), the cyclicity of the trace and the commutator equalities (2.10)–(2.13), we get

$$\begin{aligned} \int \phi\, \partial_t n \, dx &= \mathrm{Tr}\ (\phi\, \partial_t \varrho) = -\frac{i}{\hbar}\mathrm{Tr}\ (\phi\, [\mathcal{H}, \varrho]) = -\frac{i}{\hbar}\mathrm{Tr}\left(\phi\left[-\frac{\hbar^2}{2}\Delta + V, \varrho\right]\right) \\ &= -\frac{i}{\hbar}\mathrm{Tr}\left(\left[\phi, -\frac{\hbar^2}{2}\Delta + V\right]\varrho\right) = -\frac{i\hbar}{2}\mathrm{Tr}\ ((\Delta\phi + 2\nabla\phi \cdot \nabla)\varrho). \end{aligned}$$

Now we can use property (2.7) to write:

$$\int \phi\, \partial_t n\, dx = -\frac{i\hbar}{2} \int n\Delta\phi\, dx + \int nu \cdot \nabla\phi\, dx + \frac{i\hbar}{2} \int n\nabla \cdot (\nabla\phi)\, dx = \int nu \cdot \nabla\phi\, dx.$$

This is the weak formulation of the equation of conservation of mass:

$$\partial_t n + \nabla \cdot nu = 0. \tag{2.35}$$

In order to obtain the second moment equation, we compose the collisional Liouville equation (2.32) with the operator $W^{-1}(p \cdot \Phi) = -i\hbar(\Phi \cdot \nabla + \frac{1}{2}(\nabla \cdot \Phi))$. Thanks to (2.33), we obtain

$$\forall \Phi \qquad \int \Phi \cdot \partial_t(nu)\, dx = -\mathrm{Tr}\, \left([\mathcal{H}, \varrho] \left(\Phi \cdot \nabla + \frac{1}{2}(\nabla \cdot \Phi) \right) \right). \tag{2.36}$$

It is readily seen that, with no further assumption, the right-hand side of (2.36) cannot be expressed in terms of n, nu and the test function Φ only. We just recover here the fact that the system (2.35), (2.36) – which is equivalent to (1.1), (1.2), (1.3) after Wigner transformation – is not closed.

Hence, by analogy with Levermore's methodology [20] and according to [10], we modify this system by replacing ϱ in the right-hand side of (2.36) by the Ansatz $\varrho^{eq}_{n,nu}$, which plays the role of a Maxwellian here. This Ansatz corresponds to the modeling assumptions (i) and (ii) made on $\mathcal{Q}$, and represents the most likely quantum microscopic state which possesses the moments n and nu, according to the statistics that has been chosen, *i.e.* the function s. We point out the fact that $\varrho^{eq}_{n,nu}$ depends locally in time but globally in space on n and nu. Let us now gather the equations forming the quantum Euler model. This system is composed of the two equations governing the time evolution of n and nu, (2.35) and

$$\forall \Phi \qquad \int \Phi \cdot \partial_t(nu)\, dx = -\mathrm{Tr}\, \left([\mathcal{H}, \varrho^{eq}_{n,nu}] \left(\Phi \cdot \nabla + \frac{1}{2}(\nabla \cdot \Phi) \right) \right), \tag{2.37}$$

coupled to the constitutive equations

$$\varrho^{eq}_{n,nu} = (s')^{-1} \left(-\frac{1}{T} H(A, B) \right) = (s')^{-1} \left(-\frac{1}{2T} (i\hbar\nabla + B)^2 - \frac{A}{T} \right). \tag{2.38}$$

$$\forall \phi \qquad \mathrm{Tr}\, \left(\varrho^{eq}_{n,nu}\, \phi \right) = \int n\phi\, dx, \tag{2.39}$$

$$\forall \Phi \qquad -i\hbar \mathrm{Tr}\, \left(\varrho^{eq}_{n,nu} \left(\Phi \cdot \nabla + \frac{1}{2}(\nabla \cdot \Phi) \right) \right) = \int nu \cdot \Phi\, dx. \tag{2.40}$$

The main result of this section is the following:

Theorem 2.5 *The above described quantum Euler system* (2.35), (2.36), (2.38), (2.39), (2.40) *is formally equivalent to the following system of equations:*

$$\partial_t n + \nabla \cdot nu = 0, \tag{2.41}$$

$$\partial_t(nu) + \nabla \cdot (nu \otimes B) + n(\nabla B) \cdot (u - B) + n\nabla(V - A) = 0, \tag{2.42}$$

where the extensive quantities n and nu and the associated intensive ones A and B are linked by the following constitutive equations:

$$n = \sum_{p\in\mathbb{N}} (s')^{-1}\left(-\frac{\lambda_p}{T}\right)|\psi_p|^2, \qquad nu = \sum_{p\in\mathbb{N}} (s')^{-1}\left(-\frac{\lambda_p}{T}\right)\mathcal{I}m\left(\hbar\nabla\psi_p\,\overline{\psi_p}\right), \tag{2.43}$$

and where $(\lambda_p, \psi_p)_{p\in\mathbb{N}}$ denotes the complete set of eigenvalues and normalized eigenvectors of the modified Hamiltonian defined by

$$H(A,B) = \frac{1}{2}\left(i\hbar\nabla + B\right)^2 + A. \tag{2.44}$$

Moreover, the time evolution of the macroscopic quantum free energy

$$\mathcal{G}(t) = \mathrm{Tr}\left(Ts(\varrho^{eq}_{n,nu}) + \left(-\frac{\hbar^2}{2}\Delta + V\right)\varrho^{eq}_{n,nu}\right), \quad \textit{where } \varrho^{eq}_{n,nu} \textit{ is defined by (2.38)}, \tag{2.45}$$

is simply given by:

$$\frac{d}{dt}\mathcal{G}(t) = \int n\,\partial_t V\,dx. \tag{2.46}$$

Proof. Let us first prove (2.42). Noticing that the Hamiltonian $\mathcal{H}$ can be rewritten as:

$$\mathcal{H} = H(A,B) - ihB\cdot\nabla - \frac{i\hbar}{2}(\nabla\cdot B) + V - A - \frac{1}{2}B^2$$

and that $H(A,B)$ commutes with $\varrho^{eq}_{n,nu}$ (denoted shortly ϱ in the remainder of the proof), we obtain from (2.37):

$$\begin{aligned}\int \Phi\cdot\partial_t(nu)\,dx &= \mathrm{Tr}\left((\Phi\cdot\nabla)\left[i\hbar B\cdot\nabla + \frac{i\hbar}{2}(\nabla\cdot B) - V + A + \frac{1}{2}B^2, \varrho\right]\right)\\ &\quad + \frac{1}{2}\mathrm{Tr}\left((\nabla\cdot\Phi)\left[i\hbar B\cdot\nabla + \frac{i\hbar}{2}(\nabla\cdot B) - V + A + \frac{1}{2}B^2, \varrho\right]\right)\\ &= (I) + (II) + (III) + (IV)\end{aligned}$$

with

$$(I) = i\hbar\mathrm{Tr}\,\left([\Phi\cdot\nabla, B\cdot\nabla]\varrho\right) \quad , \qquad (II) = -\frac{i\hbar}{2}\mathrm{Tr}\,\left([\nabla\cdot B, \Phi\cdot\nabla]\varrho\right)$$

$$(III) = \mathrm{Tr}\left(\left[V - A - \frac{1}{2}B^2, \Phi\cdot\nabla\right]\varrho\right) \quad , \qquad (IV) = \frac{i\hbar}{2}\mathrm{Tr}\,\left([\nabla\cdot\Phi, B\cdot\nabla]\varrho\right).$$

It remains to make these four terms more explicit. The use of the commutator equality (2.12) and the use of property (2.7) give:

$$\begin{aligned}(I) &= i\hbar\mathrm{Tr}\,\left(\varrho\left((\Phi\cdot\nabla)B - (B\cdot\nabla)\Phi\right)\cdot\nabla\right)\\ &= -\int nu\cdot\left((\Phi\cdot\nabla)B - (B\cdot\nabla)\Phi\right)dx - \frac{i\hbar}{2}\int n\nabla\cdot\left((\Phi\cdot\nabla)B - (B\cdot\nabla)\Phi\right)dx.\end{aligned}$$

A direct computation of the commutators (using (2.11)) in (II), (III) and (IV) gives then:

$$\begin{aligned}(II) &= \frac{i\hbar}{2}\mathrm{Tr}\,\left(((\Phi\cdot\nabla)\nabla\cdot B)\varrho\right) = \frac{i\hbar}{2}\int n(\Phi\cdot\nabla)\nabla\cdot B\,dx,\\ (III) &= -\mathrm{Tr}\left(\left(\Phi\cdot\nabla\left(V - A - \frac{1}{2}B^2\right)\right)\varrho\right) = -\int n(\Phi\cdot\nabla)\left(V - A - \frac{1}{2}B^2\right)dx,\\ (IV) &= -\frac{i\hbar}{2}\mathrm{Tr}\,\left(B\cdot\nabla\nabla\cdot\Phi\varrho\right) = -\frac{i\hbar}{2}\int nB\cdot\nabla\nabla\cdot\Phi\,dx.\end{aligned}$$

It is easy to check that the sum of (II), (IV) and the imaginary part of (I) vanishes. It remains:

$$\int \Phi \cdot \partial_t(nu)\, dx = -\int nu \cdot ((\Phi \cdot \nabla)B - (B \cdot \nabla)\Phi)\, dx - \int n\Phi \cdot \nabla \left(V - A - \frac{1}{2}B^2\right) dx,$$

which after an integration by parts gives the second equation of the quantum Euler system (2.42). This last equation reads componentwise (we use Einstein's convention for the implicit summation on j):

$$\partial_t(nu_i) + \partial_j(nu_iB_j) + n(u_j - B_j)\partial_iB_j + n\partial_i(V - A) = 0.$$

Finally, let us show the equation (2.46) for the quantum free energy. To do so, we recall that the derivative of the quantum entropy $S(\varrho) = \mathrm{Tr}\ (s(\varrho))$ with respect to ϱ is (see [10]):

$$dS(\varrho) \cdot \delta\varrho = \mathrm{Tr}\ \left(s'(\varrho)\delta\varrho\right).$$

The derivative of the quantum free energy G defined by (2.15) with respect to ϱ is then:

$$dG(\varrho) \cdot \delta\varrho = \mathrm{Tr}\ \left((Ts'(\varrho) + \mathcal{H})\delta\varrho\right). \tag{2.47}$$

It allows to compute the derivative of $\mathcal{G} = G(\varrho(t))$ with respect to t which is given by:

$$\frac{d}{dt}\mathcal{G} = \mathrm{Tr}\ \left((Ts'(\varrho) + \mathcal{H})\partial_t\varrho\right) + \int n\, \partial_t V\, dx, \tag{2.48}$$

where we remarked that $\mathrm{Tr}\ ((\partial_t V)\varrho) = \int n\, \partial_t V\, dx$. Then, we use the Ansatz

$$\varrho = (s')^{-1}\left(-\frac{1}{T}H(A,B)\right),$$

which gives

$$\begin{aligned}
\mathrm{Tr}\ \left((Ts'(\varrho) + \mathcal{H})\partial_t\varrho\right) &= \mathrm{Tr}\ ((-H(A,B) + \mathcal{H})\partial_t\varrho) \\
&= \mathrm{Tr}\ \left(\left(-ihB \cdot \nabla - \frac{i\hbar}{2}(\nabla \cdot B) + V - A - \frac{1}{2}B^2\right)\partial_t\varrho\right) \\
&= \int \left(B \cdot \partial_t(nu) + \partial_t n\left(V - A - \frac{1}{2}B^2\right)\right) dx.
\end{aligned}$$

Using the two equations of the quantum Euler system (2.41), (2.42), we obtain:

$$\begin{aligned}
\mathrm{Tr}\ \left((Ts'(\varrho) + \mathcal{H})\partial_t\varrho\right) &= \int B \cdot (-\nabla \cdot (nu \otimes B) - n(\nabla B) \cdot (u - B) - n\nabla\,(V - A))\, dx \\
&\quad - \int \nabla \cdot nu\left(V - A - \frac{1}{2}B^2\right) dx.
\end{aligned}$$

The first line in the right-hand side can be simplified after integrations by parts:

$$\begin{aligned}
&\int (-B_i\partial_j(nu_iB_j) - nB_i(u_j - B_j)(\partial_iB_j) - nB_i\partial_i(V - A))\, dx \\
&\qquad = \int \nabla \cdot nB\left(V - A - \frac{1}{2}B^2\right) dx.
\end{aligned}$$

So we finally obtain:

$$\text{Tr } \left((Ts'(\varrho)+\mathcal{H})\partial_t\varrho\right) = -\int \nabla\cdot(nu-nB)\left(V-A-\frac{1}{2}B^2\right)dx.$$

This last term vanishes using Lemma 2.4, and finally (2.48) yields (2.46). □

Let us now write several equivalent formulations of the second equation (2.42), that will be useful further. Direct calculations using (2.41), (2.42) and (2.31) lead to the following equations, which can replace (2.42) in the whole quantum Euler system:

$$\partial_t(nu)+\nabla\cdot(nu\otimes u)+n(\nabla\times u)\times(B-u)+n\nabla\left(V-A-\frac{1}{2}|B-u|^2\right)=0, \quad (2.49)$$

$$\text{or} \qquad \partial_t u+(B\cdot\nabla)u+(\nabla B)\cdot(u-B)+\nabla(V-A)=0, \quad (2.50)$$

$$\text{or again,} \qquad \partial_t u+(\nabla\times u)\times B+\nabla\left(u\cdot B-\frac{1}{2}B^2+V-A\right)=0. \quad (2.51)$$

Remark 2.6 *If we choose for the entropy function $s(\varrho)$ the Boltzmann entropy:*

$$s(\varrho)=\varrho(\log\varrho-1), \quad (2.52)$$

then the corresponding solution of the quantum free energy minimization problem (2.17) is the equilibrium introduced in [10] as a "quantum equilibrium" and referred to as "quantum Maxwellian" in [8]:

$$\varrho^m=\exp\left(-\frac{1}{T}H(A,B)\right). \quad (2.53)$$

The macroscopic quantum free energy corresponding to the Boltzmann entropy reads (dropping the constant term $\int nTdx$):

$$\text{Tr } \left(Ts(\varrho^m)+\left(-\frac{\hbar^2}{2}\Delta+V\right)\varrho^m\right)=\int\left(nu\cdot B+n\left(V-A-\frac{1}{2}B^2\right)\right)dx. \quad (2.54)$$

We have shown in Theorem 2.5 that if the electric potential V is independent of time, then this quantum free energy is conserved. In the case where the electrical potential is the sum of an external potential V^{ext} independent of time and a self-consistent potentiel V^s linked to the charge density by the Poisson equation:

$$-\alpha^2\Delta V^s=n, \quad (2.55)$$

with α the scaled Debye length, then the conserved quantity reads:

$$\int\left(nu\cdot B+n\left(V^{ext}-A-\frac{1}{2}B^2\right)\right)dx+\frac{\alpha^2}{2}\int|\nabla V^s|^2\,dx.$$

2.4 Special case of irrotational flows

We conclude this section by dealing with the special case of irrotational flows. Before giving the main proposition which is Proposition 2.8, we state the following lemma:

Lemma 2.7 *Let n, nu, A, B be given according to Definition 2.1. Assume moreover that u is an irrotational vector field, i.e. that there exists $S(x)$ such that $u = \nabla S$. Then B is defined by*

$$B = u = \nabla S \tag{2.56}$$

and we have

$$\varrho^{eq}_{n,nu} = e^{iS/\hbar}\, \varrho^{eq}_{n,0}\, e^{-iS/\hbar}, \tag{2.57}$$

where the two equilibrium density operators $\varrho^{eq}_{n,nu}$ and $\varrho^{eq}_{n,0}$ are given according to Definition 2.1. If we note $n(A,B)$ the density associated with A and B, we have moreover:

$$n(A,B) = n(A,0). \tag{2.58}$$

Proof. See Appendix A. □

Proposition 2.8 *Let n, nu satisfy the quantum Euler system (2.41)–(2.44). Then $\omega = \nabla \times u$ satisfies formally the following transport equation:*

$$\partial_t \omega + \nabla \times (\omega \times B) = 0. \tag{2.59}$$

Moreover, assume that at $t = 0$ the velocity is irrotational, i.e. that we have

$$\omega(t=0) = \nabla \times u(t=0) = 0, \tag{2.60}$$

and that the solution of (2.41)–(2.44) is smooth. Then for all time we have $\omega = \nabla \times u = 0$. In this case, the quantum Euler system (2.41)–(2.44) can be rewritten as follows:

$$\partial_t n + \nabla \cdot nu = 0, \tag{2.61}$$

$$\partial_t (nu) + \nabla \cdot (nu \otimes u) + n\nabla(V - A) = 0, \tag{2.62}$$

where n and A are coupled by the constitutive equation:

$$n = \sum_{p\in\mathbb{N}} (s')^{-1}\left(-\frac{\lambda_p}{T}\right) |\psi_p|^2, \tag{2.63}$$

and where $(\lambda_p, \psi_p)_{p\in\mathbb{N}}$ denotes the complete set of eigenvalues and normalized eigenvectors of the modified Hamiltonian defined by

$$H(A,0) = -\frac{\hbar^2}{2}\Delta + A. \tag{2.64}$$

Proof. The equation for the curl (2.59) is a direct consequence of (2.51). Now, multiply (2.59) by ω and integrate on $\mathbb{R}^3$. Straightforward calculations lead to the following equation, governing the evolution of the L^2 norm of ω:

$$\frac{d}{dt}\int |\omega|^2\, dx = -\int (\nabla \cdot B)\, |\omega|^2\, dx + \int (\nabla B) : (\omega \otimes \omega)\, dx. \tag{2.65}$$

Hence, applying a Cauchy-Schwarz inequality, we get

$$\frac{d}{dt}\int |\omega|^2\, dx \le C\, \|\nabla B\|_{L^\infty} \int |\omega|^2\, dx,$$

which gives $\omega \equiv 0$ as soon as $\omega(t=0) = 0$, by the Gronwall lemma. Then $\nabla \times u = 0$ implies that the results of Lemma 2.7 hold true for all time. Hence $u = B$, together with (2.42) (or (2.49)), gives (2.62), while $n(A,B) = n(A,0)$ is equivalent to (2.63), (2.64), and the proof is complete. □

Remark 2.9 *In this situation of irrotational flows, the "quantum part" of the model is simpler than in the general case of Theorem 2.5, since the underlying minimization problem is (A.95) given in Appendix, with only the constraint of the first moment n, instead of (2.16). In the specific case of dimension 1, the flow is obviously generically irrotational, so the quantum Euler system always appears under the reduced form (2.61)–(2.64).*

3 Formal asymptotics

We investigate here various asymptotic approximations of the quantum Euler system as dimensionless parameters go to zero. Our aim here is to draw some connections between this model and several other existing models. All the proofs given in this section use formal arguments.

3.1 Semiclassical asymptotics

If we choose for the entropy function s the Boltzmann entropy (2.52), then an $\hbar$ expansion of the "quantum Maxwellian" $\varrho^{eq}_{n,nu}$ can be performed. By keeping in this expansion the terms up to the order $\mathcal{O}(\hbar^2)$, one gets formally some approximate constitutive equations linking (n, nu) and (A, B):

Lemma 3.1 (formal) *Let n, nu, A, B be smooth functions linked according to Definition 2.1 with the entropy function s being the Boltzmann entropy (2.52). As the dimensionless Planck constant $\hbar$ goes to 0, the quantities A and B admit the following asymptotic expansions:*

$$A = T\ln n_0 - T\ln n + \frac{\hbar^2}{6}\frac{\Delta\sqrt{n}}{\sqrt{n}} - \frac{\hbar^2}{24}|\omega|^2 + \mathcal{O}(\hbar^4), \tag{3.66}$$

$$nB = nu + \frac{\hbar^2}{12}\nabla\times(n\omega) + \mathcal{O}(\hbar^4), \tag{3.67}$$

where we have denoted $\omega = \nabla\times u$ and n_0 is the effective density of state $n_0 = \left(\frac{T}{2\pi\hbar^2}\right)^{3/2}$.

Proof. See Appendix B. □

Remark 3.2 *In reduced dimension $d = 2$ or $d = 1$, the expression of the effective density of state n_0 has to be replaced by $n_0 = \left(\frac{T}{2\pi h^2}\right)^{d/2}$.*

Then, inserting these equations (3.66), (3.67) into (2.41), (2.49), one gets an approximate quantum Euler model.

Theorem 3.3 (Semiclassical formal limit) *Let the entropy function s be the Boltzmann entropy (2.52). Then, as the dimensionless Planck constant $\hbar$ goes to 0, the quantum Euler system admits the following asymptotic expansion:*

$$\partial_t n + \nabla\cdot nu = 0, \tag{3.68}$$

$$\partial_t(nu) + \nabla\cdot(nu\otimes u) + T\nabla n + n\nabla V - \frac{\hbar^2}{6}n\nabla\left(\frac{\Delta\sqrt{n}}{\sqrt{n}}\right) + \frac{\hbar^2}{12}\omega\times(\nabla\times(n\omega)) + \frac{\hbar^2}{24}n\nabla(|\omega|^2) = \mathcal{O}(\hbar^4), \tag{3.69}$$

where we have denoted $\omega = \nabla \times u$.

It is readily seen from (3.68) and (3.69) that, as $\hbar \to 0$, the quantum Euler system converges formally to the isothermal Euler system. Moreover, if we drop the terms $\mathcal{O}(\hbar^4)$ in (3.68), (3.69), the obtained model is the so-called quantum hydrodynamic model [18], up to additional terms depending only on $\omega = \nabla \times u$. For irrotational flows, we recover the quantum hydrodynamic model. These observations were already made in [19]. We point out the fact that, if the obtained equations (3.68), (3.69) are rigourously equivalent to the ones obtained by Jüngel and Matthes, *i.e.* (5) and (6) of [19], the method to get them is simpler here and does not require an expansion of the second order moments (1.4) of the Wigner function.

3.2 The zero-temperature limit

An opposite limit to the semiclassical asymptotics is the zero-temperature limit. Before investigating the formal limit of (2.41)–(2.44) as $T \to 0$, let us claim that, when B is a gradient, the functions A and B can always be explicitly deduced from the ground state of the modified Hamiltonian. Indeed, straightforward (formal) calculations lead to the following lemma:

Lemma 3.4 *Let A and B be given real functions, respectively scalar and vector valued, and assume the existence of a scalar potential $\varphi(x)$ such that $B = \nabla\varphi$. Consider the operator*

$$H(A,B) = \frac{1}{2}(i\hbar\nabla + B)^2 + A$$

and assume that the problem of minimization of the energy

$$\min_{|\psi|_{L^2}=1} \int (H(A,B)\psi)\,\overline{\psi}\,dx = \min_{|\psi|_{L^2}=1} \int \left(\frac{1}{2}\,|i\hbar\nabla\psi + B\psi|^2 + A\,|\psi|^2\right) dx$$

is attained on the ground state $\psi_0 = \sqrt{n_0}\,e^{iS_0/\hbar}$. Then we have the identities

$$A = \frac{\hbar^2}{2}\,\frac{\Delta\sqrt{n_0}}{\sqrt{n_0}} - C, \qquad B = \nabla S_0\,, \tag{3.70}$$

where C is a constant (the Lagrange multiplier corresponding to the constraint).

Proof. We remark that the energy of a wavefunction $\psi = \sqrt{n}\,e^{iS/\hbar}$ can be rewritten in terms of n and S:

$$\int \left(\frac{1}{2}\,|i\hbar\nabla\psi + B\psi|^2 + A\,|\psi|^2\right) dx = \int \left(\frac{1}{2}\,n\,|\nabla(S-\varphi)|^2 + \frac{\hbar^2}{2}|\nabla\sqrt{n}|^2 + A\,n\right) dx.$$

By writing that $(n_0,\ S_0)$ minimizes this expression and that $\sqrt{n_0}$ solves the corresponding Euler-Lagrange equation, we get

$$A = \frac{\hbar^2}{2}\,\frac{\Delta\sqrt{n_0}}{\sqrt{n_0}} - C, \qquad \nabla(S_0 - \varphi) = 0$$

where C is the Lagrange multiplier corresponding to the equality constraint ($|\psi|_{L^2} = 1$) and the proof is complete. Note that, since ψ_0 is a ground state, by Krein-Rutman's theorem we have $n_0 > 0$ everywhere, hence we do not have to introduce a Lagrange multiplier for the positivity constraint. □

We can now claim the following formal result:

Theorem 3.5 (Zero temperature formal limit) *Assume that the entropy function s is such that $\lim_{+\infty}(s')^{-1} = +\infty$ and $\lim_{-\infty}(s')^{-1} = 0$. Assume that the solution $(n^T, n^T u^T, A^T, B^T)$ of the quantum Euler system (2.41)–(2.44) with temperature T, admits a non trivial limit (n, nu, A, B) as the dimensionless temperature T goes to zero. Then these functions satisfy the Madelung equations:*

$$\partial_t n + \nabla \cdot nu = 0, \tag{3.71}$$

$$\partial_t u + (u \cdot \nabla)u + \nabla V - \frac{\hbar^2}{2} \nabla \left(\frac{\Delta \sqrt{n}}{\sqrt{n}} \right) = 0, \tag{3.72}$$

$$A = \frac{\hbar^2}{2} \frac{\Delta \sqrt{n}}{\sqrt{n}} - C, \qquad B = u\,, \tag{3.73}$$

where C is a constant and the system is described by a pure-state:

$$\underline{\varrho}(x, x') = \psi(x)\, \overline{\psi(x')}, \tag{3.74}$$

with

$$\psi = \sqrt{n}\, e^{iS/\hbar} \quad \text{and} \quad \nabla S = u.$$

Proof. By assumption, if A^T and B^T admit a smooth limit, the modified Hamiltonian defined by (2.44) does not behave singularly and its eigenvalues $(\lambda_p^T)_{p\in\mathbb{N}}$ and eigenfunctions $(\psi_p^T)_{p\in\mathbb{N}}$ also converge to some limits as $T \to 0$. The limit ground state ψ_0 is not degenerate. Therefore, it follows from the assumption on s and from (2.43) that λ_0^T must converge to 0, otherwise n would be either infinite, or zero (note that the limit density n is assumed to be non trivial). Due to the gap between the first eigenvalue λ_0 and the other ones λ_p, $p > 0$ (this gap is supposed to be a consequence of the fact that A^T and B^T admit a smooth limit, as well as the non degeneracy of the ground state – this is a strong assumption), we have $-\lambda_p/T \to -\infty$ and one can deduce from (2.43) that the occupation factor of the state ψ_p converges to 0 if $p > 0$. Consequently, the limit density operator is that of a pure-state, given by (3.74). Remark that one must have the following asymptotic behavior for the ground state energy λ_0^T:

$$\lambda_0^T \sim -T s' \left(\int n\, dx \right) \quad \text{as } T \to 0.$$

Since at the limit the dynamic is given by the ground state, the corresponding velocity is a gradient: $u = \nabla S$, thus by Lemma 2.7, we have $B = \nabla S$. Next, by applying Lemma 3.4 we obtain (3.73). Finally, by inserting these relations into (2.50), we obtain the Madelung equation (3.72). □

Remark 3.6 *The Boltzmann distribution $(s')^{-1} = \exp$ corresponding to the entropy $s(\varrho) = \varrho \ln(\varrho) - \varrho$ satisfies the assumption of Theorem 3.5. But the Fermi-Dirac distribution does not. In this case, since the occupation factors converge to 1 as $-\lambda_p/T$ tends to $-\infty$, one can see that the limit density operator may not be a pure-state but rather a finite rank projector*

$$\underline{\varrho}(x, x') = \sum_{k=1}^{K} \psi_k(x)\, \overline{\psi_k(x')},$$

which unfortunately does not enable us to obtain the simplified constitutive equations (3.73).

3.3 System with relaxation, long-time behavior, diffusive limit

In this section, we come back to the derivation of the quantum Euler system and modify the microscopic description. We rewrite the quantum Liouville equation (2.32), assuming now that the collision operator is composed of two parts, in order to take into account the coexistence of different types of collisions:

$$\partial_t \varrho = -\frac{i}{\hbar}[\mathcal{H}, \varrho] + \frac{1}{\varepsilon_1}\mathcal{Q}_{hi}(\varrho) + \frac{1}{\varepsilon_2}\mathcal{Q}_{di}(\varrho). \tag{3.75}$$

The mean collision times ε_1 and ε_2 are both assumed to be small, but such that $\varepsilon_1 \ll \varepsilon_2$, which means there is a hierarchy between the collision phenomena. The predominant collision operator $\mathcal{Q}_{hi}$ is supposed to be similar to the one in section 2.3, satisfying the same two assumptions (i) and (ii), whereas the new operator $\mathcal{Q}_{di}$ models collisions which do not preserve momentum. To make the analysis simpler, we choose for $\mathcal{Q}_{di}$ the quantum BGK operator that was introduced in [9]. It reads

$$\mathcal{Q}_{di}(\varrho) = \varrho^{eq}_{n,0} - \varrho\,,$$

since one can see (e.g. in the proof of Lemma 2.7 in the Appendix A) that the equilibrium function with vanishing current $\varrho^{eq}_{n,0}$ realizes the following minimization problem with mass density constraint:

$$\min\left\{G(\varrho) \text{ such that } \quad \forall \phi \quad \mathrm{Tr}\ (\varrho\phi) = \int n\phi\ dx\right\}. \tag{3.76}$$

In [9], the diffusive limit of (3.75) without the $\mathcal{Q}_{hi}$ operator was performed and lead to a model called the entropic quantum drift-diffusion (QDD) system (the study of this model was continued in [8, 11, 7]). In this section, we follow a different route, that will finally lead to the same model. We perform formally successively two limits. First, in the first Theorem 3.8 of this section, we make ε_1 tend to 0 in (3.75), which corresponds to the *hydrodynamic* asymptotics. The so-obtained model is the quantum Euler system with a relaxation term induced by the new collision operator $\mathcal{Q}_{di}$. We show that this model is entropic and that its equilibria are the usual *global* quantum equilibria. Then, we let ε_2 tend to 0, which corresponds to the *diffusive* asymptotics. During this step performed in Theorem 3.9, we recover the QDD model. In order to prepare this second step, it is now more convenient to rescale the time variable in (3.75), setting $t = t'/\varepsilon_2$ (and then dropping the prime):

$$\varepsilon_2\partial_t \varrho = -\frac{i}{\hbar}[\mathcal{H}, \varrho] + \frac{1}{\varepsilon_1}\mathcal{Q}_{hi}(\varrho) + \frac{1}{\varepsilon_2}\mathcal{Q}_{di}(\varrho). \tag{3.77}$$

Before giving the main result of this section (Theorem 3.8), let us give a lemma which will be needed in the proof:

Lemma 3.7 *Let n, nu, A, B be given according to Definition 2.1. Then we have*

$$\int nu \cdot B\, dx \geq 0, \tag{3.78}$$

and this integral vanishes if and only if $u = B = 0$.

Proof. See Appendix C. □

Theorem 3.8 (Hydrodynamic formal limit) *Consider a solution of the quantum Liouville equation (3.77), denoted by $\varrho^{\varepsilon_1,\varepsilon_2}$. As ε_1 goes to 0, this density operator converges formally to the solution*

$$\varrho^{\varepsilon_2} = (s')^{-1}\left(-\frac{1}{T}H(A,B)\right)$$

of the following quantum Euler system with relaxation:

$$\varepsilon_2\partial_t n + \nabla\cdot nu = 0, \tag{3.79}$$

$$\varepsilon_2\partial_t(nu) + \nabla\cdot(nu\otimes B) + n(\nabla B)\cdot(u-B) + n\nabla(V-A) = -\frac{1}{\varepsilon_2}nu, \tag{3.80}$$

$$n = \sum_{p\in\mathbb{N}}(s')^{-1}\left(-\frac{\lambda_p}{T}\right)|\psi_p|^2, \qquad nu = \sum_{p\in\mathbb{N}}(s')^{-1}\left(-\frac{\lambda_p}{T}\right)\mathcal{I}m\left(\hbar\nabla\psi_p\,\overline{\psi_p}\right), \tag{3.81}$$

where $(\lambda_p,\psi_p)_{p\in\mathbb{N}}$ denotes the complete set of eigenvalues and normalized eigenvectors of the modified Hamiltonian defined by

$$H(A,B) = \frac{1}{2}\left(i\hbar\nabla + B\right)^2 + A. \tag{3.82}$$

Assume now that the potential V is independent of time. Then the above model is entropic, i.e. dissipates the quantum free energy defined by (2.15):

$$\frac{d}{dt}G(\varrho^{\varepsilon_2}(t)) = -\frac{1}{\varepsilon_2^2}\int nu\cdot B\,dx \le 0. \tag{3.83}$$

This suggests that its solution ϱ^{ε_2} converges at $t\to+\infty$ to the global quantum equilibria

$$\varrho_\infty = (s')^{-1}\left(-\frac{1}{T}\left(-\frac{\hbar^2}{2}\Delta + V - \mu_F\right)\right),$$

where the Fermi level μ_F is a constant.

Proof. The first part of this theorem is mainly an adaptation of the proof of Theorem 2.5. Indeed, by multiplying (3.77) by ε_1 and using $\varepsilon_1 \ll \varepsilon_2$, we obtain formally that

$$\mathcal{Q}_{hi}(\varrho^{\varepsilon_1,\varepsilon_2}) \to 0 \quad \text{as } \varepsilon_1 \to 0.$$

Hence, if $\varrho^{\varepsilon_1,\varepsilon_2}$ converges to a certain ϱ^{ε_2}, then we have $\mathcal{Q}_{hi}(\varrho^{\varepsilon_2}) = 0$, and the assumption (2.34) made on $\mathcal{Q}_{hi}$ implies the existence of A and B such that

$$\varrho^{\varepsilon_2} = (s')^{-1}\left(-\frac{1}{T}\left((i\hbar\nabla + B)^2 + A\right)\right),$$

or, in other terms, that $\varrho^{\varepsilon_2} = \varrho^{eq}_{n,nu}$. To conclude, it remains to write the equations satisfied by the two first moments of $\varrho^{\varepsilon_1,\varepsilon_2}$ and to close this system thanks to this expression. The same calculations as for Theorem 2.5 lead to (3.79) and (3.80), taking care of the right-hand sides, which are obtained from $\mathcal{Q}_{di}$ by remarking that

$$\forall\phi \quad \mathrm{Tr}\ (\mathcal{Q}_{di}(\varrho)\phi) = \mathrm{Tr}\ \left((\varrho^{eq}_{n,0} - \varrho)\phi\right) = 0,$$

$$\forall \Phi \quad -i\hbar \mathrm{Tr}\left(\mathcal{Q}_{di}(\varrho)\left(\Phi\cdot\nabla+\tfrac{1}{2}(\nabla\cdot\Phi)\right)\right) = -i\hbar \mathrm{Tr}\left(\left(\varrho_{n,0}^{eq}-\varrho\right)\left(\Phi\cdot\nabla+\tfrac{1}{2}(\nabla\cdot\Phi)\right)\right)$$
$$= -\int nu\cdot\Phi\,dx,$$

thanks to the definition of $\varrho_{n,0}^{eq}$ and by (2.6).

Moreover, by adapting the proof of (2.46) in Theorem 2.5, one gets easily the equation (3.83) for the evolution of the free energy. Note that the nonpositivity of this term is not trivial and comes from the inequality (3.78) of Lemma 3.7. Finally, by simply considering (3.83), we claim that, as $t\to+\infty$, the relaxation term created by $\mathcal{Q}_{di}$ drives the system to equilibria such that $\int nu\cdot B\,dx=0$. Hence, by the second part of Lemma 3.7, these equilibria must be such that $nu=0$. Then, from (3.80), we get $n\nabla(V-A)=0$ and $A=V-\mu_F$. □

Theorem 3.9 (Diffusive formal limit) *Consider a solution ϱ^{ε_2} of the quantum Euler model with relaxation (3.79)–(3.82). Then, as ε_2 goes to zero, ϱ^{ε_2} converges formally to the solution*

$$\varrho = (s')^{-1}\left(-\frac{1}{T}H(A,0)\right) \tag{3.84}$$

of the quantum drift-diffusion system:

$$\partial_t n + \nabla\cdot(n\nabla(A-V)) = 0, \tag{3.85}$$

$$n = \sum_{p\in\mathbb{N}} (s')^{-1}\left(-\frac{\lambda_p}{T}\right)|\psi_p|^2, \tag{3.86}$$

where $(\lambda_p,\psi_p)_{p\in\mathbb{N}}$ denotes the complete set of eigenvalues and normalized eigenvectors of the modified Hamiltonian defined by

$$H(A,0) = -\frac{\hbar^2}{2}\Delta + A. \tag{3.87}$$

Proof. Multiplying (3.80) by ε_2, one can see that $nu=\mathcal{O}(\varepsilon_2)$. Hence, from Lemma 2.7, and assuming that the relation between $(n,\,nu)$ and $(A,\,B)$ is smooth, we infer $B=\mathcal{O}(\varepsilon_2)$. As a first consequence, we obtain that ϱ^{ε_2} converges to a certain ϱ given by (3.84). Secondly, by using again (3.80) and identifying the terms of order zero in ε_2, we get

$$-\frac{1}{\varepsilon_2}nu = n\nabla(V-A)+\mathcal{O}(\varepsilon_2). \tag{3.88}$$

By inserting this identity into (3.79) and passing to the limit $\varepsilon_2\to 0$, we deduce (3.85). □

Remark 3.10 *The QDD model, obtained as the limit of an entropic model, is also entropic. Let us give the expression of the corresponding entropy flux. At the diffusive limit $\varepsilon_2\to 0$, (3.88) shows that u/ε_2 converges to the gradient function $-\nabla(V-A)$, so Lemma 2.7 gives that, asymptotically, we have $B=u$. Therefore, one deduces from (3.83) that the solution of the QDD system (3.85)–(3.87) satisfies*

$$\frac{d}{dt}G(\varrho(t)) = -\int n|\nabla(V-A)|^2\,dx \le 0.$$

We recover here an identity that was shown in [9] and, again, the fact that the equilibria are such that $V-A$ is constant.

4 Numerical results

We have implemented a 1D numerical scheme for solving the quantum Euler system with relaxation coupled to the Poisson equation on the domain $\Omega = [0,1]$ in the case where the entropy s is the Boltzmann entropy. As noticed in Remark 2.9, the quantum Euler system in one dimension takes the reduced form (2.61)–(2.64). Let $\Delta t > 0$ be the time step and $\Delta x = 1/N (N \in \mathbb{N})$ the space grid size. The grid is composed of the points $x_i = i\Delta x$ for $0 \leq i \leq N+1$ and we note the unknowns at time $t = k\Delta t$ as vectors $n^k = (n_i^k)_{0\leq i\leq N+1}$, $u^k = (u_i^k)_{0\leq i\leq N+1}$, $A^k = (A_i^k)_{0\leq k\leq N+1}$, $V^{s,k} = (V_i^{s,k})_{0\leq i\leq N+1}$. For the sake of readability, we also introduce as intermediate unknowns the density and velocity fluxes noted $j^{k+1/2} = (j_i^{k+1/2})_{0\leq i\leq N+1}$ and $\varphi^{k+1/2} = (\varphi_i^{k+1/2})_{0\leq i\leq N+1}$. The discretized model reads for $1 \leq i \leq N$:

$$\varepsilon_2 \frac{n_i^{k+1} - n_i^k}{\Delta t} + \frac{j_i^{k+1/2} - j_{i-1}^{k+1/2}}{\Delta x} = 0, \tag{4.89}$$

$$\varepsilon_2 \frac{u_i^{k+1} - u_i^k}{\Delta t} + \frac{\varphi_{i+1}^{k+1/2} - \varphi_i^{k+1/2}}{\Delta x} = -\frac{u_i^{k+1}}{\varepsilon_2}, \tag{4.90}$$

$$j_i^{k+1/2} = n_i^k u_i^{k+1} \tag{4.91}$$

$$\varphi_i^{k+1/2} = \frac{\left(u_i^k\right)^2}{2} + V_i^{ext} + V_i^{s,k+1} - A_i^{k+1} \tag{4.92}$$

$$-\alpha^2 \frac{V_{i+1}^{s,k+1} - 2V_i^{s,k+1} + V_{i-1}^{s,k+1}}{\Delta x^2} = n_i^{k+1} \tag{4.93}$$

$$n_i^{k+1} = \sum_{1\leq p\leq N} e^{-\frac{\lambda_p(A^{k+1})}{T}} |\psi_{p,i}(A^{k+1})|^2, \tag{4.94}$$

where $(\lambda_p(A^{k+1}), \psi_p(A^{k+1}))_{1\leq p\leq N}$ denotes the eigenvalues and normalized eigenvectors of the $N \times N$ matrix discretizing the modified Hamiltonian (we put Dirichlet conditions on the eigenfunctions):

$$H(A^{k+1}, 0) = -\frac{\hbar^2}{2\Delta x^2} \begin{pmatrix} -2 & 1 & 0 & \dots \\ 1 & \ddots & \ddots & 0 \\ 0 & \ddots & \ddots & 1 \\ \vdots & 0 & 1 & -2 \end{pmatrix} + \mathrm{Diag}\left((A_i^{k+1})_{1\leq i\leq N}\right).$$

We use for boundary conditions a zero-flux condition which reads:

$$\varphi_{N+1}^{k+1/2} = \varphi_N^{k+1/2} \quad ; \quad \varphi_0^{k+1/2} = \varphi_1^{k+1/2}.$$

This scheme draws its inspiration from the ones used for the entropic Quantum Drift-Diffusion model in [11, 7]. In order to solve this scheme, we first eliminate u_i^{k+1}, $j_i^{k+1/2}$ and $\varphi_i^{k+1/2}$ in equation (4.89) using equations (4.90), (4.91) and (4.92). Then we write n_i^{k+1} as a function of A^{k+1} in (4.89) using equation (4.94). We obtain a non linear (and not local) system with unknowns A_i^{k+1} and $V_i^{s,k+1}$. It can be shown that this system has a good variational formulation (inspired by Remark 2.2) and can be solved using the Newton algorithm. A future article will be devoted to the study of this scheme. A validation of the model is also needed and comparisons will

be performed with other existing models stated above (the quantum hydrodynamics model, the Schrödinger model and the entropic quantum drift-diffusion model).

The values of the parameters are given in Table IV.1. We choose for initial density $n^0(x)$ a density concentrated on the left of the device and for initial velocity $u^0(x) = 0$. The external potential V^{ext} is chosen to be a double barrier (in fact, the device here is a simplified Resonant Tunneling Diode without doping) and Figures IV.2, IV.3 show the evolution of the electron density n^k on the left, and the velocity u^k on the right for $k = 1, 4, 20, 100$ and 200. We can see electrons going through the barriers by tunneling effect. At time step $k = 200$ the system seems to achieve an equilibrium. This is confirmed by next Figure IV.1 which shows that the free energy $G(k) = \int \left(n^k \left(V^{ext} - A^k + (\frac{u^2}{2})^k \right) \right) dx + \frac{\alpha^2}{2} \int |\nabla V^{s,k}|^2 \, dx$ no longer evolves. We can see on this last graph that, as expected, the free energy is a decreasing function of time.

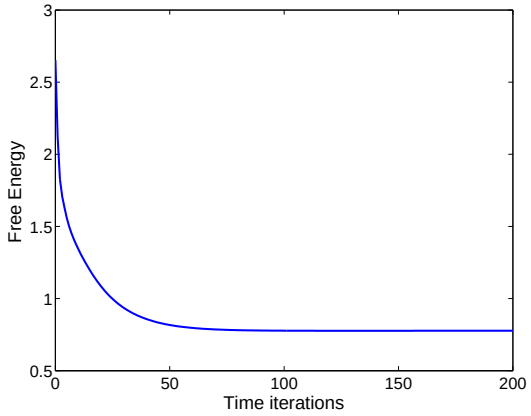

Figure IV.1: Evolution of the free energy G^k as a function of the time iteration k.

Δx	Δt	$\hbar^2/2T$	α^2	ε_2
0.01	0.005	0.02	0.1	0.1

Table IV.1: Values of the parameters for the numerical simulation.

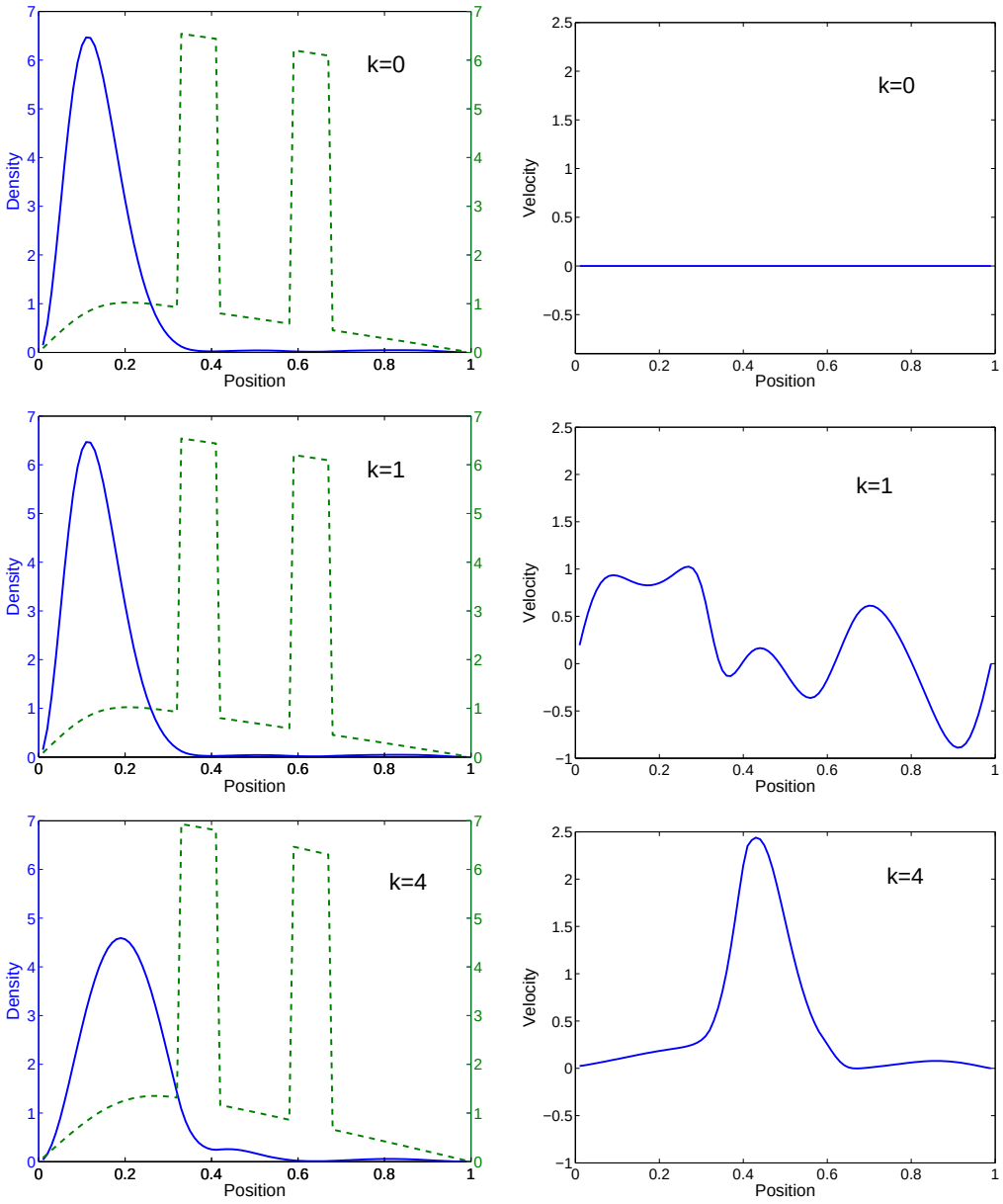

Figure IV.2: Numerical solution of the quantum Euler model with relaxation: $k = 0$ corresponds to the initial data while $k = 1$ and $k = 4$ correspond to the solution of the scheme after 1 and 4 iterations. Left: density $n^k(x)$ (solid line) and total electrical potential $(V^{s,k} + V^{ext})(x)$ (dashed line) as functions of the position x. Right: velocity $u^k(x)$ as function of the position x.

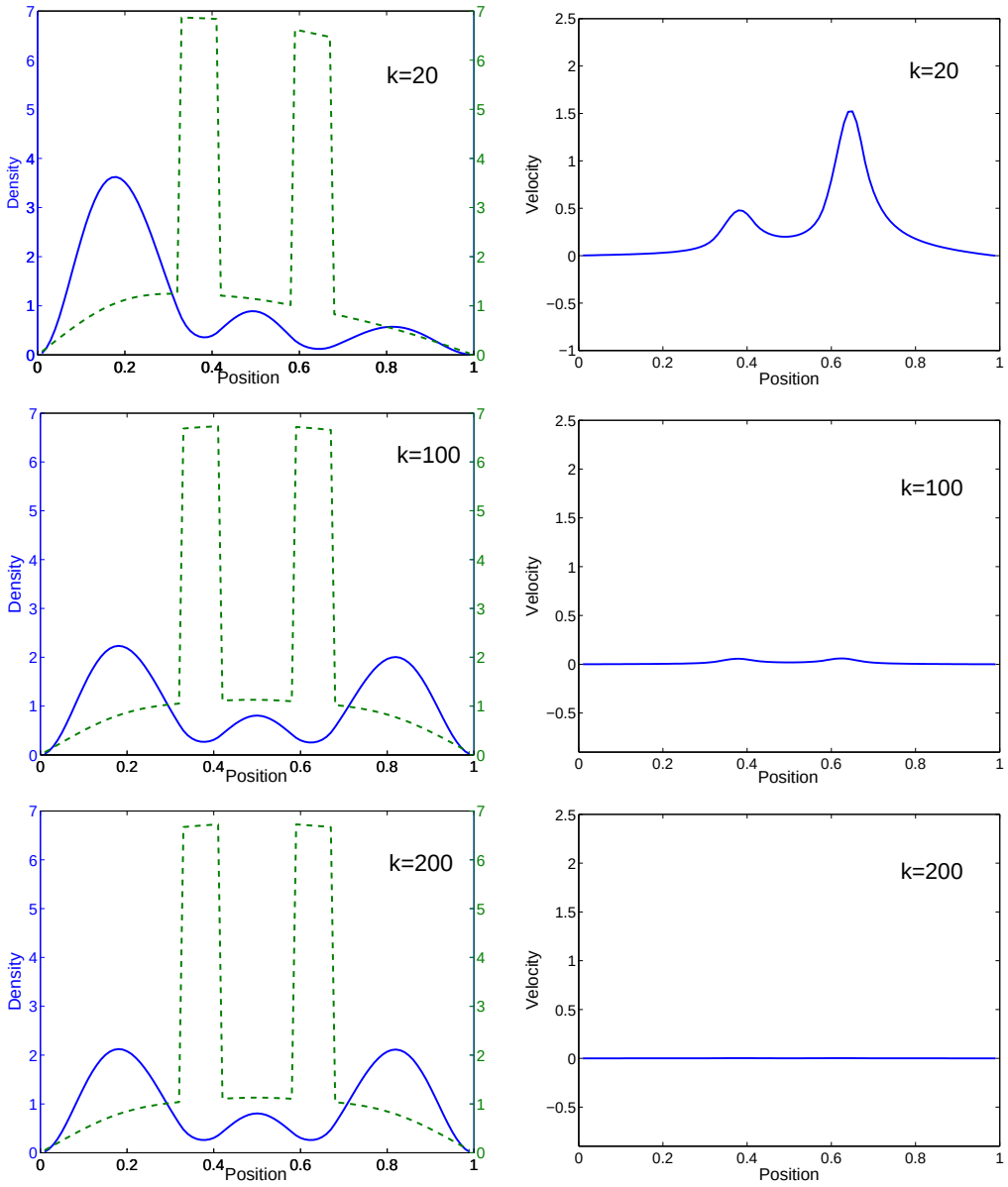

Figure IV.3: Numerical solution of the quantum Euler model with relaxation after 20, 100 and 200 iterations. Left: density $n^k(x)$ (solid line) and total electrical potential $(V^{s,k} + V^{ext})(x)$ (dashed line) as functions of the position x. Right: velocity $u^k(x)$ as function of the position x.

5 Conclusion and perspectives

In this chapter, we have rewritten in a simpler and differential way the isothermal version of the quantum hydrodynamic model derived in [10]. A remarkable gauge invariance property for this system has been exhibited. As a by-product, a constraint between the velocity u and its adjoint variable B has been discovered. Several equivalent formulations of the model are possible. We have then written some formal asymptotics of the model as dimensionless parameters tend to zero. It appears formally that the semiclassical limit of the model is the Classical isothermal Euler system while the zero temperature limit of the model gives the Madelung equations, finally, the diffusive limit permits to show a link with the recently derived entropic Quantum Drift-Diffusion model. We have also written several simplifications of the model when the velocity is irrotational, since in this case, $u = B$ and the problem depends on A only, which reduces the size of the moment reconstruction problem (i.e. the inversion of the mapping $A \to n$). This simplification allows to perform one-dimensional numerical simulations on a simple device. These preliminary numerical simulations seem to indicate that the model gives meaningful results in realistic situations. The study of the numerical scheme together with comparisons with other models will be presented in a future article. An analytical computation of the closure relations in the case of the full QHD model (as done for the isothermal case) is certainly at reach but needs further investigations.

Appendix

In these appendices, we write the proofs of several useful lemmas giving relations between the pairs (n, nu) and (A, B), as soon as they are linked according to Definition 2.1.

A Proof of Lemma 2.7

Consider the following minimization problem with the only constraint of first moment:

$$\min \{G(\varrho) \text{ such that } \varrho \text{ is a density operator satisfying (2.5)}\}. \tag{A.95}$$

Following [9] and with assumptions similar to the ones done in subsection 2.2, this minimization problem (A.95) is attained on a density operator which reads

$$\varrho_0 = (s')^{-1}\left(-\frac{1}{T}H(\alpha, 0)\right),$$

where α is a scalar function and $H(\alpha, 0)$ is still defined according to (2.18). Due to the fact that the Wigner function of ϱ_0 is even (see [9]), this density operator carries no current, *i.e.* for any test function Φ we have

$$-i\hbar \mathrm{Tr}\left(\varrho_0\left(\Phi\cdot\nabla + \frac{1}{2}\nabla\cdot\Phi\right)\right) = 0. \tag{A.96}$$

This is enough to conclude that $\varrho_0 = \varrho^{eq}_{n,0}$ (following Definition 2.1) or, equivalently, that (following the definitions (2.19), (2.20))

$$n(\alpha, 0) = n, \qquad (nu)(\alpha, 0) = 0.$$

Denote now

$$\varrho_S = (s')^{-1}\left(-\frac{1}{T}H(\alpha, \nabla S)\right).$$

Applying the Gauge invariance of Lemma 2.3, we have:

$$H(\alpha, \nabla S) = e^{iS/\hbar}\, H(\alpha, 0)\, e^{-iS/\hbar},$$

it is immediate to deduce from elementary functional calculus that

$$\varrho_S = e^{iS/\hbar}\, \varrho_0\, e^{-iS/\hbar}.$$

Note then that, by definition, the mass density and the current density corresponding to ϱ_S are respectively $n(\alpha, \nabla S)$ and $(nu)(\alpha, \nabla S)$ and, as a direct consequence of (2.26), we have

$$n(\alpha, \nabla S) = n(\alpha, 0) = n, \qquad (nu)(\alpha, \nabla S) = (nu)(\alpha, 0) + n\nabla S = nu.$$

Therefore, according to the property of uniqueness of the Lagrange multipliers A and B assumed in subsection 2.2, we deduce that $A = \alpha$ and $B = \nabla S$ and the proof is complete.

Remark A.1 *Note that we can prove the last part of the lemma, $n(A,B) = n(A,0)$, by a direct computation of the derivative of $n = \sum_p (s')^{-1}(-\frac{\lambda_p}{T})\,|\psi_p|^2$, (where $(\lambda_p, \psi_p)_{p\in\mathbb{N}}$ are the eigenelements of the Hamiltonian $H(A,B)$). A perturbation calculus gives us:*

$$dn(A,B)\cdot(\delta A,\delta B) = \sum_{p,q} T\frac{(s')^{-1}(-\frac{\lambda_p}{T}) - (s')^{-1}(-\frac{\lambda_q}{T})}{\lambda_p-\lambda_q} Re\Big[\Big(\int -\frac{i\hbar}{2}\,\delta B\cdot\overline{\nabla\psi_q}\psi_p + \frac{i\hbar}{2}\,\delta B\cdot\nabla\psi_p\overline{\psi_q} + (\delta A + B\cdot\delta B)\psi_p\overline{\psi_q}\,dx\Big)\overline{\psi_p}\psi_q\Big], \quad \text{(A.97)}$$

where $T\frac{(s')^{-1}(-\frac{\lambda_p}{T})-(s')^{-1}(-\frac{\lambda_q}{T})}{\lambda_p-\lambda_q}$ conventionally equals $-((s')^{-1})'$ if $\lambda_p = \lambda_q$. Now, assume that $u = B = \nabla S$ and let us note $\tilde{\psi}_p = e^{-iS/\hbar}\psi_p$. It is straightforward to check that the sequence $(\tilde{\psi}_p)_{p\in\mathbb{N}}$ forms an orthogonal basis of real eigenfunctions of the Hamiltonian $H(A,0)$, so that we can write $\psi_p = e^{iS/\hbar}\tilde{\psi}_p$ with $\tilde{\psi}_p$ real. Then , substituting this last equality in (A.97) and using the fact that $B = \nabla S$, we get:

$$dn(A,B)\cdot(\delta A,\delta B) = \sum_{p,q} T\frac{(s')^{-1}(-\frac{\lambda_p}{T}) - (s')^{-1}(-\frac{\lambda_q}{T})}{\lambda_p-\lambda_q}\Big(\int \delta A\tilde{\psi}_p\tilde{\psi}_q\,dx\Big)\tilde{\psi}_p\tilde{\psi}_q, \quad \text{(A.98)}$$

and we see that the derivative of the density with respect to B is zero, so that $n(A,B) = n(A,0)$. Note that we use this property in order to solve our numerical scheme in 1D (see section 4). We use indeed the derivative of the density (A.98) in the Newton algorithm.

B Proof of Lemma 3.1

In order to perform expansions (3.66) and (3.67), we are going to use the Wigner formalism in which the density and the current density are given according to:

$$n = \int \mathcal{E}\mathrm{xp}\left(-\frac{1}{T}\left(\frac{1}{2}(p-B)^2 + A\right)\right)\frac{dp}{(2\pi\hbar)^3}, \quad \text{(B.99)}$$

$$nu = \int p\,\mathcal{E}\mathrm{xp}\left(-\frac{1}{T}\left(\frac{1}{2}(p-B)^2 + A\right)\right)\frac{dp}{(2\pi\hbar)^3}, \quad \text{(B.100)}$$

where $\mathcal{E}\mathrm{xp}$ is the quantum exponential $\mathcal{E}\mathrm{xp} = W\circ\exp\circ W^{-1}$ introduced in [9]. Using Proposition 5.3 of [9] which gives the $\hbar$ expansion of $\mathcal{E}\mathrm{xp}(a)$ for an arbitrary symbol a, we find for the symbol $-\frac{1}{T}\left(\frac{1}{2}(p-B)^2 + A\right)$ the following expansion:

$$\mathcal{E}\mathrm{xp}\left(-\frac{1}{T}\left(\frac{1}{2}(p-B)^2 + A\right)\right) = \exp\left(-\frac{1}{T}\left(\frac{1}{2}(p-B)^2 + A\right)\right)\Big[1 + \frac{\hbar^2}{8T^2}\Big(-\Delta A + \Delta B\cdot(p-B) + \partial_i B_j(\partial_j B_i - \partial_i B_j) + \frac{1}{3T}(\partial_{ij}A - \partial_{ij}B\cdot(p-B) + \partial_i B\cdot\partial_j B)(p_i - B_i)(p_j - B_j) + \frac{2}{3T}\partial_i B_j(p_i - B_i)(\partial_j A - \partial_j B\cdot(p-B)) + \frac{1}{3T}|\nabla A - \nabla B_j(p_j - B_j)|^2\Big)\Big] + \mathcal{O}(\hbar^4),$$

where ∂_i denotes the partial derivative $\partial/\partial x_i$ and where we used Einstein's summation convention. It remains to calculate the integrals (B.99) and (B.100). We use the fact that:

$$\begin{aligned}
\int e^{-p^2/(2T)} dp &= (2\pi T)^{3/2}, \\
\int e^{-p^2/(2T)} p_i dp &= 0, \\
\int e^{-p^2/(2T)} p_i p_j dp &= T(2\pi T)^{3/2}\delta_{ij}, \\
\int e^{-p^2/(2T)} p_i p_j p_k dp &= 0, \\
\int e^{-p^2/(2T)} p_i p_j p_k p_l dp &= T^2(2\pi T)^{3/2}(\delta_{ij}\delta_{kl} + \delta_{ik}\delta_{jl} + \delta_{il}\delta_{jk}),
\end{aligned}$$

and we notice that $\partial_i B_j(\partial_j B_i - \partial_i B_j) = -|\nabla \times B|^2$ to obtain the expansion of the density:

$$n = n_0 e^{-A/T}\left[1 + \frac{\hbar^2}{24T}\left(-2\Delta\left(\frac{A}{T}\right) + \left|\nabla\left(\frac{A}{T}\right)\right|^2 - \frac{1}{T}|\nabla \times B|^2\right)\right] + \mathcal{O}(\hbar^4). \tag{B.101}$$

In order to calculate the second integral (B.100), we write:

$$\begin{aligned}
nu &= \int (p - B)\,\mathcal{E}\mathrm{xp}\left(-\frac{1}{T}\left(\frac{1}{2}(p-B)^2 + A\right)\right) \\
&\qquad + B\,\mathcal{E}\mathrm{xp}\left(-\frac{1}{T}\left(\frac{1}{2}(p-B)^2 + A\right)\right)\frac{dp}{(2\pi\hbar)^3}, \\
&= \int (p - B)\,\mathcal{E}\mathrm{xp}\left(-\frac{1}{T}\left(\frac{1}{2}(p-B)^2 + A\right)\right)\frac{dp}{(2\pi\hbar)^3} + nB,
\end{aligned}$$

and computing this last integral for a component nu_k, we obtain:

$$nu_k = nB_k + \frac{\hbar^2}{12} n_0 e^{-A/T}\left(-\partial_i(\partial_k B_i - \partial_i B_k) - \partial_i\left(-\frac{A}{T}\right)(\partial_k B_i - \partial_i B_k)\right) + \mathcal{O}(\hbar^4).$$

Then, we use the fact that $n = n_0 e^{-A/T} + \mathcal{O}(\hbar^2)$ and that $A = T\ln n_0 - \ln n + \mathcal{O}(\hbar^2)$ to obtain

$$nu_k = nB_k - \frac{\hbar^2}{12}\partial_i\left(n(\partial_k B_i - \partial_i B_k)\right) + \mathcal{O}(\hbar^4)$$

which is nothing else but the component value of the expansion:

$$nu = nB - \frac{\hbar^2}{12}\nabla \times (n\nabla \times B) + \mathcal{O}(\hbar^4). \tag{B.102}$$

The desired expressions of the expansions of A and B are a direct consequence of (B.101) and (B.102) noticing that

$$-2\Delta\left(\frac{A}{T}\right) + \left|\nabla\left(\frac{A}{T}\right)\right|^2 = 4\frac{\Delta\sqrt{n}}{\sqrt{n}} + \mathcal{O}(\hbar^2).$$

C Proof of Lemma 3.7

The starting point is the following fact remarked in the above proof of Lemma 2.7 (Appendix A). The density operator $\varrho_{n,0}^{eq}$ realizes the minimum of the problem (A.95), *i.e.* we have

$$G\left(\varrho_{n,nu}^{eq}\right) - G\left(\varrho_{n,0}^{eq}\right) \geq 0,$$

where we recall that the free energy was defined in (2.15). Since G is a convex differentiable function of ϱ, we deduce that

$$dG(\varrho_{n,nu}^{eq}) \cdot \left(\varrho_{n,nu}^{eq} - \varrho_{n,0}^{eq}\right) \geq G\left(\varrho_{n,nu}^{eq}\right) - G\left(\varrho_{n,0}^{eq}\right) \geq 0.$$

Now, by using the expression (2.47) of the derivative of G with respect to ϱ and recalling that

$$\varrho_{n,nu}^{eq} = (s')^{-1}\left(-\frac{1}{T}H(A,B)\right),$$

we get

$$\mathrm{Tr}\,\left((-H(A,B)+\mathcal{H})\left(\varrho_{n,nu}^{eq} - \varrho_{n,0}^{eq}\right)\right) \geq 0,$$

i.e.

$$\mathrm{Tr}\,\left(\left(-ihB\cdot\nabla - \frac{i\hbar}{2}(\nabla\cdot B) + V - A - \frac{1}{2}B^2\right)\left(\varrho_{n,nu}^{eq} - \varrho_{n,0}^{eq}\right)\right) \geq 0.$$

Therefore, the desired result (3.78) stems directly from (2.5) and (2.6). From the strict convexity of s, it is clear that this integral vanishes only in the case $nu \equiv 0$.

References

[1] A. Arnold, J. L. Lopez, P. A. Markowich, and J. Soler, *An analysis of quantum Fokker-Planck models: A Wigner function approach*, Rev. Mat. Iberoamericana **20** (2004), 771–814.

[2] R. Balian, *From Microphysics to Macrophysics*, Volume 1, Springer, Berlin, 1991.

[3] I. Burghardt, K. B. Moller, L. S. Cederbaum and E. R. Bittner, *Quantum hydrodynamics: Mixed states, dissipation, and a new hybrid quantum-classical approach*, Int. J. Quant. Chem. **100** (2004), 1153–1162.

[4] L. L. Chang, L. Esaki and R. Tsu, *Resonant tunneling in semiconductor double barriers*, Appl. Phys. Lett. **24** (1974), 593–595.

[5] Z. Chen, B. Cockburn, C. Gardner and J. Jerome, *Quantum hydrodynamic simulation of hysteresis in the resonant tunneling diode*, J. Comput. Phys. **117** (1995), 274–280.

[6] S. Datta, *Nanoscale device modeling: The Green's function method, Superlattices and Microstructures* **28** (2000), 253–278.

[7] P. Degond, S. Gallego, F. Méhats, *An entropic Quantum Drift-Diffusion model for electron transport in resonant tunneling diodes*, J. Comput. Phys. **221** (2007), 226–249.

[8] P. Degond, F. Méhats, C. Ringhofer, *Quantum hydrodynamic models derived from the entropy principle*, Contemp. Math. **371** (2005), 107–331.

[9] P. Degond, F. Méhats, C. Ringhofer, *Quantum energy-transport and drift-diffusion models*, J. Stat. Phys. **118** (2005), no. 3-4, 625–665.

[10] P. Degond, C. Ringhofer, *Quantum Moment Hydrodynamics and the Entropy Principle*, J. Stat. Phys. **112** (2003), no. 3-4, 587–628.

[11] S. Gallego, F. Méhats, *Entropic discretization of a quantum drift-diffusion model*, SIAM J. Numer. Anal. **43** (2005), no. 5, 1828–1849.

[12] C. Gardner, *The quantum hydrodynamic model for semiconductor devices*, SIAM J. Appl. Math. **54** (1994), no. 2, 409–427.

[13] C. Gardner, C. Ringhofer, *The smooth quantum potential for the hydrodynamic model*, Phys. Rev. E **53** (1996), 157–167.

[14] C. Gardner, C. Ringhofer, *The Chapman-Enskog Expansion and the Quantum Hydrodynamic Model for Semiconductor Devices*, VLSI Design **10** (2000), 415–435.

[15] I. Gasser, A. Jüngel, *The quantum hydrodynamic model for semiconductors in thermal equilibrium*, Z. Angew. Math. Phys. **48** (1997), no. 1, 45–59.

[16] I. Gasser, P. A. Markowich, *Quantum Hydrodynamics, Wigner Transforms and the Classical Limit*, Asympt. Analysis **14** (1997), no. 2, 97–116.

[17] H. Grubin, J. Kreskovsky, *Quantum moment balance equations and resonant tunneling structures*, Solid State Electr. **32** (1989), 1071–1075.

[18] A. Jüngel, *Quasi-hydrodynamic semiconductor equations*, Progress in Nonlinear Differential Equations, Birkhäuser, 2001.

[19] A. Jüngel, D. Matthes, *A derivation of the isothermal quantum hydrodynamic equations using entropy minimization*, Z. Angew. Math. Mech. **85** (2005), 806–814.

[20] C. D. Levermore, *Moment closure hierarchies for kinetic theories*, J. Stat. Phys. **83** (1996), 1021–1065.

[21] E. Madelung, *Quantentheorie in hydrodynamischer Form*, Z. Physik **40** (1926), 322–326.

[22] F. Nier, *A stationary Schrödinger-Poisson system arising from the modeling of electronic devices*, Forum Math. **2** (1990), no. 5, 489–510.

[23] E. Polizzi, *Modélisation et simulations numériques du transport quantique balistique dans les nanostructures semi-conductrices*, Ph.D. thesis, INSA, Toulouse, 2001.

[24] E. Polizzi, N. Ben Abdallah, *Self-consistent three dimensional models for quantum ballistic transport in open systems*, Phys. Rev. B, **66** (2002), 245–301.

Chapter V

On Quantum Hydrodynamic and Quantum Energy Transport Models

This chapter has given an article written in collaboration with P. Degond and F. Méhats, and published in Comm. Math. Sci. **5** (2007), no 4, 887–908.

Abstract. In this chapter, we consider two recently derived models: the Quantum Hydrodynamic model (QHD) and the Quantum Energy Transport model (QET). We propose different equivalent formulations of these models and we use a commutator formula for stating new properties of the models. A gauge invariance lemma permits to simplify the QHD model for irrotational flows. We finish by considering the special case of a slowly varying temperature and we discuss possible approximations which will be helpful for future numerical discretizations.

Key words. Density operator, quantum Liouville equation, quantum entropy, quantum local equilibrium, Quantum Hydrodynamics, Quantum Energy Transport, commutators, gauge invariance.

1 Introduction

This chapter is the continuation of series of works investigating the properties and numerical approximations of quantum hydrodynamics and diffusion models based on the entropy principle. The growing interest of the scientific community towards quantum macroscopic models arises from the fact that they are computationally less expensive than microscopic models such as the Schrödinger or Wigner equation [3, 4, 9, 30, 32, 33]. Simultaneously, collisions can be modeled without the use of quantum collision operators which are difficult to handle. The modeling of both quantum effects and collisions is particularly important for semiconductor devices where the active zone is small (sometimes less than 100 nanometers) and quantum effects are dominant while the access zones are constituted of electron reservoirs in which collisions are predominant and drive the system towards thermodynamic equilibrium. An example of such a device is the resonant tunneling diode [7] which constitutes a good candidate for testing models since it can be approximated by a one dimensional device.

The route which has been usually followed for the derivation of quantum hydrodynamics and diffusion models consists in incorporating some "quantum" correction terms, often based on the Bohm potential, into classical fluid models. This Bohm potential appears naturally in the fluid formulation of the Schrödinger equation for a single particle evolving in an external potential V. One obtains this formulation through the use of the Madelung Transform, which consists in writing the wavefunction into an exponential form $\psi = \sqrt{n}e^{iS/\hbar}$, where n is the density of mass, S is the phase and $\hbar$ denotes the scaled Planck constant. Inserting this Ansatz into the Schrödinger equation, taking the real part and the gradient of the imaginary part, we recover the "Madelung equations" consisting in a pressureless Euler system involving an additional potential, called the Bohm potential $\frac{\hbar^2}{2}\Delta\sqrt{n}/n$. The first use of this Bohm potential in the semiconductor context dates back to [1, 2] in which the Bohm potential is added to the Drift-Diffusion equations and gives rise to the so-called Density-Gradient model. This model has been used and studied in many articles [6, 28, 31]. In a diffusive setting, we can also cite [8] in which the Bohm potential is added to the Energy Transport model. In an hydrodynamic setting, many models including quantum corrections have been derived and one can cite [19, 21, 22, 23, 24, 25, 26, 27].

New quantum hydrodynamic-like models have been constructed in [15] applying the moment method to the quantum framework. These macroscopic models differ from the previous ones by the fact that they are fully quantum and do not rely on a perturbative approach when the scaled Planck constant is small. The derivation method consists in integrating the quantum Liouville equation with respect to the momentum p against a given vector of polynomials of p. Following the approach that Levermore [29] developed in the classical case, the moment system is closed by a quantum local equilibrium defined as the solution of the minimization problem for the quantum entropy subject to the constraints that its moments are given. The quantum entropy being defined globally as the trace of an operator, the relation between the extensive variables (the chosen moments) and the thermodynamic intensive variables (the Lagrange multipliers of the constraints) is non-local. An interesting special case of quantum moment method is obtained by choosing the hydrodynamic moments $(1, p, |p|^2/2)$ as moment system. This leads to the Quantum Hydrodynamic (QHD) model describing the evolution of the mass density n, the current density nu and the energy density $\mathcal{W}$. More recently, Diffusion models have been derived in

[14], namely the Quantum Energy Transport (QET) and the Quantum Drift-Diffusion (QDD) model, through diffusion limits of a collisional Wigner equation. The BGK-like collision operator used in this derivation has been constructed in order to relax the Wigner distribution function towards a quantum local equilibrium. The QDD model has been further studied in [13] and a numerical scheme for solving it has been proposed in [18]. Numerical simulations of a resonant tunneling diode and comparisons with other existing models have been reported in [10]. These simulations showed that the QDD model can provide reliable simulations of diffusive transport in nanoscale devices. Then, even more recently, the isothermal version of the QHD model (called the isothermal Quantum Euler system) has been studied in [11]. Many interesting properties of this model such as gauge invariance have been proved, and preliminary numerical simulations have been shown. A review of all this work can be found in [12].

In this chapter, we consider non isothermal models, such as the QHD and QET models, and investigate some important properties of these models. These properties are important to take care of in numerical simulations. Previous works about numerical approximations of the QDD and Quantum Euler models [18, 10, 11] have been based on the simplification of the models by means of exact commutator relations. This strategy allowed to obtain partial differential equations describing the evolutions of the moments in terms of the moments themselves and their dual variables (*i.e.* the Lagrange multipliers of the constraints in the minimization problem). The quantum feature appears in the constitutive equations which give the link between the moments and their dual Lagrange multipliers. This constitutive relation supposes the diagonalization of a suitably defined Hamiltonian (see section 2). It appears that this becomes more complex when an energy equation is added, and such a simplification is not possible in general. The evolution equations on the moments involve quantities that cannot be written in terms of a simple differential form of the moments and of their dual variables. Therefore numerical discretization will require to write the unknown moments in terms of the spectrum of the above mentioned Hamiltonian. Nevertheless, we can derive some differential constraints that link the moments and their dual Lagrange multipliers. These constraints need to be correctly approximated in any reliable numerical discretization. These constraints can be obtained via a lemma about commutators of operators the symbols of which are of the form $\lambda(x)p^\alpha$, where α is a multi-index $\alpha = (\alpha_1, \alpha_2, \alpha_3)$, *i.e.* $\lambda(x)p^\alpha = \lambda(x)p_1^{\alpha_1}p_2^{\alpha_2}p_3^{\alpha_3}$. This commutator relation was not written before (to the knowledge of the authors) and possesses an intrinsic value for future developments in this field.

The chapter is organized as follows: In section 2, we recall briefly the derivation of the QHD and QET models that can be found with more details in [15, 13, 14]. In particular in subsection 2.1 we recall the notion of quantum entropy and quantum local equilibrium, before stating the models themselves in subsection 2.2 and 2.3.

In section 3, we give four preliminary technical lemmas, the most important ones being lemma 3.2 which allows us to write all the moments and their derivatives with respect to the discrete spectrum of the modified Hamiltonian, and lemma 3.4 which gives the above-mentioned commutator relation. Note that these lemmas are useful for any quantum moment system derived by the method given in [15].

Then, section 4 deals with the remarkable properties of the QHD model. Application of the preliminary technical lemmas first allows us to write all the quantities of the QHD model in terms of the spectrum of the modified Hamiltonian defined in section 2 (lemma 4.1). It also allows us to state the differential constraints that link the

moments and their dual Lagrange multipliers (theorem 4.2). Again, these constraints should properly be taken into account in any reliable discretization of the system. Then in subsection 4.2, we state a gauge invariance lemma (lemma 4.3) which leads to gauge transformations formulas (lemma 4.4) and finally to a major simplification of the QHD model for irrotational flows (theorem 4.5 and its corollary 4.6). From these simplifications emerges a dispersive velocity term which has been found in other QHD derivations and which is discussed in subsection 4.2.2. In subsection 4.2.3 we discuss the special case of the QHD model in one dimension. In subsection 4.3, we finally discuss some simplifications of the fluxes of the QHD model when the temperature is supposed to vary slowly.

Section 5 deals with the properties of the QET model. Like for the QHD model, application of preliminary technical lemmas first allows us to write the QET model in terms of the spectrum of the modified Hamiltonian defined in section 2 (lemma 5.1). Application of the commutator lemma (lemma 3.4) also allows us to derive the differential constraints between the moments and their Lagrange multipliers (theorem 5.2) that any future discretization should take into account. In subsection 5.2 possible simplifications for the fluxes of the QET model with slowly varying temperature are discussed.

Finally, in section 6 we finish by giving a conclusion and some possible perspectives. We wish to specify that the arguments presented in this article are formal. A precise mathematical framework in which this analysis could be made rigorous is still an open subject.

2 Context

This section is a summary of previous work dealing with the Quantum hydrodynamic model [15, 13] and the Quantum Energy Transport model [14]. This summary is given here to set up the context, the notations, and for the clarity of the presentation.

2.1 Quantum entropy and quantum local equilibrium

By a density operator, we shall always mean a positive, Hermitian, trace-class operator acting on $L^2(\mathbb{R}^3)$. Let us define the first moments of a density operator ϱ, *i.e.* the mass density n,the current density nu and the energy density $\mathcal{W}$ by duality, considering scalar test functions ϕ and vector ones Φ. We set

$$\forall \phi \in C_0^\infty(\mathbb{R}^3) \qquad \int n\phi \; dx = \mathrm{Tr}\,(\varrho\,\phi), \tag{2.1}$$

$$\begin{aligned} \forall \Psi \in C_0^\infty(\mathbb{R}^3)^3 \qquad \int nu \cdot \Psi \; dx &= \mathrm{Tr}\,\left(\varrho\, W^{-1}\,(\Psi \cdot p)\right) \\ &= -i\hbar \mathrm{Tr}\,\left(\varrho\left(\Psi\cdot\nabla + \frac{1}{2}(\nabla\cdot\Psi)\right)\right), \end{aligned} \tag{2.2}$$

$$\begin{aligned} \forall \phi \in C_0^\infty(\mathbb{R}^3) \qquad \int \mathcal{W}\phi \; dx &= \mathrm{Tr}\,\left(\varrho\, W^{-1}\left(\phi\frac{|p|^2}{2}\right)\right) \\ &= -\frac{\hbar^2}{2}\mathrm{Tr}\,\left(\varrho\left(\nabla\cdot(\phi\nabla) + \frac{1}{4}\Delta\phi\right)\right). \end{aligned} \tag{2.3}$$

In (2.2) and in (2.3), W^{-1} denotes the inverse Wigner transform (or Weyl quantization). For the sake of completeness, let us recall the definition of the Wigner transform and the inverse Wigner transform. The Wigner transform maps operators on $L^2(\mathbb{R}^3)$ to symbols, *i.e.* $L^2(\mathbb{R}^3 \times \mathbb{R}^3)$ functions of the classical position and momentum variables $(x, p) \in \mathbb{R}^3 \times \mathbb{R}^3$. More precisely, one defines the integral kernel of the operator ϱ to be the distribution $\underline{\varrho}(x, x')$ such that ϱ operates on any function $\psi(x) \in L^2(\mathbb{R}^3)$ as follows:

$$\varrho\psi(x) = \int \underline{\varrho}(x, x')\psi(x')dx'.$$

Then, the Wigner transform $W(\varrho)(x, p)$ is defined by:

$$W(\varrho)(x, p) = \int \underline{\varrho}\left(x - \frac{1}{2}\eta, x + \frac{1}{2}\eta\right) e^{\frac{i\eta\cdot p}{\hbar}} d\eta. \tag{2.4}$$

The Wigner transform can be inverted and its inverse is defined for any function $w(x, p)$ as the operator acting on $\psi(x) \in L^2(\mathbb{R}^3)$ as:

$$W^{-1}(w)\psi(x) = \int w\left(\frac{x+y}{2}, p\right) \psi(y) e^{\frac{ip\cdot(x-y)}{\hbar}} \frac{dp\, dy}{(2\pi\hbar)^3}. \tag{2.5}$$

The Wigner Transform W and its inverse W^{-1} are isometries between the space of Hilbert-Schmidt operators $\mathcal{L}^2$ (the space of operators such that the product $\varrho\varrho^\dagger$ is trace class, where $\varrho^\dagger$ is the Hermitian conjugate of ϱ) and the Hilbert space $L^2(\mathbb{R}^3 \times \mathbb{R}^3)$:

$$\mathrm{Tr}\ (\varrho\sigma^\dagger) = \int W(\varrho)(x, p)\overline{W(\sigma)(x, p)} \frac{dx\, dp}{(2\pi\hbar)^3}. \tag{2.6}$$

This property allows us to define the mass density, the momentum density and the energy density in the Wigner picture, where we denote $W(\varrho) = w$:

$$\begin{pmatrix} n \\ nu \\ \mathcal{W} \end{pmatrix} = \int w \begin{pmatrix} 1 \\ p \\ \frac{|p|^2}{2} \end{pmatrix} \frac{dp}{(2\pi\hbar)^3}. \tag{2.7}$$

Definition 2.1 *Let s be a strictly convex continuously differentiable function on $\mathbb{R}^+$. We define the quantum entropy by:*

$$S(\varrho) = \mathrm{Tr}\ (s(\varrho)). \tag{2.8}$$

Let the functions n, nu and $\mathcal{W}$ be given and consider the following constrained minimization problem:

$$\min\{S(\varrho) \text{ such that } \varrho \text{ is a density operator satisfying (2.1), (2.2) and (2.3)}\}. \tag{2.9}$$

The solution, if it exists, is called the local equilibrium density operator associated to n, nu and $\mathcal{W}$. Lagrange multiplier theory for the constrained problem (2.9) (see [15]) shows that there exist scalar functions $\tilde{A}$ and $\tilde{C}$, and a vector function $\tilde{B}$, all real valued and defined on $\mathbb{R}^3$, such that this local equilibrium density operator takes necessarily the form:

$$\varrho^{eq}_{n,nu,\mathcal{W}} = (s')^{-1}\left(\tilde{H}(\tilde{A}, \tilde{B}, \tilde{C})\right), \tag{2.10}$$

where $\tilde{H}(\tilde{A},\tilde{B},\tilde{C})$ *is the following modified Hamiltonian:*

$$\begin{aligned}\tilde{H}(\tilde{A},\tilde{B},\tilde{C}) &= W^{-1}\left(\tilde{A}+\tilde{B}\cdot p+\tilde{C}|p|^2\right)\\ &= \tilde{A}-i\hbar\left(\tilde{B}\cdot\nabla+\frac{1}{2}(\nabla\cdot\tilde{B})\right)-\hbar^2\left(\nabla\cdot(\tilde{C}\nabla)+\frac{1}{4}\Delta\tilde{C}\right). \quad (2.11)\end{aligned}$$

It is convenient to change the entropic variables $(\tilde{A},\tilde{B},\tilde{C})$ into more physical variables (A,B,C) in order to write the equilibrium density operator in the form:

$$\varrho^{eq}_{n,nu,\mathcal{W}} = (s')^{-1}\left(-H(A,B,C)\right), \quad (2.12)$$

where

$$\begin{aligned}H(A,B,C) &= W^{-1}\left(\frac{1}{2C}(p-B)^2+A\right)\\ &= -\hbar^2\left(\nabla\cdot(\frac{1}{2C}\nabla)+\frac{1}{4}\Delta\frac{1}{2C}\right)\\ &\quad +i\hbar\left(\frac{B}{C}\cdot\nabla+\frac{1}{2}(\nabla\cdot\frac{B}{C})\right)+A+\frac{B^2}{2C}. \quad (2.13)\end{aligned}$$

We will call the variables A, B and C respectively the generalized chemical potential, the generalized mean velocity and the generalized temperature.

The link between $(\tilde{A},\tilde{B},\tilde{C})$ and (A,B,C) is given by:

$$A=-\tilde{A}+\frac{\tilde{B}^2}{4\tilde{C}} \;\;;\;\; B=-\frac{\tilde{B}}{2\tilde{C}} \;\;;\;\; C=-\frac{1}{2\tilde{C}}, \quad (2.14)$$

or equivalently by:

$$\tilde{A}=-A-\frac{B^2}{2C} \;\;;\;\; \tilde{B}=\frac{B}{C} \;\;;\;\; \tilde{C}=-\frac{1}{2C}. \quad (2.15)$$

This definition is obviously incomplete if no assumption is made on n, nu and $\mathcal{W}$. In fact, this result has to be understood only at a formal level. Several crucial questions remain open: in which functional spaces n, nu and $\mathcal{W}$ have to be chosen, in which spaces A, B and C have to be sought, and the question of existence and uniqueness of A, B and C. Throughout this chapter, we shall postpone this delicate question of realizability of moments, assuming that, as soon as the minimization problem (2.9) has to be solved, n, nu and $\mathcal{W}$ are such that the associate functions A, B and C are uniquely defined. Note that even in the classical setting, the question of the realizability of moments for the constrained extremal problem is already a delicate question as pointed out in [17].

2.2 The Quantum Hydrodynamic model (QHD)

In order to derive the QHD model, we start from the collisional quantum Liouville equation:

$$i\hbar\partial_t\varrho=[\mathcal{H},\varrho]+i\hbar\frac{\mathcal{Q}(\varrho)}{\varepsilon}, \quad (2.16)$$

where $\mathcal{H}$ is the Hamiltonian:

$$\mathcal{H}=-\frac{\hbar^2}{2}\Delta+V, \quad (2.17)$$

and $\mathcal{Q}(\varrho)$ is an unspecified collision operator which describes the interaction of the particles with themselves and with their environment and accounts for dissipation mechanisms (ε is the scaled relaxation time). The key property that we request is that it drives the system to the local equilibria defined in the previous subsection. This is a consequence of the two following assumptions:

(i) mass, current and energy are conserved during collision, *i.e.* for any density operator ϱ we have

$$\forall \varphi, \Psi \qquad \mathrm{Tr}\left(\mathcal{Q}(\varrho) W^{-1} \begin{pmatrix} \varphi \\ \Psi \cdot p \\ \varphi \frac{|p|^2}{2} \end{pmatrix} \right) = 0, \tag{2.18}$$

(ii) the quantum entropy is dissipated, except for the density operator in the kernel of $\mathcal{Q}$, which is explicitly described as follows:

$$\mathcal{Q}(\varrho) = 0 \text{ iff } \exists (A,\, B,\, C) \text{ such that } \varrho = (s')^{-1}\left(-H(A,B,C)\right). \tag{2.19}$$

Taking the Wigner Transform of (2.16), we get the following collisional Wigner equation for $w = W(\varrho)$:

$$\partial_t w + p \cdot \nabla w - \Theta^\hbar(V) w = \frac{Q(w)}{\varepsilon}, \tag{2.20}$$

with

$$\Theta^\hbar(V) w = \frac{i}{(2\pi)^3 \hbar} \int \left(V(x + \frac{\hbar}{2}\eta) - V(x - \frac{\hbar}{2}\eta) \right) w(x,q) e^{i\eta\cdot(p-q)} dq\, d\eta, \tag{2.21}$$

and $Q(w)$ is the Wigner Transform of $\mathcal{Q}(\varrho)$.

The moment method consists in taking the moments of the Wigner equation *i.e.* multiplying it by $\begin{pmatrix} 1 \\ p \\ \frac{|p|^2}{2} \end{pmatrix}$ and integrating over p. Due to the conservation of mass, current and energy of the collision operator, and due to the properties of $\Theta^\hbar(V)$, we obtain the following system:

$$\partial_t n + \nabla \cdot nu = 0, \tag{2.22}$$
$$\partial_t (nu) + \nabla \cdot \Pi = -n \nabla V, \tag{2.23}$$
$$\partial_t \mathcal{W} + \nabla \cdot \Phi = -nu \cdot \nabla V, \tag{2.24}$$

with the pressure tensor Π and the energy flux Φ given by:

$$\Pi = \int w (p \otimes p) \frac{dp}{(2\pi\hbar)^3}, \tag{2.25}$$
$$\Phi = \int w \frac{|p|^2}{2} p \frac{dp}{(2\pi\hbar)^3}. \tag{2.26}$$

It is readily seen that, with no further assumption, Π and Φ cannot be expressed in terms of n, nu and $\mathcal{W}$, meaning this system is not closed. Hence, by analogy

with Levermore's methodology [29] and according to [15], we modify this system by replacing $w = W(\varrho)$ by the Ansatz

$$w^{eq}_{n,nu,\mathcal{W}} = W(\varrho^{eq}_{n,nu,\mathcal{W}}) = W\left((s')^{-1}\left(-H(A,B,C)\right)\right) \tag{2.27}$$

which plays the role of a Maxwellian here. This Ansatz corresponds to the modeling assumptions (i) and (ii) made on $\mathcal{Q}$, and represents the most likely quantum microscopic state which possesses the moments n, nu and $\mathcal{W}$, according to the statistics that has been chosen, *i.e.* the function s (this Ansatz can also be justified by the hydrodynamic limit obtained when the scaled relaxation time ε tends to 0). We obtain the QHD model which consists of the following mass, current and energy conservation equations (2.22)–(2.24) with:

$$\begin{pmatrix} n \\ nu \\ \mathcal{W} \end{pmatrix} = \int w^{eq}_{n,nu,\mathcal{W}} \begin{pmatrix} 1 \\ p \\ \frac{|p|^2}{2} \end{pmatrix} \frac{dp}{(2\pi\hbar)^3}, \tag{2.28}$$

and

$$\Pi = \int w^{eq}_{n,nu,\mathcal{W}} (p \otimes p) \frac{dp}{(2\pi\hbar)^3}, \tag{2.29}$$

$$\Phi = \int w^{eq}_{n,nu,\mathcal{W}} \frac{|p|^2}{2} p \frac{dp}{(2\pi\hbar)^3}. \tag{2.30}$$

2.3 The Quantum Energy Transport model (QET)

We notice that the derivation of the QHD model did not require any knowledge of the exact form of the collision operator. For deriving a diffusion model such as the QET model from a kinetic equation, the exact form of the collision operator matters and the coefficients of the diffusion model itself depend on this collision operator. The most simple choice is a relaxation operator also called BGK operator (for Bhatnagar, Gross, Krook [5]). The collision operator expresses the relaxation of the collision operator to the local thermodynamical equilibrium. We will choose:

$$\mathcal{Q}(\varrho) = \varrho^{eq}_{n,\mathcal{W}} - \varrho, \tag{2.31}$$

or in the Wigner picture:

$$Q(w) = w^{eq}_{n,\mathcal{W}} - w, \tag{2.32}$$

where we have

$$w^{eq}_{n,\mathcal{W}} = W\left(\varrho^{eq}_{n,\mathcal{W}}\right) = W\left((s')^{-1}(-H(A,0,C))\right) \tag{2.33}$$

and the functions A and C are such that the operator $\mathcal{Q}$ conserves the mass and energy, *i.e.* :

$$\int W((s')^{-1}(-H(A,0,C))) \begin{pmatrix} 1 \\ \frac{|p|^2}{2} \end{pmatrix} \frac{dp}{(2\pi\hbar)^3} = \begin{pmatrix} n \\ \mathcal{W} \end{pmatrix}. \tag{2.34}$$

We recall that the quantum equilibrium $\varrho^{eq}_{n,\mathcal{W}}$ is a solution of the entropy minimisation principle: for n and $\mathcal{W}$ given, to find

$$\min\{S(\varrho) \text{ such that } \varrho \text{ is a density operator satisfying (2.1) and (2.3)}\}. \tag{2.35}$$

Now we consider a diffusion scaling of the collisional Wigner equation:

$$\varepsilon^2\partial_t w^\varepsilon + \varepsilon(p\nabla w^\varepsilon - \Theta^\hbar(w^\varepsilon)) = Q(w^\varepsilon), \tag{2.36}$$

where the pseudo-differential operator $\Theta^\hbar(V)$ is defined by (2.21). This scaling is obtained through the change $t \to t/\varepsilon$ which means that we are looking at long time scales. The limit $\varepsilon \to 0$ of (2.36) is the QET model which consists of the following mass and energy conservation equations:

$$\begin{aligned} \partial_t n + \nabla \cdot j_n &= 0, &(2.37)\\ \partial_t \mathcal{W} + \nabla \cdot j_{\mathcal{W}} + \nabla V \cdot j_n &= 0, &(2.38) \end{aligned}$$

$$\begin{aligned} j_n &= -\nabla \cdot \Pi - n\nabla V, &(2.39)\\ j_{\mathcal{W}} &= -\nabla \cdot \mathbb{Q} - (\mathcal{W}\mathrm{Id} + \Pi)\cdot\nabla V + \frac{\hbar^2}{8} n\nabla(\Delta V), &(2.40) \end{aligned}$$

with:

$$\begin{pmatrix} n \\ \mathcal{W} \end{pmatrix} = \int w^{eq}_{n,\mathcal{W}} \begin{pmatrix} 1 \\ \frac{|p|^2}{2} \end{pmatrix} \frac{dp}{(2\pi\hbar)^3} \tag{2.41}$$

and

$$\begin{aligned} \Pi &= \int w^{eq}_{n,\mathcal{W}} (p\otimes p) \frac{dp}{(2\pi\hbar)^3}, &(2.42)\\ \mathbb{Q} &= \int w^{eq}_{n,\mathcal{W}} (p\otimes p) \frac{|p|^2}{2} \frac{dp}{(2\pi\hbar)^3}. &(2.43) \end{aligned}$$

3 Preliminary technical lemmas

In this section, we give preliminary technical lemmas which are going to be useful for deriving properties of the QHD and QET models. Note that these lemmas can also be useful for any quantum moment systems that can be derived applying the method explained in [15]. We start by giving a lemma that can be found in [15] (lemma 3.1), and whose proof is just an exercise in Fourier transform using definition 2.5:

Lemma 3.1 *Let $\alpha = (\alpha_1, \alpha_2, \alpha_3) \in \mathbb{N}^3$ be a multi-index (with $\mathbb{N}$ the set of natural integers) and denote by $p^\alpha = p_1^{\alpha_1} p_2^{\alpha_2} p_3^{\alpha_3}$ and $\partial_x^\alpha = \partial/\partial x_1^{\alpha_1}\partial/\partial x_2^{\alpha_2}\partial/\partial x_3^{\alpha_3}$. Then for any smooth real or complex valued function $\lambda(x)$, we have the following equivalent expression of the operator $W^{-1}(\lambda p^\alpha)$:*

$$W^{-1}(\lambda p^\alpha) = (-i\hbar)^{|\alpha|} \sum_{0\le\gamma\le\alpha} \begin{pmatrix} \alpha \\ \gamma \end{pmatrix} \frac{1}{2^{|\gamma|}} (\partial_x^\gamma \lambda)\, \partial_x^{\alpha-\gamma}, \tag{3.44}$$

where $|\alpha| = \alpha_1+\alpha_2+\alpha_3$, $\begin{pmatrix} \alpha \\ \gamma \end{pmatrix} = \begin{pmatrix} \alpha_1 \\ \gamma_1 \end{pmatrix}\begin{pmatrix} \alpha_2 \\ \gamma_2 \end{pmatrix}\begin{pmatrix} \alpha_3 \\ \gamma_3 \end{pmatrix}$ are the binomial coefficients and we denote $\sum_{0\le\gamma\le\alpha} = \sum_{\gamma_1=0}^{\alpha_1}\sum_{\gamma_2=0}^{\alpha_2}\sum_{\gamma_3=0}^{\alpha_3}$.

As a consequence, we give the following lemma which allows us to write the moments and the derivative of the moments associated to a quantum equilibrium $\varrho^{eq} = (s')^{-1}(-H)$, where s is a convex function and H an operator with a discrete spectrum (we use the same notations as in the previous lemma):

Lemma 3.2 *Let $\alpha = (\alpha_1, \alpha_2, \alpha_3) \in \mathbb{N}^3$ and $\eta = (\eta_1, \eta_2, \eta_3) \in \mathbb{N}^3$ be two multi-indices. Suppose we have defined a quantum equilibrium $\varrho^{eq} = (s')^{-1}(-H)$, where s is a convex function and H an operator with a discrete spectrum that we denote $(\lambda_p, \psi_p)_{p\in\mathbb{N}}$, then we have (see lemma 3.1 for the notations):*

$$\partial_x^\eta \int p^\alpha W\left(\varrho^{eq}\right) \frac{dp}{(2\pi\hbar)^3} = (-i\hbar)^{|\alpha|} \sum_{p\in\mathbb{N}} (s')^{-1}(-\lambda_p) \times$$
$$\sum_{0\le\gamma\le\alpha} \begin{pmatrix} \alpha \\ \gamma \end{pmatrix} \left(-\frac{1}{2}\right)^{|\gamma|} \sum_{0\le\xi\le\gamma+\eta} \begin{pmatrix} \gamma+\eta \\ \xi \end{pmatrix} \left(\partial_x^{\alpha-\gamma+\xi}\psi_p\right)\left(\partial_x^{\gamma+\eta-\xi}\overline{\psi_p}\right). \quad (3.45)$$

Proof. Let $\phi(x)$ be a smooth test function, we have:

$$\begin{aligned}
&\int \left(\partial_x^\eta \int p^\alpha W\left((s')^{-1}(-H)\right) \frac{dp}{(2\pi\hbar)^3}\right)\phi\, dx \\
&\qquad = (-1)^{|\eta|} \int p^\alpha W\left((s')^{-1}(-H)\right) \partial_x^\eta\phi \frac{dp}{(2\pi\hbar)^3}\, dx \\
&\qquad = (-1)^{|\eta|} \mathrm{Tr}\ \left(W^{-1}\left(p^\alpha \partial_x^\eta\phi\right)(s')^{-1}(-H)\right) \\
&\qquad = (-1)^{|\eta|} \sum_{p\in\mathbb{N}} \left(W^{-1}\left(p^\alpha\partial_x^\eta\phi\right)(s')^{-1}(-H)\psi_p\,, \psi_p\right)_{L^2(\mathbb{R}^3)} \\
&\qquad = (-1)^{|\eta|} \sum_{p\in\mathbb{N}} (s')^{-1}(-\lambda_p)\left(W^{-1}\left(p^\alpha\partial_x^\eta\phi\right)\psi_p\,, \psi_p\right)_{L^2(\mathbb{R}^3)}.
\end{aligned}$$

Then, we use lemma 3.1, to compute $W^{-1}\left(p^\alpha\partial_x^\eta\phi\right)\psi_p$ and the desired weak formulation is obtained after integrations by parts. □

We recall now a lemma which can be found in [14] (lemma 5.4) and whose proof is a direct application of pseudo-differential calculus (see for example [34]).

Lemma 3.3 *Let us consider two symbols $w_1(x,p)$ and $w_2(x,p)$ that are infinitely differentiable. The operation $w_1 \circ_\hbar w_2$ gives the symbol of their operator product (this operation is sometimes noted $w_1 \sharp w_2$ in the literature), i.e. :*

$$w_1 \circ_\hbar w_2 = W\left(W^{-1}(w_1)W^{-1}(w_2)\right). \quad (3.46)$$

The following formal expansion holds:

$$w_1 \circ_\hbar w_2 = \sum_{n=0}^{\infty} \hbar^n w_1 \circ_n w_2 \quad (3.47)$$

with

$$w_1 \circ_n w_2(x,p) = \left(\frac{i}{2}\right)^n \sum_{\gamma,\zeta,|\gamma+\zeta|=n} \frac{(-1)^{|\gamma|}}{\gamma!\zeta!} \partial_x^\zeta\partial_p^\gamma w_1(x,p)\partial_x^\gamma\partial_p^\zeta w_2(x,p), \quad (3.48)$$

where we denote by $\lambda = (\lambda_1, \lambda_2, \lambda_3)$ and $\zeta = (\zeta_1, \zeta_2, \zeta_3)$ two multi-indices and $\lambda! = \lambda_1!\lambda_2!\lambda_3!$ (see lemma 3.1 for the other notations).

As a consequence, we give now a lemma which is helpful for commutator computations.

Lemma 3.4 *Let $\alpha = (\alpha_1, \alpha_2, \alpha_3) \in \mathbb{N}^3$ and $\beta = (\beta_1, \beta_2, \beta_3) \in \mathbb{N}^3$ be two multi-indices, and let $\lambda(x)$ and $\mu(x)$ be any smooth real or complex valued functions. Let us denote $[\lambda p^\alpha, \mu p^\beta]_\hbar$ the symbol associated to the commutator of the operators $W^{-1}(\lambda p^\alpha)$ and $W^{-1}(\mu p^\beta)$, i.e. :*

$$[\lambda p^\alpha, \mu p^\beta]_\hbar = W\left(\left[W^{-1}\left(\lambda p^\alpha\right), W^{-1}\left(\mu p^\beta\right)\right]\right). \tag{3.49}$$

The following formal expansion holds:

$$[\lambda p^\alpha, \mu p^\beta]_\hbar = \sum_{k=0}^{\lfloor (|\alpha+\beta|-1)/2 \rfloor} \hbar^{2k+1} [\lambda p^\alpha, \mu p^\beta]_{2k+1}, \tag{3.50}$$

with

$$[\lambda p^\alpha, \mu p^\beta]_{2k+1} = i\left(-\frac{1}{4}\right)^k \sum_{\substack{0\le\gamma\le\alpha,\, 0\le\zeta\le\beta \\ |\gamma+\zeta|=2k+1}} (-1)^{|\gamma|} \begin{pmatrix} \alpha \\ \gamma \end{pmatrix} \begin{pmatrix} \beta \\ \zeta \end{pmatrix} \left(\partial_x^\zeta \lambda\right) \left(\partial_x^\gamma \mu\right) p^{\alpha+\beta-\gamma-\zeta}, \tag{3.51}$$

where $\lfloor \cdot \rfloor$ denotes the floor function (see lemma 3.1 for the other notations).

Proof. By the definition of the commutator and using notations of lemma 3.3, we have:

$$\begin{aligned} [\lambda p^\alpha, \mu p^\beta]_\hbar &= \lambda p^\alpha \circ_\hbar \mu p^\beta - \mu p^\beta \circ_\hbar \lambda p^\alpha \\ &= \sum_{n=0}^{\infty} \hbar^n (\lambda p^\alpha \circ_n \mu p^\beta - \mu p^\beta \circ_n \lambda p^\alpha). \end{aligned}$$

The operation $\circ_n$ being commutative (resp. anticommutative) when n is even (resp. odd), we obtain:

$$[\lambda p^\alpha, \mu p^\beta]_\hbar = \sum_{k=0}^{\infty} \hbar^{2k+1} (2\lambda p^\alpha \circ_{2k+1} \mu p^\beta).$$

Then we apply the definition of the operation $\circ_{2k+1}$ (3.48) to obtain the coefficients $[\lambda p^\alpha, \mu p^\beta]_{2k+1}$ and we notice that these coefficients are zero as soon as $k > \lfloor (|\alpha+\beta|-1)/2 \rfloor$. □

4 Remarkable properties of QHD

4.1 Applications of the technical lemmas to QHD

All the quantities expressed in the QHD model can be written with respect to the spectrum of the modified Hamiltonian $H(A, B, C)$. This is what we do in next lemma using lemma 3.2.

Lemma 4.1 *Suppose $H(A,B,C)$ has a discrete spectrum that we denote $(\lambda_p,\psi_p)_{p\in\mathbb{N}}$, then we have:*

$$n = \sum_{p\in\mathbb{N}}(s')^{-1}(-\lambda_p)|\psi_p|^2, \tag{4.52}$$

$$nu = \hbar\sum_{p\in\mathbb{N}}(s')^{-1}(-\lambda_p)\mathcal{I}m\left(\nabla\psi_p\overline{\psi_p}\right), \tag{4.53}$$

$$\mathcal{W} = \frac{\hbar^2}{4}\sum_{p\in\mathbb{N}}(s')^{-1}(-\lambda_p)\left(|\nabla\psi_p|^2-\mathcal{R}e\left(\Delta\psi_p\overline{\psi_p}\right)\right). \tag{4.54}$$

We can also express:

$$\Pi = \frac{\hbar^2}{2}\sum_{p\in\mathbb{N}}(s')^{-1}(-\lambda_p)\mathcal{R}e\left(\nabla\psi_p\otimes\nabla\overline{\psi_p}-\overline{\psi_p}\nabla\otimes\nabla\psi_p\right), \tag{4.55}$$

$$\Phi = -\frac{\hbar^3}{8}\sum_{p\in\mathbb{N}}(s')^{-1}(-\lambda_p)\mathcal{I}m\left(2(\nabla\otimes\nabla\overline{\psi_p})\cdot\nabla\psi_p+\Delta\overline{\psi_p}\nabla\psi_p+\overline{\psi_p}\nabla\Delta\psi_p\right) \tag{4.56}$$

and the fluxes:

$$\nabla\cdot nu = \hbar\sum_{p\in\mathbb{N}}(s')^{-1}(-\lambda_p)\mathcal{I}m\left(\Delta\psi_p\overline{\psi_p}\right), \tag{4.57}$$

$$\nabla\cdot\Pi = \frac{\hbar^2}{2}\sum_{p\in\mathbb{N}}(s')^{-1}(-\lambda_p)\mathcal{R}e\left(\nabla\psi_p\Delta\overline{\psi_p}-\overline{\psi_p}\nabla\Delta\psi_p\right), \tag{4.58}$$

$$\nabla\cdot\Phi = -\frac{\hbar^3}{8}\sum_{p\in\mathbb{N}}(s')^{-1}(-\lambda_p)\mathcal{I}m\left(2\nabla\psi_p\cdot\nabla\Delta\overline{\psi_p}+\overline{\psi_p}\Delta\Delta\psi_p\right). \tag{4.59}$$

Proof. Let us denote by $\{e_1,e_2,e_3\}$ the standard basis of $\mathbb{R}^3$. We use lemma 3.2 with:

- $\eta=(0,0,0)$ and $\alpha=(0,0,0)$ to get (4.52),
- $\eta=(0,0,0)$ and $\alpha=e_i$ to get the i^{th} component of (4.53),
- $\eta=(0,0,0)$ and $\alpha=2e_j$ to get (4.54) after summation on j and division by 2,
- $\eta=(0,0,0)$ and $\alpha=e_i+e_j$ to get the coefficient (i,j) of (4.55),
- $\eta=(0,0,0)$ and $\alpha=e_i+2e_j$ to get (4.56) after summation on j and division by 2,
- $\eta=e_j$ and $\alpha=e_j$ to get (4.57) after summation on j,
- $\eta=e_j$ and $\alpha=e_i+e_j$ to get the i^{th} component of (4.58) after summation on j.
- $\eta=e_j$ and $\alpha=2e_i+e_j$ to get (4.59) after summation on i and j and division by 2.

□

We now give an application of lemma 3.4. The following theorem gives general relations involving n, nu, $\mathcal{W}$, Π, Φ and A, B, C as soon as they are linked according to (2.27)–(2.30). Any future discretization should be thought such that the following relations are respected.

Theorem 4.2 *Let n, nu, $\mathcal{W}$, Π, Φ and A, B, C be given and satisfy (2.27)–(2.30). Then we have:*

$$\nabla\cdot\frac{nu}{C} = \nabla\cdot\frac{nB}{C}, \tag{4.60}$$

$$\begin{aligned}\nabla\cdot\frac{\Pi}{C} &= \nabla\cdot\left(nu\otimes\frac{B}{C}\right)+\left(\nabla\frac{B}{C}\right)\cdot nu - n\nabla\left(A+\frac{B^2}{2C}\right)-\mathcal{W}\nabla\frac{1}{C}\\ &\quad+\frac{\hbar^2}{8}\Delta\left(n\nabla\frac{1}{C}\right),\end{aligned} \tag{4.61}$$

$$\begin{aligned}\nabla\cdot\frac{\Phi}{C^2} &= \frac{1}{C}\Pi:\left(\nabla\frac{B}{C}\right)+\frac{1}{C}\nabla\cdot\left(\frac{B}{C}\mathcal{W}\right)-\frac{1}{C}\nabla\left(A+\frac{B^2}{2C}\right)\cdot nu\\ &\quad+\frac{\hbar^2}{8C}\left(\nabla\cdot\left(nu\Delta\frac{1}{C}-n\Delta\frac{B}{C}\right)+\Delta\left(nu\cdot\nabla\frac{1}{C}\right)\right).\end{aligned} \tag{4.62}$$

Proof. Let $\mu(x)$ be a smooth test function. Using lemma 3.4, we compute:

$$\begin{aligned}\left[W\left(\tilde{H}(\tilde{A},\tilde{B},\tilde{C})\right),\mu\right]_\hbar &= \left[\tilde{A},\mu\right]_\hbar+\left[\tilde{B}\cdot p,\mu\right]_\hbar+\left[\tilde{C}|p|^2,\mu\right]_\hbar\\ &= 0-i\hbar\left(\tilde{B}\cdot\nabla\mu+2\tilde{C}\nabla\mu\cdot p\right).\end{aligned} \tag{4.63}$$

$$\begin{aligned}\left[W\left(\tilde{H}(\tilde{A},\tilde{B},\tilde{C})\right),\mu p\right]_\hbar &= \left[\tilde{A},\mu p\right]_\hbar+\left[\tilde{B}\cdot p,\mu p\right]_\hbar+\left[\tilde{C}|p|^2,\mu p\right]_\hbar\\ &= -i\hbar\Big(-\mu\nabla\tilde{A}+(\tilde{B}\cdot\nabla\mu)p-\mu(\nabla\tilde{B})\cdot p\\ &\quad+2\tilde{C}(\nabla\mu\cdot p)p-\mu\nabla\tilde{C}|p|^2+\frac{\hbar^2}{4}\nabla\tilde{C}\Delta\mu\Big)\end{aligned} \tag{4.64}$$

$$\begin{aligned}\left[W\left(\tilde{H}(\tilde{A},\tilde{B},\tilde{C})\right),\mu|p|^2\right]_\hbar &= \left[\tilde{A},\mu|p|^2\right]_\hbar+\left[\tilde{B}\cdot p,\mu|p|^2\right]_\hbar+\left[\tilde{C}|p|^2,\mu|p|^2\right]_\hbar\\ &= -i\hbar\Big(-2\mu\nabla\tilde{A}\cdot p-2\mu(p\otimes p):(\nabla\tilde{B})+\tilde{B}\cdot\nabla\mu|p|^2\\ &\quad-\frac{\hbar^2}{4}\Delta\tilde{B}\cdot\nabla\mu+2\tilde{C}\nabla\mu\cdot p|p|^2-2\mu\nabla\tilde{C}\cdot p|p|^2\\ &\quad-\frac{\hbar^2}{4}\left(2\Delta\tilde{C}\nabla\mu\cdot p-2\Delta\mu\nabla\tilde{C}\cdot p\right)\Big).\end{aligned} \tag{4.65}$$

Then due to the cyclicity of the trace, we write for the three commutators:

$$\begin{aligned}&\mathrm{Tr}\left(\left[\tilde{H}(\tilde{A},\tilde{B},\tilde{C}),W^{-1}(\mu p^\alpha)\right]\varrho^{eq}_{n,nu,\mathcal{W}}\right)=0\\ &\qquad=\int\left[W\left(\tilde{H}(\tilde{A},\tilde{B},\tilde{C})\right),\mu p^\alpha\right]_\hbar W\left(\varrho^{eq}_{n,nu,\mathcal{W}}\right)\frac{dx\,dp}{(2\pi\hbar)^3}\end{aligned}$$

which gives weakly the three desired identities after integrations by parts and the change of variable given by (2.15). □

4.2 Gauge invariance and irrotational flows

4.2.1 Gauge invariance

We now turn to look at gauge invariance, an interesting property that will simplify the model for irrotational flows.

Lemma 4.3 (Gauge invariance) *Let $\alpha = (\alpha_1, \alpha_2, \alpha_3) \in \mathbb{N}^3$ be a multi-index, and let $S(x)$ and $\lambda(x)$ be smooth functions. Then, we have:*

$$e^{iS/\hbar} H(A, B, C) e^{-iS/\hbar} = H(A, B + \nabla S, C). \tag{4.66}$$

Proof. To prove identity (4.66), we remark that for $|\alpha| \leq 2$, we have

$$e^{iS/\hbar} W^{-1}\left(\lambda p^{\alpha}\right) e^{-iS/\hbar} = W^{-1}\left(\lambda (p - \nabla S)^{\alpha}\right).$$

The modified Hamiltonian $H(A, B, C) = W^{-1}\left(\frac{1}{2C}(p - B)^2 + A\right)$ being an operator associated to a polynomial in p of order 2, we have:

$$e^{iS/\hbar} W^{-1}\left(\frac{1}{2C}(p - B)^2 + A\right) e^{-iS/\hbar} = \left(\frac{1}{2C}(p - (B + \nabla S))^2 + A\right)$$

which is (4.66). □

This gauge invariance lemma allows us to write gauge transformations which are summarized in next lemma.

Lemma 4.4 *Let us denote by $n(A, B, C)$, $nu(A, B, C)$, $\mathcal{W}(A, B, C)$, $\Pi(A, B, C)$ and $\Phi(A, B, C)$ the extensive quantities associated to the intensive quantities (A, B, C) according to (2.27)–(2.30). Then, we have the following identities:*

$$\begin{aligned}
n(A, B + \nabla S, C) &= n(A, B, C), && (4.67)\\
(nu)(A, B + \nabla S, C) &= (nu)(A, B, C) + n(A, B, C)\nabla S, && (4.68)\\
\mathcal{W}(A, B + \nabla S, C) &= \mathcal{W}(A, B, C) + (nu)(A, B, C) \cdot \nabla S \\
&\quad + \frac{1}{2} n(A, B, C)|\nabla S|^2, && (4.69)\\
\Pi(A, B + \nabla S, C) &= \Pi(A, B, C) + (nu)(A, B, C) \otimes \nabla S \\
&\quad + \nabla S \otimes (nu)(A, B, C) + n(A, B, C)\nabla S \otimes \nabla S, && (4.70)\\
\Phi(A, B + \nabla S, C) &= \Phi(A, B, C) + (\Pi(A, B, C) + \mathcal{W}(A, B, C) Id) \cdot \nabla S \\
&\quad + \frac{1}{2} n(A, B, C)|\nabla S|^2 \nabla S + \frac{1}{2}(nu)(A, B, C)|\nabla S|^2 \\
&\quad + ((nu)(A, B, C) \cdot \nabla S)\nabla S - \frac{\hbar^2}{8} n(A, B, C)\nabla \Delta S, && (4.71)
\end{aligned}$$

which relate the mass, current, and energy densities, the pressure tensor and the energy flux for two values of B differing by a gradient.

Proof. Let $\alpha = (\alpha_1, \alpha_2, \alpha_3) \in \mathbb{N}^3$ be a multi-index and λ be a smooth test function and let us denote by $w^{eq}(A, B, C) = W\left((s')^{-1}\left(-H(A, B, C)\right)\right)$. Due to lemma 4.3,

we can write:

$$\begin{aligned}\int w^{eq}(A,B+\nabla S,C)\lambda p^{\alpha}\frac{dx\,dp}{(2\pi\hbar)^3} &= \mathrm{Tr}\,\left((s')^{-1}\left(-H(A,B+\nabla S,C)\right)W^{-1}\left(\lambda p^{\alpha}\right)\right)\\ &= \mathrm{Tr}\,\left(e^{iS/\hbar}(s')^{-1}\left(-H(A,B,C)\right)e^{-iS/\hbar}W^{-1}\left(\lambda p^{\alpha}\right)\right)\\ &= \mathrm{Tr}\,\left((s')^{-1}\left(-H(A,B,C)\right)e^{-iS/\hbar}W^{-1}\left(\lambda p^{\alpha}\right)e^{iS/\hbar}\right).\end{aligned}$$

Then as we have already noticed earlier, we use the fact that for $|\alpha|\leq 2$

$$e^{-iS/\hbar}W^{-1}\left(\lambda p^{\alpha}\right)e^{iS/\hbar}=W^{-1}\left(\lambda(p+\nabla S)^{\alpha}\right),$$

so that finally we have for $|\alpha|\leq 2$

$$\int w^{eq}(A,B+\nabla S,C)\lambda p^{\alpha}\frac{dx\,dp}{(2\pi\hbar)^3}=\int w^{eq}(A,B,C)\lambda(p+\nabla S)^{\alpha}\frac{dx\,dp}{(2\pi\hbar)^3}$$

which gives the following identity:

$$\int w^{eq}(A,B+\nabla S,C)p^{\alpha}\frac{dp}{(2\pi\hbar)^3}=\int w^{eq}(A,B,C)(p+\nabla S)^{\alpha}\frac{dp}{(2\pi\hbar)^3}.$$

Then we choose (denoting by $\{e_1,e_2,e_3\}$ the standard basis of $\mathbb{R}^3$):

- $\alpha=(0,0,0)$ to get (4.67),
- $\alpha=e_i$ to get the i^{th} component of (4.68),
- $\alpha=2e_j$ to get (4.69) after summation on j and division by 2,
- $\alpha=e_i+e_j$ to get the coefficient (i,j) of (4.70).

In order to get (4.71), we compute for $\alpha=e_i+2e_j$

$$e^{-iS/\hbar}W^{-1}\left(\lambda p^{\alpha}\right)e^{iS/\hbar}=W^{-1}\left(\lambda(p+\nabla S)^{\alpha}\right)-\frac{\hbar^2}{4}\lambda\partial_i\partial_j^2 S,$$

and we get the following identity for $\alpha=e_i+2e_j$:

$$\int w^{eq}(A,B+\nabla S,C)p^{\alpha}\frac{dp}{(2\pi\hbar)^3}=\int w^{eq}(A,B,C)\left((p+\nabla S)^{\alpha}-\frac{\hbar^2}{4}\partial_i\partial_j^2 S\right)\frac{dp}{(2\pi\hbar)^3}.$$

Finally we obtain the i^{th} component of (4.71) after summation on j and division by 2. □

4.2.2 Irrotational flows

It is now possible to give interesting properties for the special case of the QHD model with irrotational flows as stated in the next theorem.

Theorem 4.5 *Let n, nu, $\mathcal{W}$ and A, B, C be given according to Definition 2.1. Assume moreover that u is an irrotational vector field, i.e. that there exists $S(x)$ such that $u = \nabla S$. Then B is defined by*

$$B = u = \nabla S \tag{4.72}$$

and we have

$$\varrho^{eq}_{n,nu,\mathcal{W}} = e^{iS/\hbar}\, \varrho^{eq}_{n,0,\mathcal{W}}\, e^{-iS/\hbar}, \tag{4.73}$$

where the two equilibrium density operators $\varrho^{eq}_{n,nu,\mathcal{W}}$ and $\varrho^{eq}_{n,0,\mathcal{W}}$ are given according to Definition 2.1. If we denote by $n(A,B,C)$, $nu(A,B,C)$, $\mathcal{W}(A,B,C)$, $\Pi(A,B,C)$ and $\Phi(A,B,C)$ the extensive quantities associated to the intensive quantities (A,B,C) according to (2.27)–(2.30), we have moreover:

$$\begin{aligned}
n(A,B,C) &= n(A,0,C), && (4.74)\\
\mathcal{W}(A,B,C) &= \mathcal{W}(A,0,C) + \frac{1}{2} n(A,0,C)|u|^2, && (4.75)\\
\Pi(A,B,C) &= \Pi(A,0,C) + n(A,0,C)\, u \otimes u, && (4.76)\\
\Phi(A,B,C) &= (\Pi(A,0,C) + \mathcal{W}(A,0,C) Id)\cdot u + \frac{1}{2} n(A,0,C)|u|^2 u \\
&\quad - \frac{\hbar^2}{8} n(A,0,C)\Delta u. && (4.77)
\end{aligned}$$

Proof. Let n, nu and $\mathcal{W}$ be given and consider the following minimization problem with only two constraints:

$$\begin{aligned}
\min \big\{ S(\varrho) \text{ such that the density associated to } \varrho \text{ is } n \\
\text{(see (2.1)) and the energy is } \mathcal{W} - \tfrac{1}{2} n u^2 \text{ (see (2.3))} \big\}. \quad (4.78)
\end{aligned}$$

Following [14], this minimization problem (4.78) is attained on a density operator which reads

$$\varrho_0 = (s')^{-1}\left(-H(\alpha, 0, \gamma)\right),$$

where α and γ are two scalar functions and $H(\alpha,0,\gamma)$ is still defined according to (2.11). Due to the fact that the Wigner function of ϱ_0 is even (see [14]), this density operator carries no current. This is enough to conclude that $\varrho_0 = \varrho^{eq}_{n,0,\mathcal{W}-\frac{1}{2}nu^2}$ (following Definition 2.1) or, equivalently, that

$$n(\alpha,0,\gamma) = n, \qquad (nu)(\alpha,0,\gamma) = 0, \qquad \mathcal{W}(\alpha,0,\gamma) = \mathcal{W} - \frac{1}{2} n u^2.$$

Denote now

$$\varrho_S = (s')^{-1}\left(-H(\alpha, \nabla S, \gamma)\right).$$

Applying the Gauge invariance of Lemma 4.3, we have:

$$H(\alpha, \nabla S, \gamma) = e^{iS/\hbar}\, H(\alpha, 0, \gamma)\, e^{-iS/\hbar},$$

it is immediate to deduce from elementary functional calculus that

$$\varrho_S = e^{iS/\hbar}\, \varrho_0\, e^{-iS/\hbar}.$$

Note then that, by definition, the mass density, the current density and the energy density corresponding to ϱ_S are respectively $n(\alpha, \nabla S, \gamma)$, $(nu)(\alpha, \nabla S, \gamma)$ and $\mathcal{W}(\alpha, \nabla S, \gamma)$ and, as a direct consequence of lemma 4.4, we have

$$\begin{aligned}
&n(\alpha, \nabla S, \gamma) = n(\alpha, 0, \gamma) = n,\\
&(nu)(\alpha, \nabla S, \gamma) = (nu)(\alpha, 0, \gamma) + n(\alpha, 0, \gamma)\nabla S = nu,\\
&\mathcal{W}(\alpha, \nabla S, \gamma) = \mathcal{W}(\alpha, 0, \gamma) + (nu)(\alpha, 0, \gamma)\nabla S + \frac{1}{2}n(\alpha, 0, \gamma)|\nabla S|^2 = \mathcal{W}.
\end{aligned}$$

Therefore, according to the property of uniqueness of the Lagrange multipliers A, B and C assumed in subsection 2.1, we deduce that $A = \alpha$, $B = \nabla S$ and $C = \gamma$.

The last part of the theorem (identities (4.74)-(4.77)) is a direct consequence of lemma 4.4. □

Corollary 4.6 *For irrotational flows, the QHD model reads:*

$$\partial_t n + \nabla \cdot nu = 0, \tag{4.79}$$

$$\partial_t (nu) + \nabla \cdot \Pi = -n\nabla V, \tag{4.80}$$

$$\partial_t \mathcal{W} + \nabla \cdot \left((\Pi + \mathcal{W} Id) \cdot u - n|u|^2 u - \frac{\hbar^2}{8} n \Delta u \right) = -nu \cdot \nabla V, \tag{4.81}$$

with

$$n = \int w^{eq}_{n,\mathcal{W}} \frac{dp}{(2\pi\hbar)^3}, \tag{4.82}$$

$$\mathcal{W} = \frac{1}{2} n|u|^2 + \int w^{eq}_{n,\mathcal{W}} \frac{|p|^2}{2} \frac{dp}{(2\pi\hbar)^3}, \tag{4.83}$$

and

$$\Pi = nu \otimes u + \int w^{eq}_{n,\mathcal{W}} (p \otimes p) \frac{dp}{(2\pi\hbar)^3}, . \tag{4.84}$$

The quantum local equilibrium $w^{eq}_{n,\mathcal{W}}$ is defined by

$$w^{eq}_{n,\mathcal{W}} = W\left(\varrho^{eq}_{n,\mathcal{W}}\right) = W\left((s')^{-1}\left(-H(A, 0, C)\right)\right), \tag{4.85}$$

where $H(A, 0, C)$ is the following modified Hamiltonian

$$H(A, 0, C) = W^{-1}\left(\frac{1}{2C}p^2 + A\right) \tag{4.86}$$

$$= -\hbar^2 \left(\nabla \cdot (\frac{1}{2C}\nabla) + \frac{1}{4}\Delta \frac{1}{2C} \right) + A. \tag{4.87}$$

Proof. The proof is straightforward using theorem 4.5. □

Let us summarize the simplifications obtained for the QHD model with irrotational flows. Firstly, two unknowns have been canceled, namely the energy flux Φ and the generalized mean velocity B. Secondly, the link between the moments and their dual variables is simpler. The underlying minimization problem is now (4.78), with only the constraint on the density and the energy, instead of (2.9). The local equilibrium

$\varrho^{eq}_{n,\mathcal{W}} = (s')^{-1}(-H(A,0,C))$ is the same as the one of the QET model and in the case where its spectrum is discrete, this spectrum has the advantage of being real. In addition, notice that the dispersive velocity term $-\frac{\hbar^2}{8}\nabla\cdot(n\Delta u)$ appearing in the divergence of the energy flux (4.81) also appears in other QHD derivations. It has been derived in [20] from a mixed-state Wigner model and interpreted as a dispersive "heat flux". It also appears in the QHD equations of [22] involving a "smoothed" potential, derived from the quantum Liouville equation by a Chapman-Enskog expansion. Finally, it appears in [27] where an $\hbar$ expansion of the QHD model presented here (with a Boltzmann statistics) is performed. It has been noted in [27] that an interesting feature of this dispersive term is that it stabilizes the QHD system numerically.

4.2.3 One-dimensional flows

A special case of irrotational flows is one-dimensional flows. It is natural to wonder if the 1D QHD model can be written in a simple way. It appears that this is a delicate question and we see two possibilities:

1. If the transport is confined in one dimension (for example if we want to model quantum transport confined on a wire [16], we can suppose that the temperature is anisotropic and the momentum p is confined on a line with coordinate $x_1 \in \mathbb{R}$), then we can start from a 1D Wigner equation, define a 1D quantum local equilibrium and in this case we obtain the following model:

$$\partial_t n + \partial_{x_1}(nu) = 0, \tag{4.88}$$

$$\partial_t(nu) + 2\partial_{x_1}\mathcal{W} = -n\partial_{x_1}V, \tag{4.89}$$

$$\partial_t\mathcal{W} + \partial_{x_1}\left(3\mathcal{W}u - nu^3 - \frac{\hbar^2}{8}n\partial^2_{x_1}u\right) = -nu\partial_{x_1}V. \tag{4.90}$$

   Notice that these 3 equations are now decoupled from the constitutive equations linking $(n, nu, \mathcal{W})$ to (A, B, C). This model is exact (without any approximation) and its only quantum character reduces to the dispersive velocity term $-\frac{\hbar^2}{8}\partial_{x_1}(n\partial^2_{x_1}u)$. A surprising fact is that this model coincides with its $\hbar$ expansion up to second order, proving that the higher order terms are equal to zero independently of the chosen statistics. Notice also that in the semiclassical limit ($\hbar \to 0$), we do not recover the classical hydrodynamic equations used in the literature.

2. If the problem is in dimension three (for the momentum p) but all the quantities depend only on one space variable (say on x_1), then the derivation of the 1D model from the 3D model (4.79)–(4.86) is not possible without some more assumptions. This statement needs some precisions. Let consider the stress tensor $\mathbb{P} = \int w^{eq}_{n,\mathcal{W}}(p\otimes p)\frac{dp}{(2\pi\hbar)^3}$ appearing in the pressure tensor Π (4.84). Without any assumption, this tensor is not diagonal contrary to the classical case (as already noticed in [14]). With the assumption that all the quantities depend only on the variable x_1, and if we suppose that the function $(s')^{-1}(\cdot)$ is expandable as a power series, it is possible to show that $w^{eq}_{n,\mathcal{W}}$ is even with respect to p_2 and p_3. Using lemma 3.3, we prove indeed that any power of $H(A,0,C)$ is a symbol depending only on (x_1,p) and even with respect to p_2, p_3, and thus $\mathbb{P}$ is diagonal. But nevertheless it is not scalar. If we suppose moreover that $\mathbb{P}$ is scalar, using

the constraint that its trace must be equal to $2\mathcal{W} - n|u|^2$, we can suppose that $\mathbb{P} = (2\mathcal{W} - n|u|^2)/3\mathrm{Id}$. We obtain then the following 1D QHD model:

$$\partial_t n + \partial_{x_1}(nu) = 0, \tag{4.91}$$

$$\partial_t(nu) + \frac{2}{3}\partial_{x_1}(\mathcal{W} + nu^2) = -n\partial_{x_1}V, \tag{4.92}$$

$$\partial_t \mathcal{W} + \partial_{x_1}\left(\frac{5}{3}\mathcal{W}u - \frac{1}{3}nu^3 - \frac{\hbar^2}{8}n\partial_{x_1}^2 u\right) = -nu\partial_{x_1}V. \tag{4.93}$$

Here we do not measure the error arising from the assumption that the stress tensor is scalar but we recover the classical hydrodynamic equations used in the literature at the semiclassical limit ($\hbar \to 0$).

4.3 Simplification of fluxes and QHD with slowly varying temperature

In three dimensions, the QHD model is more complicated and the relations of lemma 4.1 are non local and difficult to handle numerically. We would like, at least for the pressure tensor Π and the energy flux Φ to give local expressions (as it has been done for the isothermal Quantum Euler system [11]), *i.e.* to express $\nabla \cdot \Pi$ and $\nabla \cdot \Phi$ in a differential way involving only the extensive variables n, nu, $\mathcal{W}$, and the intensive ones A, B, C. Unfortunately, we have not succeeded yet but theorem 4.2 constitutes one step in this direction. It gives us $\nabla \cdot \frac{\Pi}{C}$ and $\nabla \cdot \frac{\Phi}{C^2}$ instead of $\nabla \cdot \Pi$ and $\nabla \cdot \Phi$. If we suppose that the generalized temperature is slowly varying, we can suppose that

$$\left|\frac{\nabla C}{C}\right| = \varepsilon \ll 1 \tag{4.94}$$

with ε a small positive parameter.

Using lemma 4.2, we obtain the following approximation for the divergence of the pressure tensor:

$$\nabla \cdot \Pi = \nabla(nu \otimes B) + (\nabla B) \cdot nu - n\nabla\left(AC + \frac{B^2}{2}\right) + \mathcal{O}(\varepsilon). \tag{4.95}$$

Note that if we take $C = T$ to be a constant, we find the expression of $\nabla \cdot \Pi$ already found for the Isothermal Quantum Euler model [11].

In the same manner we obtain the following approximation for the energy flux:

$$\nabla \cdot \Phi = (\Pi\nabla) \cdot B + \nabla \cdot (B\mathcal{W}) - nu \cdot \nabla\left(AC + \frac{B^2}{2}\right) - \frac{\hbar^2}{8}\nabla \cdot (n\Delta B) + \mathcal{O}(\varepsilon). \tag{4.96}$$

In this last expression, we see that $\nabla \cdot \Phi$ depends on Π and unfortunately, we do not know any approximation for it and we have not been able to find one which is compatible with the approximation made on $\nabla \cdot \Pi$ in expression (4.95).

5 Remarkable properties of QET

5.1 Applications of the technical lemmas to QET

All the quantities expressed in the QET model can also be written with respect to the spectrum of the modified Hamiltonian $H(A, 0, C)$. Suppose $H(A, 0, C)$ has a discrete

spectrum that we denote $(\lambda_p, \psi_p)_{p\in\mathbb{N}}$, this spectrum is real and lemma 3.2 allows us to compute the moments n and $\mathcal{W}$ as it has been done in lemma 4.1. In the same lemma, we have given the expression for Π and $\nabla\cdot\Pi$. In the next lemma, we complete this list for the QET model.

Lemma 5.1 *Suppose $H(A,0,C)$ has a discrete spectrum that we denote $(\lambda_p,\psi_p)_{p\in\mathbb{N}}$, we have:*

$$\begin{aligned}\mathbb{Q} &= -\frac{\hbar^4}{16}\sum_{p\in\mathbb{N}}(s')^{-1}(-\lambda_p)\Big(\nabla\psi_p\otimes\nabla\Delta\psi_p - 2(\nabla\otimes\nabla\psi_p)^2 + \nabla\Delta\psi_p\otimes\nabla\psi_p\\ &\quad -\Delta\psi_p(\nabla\otimes\nabla\psi_p) + 2(\nabla\otimes\nabla\otimes\nabla\psi_p)\cdot\nabla\psi_p - \psi_p(\nabla\otimes\nabla\Delta\psi_p)\Big), \quad (5.97)\\ \nabla\cdot\mathbb{Q} &= -\frac{\hbar^4}{16}\sum_{p\in\mathbb{N}}(s')^{-1}(-\lambda_p)\Big(-2(\nabla\otimes\nabla\psi_p)\cdot\nabla\Delta\psi_p + \Delta\Delta\psi_p\nabla\psi_p\\ &\quad +2(\nabla\otimes\nabla\Delta\psi_p)\cdot\nabla\psi_p - \psi_p\nabla\Delta\Delta\psi_p\Big), \quad (5.98)\\ \nabla\cdot\nabla\cdot\mathbb{Q} &= -\frac{\hbar^4}{16}\sum_{p\in\mathbb{N}}(s')^{-1}(-\lambda_p)\Big(\Delta\Delta\psi_p\Delta\psi_p + 2\nabla\psi_p\cdot\nabla\Delta\Delta\psi_p\\ &\quad -\psi_p\Delta\Delta\Delta\psi_p - 2|\nabla\Delta\psi_p|^2\Big). \quad (5.99)\end{aligned}$$

We have also:

$$\nabla\cdot\nabla\cdot\Pi = \frac{\hbar^2}{2}\sum_{p\in\mathbb{N}}(s')^{-1}(-\lambda_p)(|\Delta\psi_p|^2 - \psi_p\Delta\Delta\psi_p), \quad (5.100)$$

$$\nabla\cdot(\mathcal{W}Id) = \frac{\hbar^2}{4}\sum_{p\in\mathbb{N}}(s')^{-1}(-\lambda_p)\left(2(\nabla\otimes\nabla\psi_p)\cdot\nabla\psi_p - \nabla\psi_p\Delta\psi_p - \psi_p\nabla\Delta\psi_p\right). \quad (5.101)$$

Proof. Let us denote by $\{e_1,e_2,e_3\}$ the standard basis of $\mathbb{R}^3$. We use lemma 3.2 with:

- $\eta=(0,0,0)$ and $\alpha=e_i+e_j+2e_k$ to get the coefficient (i,j) of (5.97) after summation on k and division by 2,
- $\eta=e_j$ and $\alpha=e_i+e_j+2e_k$ to get the i^{th} component of (5.98) after summation on j and k and division by 2,
- $\eta=e_i+e_j$ and $\alpha=e_i+e_j+2e_k$ to get (5.99) after summation on i, j and k and division by 2,
- $\eta=e_i+e_j$ and $\alpha=e_i+e_j$ to get (5.100) after summation on i and j,
- $\eta=e_i$ and $\alpha=2e_j$ to get the i^{th} component of (5.101) after summation on j and division by 2.

□

As it has been done in theorem 4.2, we now state some general properties involving Π, $\mathbb{Q}$ and some differential expressions of the extensive quantities n, $\mathcal{W}$ and intensive ones A and C.

Theorem 5.2 *Let n, $\mathcal{W}$, Π, $\mathbb{Q}$ and A, C be given and satisfy (2.33), (2.41)–(2.43). Then we have:*

$$\nabla\cdot\frac{\Pi}{C}=-n\nabla A-\mathcal{W}\nabla\frac{1}{C}+\frac{\hbar^2}{8}\Delta\left(n\nabla\frac{1}{C}\right), \tag{5.102}$$

$$\begin{aligned}\nabla\cdot\frac{\mathbb{Q}}{C^2}+\frac{1}{2C}\mathrm{Tr}\,\mathbb{Q}\nabla\frac{1}{C}=&-(\Pi+\mathcal{W}Id)\cdot\frac{\nabla A}{C}+\frac{\hbar^2}{8C}\Bigg(n\nabla\Delta A+\mathcal{W}\nabla\Delta\frac{1}{C}\\&+\nabla\cdot\left(\Pi\Delta\frac{1}{C}\right)+2\nabla\cdot\left(\left(\nabla\otimes\nabla\frac{1}{C}\right)\Pi\right)+\Delta\left((\Pi+\mathcal{W}Id)\cdot\nabla\frac{1}{C}\right)\Bigg)\\&-\frac{\hbar^4}{64C}\Delta\left(n\nabla\Delta\frac{1}{C}\right).\end{aligned} \tag{5.103}$$

Proof. For the first identity, we use (4.61) with $B=0$. For the second identity, we use again lemma 3.4. Let $\mu(x)$ be a smooth test function, we compute:

$$\begin{aligned}\left[W\left(\tilde{H}(\tilde{A},0,\tilde{C})\right),\mu|p|^2p\right]_\hbar&=\left[\tilde{A},\mu|p|^2p\right]_\hbar+\left[\tilde{C}|p|^2,\mu|p|^2p\right]_\hbar\\&=-i\hbar\Bigg(-2\mu(\nabla\tilde{A}\cdot p)p-\mu|p|^2\nabla\tilde{A}+\frac{\hbar^2}{4}\mu\nabla\Delta\tilde{A}\\&-2\mu(\nabla\tilde{C}\cdot p)|p|^2p-\mu\nabla\tilde{C}|p|^2|p|^2+2\tilde{C}(\nabla\mu\cdot p)|p|^2p\\&-\frac{\hbar^2}{4}\Bigg(-\mu\nabla\Delta\tilde{C}|p|^2+2(\nabla\mu\cdot p)\Delta\tilde{C}p+4\left((\nabla\otimes\nabla\tilde{C})(p\otimes p)\right)\cdot\nabla\mu\\&-2\Delta\mu(\nabla\tilde{C}\cdot p)p-\Delta\mu\nabla\tilde{C}|p|^2\Bigg)-\frac{\hbar^4}{16}\Delta\mu\nabla\Delta\tilde{C}\Bigg).\end{aligned} \tag{5.104}$$

Then due to the cyclicity of the trace, we write:

$$\begin{aligned}\mathrm{Tr}\,\left(\left[\tilde{H}(\tilde{A},\tilde{B},\tilde{C}),W^{-1}(\mu|p|^2p)\right]\varrho^{eq}_{n,\mathcal{W}}\right)&=0\\&=\int\left[W\left(\tilde{H}(\tilde{A},0,\tilde{C})\right),\mu|p|^2p\right]_\hbar W\left(\varrho^{eq}_{n,\mathcal{W}}\right)\frac{dx\,dp}{(2\pi\hbar)^3}\end{aligned}$$

which gives weakly the desired identity after integrations by parts and the change of variable given by (2.15) (with $B=\tilde{B}=0$). □

5.2 Simplification of fluxes and QET with slowly varying temperature

As it has been done for the QHD model, we can discuss the case of slowly varying temperature for the QET model. Let us note again $\left|\frac{\nabla C}{C}\right|=\varepsilon\ll 1$. Using theorem 5.2, we obtain the following approximation for the divergence of the pressure tensor:

$$\nabla\cdot\Pi=-n\nabla(AC)+\mathcal{O}(\varepsilon). \tag{5.105}$$

Note that if we take $C=T$ to be a constant, we find the expression of $\nabla\cdot\Pi$ already found for the Quantum Drift-Diffusion model [13, 18, 10].

For the divergence of the heat flux tensor, we find the following approximation:

$$\nabla\cdot\mathbb{Q}=-(\Pi+\mathcal{W}\mathrm{Id})\cdot\nabla(AC)+\frac{\hbar^2}{8}n\nabla\Delta(AC)+\mathcal{O}(\varepsilon), \tag{5.106}$$

so that the currents can be approximated by

$$j_n = n\nabla(AC - V) + \mathcal{O}(\varepsilon) \tag{5.107}$$

$$j_{\mathcal{W}} = (\mathcal{W}\mathrm{Id} + \Pi) \cdot \nabla(AC - V) - \frac{\hbar^2}{8} n\nabla\left(\Delta(AC - V)\right) + \mathcal{O}(\varepsilon). \tag{5.108}$$

Unfortunately again, we do not know any approximation for Π and we have not been able to find one which is compatible with the approximation made on $\nabla \cdot \Pi$ in expression (5.105). Except in one dimension, where we see again two possibilities.

1. If we suppose that the transport is confined in dimension one (the momentum p being confined on a line with coordinate $x_1 \in \mathbb{R}$), and if we suppose that $\left|\frac{\partial_{x_1} C}{C}\right| = \varepsilon \ll 1$, the 1D QET model reads:

$$\begin{aligned} \partial_t n + \partial_{x_1} j_n &= 0, & (5.109)\\ \partial_t \mathcal{W} + \partial_{x_1} j_{\mathcal{W}} + (\partial_{x_1} V) j_n &= 0, & (5.110) \end{aligned}$$

$$\begin{aligned} j_n &= -2\partial_{x_1}\mathcal{W} - n\partial_{x_1} V, & (5.111)\\ j_{\mathcal{W}} &= 3\mathcal{W}\partial_{x_1}(AC - V) - \frac{\hbar^2}{8} n\partial_{x_1}^3(AC - V) + \mathcal{O}(\varepsilon), & (5.112) \end{aligned}$$

with:

$$\begin{pmatrix} n \\ \mathcal{W} \end{pmatrix} = \int w_{n,\mathcal{W}}^{eq} \begin{pmatrix} 1 \\ \frac{p_1^2}{2} \end{pmatrix} \frac{dp_1}{2\pi\hbar}. \tag{5.113}$$

The quantum local equilibrium is defined by

$$w_{n,\mathcal{W}}^{eq} = W\left(\varrho_{n,\mathcal{W}}^{eq}\right) = W\left((s')^{-1}\left(-H(A,0,C)\right)\right), \tag{5.114}$$

where $H(A,0,C)$ is the following modified Hamiltonian

$$\begin{aligned} H(A,0,C) &= W^{-1}\left(\frac{p_1^2}{2C} + A\right) \\ &= -\hbar^2\left(\partial_{x_1}\left(\frac{1}{2C}\partial_{x_1}\right) + \frac{1}{4}\partial_{x_1}^2\frac{1}{2C}\right) + A. \end{aligned} \tag{5.115}$$

2. If the problem is in dimension 3 but all the quantities depend only on one space variable (say x_1), it is possible to show that the tensor Π is diagonal (see subsection 4.2.3). If we suppose that this tensor is scalar and equal to $2\mathcal{W}/3\mathrm{Id}$, then the expressions of the currents (5.111) and (5.112) have to be replaced by:

$$\begin{aligned} j_n &= -\frac{2}{3}\partial_{x_1}\mathcal{W} - n\partial_{x_1} V, & (5.116)\\ j_{\mathcal{W}} &= \frac{5}{3}\mathcal{W}\partial_{x_1}(AC - V) - \frac{\hbar^2}{8} n\partial_{x_1}^3(AC - V) + \mathcal{O}(\varepsilon), & (5.117) \end{aligned}$$

6 Conclusion and perspectives

In this chapter, we have given the expressions of the QHD and QET models with respect to the spectrum of the modified Hamiltonians $H(A, B, C)$ and $H(A, 0, C)$. We have then given some differential constraints that link the moments and their dual Lagrange multipliers. Concerning specifically the QHD model, a gauge invariance lemma allows us to simplify the model for irrotational flows. All these properties allow us to discuss some possible approximations of the models in the special cases of slowly varying temperature and/or of one dimensional flows which will facilitate future numerical approximations. The use of the commutator lemma should also allow us to study other quantum hydrodynamic-like models that have been derived with the same methodology based on the entropy principle, but involving other moments.

References

[1] M. G. Ancona, G. J. Iafrate, *Quantum correction of the equation of state of an electron gas in a semiconductor*, Phys. Rev. B **39** (1989), 9536–9540.

[2] M. G. Ancona, H. F. Tiersten, *Macroscopic physics of the silicon inversion layer*, Pys. review, B **39** (1987), 7959–7965.

[3] A. Arnold, J. L. Lopez, P. A. Markowich, and J. Soler, *An analysis of quantum Fokker-Planck models: A Wigner function approach*, Rev. Mat. Iberoamericana **20** (2004), 771–814.

[4] A. Arnold, F. Nier, *The two-dimensional Wigner-Poisson problem for an electron gas in the charge neutral case*, Math. Methods Appl. Sci. **14** (1991), no. 9, 595–613.

[5] P. Bhatnagar, E. Gross, M. Krook, *A model for collision processes in gases. I. Small amplitude processes in charged and neutral one-component systems*, Phys. Review **94** (1954), 511–525.

[6] N. Ben Abdallah, A. Unterreiter, *On the stationary quantum driftdiffusion model*, Z. Angew. Math. Phys. **49** (1998), no. 2, 251–275.

[7] L. L. Chang, L. Esaki, R. Tsu, *Resonant tunneling in semiconductor double barriers*, Appl. Phys. Lett. **24** (1974), 593–595.

[8] R.-C. Chen, J.-L. Liu, *A quantum corrected energy-transport model for nanoscale semiconductor devices*, J. Comput. Phys. **204** (2005), 131–156.

[9] S. Datta, *Nanoscale device modeling: The Green's function method, Superlattices and Microstructures* **28** (2000), 253–278.

[10] P. Degond, S. Gallego, F. Méhats, *An entropic Quantum Drift-Diffusion model for electron transport in resonant tunneling diodes*, J. Comput. Phys. **221** (2007), 226–249.

[11] P. Degond, S. Gallego, F. Méhats, *Isothermal quantum hydrodynamics: derivation, asymptotic analysis and simulation*, SIAM Multiscale Model. Simul. **6** (2007), no. 1, 246–272.

[12] P. Degond, S. Gallego, F. Méhats, C. Ringhofer, *Quantum hydrodynamic and diffusion models derived from the entropy principle*, to be published in Springer Lecture Notes in Mathematics.

[13] P. Degond, F. Méhats, C. Ringhofer, *Quantum hydrodynamic models derived from the entropy principle*, Contemp. Math. **371** (2005), 107–331.

[14] P. Degond, F. Méhats, C. Ringhofer, *Quantum Energy-Transport and Drift-Diffusion models*, J. Stat. Phys. **118** (2005), no. 3-4, 625–665.

[15] P. Degond, C. Ringhofer, *Quantum Moment Hydrodynamics and the Entropy Principle*, J. Stat. Phys. **112** (2003), no. 3-4, 587–628.

[16] F. Dubin, R. Melet, T. Barisien, R. Grousson, L. Legrand, M. Schott, V. Voliotis, *Macroscopic coherence of a single exciton state in an organic quantum wire*, Nature Phys. **2** (2006), 32–35.

[17] W. Dreyer, M. Junk, M. Kunik, *On the approximation of the FokkerŰPlanck equation by moment systems*, Nonlinearity **14** (2001), 881–906.

[18] S. Gallego, F. Méhats, *Entropic discretization of a Quantum Drift-Diffusion model*, SIAM J. Numer. Anal. **43** (2005), no. 5, 1828–1849.

[19] C. Gardner, *The quantum hydrodynamic model for semiconductor devices*, SIAM J. Appl. Math. **54** (1994), no. 2, 409–427.

[20] C. Gardner, *Resonant tunneling in the quantum hydrodynamic model*, VLSI Design **3** (1995), 201–210.

[21] C. Gardner, C. Ringhofer, *The smooth quantum potential for the hydrodynamic model*, Phys. Rev. E **53** (1996), 157–167.

[22] C. Gardner, C. Ringhofer, *The Chapman-Enskog Expansion and the Quantum Hydrodynamic Model for Semiconductor Devices*, VLSI Design **10** (2000), 415–435.

[23] I. Gasser, A. Jüngel, *The quantum hydrodynamic model for semiconductors in thermal equilibrium*, Z. Angew. Math. Phys. **48** (1997), no. 1, 45–59.

[24] I. Gasser, P. A. Markowich, *Quantum Hydrodynamics, Wigner Transforms and the Classical Limit*, Asympt. Analysis **14** (1997), no. 2, 97–116.

[25] A. Jüngel, *Quasi-hydrodynamic semiconductor equations*, Progress in Nonlinear Differential Equations, Birkhäuser, 2001.

[26] A. Jüngel, D. Matthes, *A derivation of the isothermal quantum hydrodynamic equations using entropy minimization*, Z. Angew. Math. Mech. **85** (2005), 806–814.

[27] A. Jüngel, D. Matthes, J.P. Milisic, *Derivation of new quantum hydrodynamic equations using entropy minimization*, SIAM J. Appl. Math. **67** (2006), 46–68.

[28] A. Jüngel, R. Pinnau, *A positivity preserving numerical scheme for a fourth-order parabolic equation*, SIAM J. Num. Anal. **39** (2001), no. 2, 385–406.

[29] C. D. Levermore, *Moment closure hierarchies for kinetic theories*, J. Stat. Phys. **83** (1996), 1021–1065.

[30] F. Nier, *A stationary Schrödinger-Poisson system arising from the modeling of electronic devices*, Forum Math. **2** (1990), no. 5, 489–510.

[31] A. Unterreiter, R. Pinnau, *The stationary current-voltage characteristics of the Quantum Drift-Diffusion model*, SIAM J. Num. Anal. **37** (1999), no. 1, 211–245.

[32] E. Polizzi, *Modélisation et simulations numériques du transport quantique balistique dans les nanostructures semi-conductrices*, Ph.D. thesis, INSA, Toulouse, 2001.

[33] E. Polizzi, N. Ben Abdallah, *Self-consistent three dimensional models for quantum ballistic transport in open systems*, Phys. Rev. B, **66** (2002), 245–301.

[34] D. Robert, *Autour de l'Approximation Semi-Classique*, Birkhäuser, Boston, 1987.

Chapter VI

An asymptotic preserving scheme for the Schrödinger equation in the semiclassical limit

This chapter has given a note written in collaboration with P. Degond and F. Méhats, and published in C. R. Math. Acad. Sci. Paris **345** (2007), no. 9, 531–536.

Abstract. This chapter is devoted to the discretization of the fluid formulation of the Schrödinger equation (the Madelung system). We explore both the discretization of the system in eulerian coordinates and lagrangian coordinates. We propose schemes for these two formulations which are implicit in the mass flux term. This feature allows us to show that these schemes are asymptotic preserving i.e. they provides discretizations of the semi-classical Hamilton-Jacobi equation when the scaled Planck constant ε tends to 0. An analysis performed on the linearized systems also shows that they are asymptotically stable i.e. their stability condition remains bounded as ε tends to 0. Numerical simulations are given ; they confirm that the considered schemes allow us to numerically bridge the quantum and semi-classical scales.

Key words. Schrödinger, Madelung, asymptotic preserving scheme, semiclassical limit, linear analysis, asymptotic stability, lagrangian coordinates.

1 Introduction

It is known since Madelung [5] that the Schrödinger equation $i\varepsilon\partial_t\psi = -\frac{\varepsilon^2}{2}\Delta\psi + V\psi$ (ε is the scaled Planck constant) can be expressed equivalently in a fluid dynamical way using the Madelung Transform. This consists in writing the wave function in WKB form $\psi = \sqrt{n}e^{i\frac{S}{\varepsilon}}$ where n is the density and S is the phase. Inserting this ansatz in the Schrödinger equation and taking the real part and the gradient of the imaginary part, one obtains the following so-called Madelung system with unknowns the density n and the current $q = n\nabla S$:

$$\partial_t n + \nabla \cdot q = 0, \tag{1.1}$$

$$\partial_t q + \nabla \cdot \left(\frac{q \otimes q}{n}\right) + n\nabla(V + V^B) = 0, \tag{1.2}$$

$$V^B = -\frac{\varepsilon^2}{2}\frac{\Delta\sqrt{n}}{\sqrt{n}}. \tag{1.3}$$

These equations consist in the classical pressureless Euler equations involving an additional quantum potential called the Bohm potential V^B.

These equations are nonlinear by contrast to the Schrödinger equation. In spite of this additional complexity (compared to the linear Schrödinger) the Madelung formulation can be useful from a numerical point of view. Indeed, in the semiclassical regime when the scaled Planck constant ε is small, the wave function develop oscillations of order ε and, in the Schrödinger formulation, the space discretization needs to resolve these oscillations. Since the values of the physical observables depend on the gradient of the phases, their accurate computation is often very difficult. Some schemes for the Schrödinger formulation have been analyzed by means of Wigner measures in the semiclassical limit such as e.g. the Crank-Nicolson scheme and the leap frog scheme in [6] and the Dufort-Frankel scheme in [7]. These analyses show that the space and time discretizations must satisfy $\Delta x = o(\varepsilon)$ and $\Delta t = o(\varepsilon)$. Time splitting spectral approximations are more efficient [1] but the constraints on the space and time discretizations are still very stringent: $\Delta t = O(\varepsilon)$ and $\Delta x = o(\varepsilon)$. In a closer spirit to this chapter, the Madelung formulation (also called Bohmian mechanics or quantum trajectory methods) has been used for a long time and has recently been subject to a revived interest for quantum chemistry applications [10, 2, 4, 8, 9, 11].

In this chapter, we propose a semi-implicit scheme (which has the same cost as an explicit scheme) to solve the Madelung system in eulerian and lagrangian coordinates. The scheme is implicit in the mass flux term. The main advantage of this method is asymptotically stable and preserving when $\varepsilon \to 0$ i.e. the stability condition remains finite as $\varepsilon \to 0$ and in this limit, the scheme provides a discretization of the semiclassical Hamilton-Jacobi equations.

2 The method

Numerical schemes: We first propose a scheme for the one-dimensional Madelung system in eulerian coordinates (1.1)–(1.3). Motivated by the linear analysis presented in next section, we choose a semi-implicit discretization in time and a centered finite

discretization in space:

$$n_j^{k+1} = n_j^k - \frac{\Delta t}{2\Delta x}(q_{j+1}^{k+1} - q_{j-1}^{k+1}) = 0, \tag{2.4}$$

$$q_j^{k+1} = q_j^k - \frac{\Delta t}{2\Delta x}(\frac{{q_{j+1}^k}^2}{n_{j+1}^k} - \frac{{q_{j-1}^k}^2}{n_{j-1}^k}) - \frac{\Delta t}{2\Delta x} n_j^k (V_{B,j+1}^k + V_{j+1} - V_{j-1}^{B,k} - V_{j-1}) = 0 \tag{2.5}$$

$$V_{B,j}^k = -\frac{\varepsilon^2}{2} \frac{\sqrt{n_{j+1}^k} - 2\sqrt{n_j^k} + \sqrt{n_{j-1}^k}}{\sqrt{n_j^k}\Delta x^2}. \tag{2.6}$$

This scheme is clearly asymptotic preserving. We show below that, at least for the linearized system, the scheme is also asymptotically stable.

This scheme has also a Lagrangian version. Let us transform the 1D Madelung system in lagrangian coordinates. Suppose the total mass of the system is finite and equal to M. We introduce the new variables $m : \mathbb{R} \to [0, M], m(x) = \int_{-\infty}^{x} n(y,t)dy$ and its inverse: $X : [0, M] \to \mathbb{R}, m \to X(m,t)$ such that $X(m(x,t),t) = x$. Let us also introduce the velocity and specific volume in lagrangian coordinates $v(m,t) = q(X(m,t),t)/n(X(m,t),t)$ and $\tau(m,t) = 1/n(X(m,t),t)$. If we write the equations for the evolution of the system with unknowns τ and v with respect of the variables t and m, we obtain:

$$\partial_t \tau - \partial_m v = 0, \tag{2.7}$$

$$\partial_t v + \frac{1}{\tau}\partial_m(\overline{V} + \overline{V_B}) = 0, \tag{2.8}$$

$$\overline{V_B} = \frac{\varepsilon^2}{4\sqrt{\tau}}\partial_m\left(\frac{\partial_m \tau}{\tau^{5/2}}\right), \tag{2.9}$$

$$\overline{V} = V(X(m,t),t), \tag{2.10}$$

with $\partial_t X = v$. Motivated by the same linear analysis as for the Madelung system in eulerian coordinates, we choose a semi-implicit discretization in time and a centered finite discretization in mass. The interpolations for the passage from the lagrangian to the eulerian coordinates are performed using cubic splines.

Linear analysis: We assume that the potential V is constant and we want to study the linearized Madelung system about the stationary state $n_0 = 1$ and $q_0 = 0$:

$$\partial_t n + \nabla \cdot q = 0,$$
$$\partial_t q - \frac{\varepsilon^2}{4}\nabla\Delta n = 0.$$

Notice that by linearizing the Madelung system in lagrangian coordinates with a null potential about $\tau_0 = 1$, the first three equations (2.7)–(2.9) have the same linearization as the system in eulerian coordinates, with the substitution $n \to \tau$, $q \to -v$ and $x \to m$.

We first start by studying a time discretization of the linearized system. Note that the density is solution of a wave equation for the bilaplacian operator $\partial_t^2 n + \frac{\varepsilon^2}{4}\Delta^2 n = 0$. Let us consider the following semi-implicit discretization in time of the system, where Δt is the time step:

$$\frac{n^{k+1} - n^k}{\Delta t} + \nabla \cdot q^{k+1} = 0, \tag{2.11}$$

$$\frac{q^{k+1} - q^k}{\Delta t} - \frac{\varepsilon^2}{4}\nabla\Delta n^k = 0, \tag{2.12}$$

which corresponds to the explicit discretization of the wave equation form. By a partial Fourier transform on the variable x, and denoting $\hat{n}$ the transform of n, we obtain $\frac{\hat{n}^{k+1}-2\hat{n}^k+\hat{n}^{k-1}}{\Delta t^2} + \frac{\varepsilon^2}{4}\xi^4\hat{n}^k = 0$. The necessary condition for this scheme to be stable is $\frac{\varepsilon\xi^2\Delta t}{4} < 1$. In view of the space discretization of mesh size Δx, we assume that the range of admissible wave-number ξ is $[0, \xi^* = 2\pi/\Delta x]$. This gives the following stability criterion:

$$\Delta t < \frac{\Delta x^2}{\varepsilon\pi^2}. \tag{2.13}$$

Note that this semi-implicit treatment does not require more computational effort than the explicit scheme. Knowing q^k and n^k for a given time step, it suffices to solve (2.12) to get q^{k+1} first, and then (2.11) to get n^{k+1}.

In order to mimic the influence of a decentered space discretization, we have considered a viscous perturbation of the linearized Madelung system. It appears that even if the numerical viscosity stabilizes the scheme, the viscosity must be smaller than ε in order not to destroy the dispersive behavior of the Schrödinger equation and provide a correct discretization of the semi-classical limit. For this reason, we favored a centered space discretization with centered finite-differences.

3 Numerical results

We are going to test both schemes in eulerian and lagrangian coordinates on a bounded domain $[0, 1]$ with periodic boundary conditions and a constant potential $V(x) = 100$.

The first test case is taken from [6, 7, 1]. The initial density is given by $n^0 = e^{-50(x-0.5)^2}$ and the initial current is given by $q^0 = 0.2(2x-1)n^0$. Figure VI.1 shows the results for the scheme in eulerian coordinates (2.4)–(2.6). We plot the density, current and bohm potential at $t = 0.54$ for different ε. As ε tends to zero, the density and the current tend to smooth limits as already noted in [6, 7, 1]. In our simulations, the mesh size is fixed and equal to $\Delta x = 0.01$. The time step Δt is taken proportional to $1/\varepsilon$: for $\varepsilon = 0.0256$, $\Delta t = 2 \times 10^{-4}$, for $\varepsilon = 0.0064$, $\Delta t = 8 \times 10^{-4}$ and for $\varepsilon = 0.0001$, $\Delta t = 6 \times 10^{-2}$ so that the stability criterion (2.13) is respected. We see clearly here the advantage of using our scheme based on the Madelung formulation compared to any scheme using the Schrödinger formulation. We would like to point out that other test cases exhibiting densities near vacuum can create instabilities. This has already been noted in the literature for the pressureless Euler system [3] and the addition of the Bohm potential makes things harder (see the square root of the density at the denominator of the expression giving the Bohm potential in (1.3)). The scheme in the lagrangian coordinates is even more unstable since vacuum corresponds to a singularity of the specific volume τ.

The second test case allows to compare the schemes in lagrangian and eulerian coordinates. We choose an initial density which is uniformly bounded from below by a positive constant $n^0 = 0.1 + e^{-50(x-0.5)^2}$ and we choose for initial current $q^0 = 0.1\sin(2\pi x)n^0$. We plot on figure VI.2 the density and current at time $t = 0.2$ for $\varepsilon = 0.05$ and $\varepsilon = 0.001$, using the eulerian scheme (solid line) and the lagrangian scheme (dashed line). We take again for the eulerian scheme $\Delta x = 0.01$. Concerning the lagrangian scheme, the total mass is equal to 0.3507 and we take for mass discretization $\Delta m = 0.003507$. Again the time step can be taken proportional to $1/\varepsilon$ and both schemes are stable.

The third test case shows the advantage of using the scheme in lagrangian coordinates since it allows to consider higher currents. This test corresponds to a traveling gaussian. We choose the same initial $n^0 = 0.1 + e^{-50(x-0.5)^2}$, but we take now a higher initial current $q^0 = 10n^0$. For $\varepsilon = 0$, it is easy to check that the soliton $n(x) = n^0(x - 10t)$, $q(x) = q^0(x - 10t)$ is the solution of the problem so that for $t = 0.1$, we have $n(x) = n^0(x)$ and $q(x) = q^0(x)$ (due to the periodic boundary conditions). Figure VI.3 show the density and current at time $t = 0.1$ for different ε. We take the same mesh size as the second test case and the time step can again be taken proportional to $1/\varepsilon$. Results obtained with the scheme in eulerian coordinates on this test case are not presented because they are unstable.

4 Conclusion

We have presented two asymptotic preserving schemes for the Schrödinger equations in the semiclassical limit, based on the Madelung formulation of Schrödinger's equation in terms of the density and flux. Both eulerian and lagrangian coordinate systems have been considered. A stability analysis of the linearized Madelung system shows that these schemes are asymptotically stable. The numerical results confirm this analysis and demonstrate that, for a fixed Δx, the time step can scale like $1/\varepsilon$, while the best meshing strategy for any scheme using the Schrödinger formulation is $\Delta t = O(\varepsilon)$ and $\Delta x = o(\varepsilon)$. These schemes however develop an instability near vacuum. More tests are under progress, in particular to evaluate the ability of the scheme to cross the caustics.

References

[1] W. Bao, S. Jin, P.A. Markowich, *On time-splitting spectral approximations for the Schrödinger equation in the semiclassical regime*, J. Comput. Phys. **175** (2002), 487–524.

[2] E. R. Bittner, *Quantum tunneling dynamics using hydrodynamic trajectories*, J. Chem. Phys. **112** (2000), no. 22, 9703–9710.

[3] G.-Q Chen, H. Liu, *Formation of δ-Schocks and Vacuum states in the Vanishing Pressure Limit of Solutions to the Isentropic Euler Equations*, SIAM J. Math. Anal. **34** (2003), 925–938.

[4] C. L. Lopreore, R. E. Wyatt *Quantum wave packet dynamics with trajectories*, Phys. Rev. **82** (1999), no. 26, 5190–5193.

[5] E. Madelung, *Quanten theorie in Hydrodynamischer Form*, Z. Physik **40** (1927), 322.

[6] P. A. Markowich, P. Pietra, and C. Pohl, *Numerical approximation of quadratic observables of Schrödinger type equations in the semi-classical limit*, Numer. Math. **81** (1999), 595–630.

[7] P. A. Markowich, P. Pietra, C. Pohl, H. P. Stimming, *A Wigner-measure analysis of the Dufort-Frankel scheme for the Schrödinger equation*, SIAM J. Numer. Anal. **40** (2002), 1281–1310.

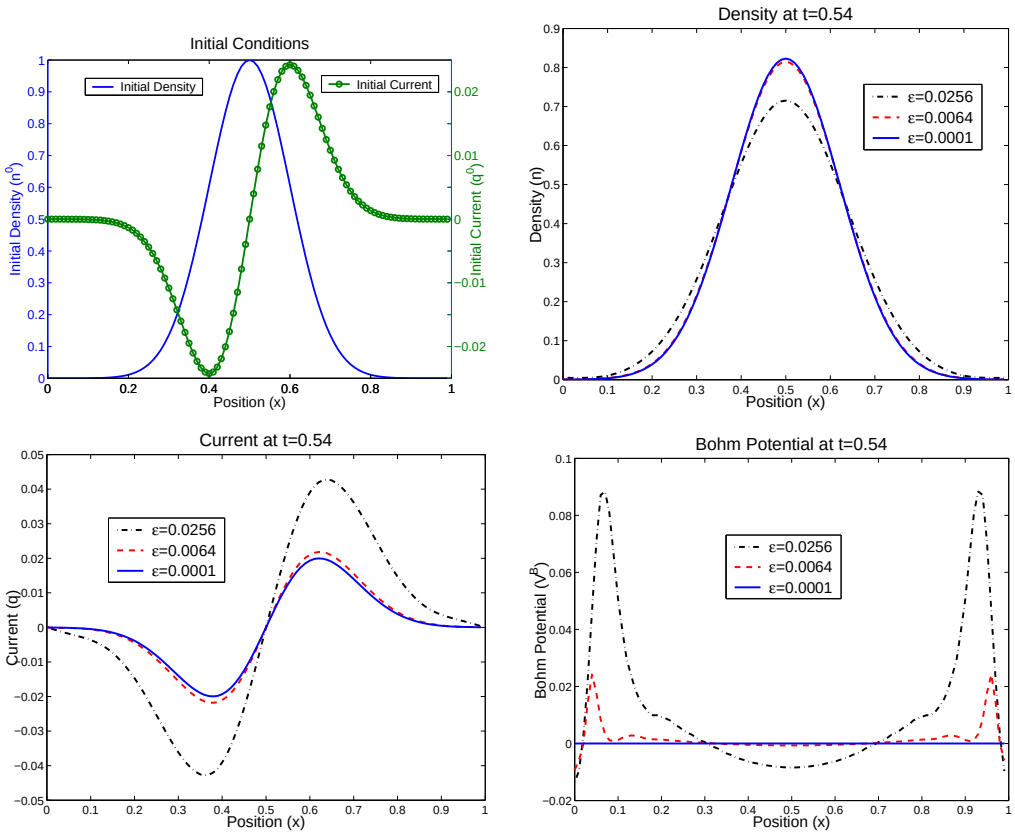

Figure VI.1: Numerical solutions for the first test case (eulerian scheme). Top left: Initial conditions as function of the position x; top right, bottom left and bottom right: density, current and bohm potential at time $t = 0.54$ as functions of the position x for $\varepsilon = 0.0256$ (dash-dot line), $\varepsilon = 0.0064$ (dashed line) and $\varepsilon = 0.0001$ (solid line).

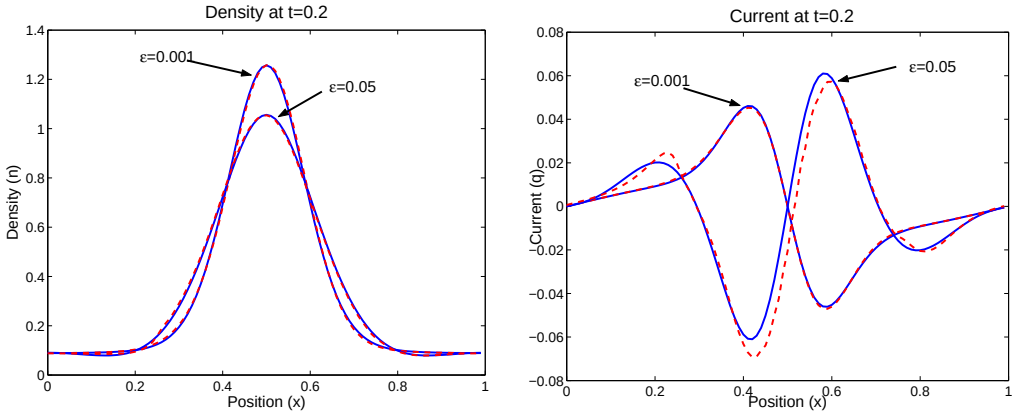

Figure VI.2: Numerical solutions for the second test case (eulerian and lagrangian schemes). Density and current at time $t = 0.2$ as functions of the position x for $\varepsilon = 0.05$ and $\varepsilon = 0.001$ using the eulerian scheme (solid line) and the lagrangian scheme (dashed line).

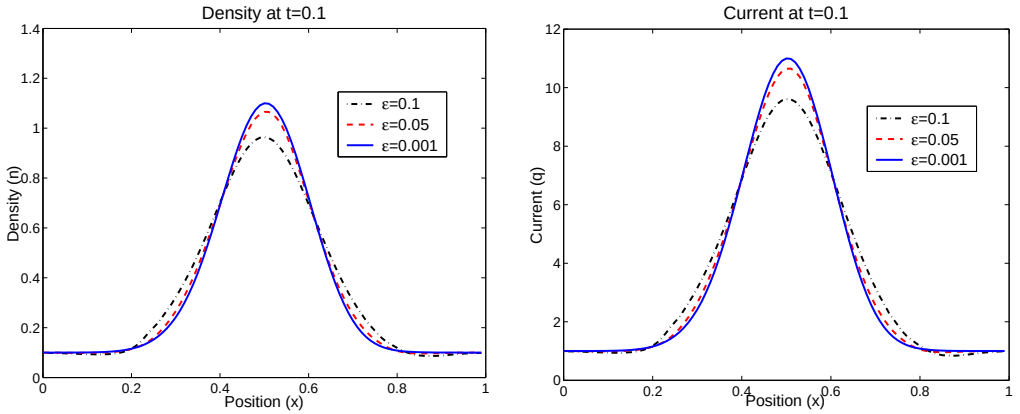

Figure VI.3: Numerical solutions for the third test case (lagrangian scheme). Density and current at time $t = 0.1$ as functions of the position x for $\varepsilon = 0.1$ (dash-dot line), $\varepsilon = 0.05$ (dashed line) and $\varepsilon = 0.001$ (solid line). Note that the scheme in eulerian coordinates is unstable on this test case due to the high current.

[8] F. S. Mayor, A. Askar, H. A. Rabitz, *Quantum fluid dynamics in the lagrangian representation and applications to photodissociation problems*, J. Chem. Phys. **111** (1999), no. 6, 2423–2435.

[9] K. Na, R. E. Wyatt *Quantum trajectories for resonant scattering*, Internat. J. Quantum Chem. **81** (2001), no. 3, 206–213.

[10] J. H. Weiner, A. Askar, *Particle method for numerical solution of the time-dependant Schrödinger equation*, J. Chem. Phys. **54** (1971), no. 8, 3534–3541.

[11] R. E. Wyatt, C. L. Lopreore, G. Parlant *Electronic transitions with quantum trajectories*, J. Chem. Phys. **114** (2001), no. 12, 5113–5116.

Conclusion générale et perspectives (version française)

Dans cette thèse, nous avons étudié quelques modèles fluides quantiques issus du principe de minimisation d'entropie:

- le modèle de Dérive-Diffusion Quantique (QDD) dans les chapitres I, II et III,
- le modèle d'Euler Quantique Isotherme dans le chapitre IV,
- les modèles d'Hydrodynamique Quantique (QHD) et de Transport d'Énergie Quantique (QET) dans le chapitre V.

Sur le plan numérique, nous avons clairement porté l'essentiel de nos efforts sur le modèle QDD. Nous avons d'abord proposé une discrétisation en temps puis en espace du modèle couplé à l'équation de Poisson avec des conditions aux bords fermées, nous avons effectué une analyse numérique de ce schéma et démontré que ce schéma a de bonnes propriétés (le schéma est bien posé, la stricte positivité de la densité est garantie pour tout temps, la charge totale dans le domaine est conservée et une énergie libre quantique discrète est décroissante au cours du temps). Nous avons par la suite proposé des conditions aux bords ouvertes et nous avons effectué une batterie de tests sur la diode à effet tunnel résonnant (RTD) puis nous avons comparé le modèle QDD avec d'autres modèles existants. Enfin nous avons proposé d'inclure des conditions aux bords transparentes qui semblent plus réalistes d'un point de vue physique.

Cependant, il reste encore du travail à achever concernant le modèle QDD. Grâce à la propriété de décroissance de l'énergie libre, la démonstration de la convergence en temps du modèle (tout au moins pour le modèle discrétisé) semble possible mais nécessite encore quelques efforts. Par ailleurs, concernant les conditions aux bords transparentes, nous ne sommes pas capables dans l'état actuel de capturer suffisamment bien les résonances de la RTD pour tracer des caractéristiques courant-tension (la méthode de Gummel appliquée pour le modèle stationnaire ne converge pas pour des biais appliqués trop grands et on n'a pas encore trouvé de remède à ce mauvais comportement) et la nécessité de prendre un très petit pas de discrétisation pour l'impulsion fait exploser le temps de calcul pour le modèle instationnaire. La prise en compte d'un pas d'impulsion adaptatif devrait permettre dans le futur de diminuer les coûts de calculs. On peut penser à beaucoup d'autres extensions: choisir d'autres statistiques que celle de Boltzmann, comme celle de Fermi-Dirac par exemple, effectuer un couplage du modèle QDD avec le modèle de Dérive-Diffusion classique au niveau des réservoirs d'électrons, appliquer le modèle à d'autres domaines comme la chimie quantique par exemple, etc...

Concernant le modèle d'Euler Quantique Isotherme, plusieurs propriétés ont été démontrées qui reposent pour la plupart sur une propriété d'invariance de jauge, ce qui permet d'écrire de grosses simplifications pour le modèle irrotationnel, et donc pour le modèle 1D. Ceci nous a permis de présenter des simulations numériques préliminaires sur une diode à effet tunnel simplifiée. Il reste pour ce modèle encore beaucoup de travail, le même programme que pour QDD pouvant s'appliquer (étude du schéma numérique, application du modèle sur un cas-test physique, comparaison avec des modèles existants, prise en compte de conditions aux bords transparentes...).

Pour les modèles QHD et QET, tout reste à faire même si le chapitre V devrait faciliter l'implémentation numérique de ces modèles. On peut aussi imaginer étudier d'autres modèles fluides quantiques issus du principe de minimisation d'entropie, comme par exemple des modèles hydrodynamiques avec des moments d'ordre supérieurs à deux. Beaucoup de questions théoriques restent ouvertes concernant tous ces modèles. En effet l'existence même des équilibres locaux quantiques définis comme minimiseurs d'une entropie quantique est à démontrer et pour cela, il va falloir créer un cadre fonctionnel qui est pour l'instant absent.

Enfin, dans le dernier chapitre de cette thèse (chapitre VI), nous avons proposé un schéma numérique pour l'équation de Schrödinger écrite sous forme fluide: le système de Madelung. L'analyse du schéma pour le système linéarisé nous montre que celui-ci est asymptotiquement stable dans la limite semi-classique. Un travail possible pour le futur pourrait être de démontrer la stabilité du schéma non-linéaire. Par ailleurs, de nombreux problèmes apparaissent et sont en cours d'étude, comme la gestion d'instabilités liées aux faibles densités et la prise en compte de potentiels extérieurs non constants par exemple.

General conclusion and perspectives (english version)

In this thesis, we have studied some quantum fluid models derived from the entropy principle:

- the Quantum Drift-Diffusion model (QDD) in chapters I, II and III,
- the Isothermal Quantum Euler model in chapter IV,
- the Quantum Hydrodynamic (QHD) and Quantum Energy Transport (QET) models in chapter V.

From a numerical point of view, most efforts have been made on the QDD model. We have first proposed a time and space discretization of the model coupled to the Poisson equation with insulating boundary conditions, a numerical analysis of the scheme has been performed and we have shown that this scheme has nice properties (the scheme is well posed, the strict positivity of the density is granted for all time, the total charge on the domain is conserved and a discrete quantum free energy is dissipated). We have then proposed some open boundary conditions and we have performed some tests on the resonant tunneling diode (RTD), these tests have been compared with those obtained with other existing models. Finally, we have suggested to include transparent boundary conditions to the QDD model which seem more realistic from a physical point of view.

Nevertheless, some work need to be completed concerning the QDD model. Thanks to the decrease of the quantum free energy, the proof of convergence of the model (at least for the discretized model) seems possible but needs more investigations. In addition, concerning the transparent boundary conditions, we are not able at the moment to capture correctly resonances of a realistic RTD in order to plot current-voltage characteristics (the Gummel method applied for the stationary model does not converge for large applied bias and we have not been able to find a cure for this ill-behavior yet) and the need to take a very small momentum step makes explode the computation time for the transient model. The use of an adaptative mesh size for the momentum should allow to decrease the computation cost but is still to be implemented. We can think about many other extensions: choosing other statistics than the Boltzmann statistics, such as the Fermi-Dirac statistics, coupling the QDD model with the classical drift-diffusion model (inside the reservoirs of electrons for instance), applying the model to other domains such as quantum chemistry, etc...

Concerning the Isothermal Quantum Euler model, some properties have been proved which rely essentially on a gauge invariance property. These properties permit

to perform simplifications for the special case of irrotational flows, and thus for the 1D model. These simplifications allowed us to present preliminary numerical simulations on a simplified RTD. It remains a lot of work on this model and the same program as for the QDD model can be followed (study of the numerical scheme, application on a physical test case, comparison with existing models, implementation of transparent boundary conditions,...).

Regarding the QHD and QET models, almost everything has to be done even if chapter V should facilitate numerical implementations of these models. We can also imagine studying other quantum fluid models based on the entropy principle, such as hydrodynamic-like models with moments of order greater than two. A lot of open questions remain concerning all of these models. The existence of quantum local equilibrium defined as the minimizers of a quantum entropy is to be shown and to this purpose, a functional framework needs to be created.

Finally, in the last chapter of this thesis (chapter VI), we have proposed a numerical scheme for the Schrödinger equation written in its fluid formulation: the Madelung system. The linear analysis of the scheme shows that this scheme is asymptotically stable in the semiclassical limit. A possible work for the future could be to show the stability of the nonlinear scheme. Furthermore, a lot of problems are under considerations, such as dealing with instabilities linked to low densities and taking non contant external potentials for instance.

Résumé

Le sujet de la thèse porte sur l'étude d'une nouvelle classe de modèles de transport quantique: les modèles fluides quantiques issus du principe de minimisation d'entropie. Ces modèles ont été dérivés dans deux articles publiés en 2003 et 2005 par Degond, Méhats et Ringhofer dans Journal of Statistical Physics en adaptant au cadre de la théorie quantique la méthode des moments développée par Levermore dans le cadre classique. Cette méthode consiste à prendre les moments de l'équation de Liouville quantique et à fermer ce système par un équilibre local (ou Maxwellienne quantique) défini comme minimiseur d'une certaine entropie quantique sous contrainte de conservation de certaines quantités physiques comme la masse, le courant, et l'énergie. Le principal intérêt des modèles quantiques ainsi obtenus provient du fait qu'étant macroscopiques, ils sont biens moins coûteux numériquement que des modèles microscopiques comme l'équation de Schrödinger ou l'équation de Wigner, et de plus, ils prennent en compte implicitement des effets de collision bien plus difficiles à modéliser à un niveau microscopique. Le but de cette thèse est donc de proposer des méthodes numériques pour implémenter ces modèles et de les tester sur des dispositifs physiques adéquats. Nous avons donc commencé dans le chapitre I par proposer une discrétisation du plus simple de ces modèles qu'est le modèle de Dérive-Diffusion Quantique sur un domaine fermé. Puis nous avons décidé dans le chapitre II et III d'appliquer ce modèle au transport d'électrons dans les semiconducteurs en choisissant comme dispositif ouvert la diode à effet tunnel résonnant. Ensuite nous nous sommes intéressés au chapitre IV à l'étude et l'implémentation du modèle d'Euler Quantique Isotherme, avant de s'attaquer aux modèles non isothermes dans le chapitre V avec l'étude des modèles d'Hydrodynamique Quantique et de Transport d'Énergie Quantique. Enfin, le chapitre VI s'intéresse à un problème un petit peu différent en proposant un schéma asymptotiquement stable dans la limite semi-classique pour l'équation de Schrödinger écrite dans sa formulation fluide: le système de Madelung.

Mots clefs. Modèles fluides quantiques, Dérive-Diffusion Quantique, Euler Quantique, Hydrodynamique Quantique, Transport d'Énergie Quantique, diode à effet tunnel résonnant, équation de Schrödinger, équation de Poisson, système de Madelung, analyse asymptotique.

Summary

The PhD thesis is concerned with the study of a new class of quantum transport models: the quantum fluid models derived from the entropy principle. These models have been derived in two articles published in 2003 and 2005 by Degond, Méhats and Ringhofer in the Journal of Statistical Physics, by adapting to the quantum framework the moment method developed by Levermore in the classical framework. This method consists in taking the moments of the Quantum Liouville equation and closing this system by a local equilibrium (or quantum Maxwellian) defined as the minimizer of a quantum entropy with constraints on some physical quantities such as the mass, current, and energy. The main interest of such macroscopic models is their low cost in terms of numerical implementation compared to microscopic models such as the Schrödinger equation or the Wigner equation. Moreover, such models take implicitly into account collisions which are much more difficult to handle with quantum microscopic models. The goal of this thesis is thus to propose numerical methods to implement these models and to test them on some physical devices. We have started in chapter I by proposing a discretization for the most simple of these models which is the Quantum Drift-Diffusion model on a closed domain. We have then decided in chapter II and III to apply this model to electron transport in semiconductors by choosing as open device the resonant tunneling diode. We have then studied in chapter IV the Isothermal Quantum Euler model, before considering in chapter V the study of non isothermal models such as the Quantum Hydrodynamic and the Quantum Energy Transport models. Finally, chapter VI is concerned with a slightly different problem which is the implementation of an asymptotically stable scheme in the semiclassical limit for the fluid formulation of the Schrödinger equation: the Madelung system.

Key words. Quantum fluid models, Quantum Drift-Diffusion, Quantum Euler, Quantum Hydrodynamics, Quantum Energy Transport, Resonant Tunneling Diode, Schrödinger equation, Poisson equation, Madelung system, asymptotic analysis.